

PAST VARIATIONS OF NATURAL RADIOCARBON AS RECORDED IN

U.K. WOOD

THESIS

submitted for the degree of

DOCTOR OF PHILOSOPHY

of the

UNIVERSITY OF GLASGOW

by

JOHN ALLAN CAMPBELL

Department of Chemistry

November 1977

ProQuest Number: 13804133

All rights reserved

INFORMATION TO ALL USERS

The quality of this reproduction is dependent upon the quality of the copy submitted.

In the unlikely event that the author did not send a complete manuscript and there are missing pages, these will be noted. Also, if material had to be removed, a note will indicate the deletion.



ProQuest 13804133

Published by ProQuest LLC (2018). Copyright of the Dissertation is held by the Author.

All rights reserved.

This work is protected against unauthorized copying under Title 17, United States Code
Microform Edition © ProQuest LLC.

ProQuest LLC.
789 East Eisenhower Parkway
P.O. Box 1346
Ann Arbor, MI 48106 – 1346

T A B L E O F C O N T E N T S

	PAGE
Acknowledgements	i
List of Tables	iii
List of Figures	v
List of Plates	viii
Summary	ix
CHAPTER 1 INTRODUCTION	
1.1 Historical	1
1.2 Variations in natural ¹⁴ C concentrations in the atmosphere	4
1.3 Artificial variations of atmospheric ¹⁴ C concentrations	15
1.4 Quantitative assessment of processes in the carbon cycle	21
1.5 Calibration of the radiocarbon timescale	27
1.6 The submerged forests of the U.K.	33
1.7 Aims of research	43
CHAPTER 2 EXPERIMENTAL METHODS	
2.1 Introduction	46
2.2 Chemical preparation of benzene	
2.2.1 Sample pretreatment	49
2.2.2 Sample combustion	53
2.2.3 Acetylene synthesis	60
2.2.4 Cyclotrimerisation of acetylene to benzene	71
2.2.5 Combustion of benzene to carbon dioxide	78
2.2.6 Summary of laboratory procedure	81

	PAGE	
2.3	Measurement of isotopic fractionation	81
2.4	The Liquid Scintillation Technique	
2.4.1	Introduction	
2.4.2	The scintillation medium	88
2.4.3	Counter electronics	90
2.4.4	Quenching	95
2.5	The ^{14}C detection system	
2.5.1	Description	96
2.5.2	Optimisation of the counting system for low level ^{14}C assay	99
2.5.3	Preparation of the standard geometry vial	102
2.5.4	Background count rate	106
2.5.5	Quench-efficiency calibration	108
2.5.6	Modern standard count rates	112
2.6	Calculation of results	120
CHAPTER 3	RESULTS	
3.1	Intercalibration samples and replicate analyses	122
3.2	Archaeological samples	124
3.3	Geochemical samples	125
CHAPTER 4	ASSESSMENT OF LABORATORY PROCEDURES	156
CHAPTER 5	DISCUSSION OF TREE-RING/RADIOCARBON RESULTS	
5.1	Preliminary results	179
5.2	Dendrochronology	181
5.3	Tree-ring/radiocarbon results	183
5.4	Conclusions and implications	214

	PAGE
CHAPTER 6 APPLICATIONS OF RADIOCARBON DATING TO ARCHAEOLOGY	
6•1 Radiocarbon dates for South Cadbury- Camelot	218
6•2 The 1976 British-Ecuadorean expedition to the Los Tayos Caves	238
APPENDIX 1 THE BACKGROUND COUNT RATE	243
APPENDIX 2 COMPUTER PROGRAMMES	256
REFERENCES	278

A C K N O W L E D G E M E N T S

I wish to record my sincere thanks to Dr. M.S. Baxter for his tuition and supervision during this research project and for constructive criticism and assistance during the preparation of this thesis.

Samples of dendrochronologically dated wood were largely supplied by Dr. A. Heyworth, University College Wales, Aberystwyth. I am grateful to him for this source of material and for additional diagrams and data presented here.

During the establishment of the laboratory, the assistance of Dr. D.D. Harkness of the Scottish Universities Research and Reactor Centre, both in practical advice and in sample preparation, was invaluable.

The equipment of the dating laboratory was constructed and efficiently maintained by the glassblowing, workshop and electronics sections of the Chemistry Department under the respective direction of J. Connolly, A. Hislop and A. Anderson. In addition, I wish to acknowledge the craftsmanship of D. Sinclair, for the manufacture of metal reaction vessels, and W. Goodway, for the construction of the glass high vacuum system. Further technical services were supplied by A. Miller, K. McKay and A. Ritchie (mass spectrometry). To them thanks are due.

I wish to thank J. Kay, T. Aitchison and P. Breeze of the Statistics Department in the University for assistance with the statistical aspects of the work.

I am indebted to Mrs. Janis Whitelaw for painstakingly typing this manuscript and to Dr. Brian Whiting for assistance in mounting the photographic plates.

The past and present members of the Nuclear Geochemistry Group have proved an excellent group of friends whose ready discussion and criticism, scientific and social, was greatly appreciated. They are, Drs. H.M. Blauer, N. Drndarski, A.E. Fallick, J.G. Farmer, T.D.B. Lyon, A.B. MacKenzie and M.J. Stenhouse and Messrs. R.W. Crawford, I.G. McKinley, A. Saad, J. Smith-Briggs and D.S. Swan.

I have been faithfully supported through this period of study by my parents and to them I express my gratitude.

It was a pleasure and a privilege to spend the summer months of 1976 as a participant in the Los Tayos expedition. To the Expedition Trust and to the members of the party, scientific and military, I extend my thanks.

Lastly, the financial support of the Natural Environment Research Council is gratefully acknowledged.

JOHN A. CAMPBELL

NOVEMBER 1977

L I S T O F T A B L E S

	PAGE	
1-1	Residence times (years) for ^{14}C in the atmosphere	25
2-1	Errors caused by sample contamination	51
2-2	Analyses of Brain Standard against Tree-Ring standard	85
2-3	Common primary scintillators	89
2-4	Background data 1 - Marble	109
2-5	Background data 2 - Scintillation grade benzene	110
2-6	Quench-efficiency calibration	110
2-7	Modern standard - M6	118
2-8	N.B.S. Oxalic Acid standards	119
3-1-1	Intercalibration samples	127
3-1-2	Ynyslas 1 replicate analyses	128 and 129
3-1-3	Rice standard replicate analyses	130
3-1-4	Calibration of micro-combustion system - replicate measurements on scintillation grade benzene	131
3-1-5	Calibration of micro-combustion system - replicate analyses on wood cellulose	132
3-1-6	Stable carbon isotope data for Stolford 4	133
3-1-7	Stable carbon isotope data for Stolford 5	134 and 135
3-2-1	Archaeological samples	136 and 137
3-3-1	Radiocarbon dates for submerged forest sites	138
3-3-2	Borth 1 Pine - Tree-ring/radiocarbon analyses	139
3-3-3	Borth 4 Oak - Tree-ring/radiocarbon analyses	140
3-3-4	Borth 6 Oak - Tree-ring/radiocarbon analyses	141 and 142

	PAGE
3-3-5 Ynyslas 1 Pine - Tree-ring/radiocarbon analyses	143
3-3-6 Stolford 4 Oak - Tree-ring/radiocarbon analyses	144
3-3-7 Stolford 5 Oak - Tree-ring/radiocarbon analyses	145 and 146
3-3-8 Cullykhan 1 Oak - Tree-ring/radiocarbon analyses	147 and 148
5-1 Linear least squares analysis of submerged forest floating chronologies	185
5-2 Weighted linear least squares analysis of submerged forest floating chronologies	188
5-3 Statistical calibration of floating chronologies against a master chronology	207
6-1 Radiocarbon dates for South Cadbury - Camelot	229
6-2 Radiocarbon dates for South Cadbury "massacre"	233
6-3 Sources of error in radiocarbon dating	237
A1-1 Weight of scintillation vials in a 50-vial tray	245
A1-2 Background count rate for selected vials	247
A1-3 Background count rate observed under different counting conditions	251
A1-4 Background components for a standard 10ml geometry vial	254

LIST OF FIGURES

	PAGE	
1-1	The Carbon Cycle	2
1-2	Secular variations of atmospheric ^{14}C concentrations during the last 12 millenia	7
1-3	^{14}C concentrations in the northern hemisphere troposphere (1890-1974)	17
1-4	Typical box models describing the natural radiocarbon system	22
1-5	Radiocarbon dates for U.K. submerged forest exposures	35
1-6	Sea-level curves	36
2-1	Sample combustion vessel	55
2-2A	CO_2 collection system	56
2-2B	CO_2 distillation, measurement and storage system	57
2-3	Stainless steel reaction vessel for conversion of CO_2 to C_2H_2	62
2-4A	C_2H_2 preparation and collection system	64
2-4B	C_2H_2 purification, measurement and storage system	65
2-5	CO_2 to C_2H_2 conversion yields	69
2-6	Benzene synthesis system	72
2-7	C_2H_2 to C_6H_6 conversion yields	75
2-8	Microcombustion bomb	80
2-9	Micro-combustion gas handling system	82
2-10	Flow diagram of laboratory procedure	83
2-11	Energy transfer scheme in a liquid scintillator	87
2-12	Structural formulae of common liquid scintillators	91
2-13	Schematic diagram of a photomultiplier tube	93
2-14	Schematic diagram of counting system electronics	98

	PAGE	
2-15	Variation of the count rate of a ^{14}C spike sample with high voltage	101
2-16	^{14}C pulse height spectrum	103
2-17	^3H pulse height spectrum	104
2-18	Background pulse height spectrum	105
2-19	Nomogram for preparation of standard 10ml. counting vial	107
2-20	Quench calibration curve	113
2-21	Quench calibration line (for samples with $R < 2.5$, i.e. small quench effect)	114
2-22	Sample hydrolysis/wet oxidation system	116
3-1	Borth 1 - Radiocarbon analyses	149
3-2	Borth 4 - Radiocarbon analyses	150
3-3	Borth 6 - Radiocarbon analyses	151
3-4	Ynyslas 1 - Radiocarbon analyses	152
3-5	Stolford 4 - Radiocarbon analyses	153
3-6	Stolford 5 - Radiocarbon analyses	154
3-7	Cullykhan 1 - Radiocarbon analyses	155
4-1	NBS oxalic acid standard M6 - count rate versus time October 1975 - September 1976	159
4-2	Background count rate versus time July 1975 - April 1976	160
4-3	Stolford 4/6 (GU 760) - Number of counts accumulated in successive 100 minute counts	171
4-4	Wood replicate 8 (GU 676)-Number of counts accumulated in successive 100 minute counts	172
4-5	Wood replicate 21 (GU 689) - Number of counts accumulated in successive 100 minute counts	173
5-1	Tree-ring curves for Stolford and Borth oak chronologies	182
5-2	Comparison of sampling frequencies	189

	PAGE
5-3A Stolford 5 - 5 x 10 samples per century, alternate analyses Case A	191
5-3B Stolford 5 - 5 x 10 samples per century, alternate analyses Case B	192
5-3C Stolford 5 - 5 x 20 samples per century, adjacent averaged analyses Case C	193
5-4 Least squares approximations for Cullykhan data	195
5-5 Least squares approximations for Stolford data	197
5-6 Least squares approximations for Borth (oak) data	198
5-7 Least squares approximations for Ynyslas (pine) data	200
5-8 Least squares approximations for Borth (pine) data	201
5-9 Statistical calibration of Cullykhan oak chronology against bristlecone pine	208
5-10 Statistical calibration of Stolford oak chronology against bristlecone pine	209
5-11 Statistical calibration of Borth 4 oak chronology against bristlecone pine	211
5-12 Statistical calibration of Borth and Ynyslas pine chronologies against bristlecone pine	212
5-13 Statistical calibration against bristle- cone pine: relative positions of Stolford (oak) and Ynyslas (pine) chronologies	213
A1-1 Background count rate (10ml. geometry) versus scintillation vial weight	248
A1-2 Background count rate (10ml. geometry) versus clear height	249

L I S T O F P L A T E S

		PAGE
1.	Submerged forest exposure at Ynyslas, Cardigan Bay, Wales	39
2.	Cutting a section from a fallen trunk	40
3.	Removal of section	41

S U M M A R Y

Past variations in the natural radiocarbon content of the atmosphere over recent millenia have previously been documented through analyses of precisely dated organic materials, principally tree rings of bristlecone pine wood. Evidence for the causal factors of the secular variations has been obtained by correlation of the ^{14}C profile with geophysical parameters such as the Earth's magnetic field, solar activity and climatic data. While the long-term trend in atmospheric ^{14}C concentration and its origins are now firmly established, the existence of short-term fluctuations and the factors which could produce them are still in dispute. Bristlecone pine calibration of the radiocarbon timescale has produced a means of correcting archaeological data for past fluctuations, but this data record has subsequently been criticised, the main objections being that the ^{14}C concentration of that wood may be atypical of world-wide ^{14}C concentrations, as a result of its extreme growth conditions. Alternative dendrochronologies are at present being developed and subsequent ^{14}C analyses will prove or disprove the validity of the existing data.

This thesis presents the preliminary results of a long-term project aimed at producing an absolute dendrochronology/radiocarbon calibration system for the United Kingdom. Samples for this study come from the vast areas of submerged forests around the coast of the U.K., and from archaeological sites. The principal features of the study - one of the first of this kind to make exclusive use of the liquid scintillation method - are, a) a very high sampling frequency

(10 samples/century), b) abundant sample materials in perfect preservation and c) an emphasis on inter-calibration and error assessment.

The results of radiocarbon analyses of 5 "floating" chronologies, three oak and two pine, are presented. These clearly show that short-term fluctuations in atmospheric radiocarbon do exist, the variations being of the order of 2 - 3% in 40 - 50 years. The laboratory standardisation, by replicate analysis of an aged wood sample, indicates that the total error associated with a single analysis is largely a result of counting statistics, and thus these observed fluctuations are considered to reflect real changes in atmospheric ^{14}C levels, rather than random experimental noise. Variations of this magnitude and time period have not previously been observed and it is believed that their detection in this study is a result of the enhanced sampling frequency employed. Statistical comparison of U.K. and American data has not shown reported systematic discrepancies between "normal" organic material and bristlecone pine wood but does suggest that, while longer-term trends in atmospheric ^{14}C levels are equivalent, the detailed structure of the ^{14}C profile may be different.

In addition to the major research programme described above, two short studies involving direct application of radiocarbon dating to archaeological problems were performed. The results of these have direct relevance to the limitations inherent in practical radiocarbon dating.

CHAPTER 1

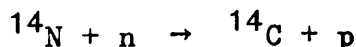
INTRODUCTION

1.1 Historical

The radiocarbon dating method involves determination of the time during which the radiocarbon concentration in a sample has decreased from its initial to its present value and therefore depends on a knowledge of these concentrations and on the rate of decay. The initial concentration of radiocarbon in a sample is the ^{14}C concentration of that sample when it ceases to assimilate carbon from and to be in equilibrium with its environment. Except for a small fractionation effect, due to the mass difference between ^{14}C and ^{12}C , the assimilation of carbon by a sample results in an equality of the environmental and initial concentrations of the sample.

After the discovery by Libby of the existence of naturally occurring radiocarbon (Anderson et al., 1947), the basic assumption that the radiocarbon concentrations of the various reservoirs in the dynamic carbon cycle (Fig. 1-1) have remained constant and equal to their present concentrations was proposed and confirmed, to the extent then possible, by Libby and his co-workers (Anderson and Libby, 1951).

Radiocarbon is produced in the atmosphere by the interaction of cosmic-ray neutrons with nitrogen



and the radiocarbon undergoes β decay to ^{14}N

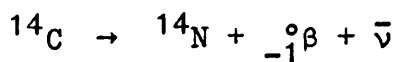
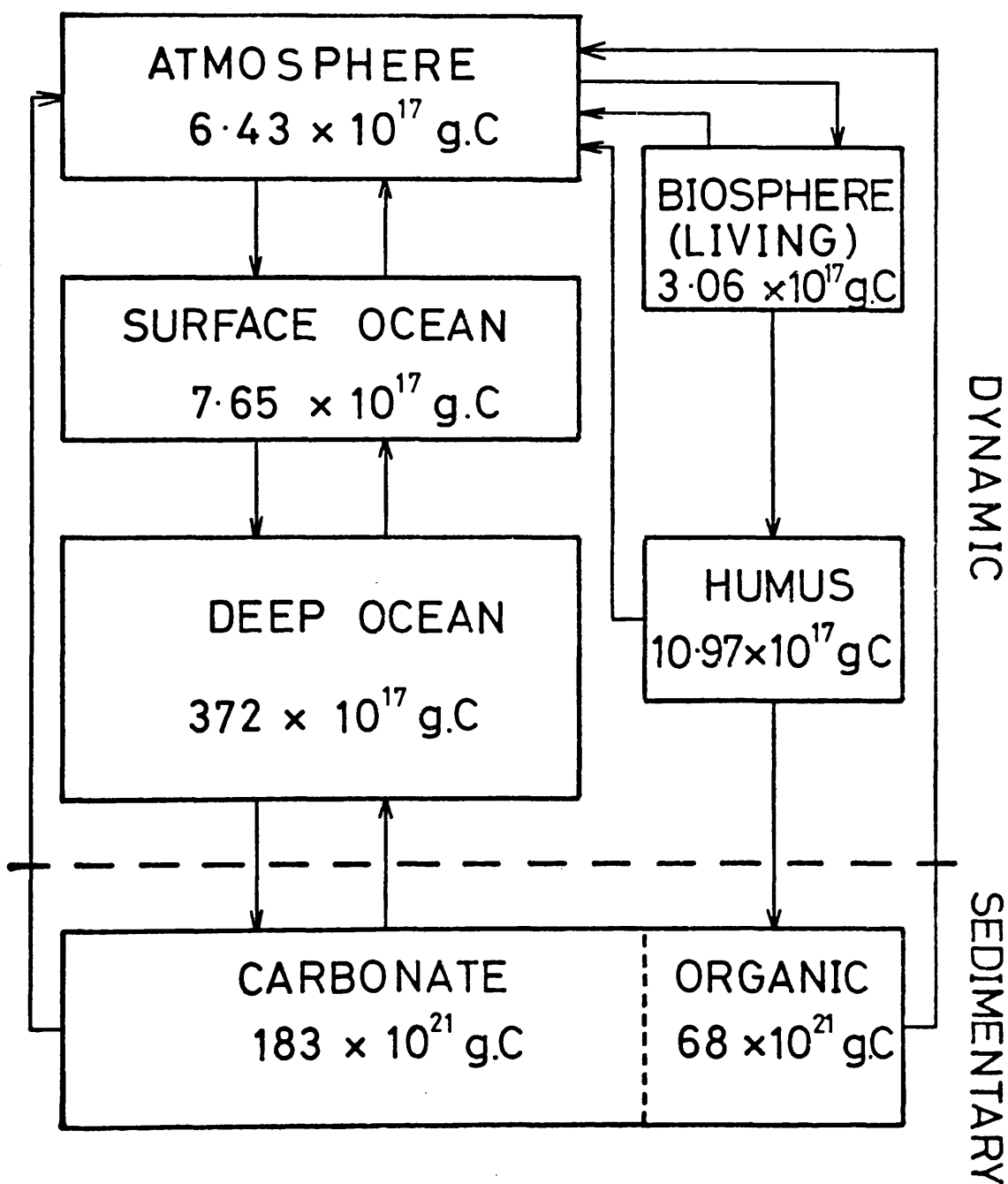


FIGURE 1-1: The Carbon Cycle



The half-life, $t_{\frac{1}{2}}$, for this decay process is 5730 ± 40 years (Godwin, 1962). After its production the radiocarbon is rapidly oxidised to CO_2 and is distributed among the various carbon-containing reservoirs, i.e. the carbon dioxide of the atmosphere, the terrestrial biosphere and the bicarbonates dissolved in the oceans. Most of the radiocarbon decay takes place in the oceans which constitute by far the largest of these reservoirs.

Thus the basic assumption of constant radiocarbon in the environment, primarily in the atmosphere, entails the following subsidiary assumptions:

1. the cosmic-ray flux incident on the atmosphere and hence the production rate of radiocarbon in the atmosphere have remained constant for several half-lives,
 2. the stable carbon content of the various reservoirs containing cosmic-ray-produced ^{14}C have remained constant over such a period of time
- and 3. the rates of ^{14}C transfer between the reservoirs, in particular from the atmosphere into the oceans, have also remained constant over this length of time.

The intensive investigation of radiocarbon concentrations in many materials over the last twenty five years has confirmed the general validity of these assumptions but has simultaneously shown the existence of small variations with time in the atmospheric $^{14}\text{C}/^{12}\text{C}$ ratio, indicating the slight failure of one or more of these criteria. The

discovery of these variations has led both to a refinement in the accuracy of radiocarbon dating and to an increased knowledge of such diverse areas of geophysics as isotope production by cosmic rays in the atmosphere and mechanisms and rates of exchange of carbon dioxide between the atmosphere and oceans.

1.2 Variations in natural ^{14}C concentrations in the atmosphere

In 1958, de Vries proved the existence of an increase in atmospheric ^{14}C concentrations for the years around A.D. 1700, of about 2%, relative to the 19th Century "natural" level, an anomaly subsequently called "the de Vries effect". The effect was detected in known age samples from different geographical locations, namely the United States, Germany and Holland. Subsequently a number of other investigators found deviations of a similar nature. A study of the variations of ^{14}C activity in a section of a California giant sequoia tree (sequoia gigantea) was made in three European laboratories (Willis et al., 1960). More or less irregular variations in ^{14}C activity of the order of 2 or 3% were recognised. Furthermore, measurements on historically dated objects from the second and third millennia B.C., mainly Egyptian, indicated a discrepancy of several hundred years between radiocarbon dates and true ages (Ralph, 1959).

The discovery of these variations in natural ^{14}C concentrations had obvious implications for the radiocarbon dating method. It was necessary to seek a method

by which the radiocarbon timescale could be compared to an independently derived absolute chronology. If this could be achieved then subsequent radiocarbon analyses on precisely dated material from the absolute chronology would allow the construction of a record of past variations of natural radiocarbon and so would enable the conversion of conventional ^{14}C ages into true calendar ages.

Such an absolute chronology was found in the dendro-chronology of bristlecone pine wood (pinus aristata) and, to a lesser extent, of giant sequoia (sequoia gigantea). The major portion of the bristlecone pine chronology was constructed during the 1960's by Ferguson (1968, 1969, 1970) and by 1972 had been extended to almost 8,000 years B.P. (Ferguson, 1972). As the chronology was being compiled, samples of precisely dated tree rings, usually spanning 10 growth increments each, were analysed for their ^{14}C content principally by the La Jolla laboratory (Suess, 1970a). A much smaller number of samples have been analysed at the Arizona, Pennsylvania and Yale laboratories (Stuiver, 1969; Ralph and Michael, 1970; Damon et al., 1970; Michael and Ralph, 1972; Damon et al., 1972).

A potentially suitable alternative for the study of ^{14}C variations prior to 10,000 years B.P. is found in varve series. Varves are the annual layers found in clays which deposit in the beds of glacial lakes. Annual layers may be identified by seasonal variations in texture of the sediment in a manner analogous to tree-ring counting.

The Swedish varve chronology of De Geer (1940) has been used to monitor ^{14}C levels back to 12,500 years B.P. Although insufficient organic carbon was present in these varves, pollen-zone boundary conditions enabled their relation to nearby peat bogs from which satisfactory samples were obtained for ^{14}C assay (Wenner, 1968; Fromm, 1970). The other major varve series is from Lake of the Clouds, Minnesota. Direct measurements on the organic matter present provided data on ^{14}C levels during the past 10,000 years (Stuiver, 1970).

The variations in atmospheric ^{14}C concentration during the past twelve millenia are illustrated in Fig. 1-2 and are based on both tree-ring and varve data. Certain major features can be seen from the curve:

1. atmosphere concentrations over the past 2,500 years have been within a few percent of the 19th Century level
- and 2. between 5,500 and 2,500 years B.P. the atmospheric ^{14}C content decreased from 10% above the natural level.

There is, in general, excellent agreement between the tree-ring and varve data up to 6,000 years B.P.

Prior to 6,000 B.P., the Swedish ^{14}C varve data show a decrease to the natural level by 12,000 B.P. In contrast, the data for Lake of the Clouds indicate a decrease to + 8% natural at 8,000 B.P. and then an increase to 12% by 10,000 B.P. The discrepancy, which is unlikely to be the result of a real difference in ^{14}C levels between the two locations, may be due to errors in either or both chronologies.

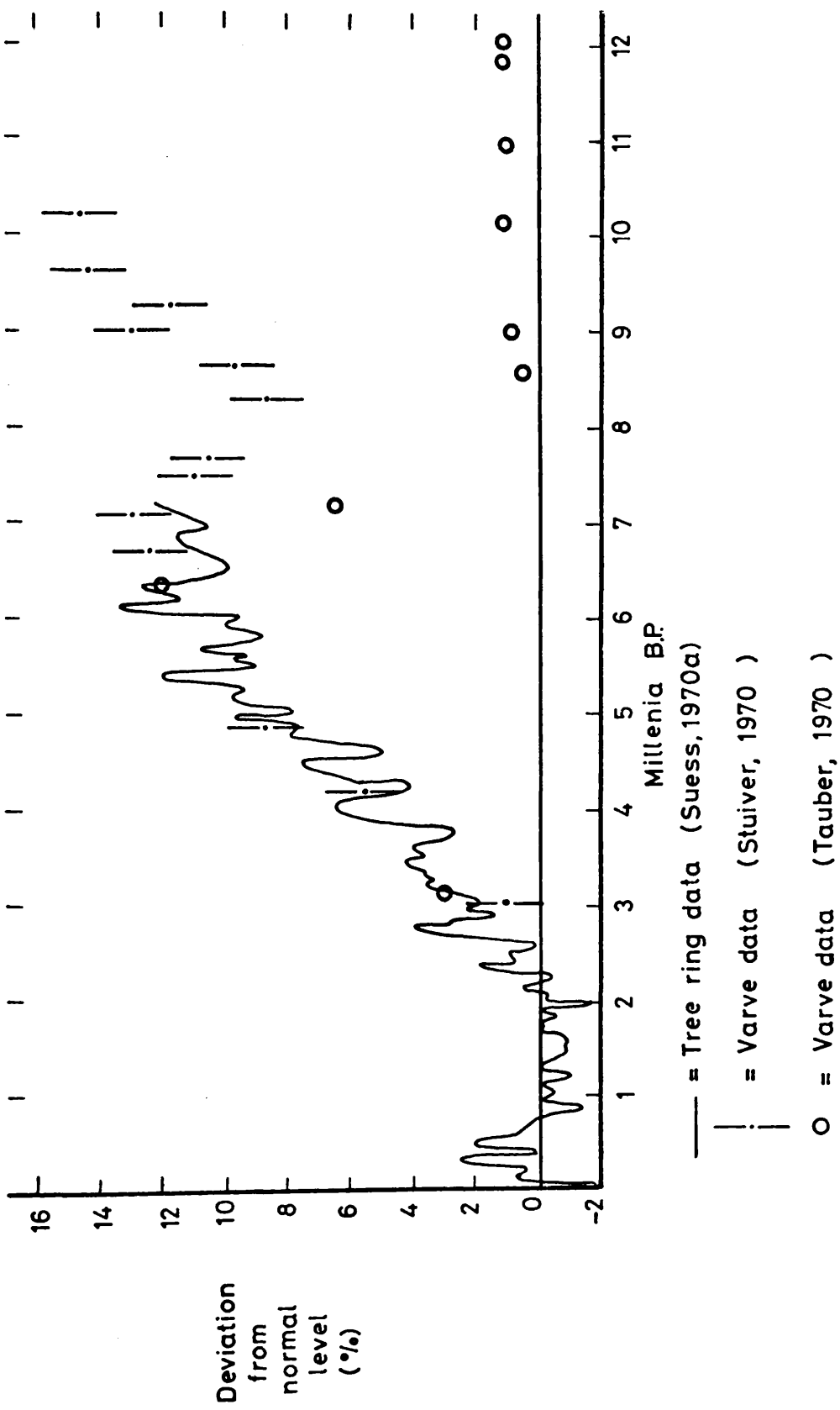


FIGURE 1-2: Secular variations of atmospheric ¹⁴C concentrations during the last 12 millenia

In addition to the long-term features, there are short-term fluctuations of 2 - 3% over 50 to 200 years and also similar variations of 400 years (Suess, 1970b). The occurrence of these short-term variations in natural ^{14}C pose particular problems for the archaeologist, since one ^{14}C age may correspond to more than one calendar age. (The problems of radio-carbon-true age calibration are discussed in Section 1.5).

The question of the correct causes of the variations in natural ^{14}C is a major topic of discussion, as yet unsettled, partly because correlations are usually, at least to some extent, subjective and also because they indicate a relationship which may only be coincidental. The following relationships are, however, generally accepted. Firstly, the large-scale variations over the last 7,000 years are probably due to varying modulation by the earth's magnetic field of the total cosmic-ray flux incident on the earth's atmosphere. The reasons for changes in the magnetic field intensity are related to hydro-magnetic processes in the boundary layer of the earth's core, an increase in intensity leading to a decrease in ^{14}C production and vice versa (Elsasser et al., 1956). Kigoshi and Hasegawa (1966) calculated variations in the atmospheric concentration of ^{14}C arising from variations in the geomagnetic dipole. A smoothed trend of observed varying geomagnetic intensity was correlated with variations in production rate using an expression derived by Wada and Yamaguchi (1962). The estimated trends of varying ^{14}C concentration agreed well with ^{14}C

concentrations obtained by assay of samples of known age. From palaeomagnetic measurements, Bucha (1970) has constructed a sinusoidal curve for the geomagnetic field intensity for the past 9,000 years, with approximate periodicity of 8,900 years. There is evidence of good inverse correlation between geomagnetic field intensity and atmospheric ^{14}C concentrations. Furthermore, Houtermans (1966) has shown that a 50% increase in the ^{14}C production rate will account for the observed change in ^{14}C activity over the past 8,000 years. This compares favourably with the observed variation in the geomagnetic field by a factor of about 2. This detailed archaeomagnetic investigation showed that, in addition to the long-term changes, fluctuations of shorter periods occur, the source of which is probably the westward drift of the non-dipole field. In consequence these fluctuations do not appear simultaneously on the whole of the earth's surface, and the temporal occurrence of their maxima and minima depends on geographical longitude. Lal and Venkatavaradan (1970) estimated a periodicity of 150 - 1,000 years for the westward drift but also cautioned that limited data may not reflect changes on a world wide basis, but only regional disturbances.

Secondly, evidence for the causal factor of the shorter-term fluctuations superimposed on the long-term trend has been derived from correlation with solar activity. Forbush (1954) was the first to observe the inverse correlation between sunspot number and cosmic-ray intensity over the 11 year solar cycle in particular. This correlation has been shown by Simpson (1963) and others

to be due to a large-scale modulation of galactic cosmic-ray intensity by interplanetary fields controlled by solar plasma. Records of solar activity over the past 2,000 years have been compiled by Schöve (1955).

The first report of an inverse correlation between the index of solar activity and atmospheric ^{14}C concentrations was made by Stuiver (1961). Thus at times of high solar activity the associated intensification of the weak magnetic field of the solar wind causes a reduction in the cosmic-ray flux near the earth and consequently a decrease in the production rate of ^{14}C . Direct measurement of cosmic radiation over three recent solar cycles (Lingenfelter, 1963; Lingenfelter and Ramaty, 1970) has verified this empirical relationship. The relationship between solar activity and ^{14}C levels is now fairly well established, Grey (1969) observing excellent agreement over the past 750 years between observed ^{14}C concentrations and those calculated from a solar cycle model.

Variations in solar activity appear to have certain periodicities and these are reflected in ^{14}C levels. Again the inverse correlation was noted for periodicities of 50 and 200 years (Houtermans et al., 1967; Houtermans, 1971). Suess (1970b), as stated earlier, has noted a minimum in $\Delta^{14}\text{C}$ occurring at intervals of approximately 400 years which may be related to reported 400 year periodicities in sunspot numbers. He has, however, also observed that the minima occurring after 400 B.C. are not in phase with those occurring earlier. The shortest observed periodicity in solar activity is the well known 11 year cycle.

A negative correlation between sunspot number and ^{14}C concentration was reported by Baxter and Walton (1971) based on ^{14}C assay of wines, spirits and plant seeds. The maximum correlation was observed with ^{14}C concentration minima preceding sunspot maxima by one year, the overall magnitude of the fluctuations being 3%. Variations of 2% were reported by Baxter and Farmer (1973), from measurements on annual growth increments of 19th and 20th Century oak wood. In contrast to the previous work, these authors found that the phase shift for maximum correlation was such that maximum ^{14}C levels were attained 5 years after sunspot minimum. Lavrukhina et al. (1973) and Alexeev et al. (1975) have also reported a correlation of ^{14}C concentration and solar activity, the amplitude of the cyclic oscillations being a maximum of 2.2%. Other workers (e.g. Damon et al., 1973) have not recorded these large variations in ^{14}C levels and have suggested that variations of natural radiocarbon during the 11 year solar cycle must be less than 5^o/oo. Measurement of radiocarbon concentrations in annual growth rings of 18th and 19th Century wood (Kocharov et al., 1974; Stuiver pers. comm.) have, however, not shown any variation which can be correlated to the 11 year solar cycle.

Solar activity may further influence the ^{14}C production rate through a positive contribution to the cosmic-ray flux by solar flares. There are no records of solar flare activity in the past, but Lingenfelter and Ramaty (1970) have estimated that sudden increases of 1% in atmospheric activity may be due to these effects.

It is possible that solar activity may not only have a direct influence on ^{14}C levels via production rate changes, but may also induce climatic variations (Suess, 1968; Damon, 1968), which may, in turn, affect the transfer and exchange of carbon dioxide in the carbon cycle. Changes in temperature can alter the distribution of carbon dioxide between the atmosphere and the bicarbonate/carbonate system of the oceans. The effects of varying climate tend, however, to be counteractive. For example, a decrease in global temperature could result in a decrease in the partial pressure of CO_2 in the atmosphere resulting in an increase in ^{14}C specific activity. On the other hand, the oceanic thermocline would be weakened resulting in much faster oceanic mixing. The resultant effect would be more rapid transport of ^{14}C into the oceans, that is a decrease in atmospheric ^{14}C . A change in atmospheric ^{14}C of 2% over a period of 100 years would require a change in the atmospheric CO_2 concentration of 20%. According to Suess (1965), a change of such an order of magnitude in the carbon dioxide content of air would occur if the average surface temperature of the oceans changed by more than 10°C , that is by more than the change that occurred at the end of the last glaciation (Emiliani, 1955).

There are, however, notable correlations between climate and ^{14}C levels, such as the de Vries effect. The relatively high ^{14}C concentrations of the 15th to 17th Centuries A.D. correspond to a period of severe climate in Europe. It should, of course, also be noted

that solar activity was unusually low during this time, a period known as the Maunder minimum (Eddy, 1976) and that the high ^{14}C level is therefore most probably a result of production rate modulation (Suess, 1968; 1970b).

Lal and Venkatavaradan (1970) have suggested that the high ^{14}C activity of 10,000 B.P. can be attributed to the last ice-age. The model presented assumes direct ^{14}C input to the deep ocean via the Antarctic outcrop. During glacial periods exchange of CO_2 between the atmosphere and ocean would be reduced as a result of increased ice cover. Hence atmospheric ^{14}C concentrations would rise. It has been suggested further (Schell et al., 1965) that world-wide melting of ice after the last glacial period may have caused a long-term decrease of $\sim 10\%$ in ^{14}C levels since 8,000 B.P. The decrease in ^{14}C is a result of the release of old carbon locked in the ice and an increase in the size of the ocean with a resultant increase in the partial pressure of CO_2 in the atmosphere. The calculated increase in the ocean reservoir size, by $\sim 2.5\%$, however, seems too small to account for this effect. It is now generally accepted (Damon, 1970) that climate-induced long-term fluctuations in atmospheric ^{14}C concentrations during the last 8 millenia appear to be of minor importance compared to those produced by variations in the intensity of the geomagnetic field.

The secular variation of atmospheric ^{14}C concentration may therefore be summarised as follows:

1. the high specific activity of ^{14}C at 10,000 B.P. was probably a result of the Ice Age,
 2. the long-term decrease since then may be related to a cyclic variation of the geomagnetic field intensity of approximate periodicity 8,000 - 10,000 years
- and 3. superimposed on the general trend, fluctuations of 2 - 3% do occur over time periods of ~100 years. These are probably the effect of varying solar activity leading primarily to variation in the production rate of ^{14}C and to a lesser extent to variations in climatic conditions which affect the exchange parameters of the carbon cycle.

The correlation of short-term fluctuations in natural radiocarbon concentration with climate-induced effects is, however, not certain. There are a large number of interrelated factors which require consideration. Such interrelated parameters as carbonate-bicarbonate exchange coefficients, the pH of the sea, atmospheric moisture concentrations, cloud cover, the relationship between the CO_2 concentration and temperature, oceanic volume, biospheric activity, albedo, atmospheric particulate levels and ozone concentrations have to be considered and quantified before definite cause and effect mechanisms can be produced to interpret the short-term fluctuations in terms of climatic factors.

Information on the constancy of the cosmic-ray radiation incident on the earth may be derived from measurement of concentrations of other terrestrial cosmic-

ray-produced radionuclides such as ^{37}Ar ($t_{1/2} = 35$ days), ^{39}Ar (270 years), ^{36}Cl (3.0×10^5 years) and ^{81}Kr (2.1×10^5 years). The present concentration of these isotopes in the atmosphere (when compared with calculated concentration ratios from production cross-section data) will reflect cosmic-ray intensity averaged over the time periods of the order of these half-lives. Accordingly the ratio of $^{39}\text{Ar}/^{81}\text{Kr}$ will reflect changes in the cosmic-ray flux over several hundred years. Measurements on ice-core samples from the polar regions have enabled study of variations in the concentration of cosmic-ray-produced radionuclides over 10^5 - 10^6 years. The precision of these determinations is, however, restricted by the slow development of appropriate counting techniques (Oeschger et al., 1970). Studies on extra-terrestrial materials, for example meteorites and lunar samples, will yield information concerning variations in the cosmic-ray flux caused by solar activity, since these materials are not subject to the geomagnetic modulation effect. From ^{36}Cl and ^{39}Ar measurements on fallen meteorites, Schaeffer (1963) has deduced that the intensity of galactic cosmic rays has been constant ($\pm 10\%$) over the past 10^5 - 10^6 years.

1.3 Artificial variations of atmospheric ^{14}C concentrations

Twentieth century atmospheric ^{14}C levels have been significantly influenced by two of man's activities:

1. the burning of fossil fuels and
2. the testing of nuclear weapons.

1. The Suess Effect

The Suess effect is the decrease in atmospheric

carbon-14 concentrations caused by the combustion of large quantities of inactive fossil fuels. It originated with the industrial revolution and was estimated by Suess (1955) to have caused a depression of about 3% in northern hemisphere atmospheric ^{14}C concentrations by 1950 (Fig. 1-3). Fergusson (1958) obtained a corresponding value of 2% for the southern hemisphere. Both figures were derived from comparison of ^{14}C concentrations in mid-19th and 20th Century wood. Before detection of the Suess effect, twentieth century wood samples were frequently used as reference standards in radiocarbon age studies. With the discovery of the effect, however, it was shown that carbon-14 ages based on these standards could be too young by about 200 years. A new standard, the National Bureau of Standards Oxalic Acid Standard, based on 19th Century levels, was then issued.

The annual input to the atmosphere of CO_2 from fossil fuel can be estimated from records of the production of coal, lignite, oil, natural gas and limestone used in cement manufacture. The rate of input has risen rapidly since 1860 except for a noticeable slowing during the depression between the two world wars. Such estimates have been employed in theoretical calculations of the "Suess effect" at particular times in the past (Revelle and Suess, 1957; Fergusson, 1958; Baxter and Walton, 1970). The values obtained may be used to correct measured 20th Century ^{14}C levels so that any natural ^{14}C fluctuations are apparent (Baxter and Walton, 1971).

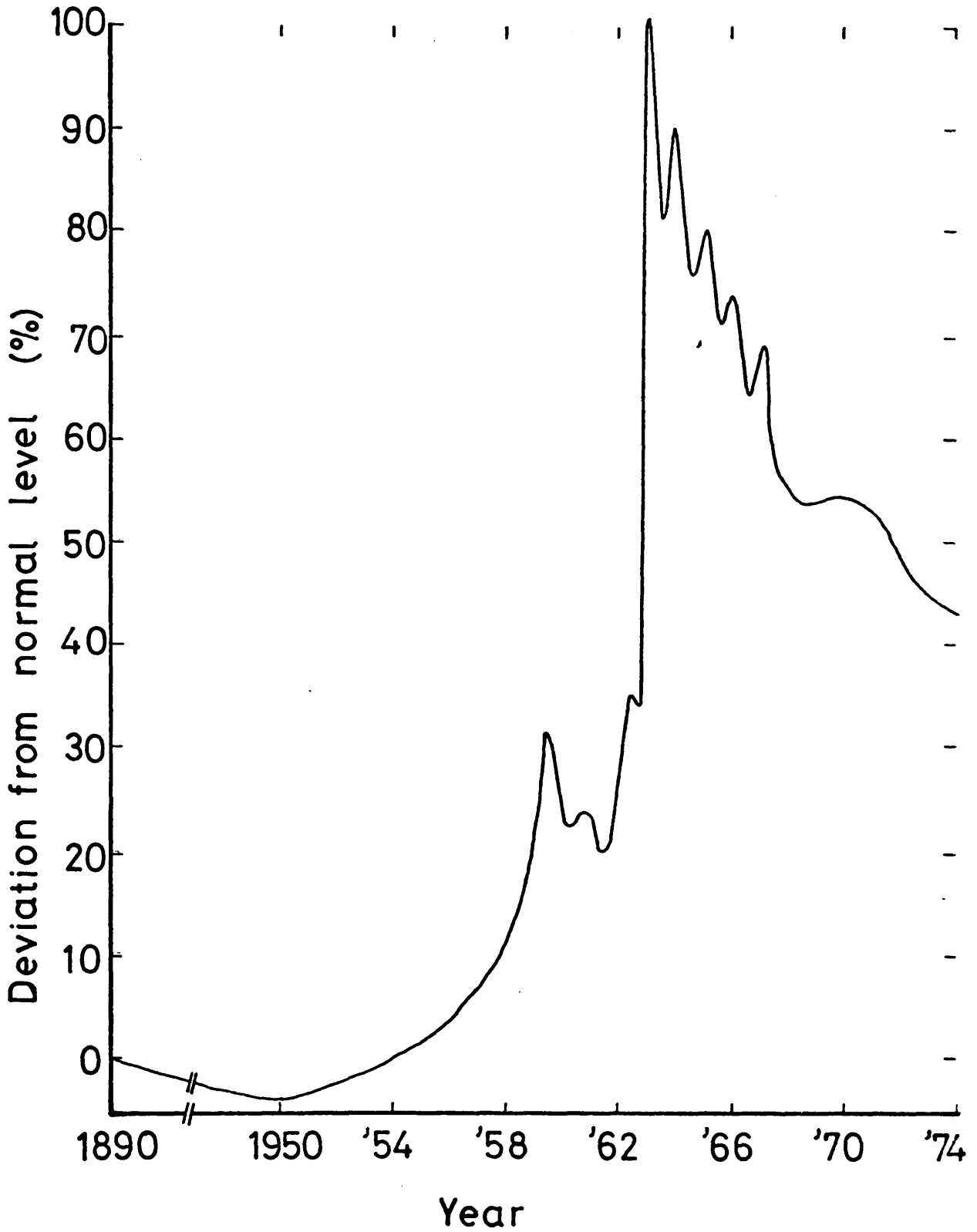


FIGURE 1-3: ^{14}C concentrations in the northern hemisphere troposphere (1890-1974)

The addition of this fossil CO_2 to the atmosphere has disturbed the dynamic equilibrium of the carbon cycle reservoirs. The observed magnitude of the "Suess effect" will depend on the distribution of this excess CO_2 throughout the carbon cycle. This has enabled calculations of exchange parameters between the various reservoirs (Craig, 1957, Revelle and Suess, 1957; Bolin and Keeling, 1963).

In 1970 the concentration of carbon dioxide in the atmosphere was 320 p.p.m. (Bolin and Bischof, 1970) compared to 290 p.p.m. in 1860 (Callendar, 1958), and the rate of increase of atmospheric CO_2 has been calculated to be $0.7 \text{ p.p.m. yr}^{-1}$ (Bischof and Bolin, 1966) which implies that the concentration of CO_2 in the atmosphere at the end of this century will be 375 p.p.m. (Bolin and Bischof, 1970; Baxter and Walton, 1970). Since CO_2 is a strong absorber and back-radiator of infra-red radiation an increase in global surface temperature could occur as a result of increasing CO_2 concentrations in the atmosphere - the "greenhouse effect". The evaluation of this effect is rather difficult because of additional factors such as associated cloud cover and atmospheric dust levels. Nevertheless, it is quite possible that the predicted increases of atmospheric CO_2 will appreciably change the climate over the next few centuries.

2. The "Bomb" Effect

The "bomb" effect is the result of the addition to the atmosphere of considerable quantities of ^{14}C produced through the activation of atmospheric nitrogen by "bomb" neutrons released during nuclear weapon tests.

The total production of ^{14}C from nuclear weapon tests is estimated at 95.6×10^{27} atoms, based on a yield of 2×10^{26} ^{14}C atoms/Mton fission or fusion for an air burst and 1×10^{26} ^{14}C atoms/Mton fission or fusion for a ground burst (Machta, 1959). Fig. 1-3 includes a profile of the irregular increase of atmospheric ^{14}C concentrations for the period 1950 - 1974 for the northern hemisphere troposphere (Broecker and Walton, 1959; Broecker and Olson, 1960; Nydal, 1963; 1968; Lal and Rama, 1966; Young and Fairhall, 1968; Walton et al., 1970; Nydal and Lösveth, 1970; Stenhouse, pers. comm.). Since the majority of the artificial ^{14}C was injected into the northern hemisphere stratosphere, the highest levels of northern hemisphere tropospheric concentrations occurred in 1963 and 1964, roughly two years after the period of maximum production. This lag is accounted for by a finite stratospheric residence time. Since the maximum levels were attained, ^{14}C concentrations have gradually decreased through mixing with the southern hemisphere troposphere and absorption by the biosphere and oceans. Using this "tracer" ^{14}C it has been possible to determine exchange parameters in the carbon cycle by model calculations.

The "box-model" approach has been used by many authors (e.g. Lal and Rama, 1966; Walton et al., 1970). The carbon cycle may be divided into compartments, for example, stratosphere, biosphere, surface ocean and deep ocean. The complexity of the model will depend on the number of compartments. The calculation of exchange rates and

residence times requires a knowledge of both the total carbon content and the excess ^{14}C for each reservoir.

Despite intense research along these lines and despite the considerable data accumulated, the values of the exchange parameters obtained by different models are not consistent. This disagreement may, of course, reflect significant variations of atmospheric CO_2 exchange rates both temporally and latitudinally. Such variations are observed annually in the northern hemisphere where the seasonally variable injection of excess ^{14}C from the stratosphere has produced the "spring leaks" shown in Fig. 1-3.

The study of natural ^{14}C fluctuations is critically dependent on samples of known age. "Bomb" ^{14}C in biospheric materials such as plants and animals participating in the carbon cycle after 1962 should also show the large increase in ^{14}C concentration observed in tropospheric air and thus the suitability of that material as an indicator of atmospheric levels can be tested (Tauber, 1967; Baxter, 1969)

As the excess ^{14}C distribution tends further to equilibrium, continued studies along this line should allow more accurate assessment of exchange rate processes. Of course, the increasing "Suess effect" must also be taken into account. It has been estimated, considering both artificial effects, that atmospheric levels will return to normal (i.e. pre-1890) by A.D. 2,000 (Harkness, 1970).

1.4 Quantitative assessment of processes in the carbon cycle

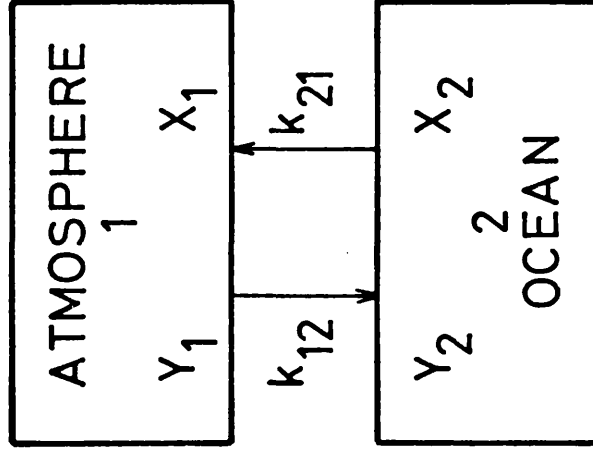
Variations in atmospheric ^{14}C concentrations are caused by the failure of one or more of the basic assumptions of the dating method (Section 1.1) and the phenomena giving rise to these variations have been outlined in Section 1.2. The response of the carbon cycle to such factors as variable production rate, varying rates of exchange of CO_2 between reservoirs and changes in the relative sizes of these reservoirs can be quantitatively assessed. The usual method of assessment is some form of "box-model".

It has been shown, in general, that a two reservoir model of the form shown in Fig. 1-4 is perfectly adequate for the particular purpose of relating long-term fluctuations in production rate to fluctuations in the atmospheric ^{14}C concentration (Houtermans, 1966; Houtermans et al., 1973). The model contains the following essential points:

1. the average delay between the production of a ^{14}C atom and the time it leaves the reservoir is non zero,
 2. the atmospheric reservoir is much smaller than the large oceanic reservoir into which the ^{14}C atoms are transferred and in which most ^{14}C atoms decay.
- and 3. the rates of exchange of ^{14}C between reservoirs are governed by first order rate constants.

The total ^{14}C produced per year is $1/8,270$ of the total ^{14}C inventory. Hence fluctuations in this production rate on a timescale small in comparison with $\sim 8,000$ years will have a very small effect on the world average ^{14}C

2 - Box model



3 - Box model

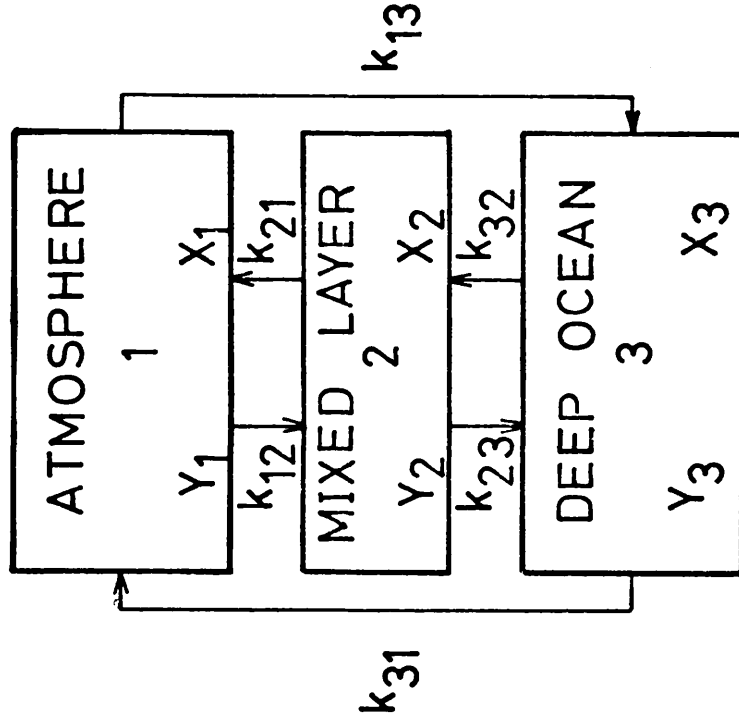


FIGURE 1-4 : Typical box models describing the natural radiocarbon system

concentration of the total exchangeable carbon. The effect will, however, be much greater on a small part of the total exchangeable carbon provided that a ^{14}C atom produced in this part (i.e. the atmosphere) does not leave this reservoir in a time short in comparison with the period of fluctuation. The transfer rate constant or its reciprocal (the residence time) for ^{14}C and CO_2 in the atmosphere is perhaps the most interesting quantity that can be derived from ^{14}C observations. The residence time is usually defined as the mean time required for a CO_2 molecule in the atmosphere to cross the atmosphere-sea (or biosphere) interface and become absorbed by the oceans (or biosphere). As long as the addition of CO_2 to the ocean is small enough that it does not change the chemical properties of sea water, this residence time of CO_2 in the atmosphere is the same as that of ^{14}C (Craig, 1957).

A set of differential equations describing the ^{14}C equilibrium in the two reservoir model are set up based on the following assumptions and notation. Reservoir i ($i = a, s$) contains Y_i atoms of ^{12}C per square centimetre of earth's surface and X_i atoms of ^{14}C . Both isotopes are internally mixed within reservoir i in a time short compared with the residence time in the reservoir. Carbon-14 is produced in the atmosphere at the variable rate of Q atoms $\text{cm}^{-2}\text{yr}^{-1}$, may leave the deep sea at the constant sedimentation rate S atoms $\text{cm}^{-2}\text{yr}^{-1}$ and decays with mean life $\tau = 1/\lambda = 8,267$ years ($T_{1/2} = 5,730$ years). The rates (atom $\text{cm}^{-2}\text{yr}^{-1}$) at which ^{14}C and ^{12}C flow from reservoir i to reservoir j are $k_{ij}X_i$ and $k_{ij}Y_i$ respectively, where first order rate constants are assumed to be the same for

^{14}C and ^{12}C . The inverse rate coefficient is $\tau_{ij} = 1/k_{ij}$ and is the residence time reservoir i with respect to removal to reservoir j .

The differential equations are:

$$\frac{dX_a}{dt(t)} = Q(t) - (\lambda + k_{as})X_a(t) + k_{sa}X_s(t)$$

$$\frac{dX_s}{dt(t)} = -S + k_{as}X_a(t) - (\lambda + k_{sa})X_s(t)$$

These equations can be solved and the data of interest extracted. Houtermans et al. (1973) derived similar equations for a three reservoir model (Fig. 1-4) and compared the effects of varying production rate, exchange rates and reservoir sizes between the two models. Of particular interest was the effect of harmonic input of ^{14}C such as might arise due to periodic solar activity. The results obtained for both two and three reservoir models indicated that short-term fluctuations in production rate, of the order of 10 years, show a high attenuation, i.e. the model can be said to act as a low-pass filter, whereas longer periodicities in production rate are attenuated to a much lesser extent. Periods of longer than 100 years can be explained by a change in production rate of less than a factor of two.

The calculations were based on assumed residence times for the atmosphere of 6 and 24 years. These values represent the approximate limits of residence times calculated for the distribution of natural ^{14}C and the distribution of fossil and bomb ^{14}C . (Table 1-1).

TABLE 1-1 RESIDENCE TIMES (YEARS) FOR ^{14}C IN
THE ATMOSPHERE

Source	Method of calculation	Residence Time (years)
Craig (1957)	Natural	7 ± 3
Revelle and Suess (1957)	Fossil	~ 10
Fergusson (1958)	Fossil	2 - 7
Rafter and Fergusson (1958)	Bomb	3.3
Lal and Rama (1966)	Bomb	4
Munnich and Roether (1967)	Bomb	5.4
Bien and Suess (1967)	Bomb	25
Young and Fairhall (1968)	Bomb	4
Nydal (1968)	Bomb	5 - 10
Nydal and Lösveh (1970)	Bomb	4 ± 1
Walton et al., (1970)	Bomb	9.3

Studies of the short-term variations have therefore made it evident that the exchange coefficients derived from the response of the different reservoirs to the bomb ^{14}C and fossil CO_2 inputs. Oeschger et al. (1975) have proposed a new model which describes the real situation more completely. The model consists of 4 reservoirs:

1. a well mixed atmosphere,
 2. biosphere,
 3. a well mixed surface ocean
- and 4. a diffusive deep ocean.

The dynamic parameters k_{am} , the atmosphere-mixed layer rate constant and K , the coefficient of vertical eddy diffusion are calculated based on pre-industrial (and pre-bomb) ^{14}C values. $k_{\text{am}} = 1/7.3$ years is in good agreement with the determination of Craig (1957) also based on the natural system (Table 1-1). This model can be used to produce a consistent description of phenomena with completely different characteristic time constants since in the box diffusion model the flux from mixed layers to deep sea increases for decreasing time constants of the perturbations.

The disturbances of the natural carbon cycle represented by the "Suess" effect and the "bomb" effect have permitted a more detailed study of the distribution of carbon in nature. The vast majority of thermonuclear weapon tests were carried out in the northern hemisphere stratosphere. Complex box model calculations, such as the 12 compartment model used by Nydal (1968), based on measurements of the dispersal of the resultant ^{14}C excess have facilitated evaluation of parameters such as stratosphere-troposphere exchange rates and northern hemisphere stratosphere to southern hemisphere

stratosphere exchange rates, which were not readily obtained from box models describing the undisturbed system. ^{14}C measurements and model calculations have, in addition, increased the understanding of the exchange processes themselves. The transfer of $^{14}\text{CO}_2$ between the stratosphere and the troposphere is thought to be primarily due to the displacement and distortion of the tropopause and from horizontal diffusion through the tropopause gap. The exchange of $^{14}\text{CO}_2$ is largely confined to periods of maximum tropopause instability viz. February - April in the northern hemisphere when the tropopause altitude increases. The injection of ^{14}C from the stratosphere to the troposphere has, however, been shown to be latitudinally and meridionally variable (Young and Fairhall, 1968). This particular factor has relevance to the global applicability of the bristlecone pine calibration (Section 1.5), since latitudinal variation in ^{14}C input during the past millenia may have given rise to localised short-term variations in atmospheric ^{14}C levels.

1.5 Calibration of the radiocarbon timescale

Radiocarbon measurements on precisely dated tree-ring samples, principally of bristlecone pine wood have provided a set of data by which radiocarbon dates may be corrected for past ^{14}C fluctuations to yield true or absolute dates. Since the introduction of this calibration (Suess, 1970a), the form of the calibration curve or tables has been a major topic of discussion.

The original calibration curve, and the most widely used one, introduced in 1970, is a hand drawn curve through some 300 data points. The curve contains a large number of "kinks" or "wiggles" which were intuitively drawn by the author, the undulations being governed by the premise that the atmospheric radiocarbon concentration does not change by more than one or two percent/century. McKerrell (1971) has produced a tabulated version of Suess' data by direct extrapolation from the graph. This curve, however, has one major drawback with respect to calibration, a given radiocarbon date may correspond to more than one "true" calendar age. This problem has been investigated by Clark and Renfrew (1974). The archaeological requirement is that some continuous function or calibration curve be constructed from the data to permit conversion of radiocarbon to calendar dates. If the radiocarbon age y and corresponding calendar age x were plotted on a graph for a large number of samples, the points (x,y) would lie exactly on a straight line $y=x$, if all the measurements were without error and if all the assumptions of the method were correct. If, however, the assumption of the secular constancy of atmospheric radiocarbon is incorrect, these ideal errorless measurements would lie on some smooth curve, expressible mathematically as

$$y = F(x)$$

The function F is the calibration function, its departure from linearity being directly related to the past secular variations in natural radiocarbon concentration. The physical assumptions imply that there is only one radiocarbon

age, y , corresponding to any given calendar age x , although several x 's may give the same value of y .

On the other hand, given a sample whose radio-carbon age has been determined as $y \pm s$, the archaeologist wishes to estimate a corresponding calendar age x implying an "inverse calibration function" allowing the determination of x and y of the form

$$x = G(y)$$

If, however, there were several possible x 's corresponding to the same y , G would not be a function in the usual mathematical sense (since a function can only have one value at any particular point).

At the present time the form of the calibration curve F is unknown and several authors have made an arbitrary choice for the approximating function f since the hand drawn curve was published in 1970. Wendland and Donley (1971) have produced from 500 pairs of observations a single third degree polynomial defining the calibration relationship for the last 7,000 years.

$$\text{Calendar age} = 112 + 0.690C + 0.152 \times 10^{-3}C^2 - 0.138 \times 10^{-7}C^3$$

This curve, however, is obtained by estimating the inverse calibration function, so that the results of this study are of limited value. Various other forms of calibration curve have been used. Houtermans (1971) used a combination of periodic functions to obtain a relationship between $\Delta^{14}C$ and calendar age. Clark and Renfrew (1973) fitted a piecewise linear curve over a restricted time range, that is, a series of straight line segments constrained to be continuous at their join points. An extension of this technique comprising segments of different polynomial functions

constrained to be continuous at their joint points has subsequently been proposed by Clark and Sowray (1974). Damon et al. (1972) have produced a table for the correction of radiocarbon dates using polynomial fitting and simple moving averages. These results are based on 600 radiocarbon dates but are statistically inadequate since the rejection of outlying data points was determined by Chauvenet's Criterion, which is known to be unsatisfactory (Anscombe, 1960). Michael and Ralph (1972), Ralph et al. (1973) and Switsur (1973) have used similar moving average methods to obtain a smooth trend curve, although the former authors' curve maintains some of the larger "wiggles" of the Suess curve. Watkins (1975) has tabulated several of the calibration methods applied to the bristlecone pine data. The procedures include the analyses referenced previously plus a "50-year averaging" calibration and a limited time-span-calibration against the Egyptian historical chronology (Edwards, 1970; Berger, 1970).

The main objection to these calibration curves and tables is that they have been derived by subjective methods. Another version of the calibration curve was produced by Clark (1975). This calibration was aimed at correcting the deficiencies in the existing curves, using all the available data relating ^{14}C and true ages and reducing to a minimum the number of arbitrary decisions in deriving the curve.

Clark's calibration is presented in graphical and tabular form. Close detail is paid to the use of the calibration curve and the evaluation of errors associated with the calibration procedure is illustrated by examples.

At present this represents the best calibration curve available to archaeologists although its appeal to the geo-scientist is limited as a result of its omission of short-term fluctuations apparently not justified by the accuracy of the data. One important outcome is, however, the assessment of the error associated with calibration. A one sigma error of ± 200 years on a calibrated radiocarbon date, resulting from the use of Clark's curve, may well be a realistic uncertainty of a calibration against the true calibration function F which may contain short-term fluctuations not appearing in a statistically derived curve.

The global applicability of the bristlecone pine calibration has been a further major source of discussion since its introduction in 1970, the main criticisms being concerned with the dating material itself and its growth environment. Bristlecone pine wood grows at extreme altitudes, namely 3,000m, at which the ambient cosmic-ray-neutron flux is approximately one order of magnitude higher than at sea level. Since these neutrons are the source of ^{14}C , it is feasible that bristlecone pine wood could be unrepresentative of normal organic material. Whether through in situ ^{14}C production or variable atmospheric mixing, bristlecone pine ^{14}C levels could experience localised effects. Neutron irradiation of bristlecone pine wood in a nuclear reactor was found not to result in ^{14}C enrichment (Harkness and Burleigh, 1974). It was suggested, however, that the absence of a measurable amount of ^{14}C produced in situ by neutron irradiation may well point to the importance of the chemical pretreatment

prior to ^{14}C assay. Even if the bulk of the original nitrogen is present in the stable structure of the wood, i.e. chemically bound to cellulose or lignin molecules, the energy release in the transmutation of ^{14}N to ^{14}C (0.622 MeV; Ashby and Catron, 1959) would be sufficient to rupture the chemical bonding in these molecules. Hence, any ^{14}C produced via the natural in situ mechanism is liable to have existed in a form readily removable by standard pretreatment procedures. Similar work by Grootes (1977) has suggested that the effects of in situ production would be significant only in samples of age $>80,000$ years. Libby and Lukens (1973) have suggested the possibility that thunderstorms may produce ^{14}C in bristlecone pines, the proposed mechanism involving production of neutrons either as a result of lightning strikes on rocks or on the tree itself.

Evidence of latitudinal variations in atmospheric ^{14}C concentrations was presented by Lerman et al. (1970) and Jansen (1970), the size of these variations being of the order of 0.5% to 2%, southern hemisphere levels being lower than contemporary northern hemisphere concentrations. Comparison of two "floating" tree-ring chronologies from Auvernier, Switzerland by Suess and Strahm (1970) with the bristlecone pine calibration (Suess, 1970a version) led to the conclusion that the radiocarbon age of Auvernier wood would have to be 50 years older on average than bristlecone pine wood of the same age in order to give a good match of the Auvernier sequences against the kinks in the master calibration curve, implying that the carbon-14 content of

Auvernier wood must be lower than that of bristlecone pine wood of the same age. A similar statistical analysis estimated the difference as 92 years (Clark and Sowray, 1974).

The world wide validity of the bristlecone pine - radiocarbon chronology is now being tested as a result of the establishment of independent dendrochronologies. At present the two major European chronologies are the Irish Bog Oak chronology (Smith et al., 1972) and the oak tree-ring chronology for central Europe, the latter now extending to 350 B.C. As yet, however, radiocarbon analyses on precisely dated European tree-ring samples are not an advanced stage.

1.6 The submerged forests of the U.K.

Around the coast of the United Kingdom are many sites where "submerged forests" are exposed at low tide. These submerged forests are the result of drowning, by the post-glacial sea-level rise, of coastal woodland. The trees grow at about mean high water mark, usually behind a coastal barrier of some kind, and were usually killed by the rising water table or by the ingress of salt water, rather than by catastrophic overwhelming on a large scale.

It was thought at one time, that the submerged forests were all formed during the same period - the "Submerged Forest Period" - however, it has since been shown by pollen analysis and radiocarbon dating that they were formed throughout most of the post-glacial period. The earliest were probably formed as soon as trees reappeared with climate

amelioration. There are not many previous dates from submerged forest sites, although there is a large volume of data on ^{14}C measurements of peats associated with the forests and from coastal boreholes. Some dates from actual submerged forest exposures are presented in Fig. 1-5 (Q 134 - Godwin and Willis, 1959; BM 29 - Barker and Mackay, 1959; BM 80 - Barker and Mackay, 1961; Q 81, Q 380, Q 398 - Godwin and Willis, 1961; Q 637 - Godwin and Willis, 1962; Q 715 - Godwin et al., 1965; NPL 113, NPL 147, NPL 148 - Callow and Hassal, 1968; I 1543 - Buckley et al., 1968; IGS-C14/32 (St 3279) - Welin et al., 1972; IGS-C14/42 (St 3402) - Welin et al., 1972; HAR 78 - Otlet and Slade, 1974; UB 744 - Smith et al., 1974). Based on these radiocarbon data the extent of eustatic sea-level rise has been charted over the last 8,500 (radiocarbon) years; the profile of sea-level rise is given in Fig. 1-6 (Shepard, 1963; Jelgersma, 1966; Mörner, 1969; Kidson and Heyworth, 1973). As can be seen from Fig. 1-6, the different workers have chosen to represent the sea-level rise by a smooth curve, whilst others hold that oscillations do occur (also Fairbridge, 1961). The supporters of the oscillating rise claim that transgressions and regressions can be recognised in widely separated localities and can be correlated with changes in eustatic sea-level and various climatic records. Supporters of the smooth exponential curve agree that the rapid rise and fall of sea-level suggested is, because of the inertia of the glacio-eustatic system, inherently improbable and that other explanations are more likely.

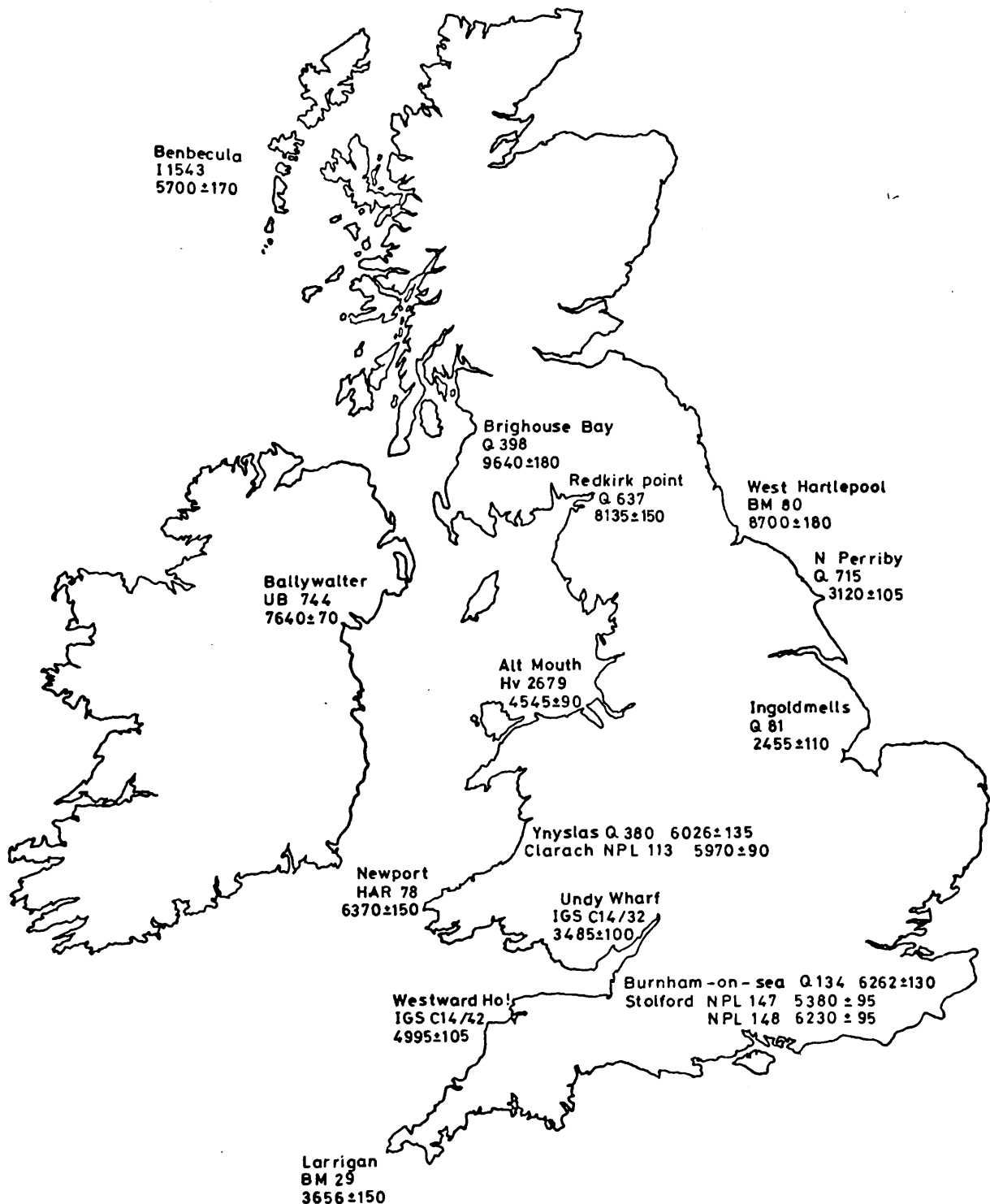


FIGURE 1-5: Radiocarbon dates for U.K. submerged forest exposures

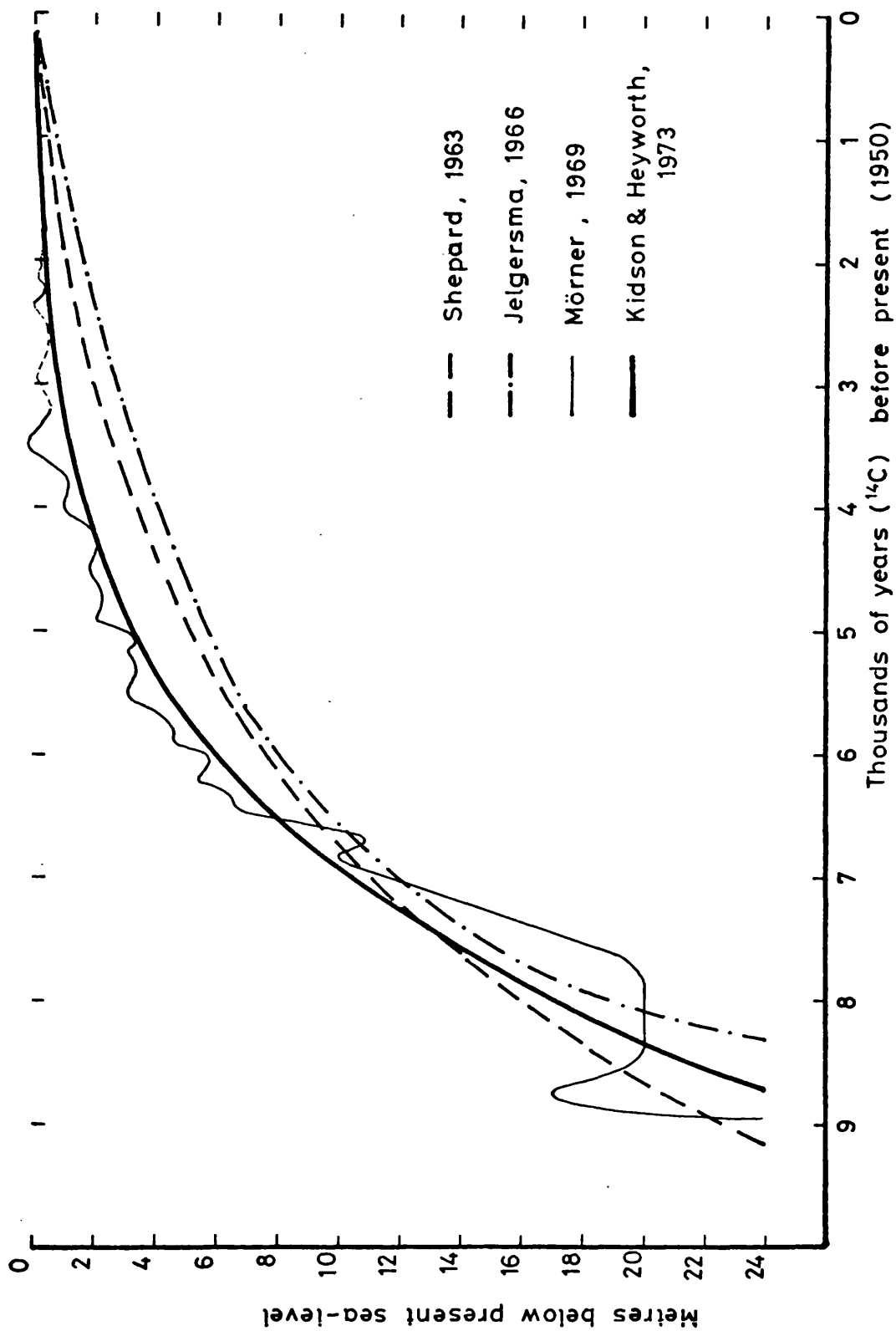


FIGURE 1-6: Sea-level curves

Submerged forests occur at all heights in the vertical range indicated (Fig. 1-6), the practical limit for dendrochronological studies being set by the lowest tides. In the Bristol Channel for instance, Low Water Spring Tide is at about -6m O.D. (zero datum). In most places this is considerably higher, about -2.5m O.D. Since the forests grow at about mean high water mark, the earliest accessible trees are, therefore, those which grew when mean high water mark was from -6m O.D. to -2.5m O.D., depending on tidal range. This would put the age limit at about 7,000 years B.P. (radiocarbon years) in the Bristol Channel, and later, c. 6,000 B.P. elsewhere.

In this respect, however, there is another important aspect. As well as the eustatic world-wide rise in sea-level, there has, during the post-glacial, been an isostatic uplift of the land, as a recovery from the depression due to ice-loading. The extent of this recovery varies, depending on the thickness of the original ice-cover. In places where ice was not present, or present only sporadically, no isostatic uplift may be manifested. The degree of isostatic uplift must be subtracted from the eustatic sea-level rise to give the relative sea-level rise in any one area. To further complicate the situation, there may be other longer-term tectonic vertical movements of the land.

In Britain, the net result of the isostatic uplift and long-term subsidence of the land is that areas north and west of a line from the Bristol Channel to the Humber have risen during the post-glacial, while areas south and east

of this line have sunk. The further north the site, the greater the degree of uplift. Thus in the Solway Firth, uplift during the past 8,000 years has been approximately equal to eustatic sea-level rise, so that the submerged forests formed at about mean high water mark 8,000 years ago are at mean high water mark now, even though there has been a rise in sea-level of 25m or more during this period.

The most common age of submerged forests is between 4,000 and 5,500 years B.P., since this was a period of a moderate rate of sea-level rise, which allowed the growth of extensive coastal forests which were progressively inundated. Before this period, sea-level rise was more rapid, so that there is only a narrow belt of submerged forest trees of any particular age, whilst after this period, sea-level rise has been so slow that there has not been a very marked marine transgression. These submerged-forest beds consist of stumps, still in the position of growth, and fallen trunks, often with associated peats. The trees may be very large and are usually extremely well preserved (Plates 1, 2 and 3). Most of the trees are oak, though at some sites pine is dominant; birch, yew and alder are also found. In general, growth was more rapid than at present, and oaks, apparently, were able to grow where they would not survive now, that is, nearer to the sea. This was presumably because they were more vigorous and thus could withstand greater exposure to salt spray. At present, oak trees can tolerate a surprising degree of fresh-waterlogging

Plate 1 (facing page): Submerged forest exposure at Ynyslas,
Cardigan Bay, Wales





Plate 2: Cutting a section from a
fallen trunk



Plate 3: Removal of section

but do not favour saline environments.

As a source of wood for dendrochronological-radiocarbon studies, the submerged forests are unique. Preliminary radiocarbon measurements, Fig. 1-5, have shown that there is a wide age range of wood available and, as the rates of isostasy and eustasy are fairly well understood, it is possible, by reference to established sea-level curves, to collect samples for analysis systematically, thus accelerating compilation of a tree-ring chronology. At any one site, particularly if the site dates from the optimum growth period, there are large numbers of trees allowing a master chronology to be constructed, this record then being overlapped with chronologies at adjacent locations. The trees are ideal for dendrochronological studies; individual growth rings are wide and the growth pattern is extremely sensitive and therefore well characterised. Calibration with other tree-ring chronologies, such as the Irish Bog Oak chronology (Smith et al., 1972) may assist in the establishment of an absolute chronology either through reinforcement and extension of developed "floating" chronologies, or by completing gaps in the individual records which could not be completed with locally collected samples.

The submerged forests, furthermore, provide excellent material for radiocarbon calibration studies. The trees of different ages all grew at the same altitude, that is,

contemporary sea level, and therefore should not experience such local effects as higher ambient ^{14}C concentration and in situ production, which may limit the previously derived bristlecone pine calibration. Plentiful supplies of wood permit collection of large samples and a higher sampling frequency than in any other study of this kind, that is 10 samples per century, with the additional benefit of duplication of samples and collaborative analyses maintaining the high level of objectivity necessary for such a project.

The dendrochronology of the submerged forests is being performed by A. Heyworth at University College Wales at Aberystwyth. Establishment of a long tree-ring record for the United Kingdom, based on the submerged-forest sites will not only be advantageous in radiocarbon calibration studies but will yield detailed information on isostatic and eustatic changes during the recent past.

1.7 Aims of research

Current theories concerning the past variations in natural radiocarbon concentration in the atmosphere are largely based on the ^{14}C measurements on precisely dated tree rings of bristlecone pine wood, and, to a lesser extent, on Varve series. The interpretation of observed variations in ^{14}C and the geophysical parameters producing them has been discussed in the preceding sections. Calibration of the radiocarbon timescale against an independently produced absolute chronology, as represented by the tree-ring record of bristlecone pine, has enabled

correction of radiocarbon ages for these secular fluctuations. The form of the relationship between the two independently derived chronologies and the errors associated with calibration procedures have provoked much discussion in the literature. In particular, the global applicability of the bristlecone pine calibration has been questioned, the extreme growth conditions of the tree and the possibility of local effects being proposed as reasons for the specific ^{14}C activity of that wood being atypical of world-wide ^{14}C concentrations. Recently, alternative sources of wood suitable for dendrochronological studies have been discovered and these present the opportunity to test the applicability of the bristlecone pine calibration through construction of a similar data record. Such a source of wood is found in the numerous submerged-forest sites on the United Kingdom shoreline. The origin and advantages of this source of material are outlined in Section 1.6.

This research project is a preliminary investigation in a long-term programme to produce an independent tree-ring/radiocarbon chronology for the United Kingdom. Samples for the investigation are collected from these submerged forest sites and from archaeological sites. The work is one of the first applications of the liquid scintillation counting method, based on synthesis of high purity benzene, to the particular field of radiocarbon calibration and is characterised by the very high sampling frequency, ten samples per century, and the emphasis on error assessment through intra and interlaboratory calibration.

While long-term trends in natural radiocarbon concentrations are reasonably well documented, short-term fluctuations, commonly known as "wiggles" or "kinks" favoured particularly in Suess' original interpretation of the bristlecone pine radiocarbon data, are still in dispute. It is hoped that, as a result of the higher sampling frequency employed in this study, the existence of such short-term fluctuations will or will not be apparent and that, if so, other variations not exhibited in the American data, through the relative sparseness of samples, will be observed.

The tree-ring sequences analysed here will be "floating" chronologies, and application of statistical techniques should permit direct comparison of U.K. data with the bristlecone pine calibration.

C H A P T E R 2

EXPERIMENTAL METHODS2.1 Introduction

The measurement of natural radiocarbon requires sophisticated physical and chemical techniques. There are two reasons for this; firstly, ^{14}C is a weak beta emitter, of maximum energy 0.156 MeV, and secondly, it is present in very low natural concentrations. The specific activity of 13.56 ± 0.07 d.p.m. gC^{-1} (Karlen et al., 1964) corresponds to approximately 1 atom ^{14}C per 10^{12} atoms C. It is therefore imperative that the monitoring system has a high detection efficiency for ^{14}C and that sample count rates are high compared to background values. Further, since a radiocarbon age determination involves precise comparison of sample and standard activities, and since long counting times of the order of 1-2 days are employed to reduce the statistical uncertainty of the measurements, the detection system must have long-term stability with respect to detection efficiency and background count rate. A ^{14}C counting system, therefore, must display the following features:

1. high beta detection efficiency,
 2. low background count rate
- and
3. long-term stability of beta detection and background characteristics,

Early ^{14}C counting systems (Libby, 1955) involved coating the inner wall of a screen-wall Geiger counter with elemental carbon prepared from the sample. The overall detection efficiency was only 5% and the "carbon black" was often

contaminated by "fall-out" isotopes. The method was soon rendered obsolete by the development of gas proportional and, more recently, of liquid scintillation techniques.

The proportional, rather than the Geiger, region is favoured for the common counting gases (CO_2 , CH_4 , C_2H_2) since only in the former is the amplitude of each output pulse a measure of the energy absorbed by the counting gas. Thus, with a proportional counter, it is possible to monitor only the energy range of interest by discrimination against lower and higher energy pulses.

A survey of counting techniques employed by radiocarbon laboratories shows that approximately 50% of the laboratories utilising the gas proportional technique have CO_2 as the counting gas. The use of acetylene and methane is favoured by the remainder in almost equal numbers. The advantage of CO_2 as a counting gas lies in the fact that the sample preparation requires only one reaction step, namely sample combustion. The counting characteristics of CO_2 , however, are very sensitive to the effect of electronegative impurities and thus rigorous purification procedures are required. On the other hand acetylene and methane are not so sensitive to impurities and the improvement of chemical procedures in methane and acetylene chemistry (Fairhall et al., 1961; Barker, 1953; Suess, 1954) have increased the appeal of these gases for proportional counting.

Considerable variation in design is possible for proportional counters, however the essential features are

as follows. The sample detector is made either from quartz or oxygen free high conductivity (O.F.H.C.) copper. The wall of the detector is the cathode and the anode is a taut wire sited along the axis of the detector. The background is caused by cosmic-ray particles and the count rate registered is far greater than the normal sample activity. Reduction of the background count rate is achieved by shielding the sample detector with lead and paraffin wax containing boric acid, the latter absorbing neutrons. The major reduction in the background is, however, not achieved by shielding alone. A guard counter, or series of guard counters, is mounted concentrically on the sample detector and is linked to the latter by anti-coincidence circuitry. This arrangement will register only events detected in the sample detector and events detected simultaneously in sample and guard counters are rejected. Generally the detection efficiency for an anti-coincidence counter is >90% making the proportional counter particularly suitable for small samples.

The liquid scintillation technique also enables energy discrimination and was first applied to radiocarbon age determinations by Arnold in 1954 via conversion of sample carbon to a mixture of hexane and octane. In the succeeding years several authors reported ^{14}C age determinations using as counting material ethanol (Arnold, 1954), dissolved acetylene (Audric and Long, 1954), methanol and partially synthesised toluene (Pringle et al., 1955), methyl borate

(Pringle et al., 1957), paraldehyde (Léger and Pichat, 1957) and dissolved carbon dioxide (Barendsen, 1957). Starting in 1959, attention turned to synthesised benzene as the scintillation solvent (Tamers, 1960; Starik et al., 1961) and steady progress has since been made on this system. The advantages of benzene are that it contains 92% carbon, has excellent liquid scintillation properties, is stable and can be produced entirely from sample carbon. Many new laboratories therefore utilise liquid scintillation counting techniques because of

1. the general improvement made in component performance (e.g. increase in figure of merit, E^2/B)
- and 2. the convenience of automatic sample counting with its time-saving advantage.

While in general the gas counting technique is more suited to analysis of small samples, say $<2\text{gC}$, for this research it was considered that liquid scintillation counting would be the appropriate system with respect to the larger sample sizes envisaged. Further details of the counting method and its principles are presented in subsequent sections.

2.2 Chemical Preparation of Benzene

2.2.1 Sample Pretreatment

It is of the utmost importance in performing a radiocarbon analysis that the sample contains only those carbon atoms which constituted the material at the time of its isolation from the carbon cycle. The nature of contamination to which a sample may be subjected depends on the chemical nature of the sample itself and on its immediate environment. Inorganic samples such as bone and shell may be contaminated by percolating

ground water containing carbonates and bicarbonates which can be incorporated via ion exchange. In general, organic materials do not undergo this form of "chemical" contamination. Typical contaminants in organic samples such as rootlets, humic acids, soil and sand are introduced by water filtration but do not enter into ion exchange processes or chemical bonding with the sample. The effect of contamination on old samples by dead and modern carbon is given in Table 2-1.

The method of pretreatment utilised depends largely on the nature of the sample. In this research, by far the majority of the samples were of wood and the rigorous pretreatment method applied to these samples will be discussed later. The remaining few samples were of charcoal, carbonised grain and soil.

Charcoal and grain samples are first of all examined visually for rootlets and other possible sources of non-contemporaneous carbon which might lead to an erroneous assay. This being done, the samples are washed with distilled water and then treated with 1M potassium hydroxide solution for 3 hours to remove humic acids. After rinsing with distilled water, the dehumified material is treated with hot dilute hydrochloric acid (~1M) for a further 3 hours. Pretreatment is completed by thoroughly washing the sample with distilled water and placing the sample in a drying oven at 80°C overnight. Soil samples are handled more gently since the chemical composition is considerably less inert than that of charcoal and grain. After the initial visual examination the samples are washed with distilled water, warm dilute hydrochloric acid and rinsed again with distilled water before drying overnight in an oven at 80°C.

TABLE 2-1: ERRORS CAUSED BY SAMPLE CONTAMINATION

(a) Contamination of old samples by "dead" carbon

True age of sample (years)	Radiocarbon age of sample (years)		
	Degree of contamination by "dead" carbon		
	1%	0.1%	0.01%
5570	5648	5576	5571
11140	11380	11160	11144
22280	23578	22394	22296

(b) Contamination of old samples by "modern" carbon

True age of sample (years)	Radiocarbon age of sample (years)		
	Degree of contamination by "modern" carbon		
	1%	0.1%	0.01%
5570	5490	5560	5570
11140	10900	11120	11140
22280	21080	22160	22270

The tree-ring samples analysed in this research are separated from the bulk wood section by hand chisel. This is considered more reproducible than using a mechanical saw, since the wood often contains irregularities which can easily be picked out when the operation is performed manually. The accuracy of separating successive 10 year growth increments depends to a large extent on the ring width in each individual section. Marker pins, inserted at the time of dendro-chronological measurement, usually at a frequency of 1 pin per 20 rings, maintain an accuracy of ± 1 ring per section. The separated 10 year increments are then cut to match stick size in preparation for cellulose extraction.

There is a wide range of opinion as to the optimum pretreatment procedure for wood samples submitted for ^{14}C analysis. Some laboratories employ both organic and inorganic solvents while others consider that either an organic or inorganic solvent is sufficient. In assessing the validity of tree rings as indicators of atmospheric ^{14}C concentrations (Fairhall and Young, 1970) have demonstrated that there are significant differences in the ^{14}C level in the different components of wood, namely cellulose, lignin and resin. Thus, depending on the pretreatment procedure adopted, the ^{14}C value obtained may or may not be a reflection of the atmospheric ^{14}C concentration at the particular time of growth. Of course, the effect of transport of resin across ring boundaries will depend on the species of tree and an effect would be more marked in a more resinous wood. It was, therefore, decided that ^{14}C assay on wood samples should be performed on the cellulose fraction only since the cellulose in each ring is not in dynamic equilibrium with the metabolism

of the tree but that, once synthesised, it remains fixed, thus fulfilling the "closed system" assumption of the radio-carbon dating method.

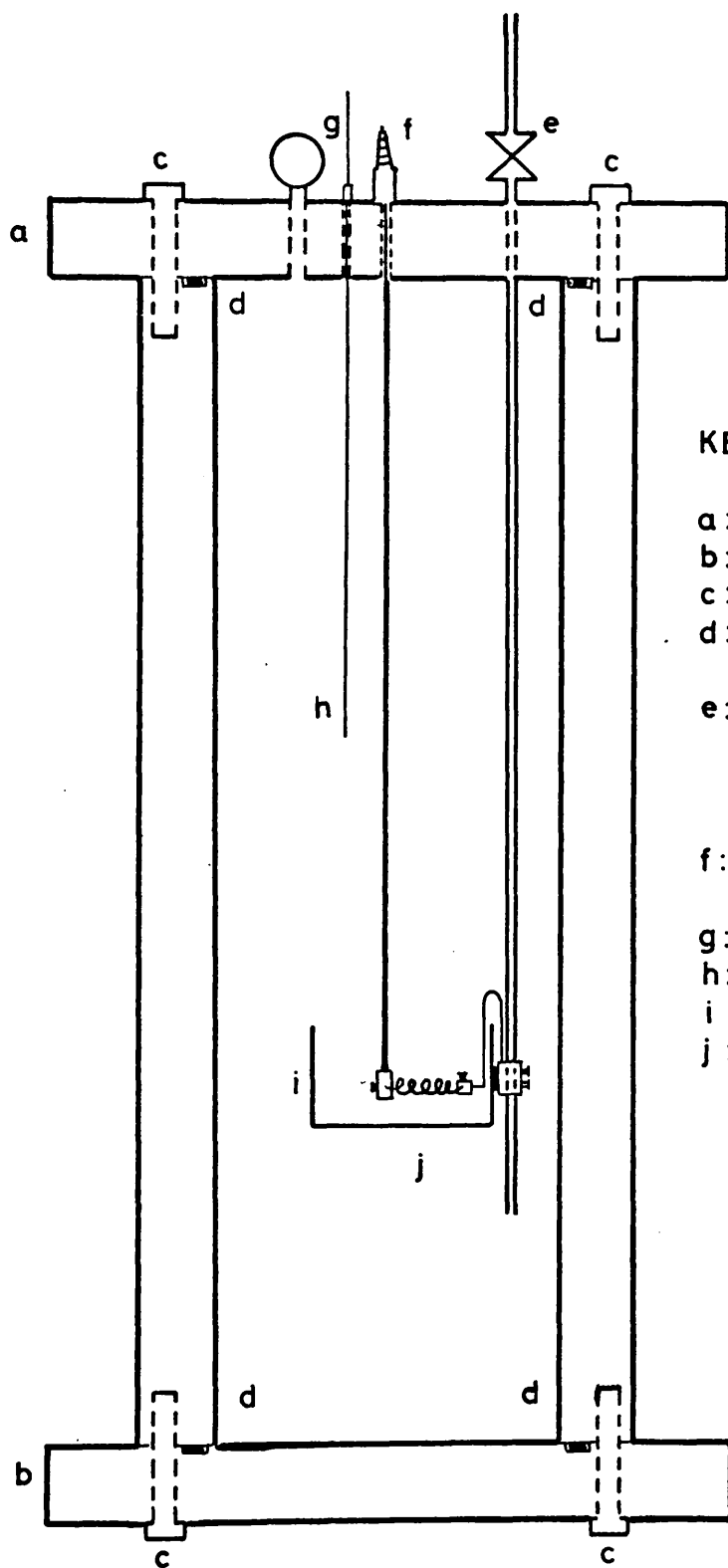
A further problem concerning the pretreatment of wood recovered from the marine environment is infestation of the samples by boring organisms. While it is, in general, possible to discard sample material which has been infested, when this is not possible the remaining carbonate of the organism plus any evaporite carbonate is removed mechanically. Subsequent pretreatment stages in acid media will then remove final traces of non-contemporaneous "carbonate" carbon.

The first step in the cellulose extraction is treatment of the wood with boiling 2M potassium hydroxide to remove any humic acids and to solubilise the lignin. The sample is then filtered and washed with distilled water. Prior to bleaching, the dehumified wood is soaked in 2M hydrochloric acid, thus neutralising any residual alkali not removed in the previous washing. The wood is now added to a bleaching solution comprising 80g NaClO_2 and 110ml of 1M HCl in 3 litres of distilled water and the temperature of the bleaching medium is maintained at 70-80°C for 48 hours. Finally the solution is filtered and the white cellulose washed with distilled water and dried at 80°C. Typically a wood sample of 40-50g will yield 12-16g of wood cellulose.

2.2.2 Sample Combustion

Organic samples are burned in a pressure combustion vessel to yield carbon dioxide. Up to 25 litre atmospheres of CO_2 can be prepared in the Glasgow system.

The combustion vessel (Fig. 2-1) is constructed of stainless steel and has a volume of approximately 6.4l. The base flange of the "bomb" is secured by 12 high tensile bolts and the seal is completed by a neoprene 'O'-ring. The top flange, secured and sealed in the same way as the basal flange, houses the filling and emptying valve, fitted with a safety bursting disc (maximum pressure 1400 p.s.i.), a pressure gauge, the ignition contacts and a thermocouple. The sample crucible, also made of stainless steel, is mounted on the oxygen filling pipe. It is important that the lower end of the O₂ supply pipe is below the lip of the crucible to prevent dispersal of finely divided samples with the subsequent possibility of a dust explosion. A coil of wire (Kanthal AB resistance wire) is connected across the contacts in the base of the crucible and the firing mechanism connected via the contact points on the top flange. The firing circuit delivers a 3.5 Ampère D.C. current through the "spark" plug and the earth contact on the filling valve. Before loading the sample, the ignition wire is tested. This also ensures that any grease on the wire as a result of handling is burnt off. The sample is then placed in the crucible and, prior to sealing, an amount of distilled water, usually 25-30ml, is added to the bomb. The combustion of wood cellulose produces small quantities of oxides of sulphur and nitrogen and the addition of the water to the combustion bomb prevents escape of these gases to the CO₂ collection system. Before charging with oxygen the sealed bomb is evacuated through the collection system (Figs. 2-2A, 2-2B). At this stage, needle valves N1 and N2 are open, stopcocks S1 and S4 are open, S2, S3 and S5 are shut and the three way stopcock, 3W1, is directing flow through the low vacuum manifold. When the Bourdon gauge B1 registers ~10 torr



KEY:

- a: Top flange
- b: Basal flange
- c: High tensile bolts
- d: 'O'-ring track and neoprene 'O' ring
- e: O₂ inlet-CO₂ outlet valve with 1400p.s.i. bursting disc and earth electrode
- f: Spark plug on "live" electrode rod
- g: Pressure gauge
- h: Thermocouple
- i: Sample crucible
- j: Ignition filament wire

FIGURE 2-1: Sample combustion vessel

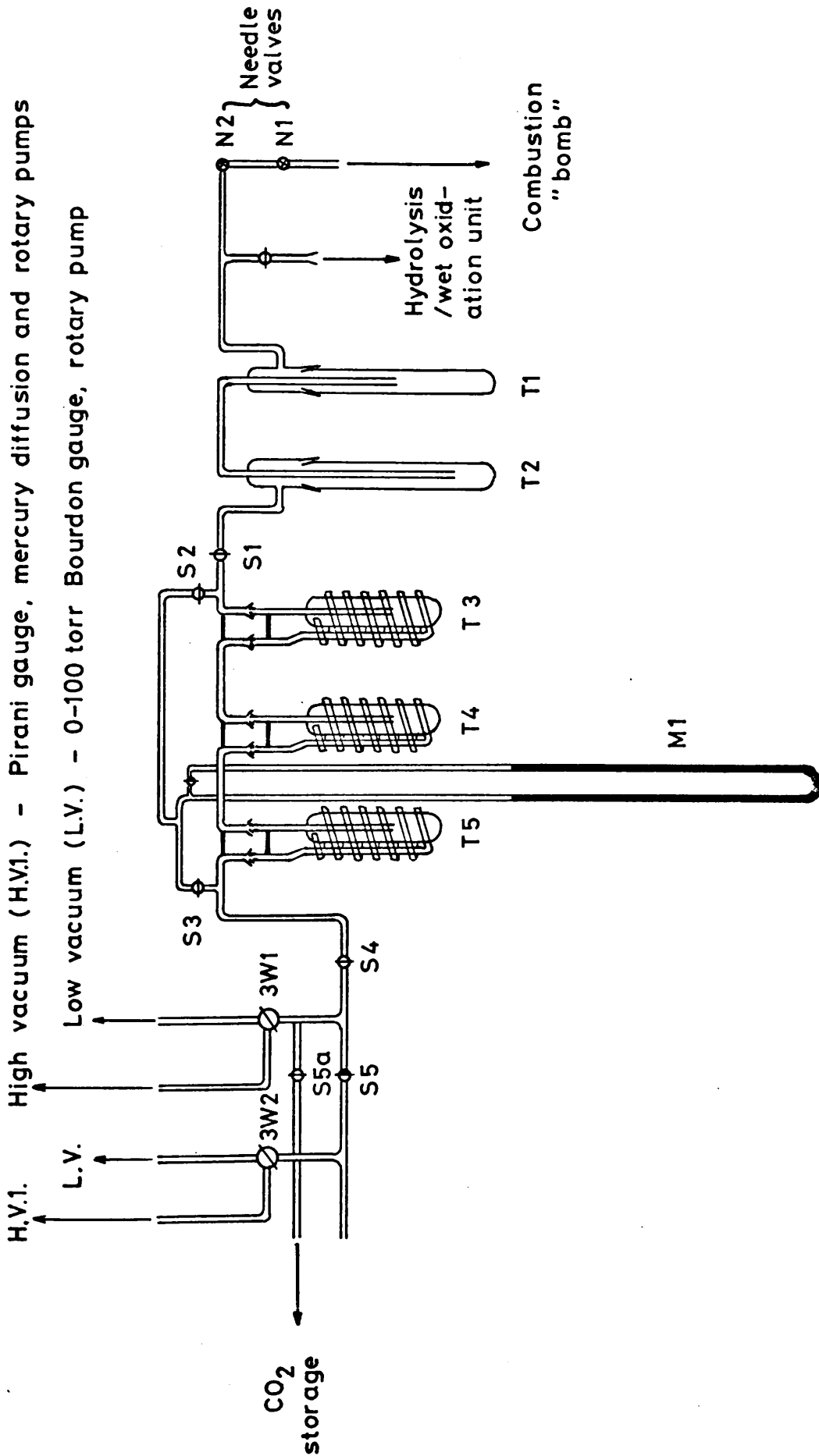


FIGURE 2-2A: CO₂ collection system

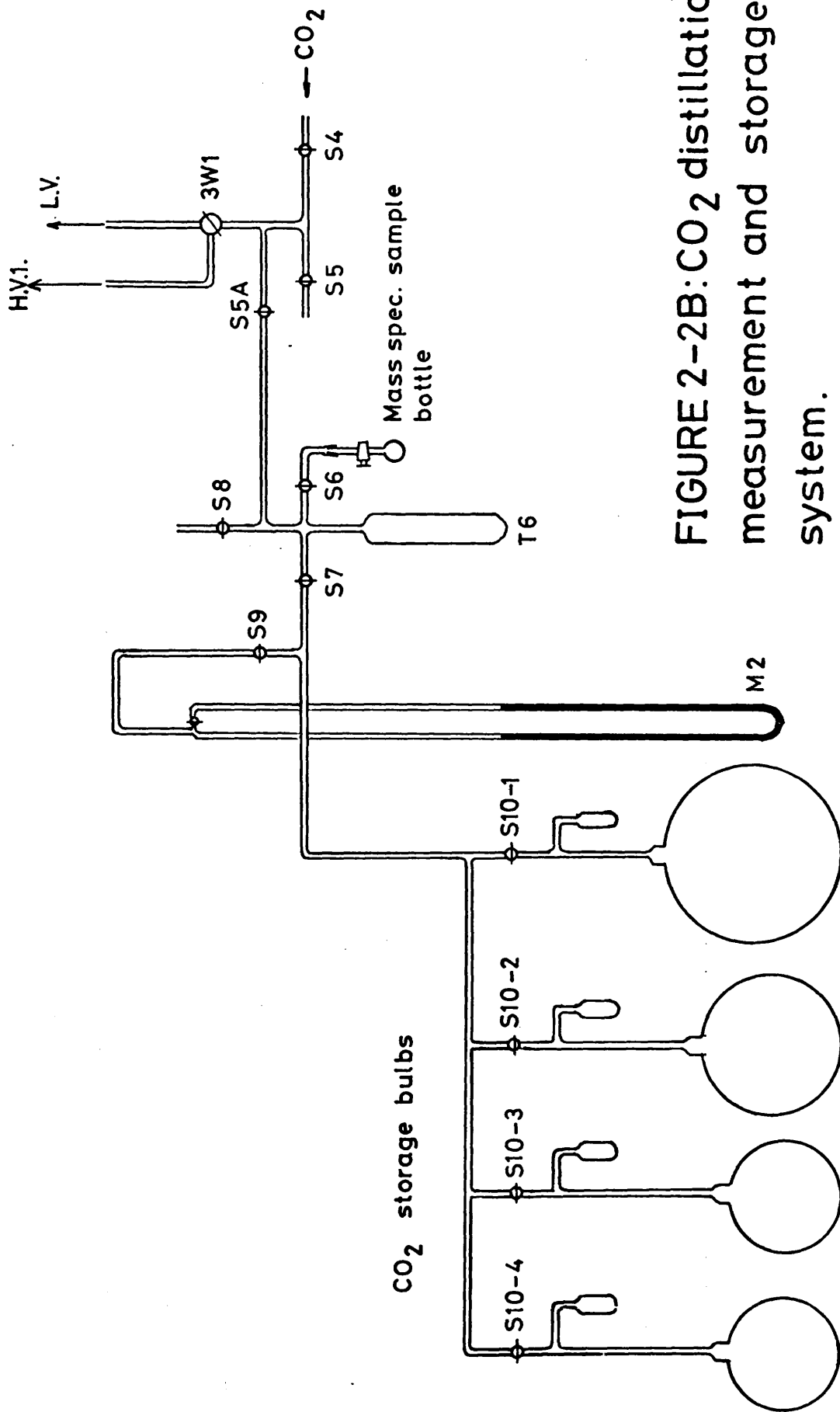


FIGURE 2-2B: CO₂ distillation, measurement and storage system.

the main valve on the bomb, valves N1 and N2 and stopcocks S1 and S4 are shut and the vacuum connection removed since this pressure is due mainly to water vapour. The bomb is then filled with O_2 to a pressure of 5 atmospheres, the tube connection from the cylinder having been flushed with gas before securing the umbilical and opening the bomb. When the bomb is pressurised, the main valve is shut, the umbilical disconnected, the electrical connections made and the sample ignited. A successful combustion is indicated by a sharp rise in pressure and temperature inside the bomb. The use of the internal thermocouple was discontinued since the lifetime of a thermocouple is very short, in the order of 10 combustions, due to the corrosive nature of the gases produced.

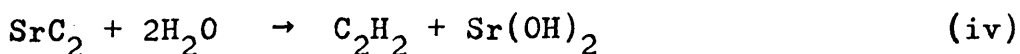
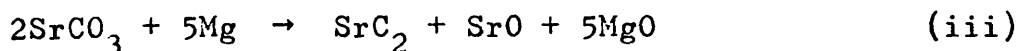
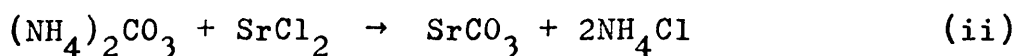
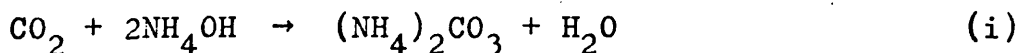
After allowing the heat generated to dissipate, the product CO_2 is collected. Traps T1 and T2 are cooled to $-78^\circ C$ with acetone/solid CO_2 slush baths to prevent water reaching the CO_2 collection traps T3, T4 and T5 which are cooled to $-196^\circ C$ by liquid nitrogen. The system is pumped out on low vacuum until the Bourdon gauge B1 gives zero reading and then, with N1 and N2 slightly open, S1, S2, and S4 open, 3W1 to low vacuum and S3 and S5 shut, the main valve on the bomb is carefully opened. The gas flow is throttled by varying the needle valve settings to maintain a pressure of 10-22 torr on the Bourdon gauge, B1, this pressure representing the excess oxygen being pumped away. The manometer M1 which is open during the collection of the CO_2 acts as a blockage detector for the CO_2 traps. In practice, using the described flow rate,

most of the CO_2 , that is, greater than 90%, is collected in trap T3. Emptying the combustion bomb takes about 45 minutes. When all the gas has been collected the main valve, N1, N2, S1 and S2 are shut and 3W1 is turned to high vacuum. The CO_2 is pumped to better than 10^{-3} torr. Purification of the CO_2 is effected by distillation and further pumping. The collection traps T3, T4 and T5 are isolated from the pumping system, 3W1 closed and stopcock S5a in the open position. The liquid nitrogen traps are removed from T3 and T4 while the trap cooling T5 is replaced by an acetone/solid CO_2 slush bath (-78°C), to ensure that any water vapour which may have passed through T1 and T2 during the collection procedure does not enter the storage area. The gas is sublimed into the cold finger T6 which is cooled to -196°C . When all the gas has been transferred, S4 is closed and the CO_2 is pumped on high vacuum via 3W1 to less than 10^{-3} torr. The CO_2 storage area consists of four bulbs of known volume, two bulbs approximately 6 ℓ in volume and two of approximately 12 ℓ and 25 ℓ respectively. This arrangement facilitates the long-term storage of a wide range of CO_2 quantities under conditions which reduce the problems of leakage or blow-out arising from gas pressures which are either too low or too high for a particular size of bulb. The yield of CO_2 which will be produced by combustion of a wood sample may be predicted using the following empirical calculation. Assuming a carbon content in cellulose of

~44%, then 1g of cellulose should produce 0.83 litre atmospheres of CO₂. Prior to collection of a CO₂ sample, the designated storage bulb, x, is pumped to better than 10⁻³ torr to eliminate possible CO₂ memory effects. The CO₂ is then transferred from T6 to the cold finger on the storage bulb with 3W1, S5a, S6 and S8 closed and S7, S9 and S10-x opened. Once this has been completed, S7 is closed and the gas allowed to expand into the bulb and manometer system, M2, when the yield of CO₂ produced is measured. An aliquot of CO₂ is then removed for subsequent mass spectrometric analysis.

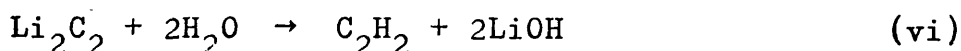
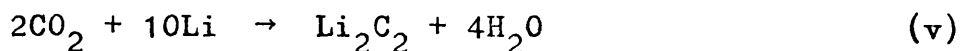
2.2.3 Acetylene Synthesis

Two methods of conversion of carbon dioxide to acetylene are currently being utilised by radiocarbon laboratories. Firstly, and less commonly, the CO₂ produced from sample combustion (or sample hydrolysis) is bubbled through ammonium hydroxide producing ammonium carbonate. Addition of strontium chloride precipitates strontium carbonate. The carbonate is then reduced with magnesium to give the carbide which is hydrolysed to produce acetylene. The complete reaction scheme is given below (Suess, 1954):



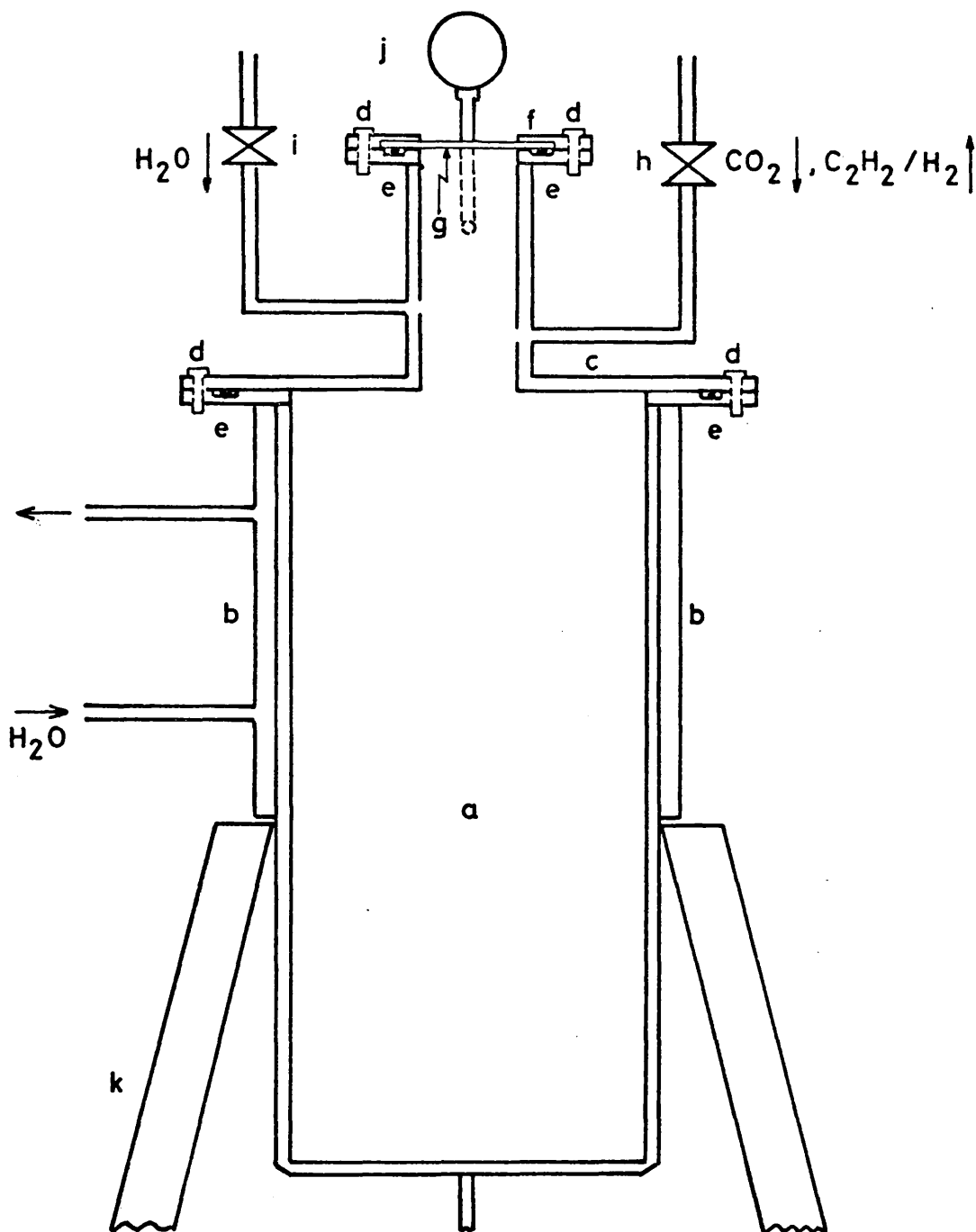
The second method, that used in this research, was developed by Barker (1953) and involves the direct reaction of carbon dioxide and molten lithium followed by hydrolysis

of the carbide. This method was developed from earlier work by Arrol and Glascock (1947) who used barium metal instead of lithium metal. The reaction scheme for Barker's process is as follows:



The carbide synthesis and hydrolysis are performed in a stainless steel vessel with an approximate volume of 6.7 l (Fig. 2-3). The top half of the main body of the reaction chamber is water cooled to prevent evaporation of molten lithium from the base of the vessel to the upper part of the walls thus rendering it unreactive toward CO_2 . The main flange, housing the gas inlet-outlet valve, the water inlet, a 0-760 torr Bourdon gauge and the view port flange, is secured to the main body of the vessel by six high tensile bolts and the seal completed by a Viton 'O'-ring. This flange is in position prior to addition of the lithium charge to minimise the time required to seal and evacuate the vessel, and thus to reduce the amount of oxidation of the lithium. A diagram of the acetylene system is given in Figs. 2-4A and 2-4B and the laboratory procedures are as follows.

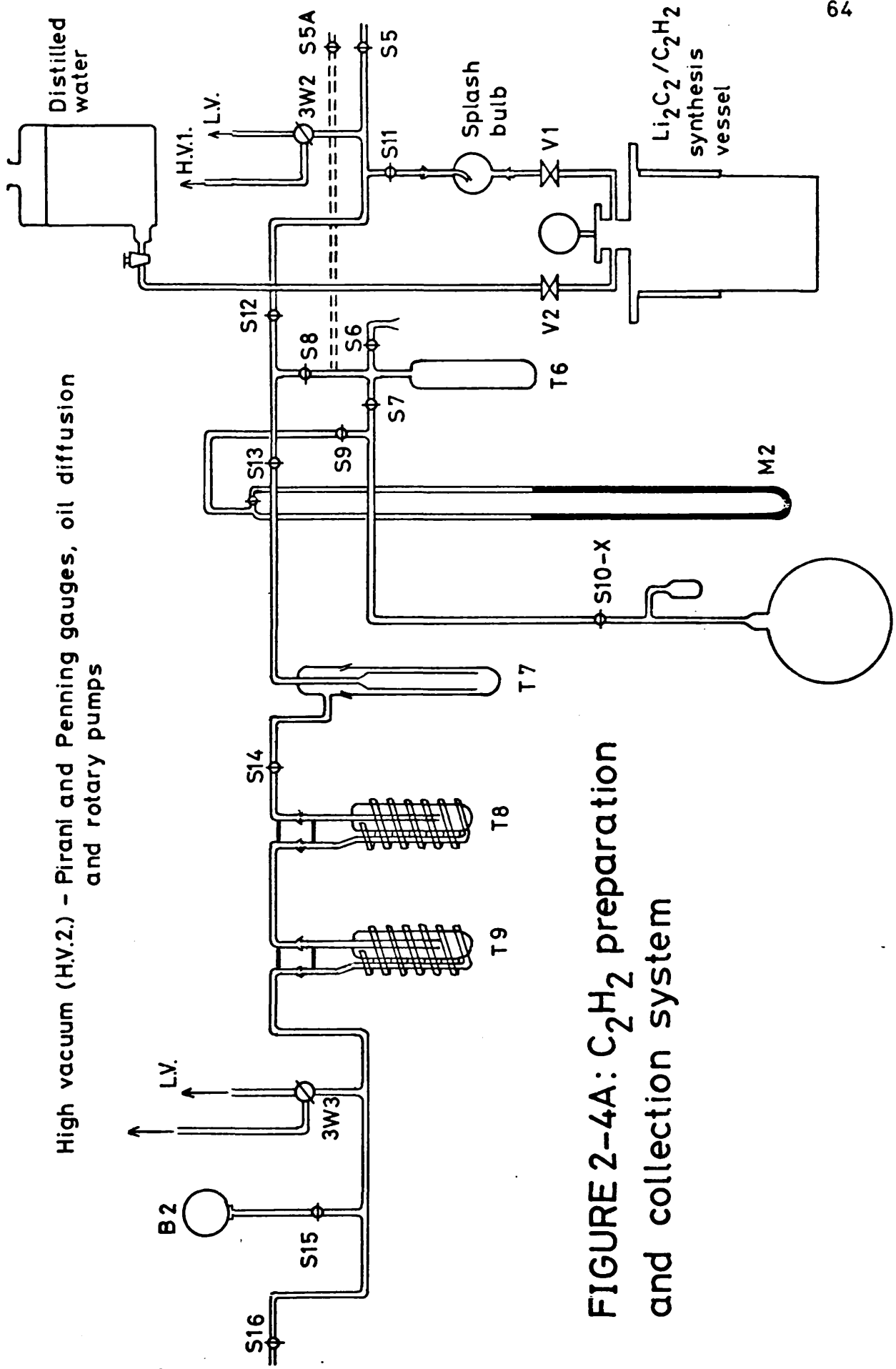
A quantity of lithium metal, (lithium metal ingots supplied by Associated Lead, Newcastle) 50% in excess of the stoichiometric quantity is scrubbed under petroleum ether to remove the oxide layer. The cleaned metal is then added to the reaction vessel through the view port



KEY: a-Main reaction chamber; b-Cooling jacket; c-Top flange;
 d-High tensile bolts; e-'O'-ring track & "viton" 'O'-ring
 f-Viewport flange; g-Quartz viewport; h-Gas inlet/outlet
 valve; i-Water inlet valve; j-0-760 torr Bourdon gauge;
 k-Tripod stand

FIGURE 2-3: Stainless steel reaction vessel
 for conversion of CO₂ to C₂H₂

hole and the chamber is sealed and evacuated (valve V1 open, V2 shut, stopcock S11 open, 3W2 in the low vacuum position, all other stopcocks closed). The three "Amal" burners are lit and the water for the cooling jacket is turned on. Pumping is continued for 15-20 minutes, by which time the pressure in the reaction vessel is approaching 10^{-2} torr, and then the chamber is isolated (3W2 to the off position, V1 shut) with continued heating. After 40-45 minutes the molten lithium is hot enough for admission of the CO_2 . With stopcocks S11, S12, S8, S7, S9 (to manometer M2) all in the open position, S10-x is opened, 'x' being the number of the appropriate storage vessel, and the sample gas expanded to valve V1. At this point S10-x is closed again to prevent contamination of the bulk of the sample in the event of problems in the reaction vessel. Valve V1 is opened. The silvery surface of the hot metal discolours to black as the CO_2 reacts and then, as heat of reaction is evolved, the temperature of the reaction mixture increases to reddish-orange heat (800°C). V1 is closed and S10-x quickly reopened and, using V1 as control, the rest of the CO_2 is admitted to the reaction chamber. The consumption of CO_2 is noted by the equalising of the mercury levels in manometer M2. Normally 10% of CO_2 will react in 15-20 minutes. At no time during the reaction is the pressure inside the reaction vessel allowed to exceed 300 torr, since above that temperature the reaction proceeds at too fast a rate resulting in a lower-



High vacuum (HV.2.) - Pirani and Penning gauges, oil diffusion and rotary pumps

FIGURE 2-4A: C_2H_2 preparation and collection system

H.V.2.

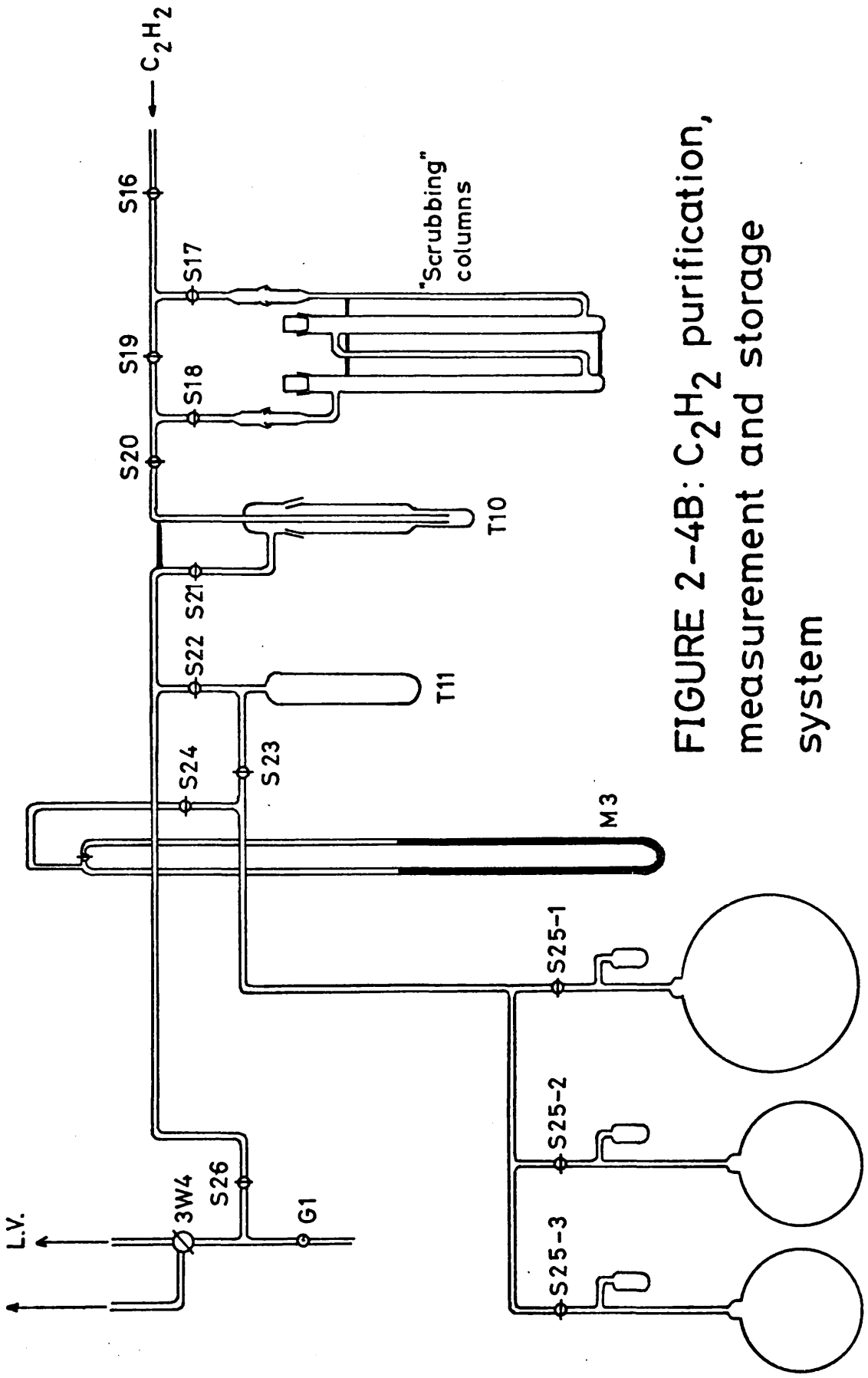


FIGURE 2-4B: C₂H₂ purification, measurement and storage system

ing of the final acetylene yield. When virtually all (>95%) of the carbon dioxide has been added to the lithium, valve V1 is closed and the remaining gas is condensed into the cold finger T6. The storage bulb is then closed off (S10-x to the shut position) and the CO₂ allowed to expand into the reduced volume and then into the reaction vessel. The CO₂ storage system is now closed off, S9, S7, S8 and S12 all being turned to the closed position. Heating is continued for 10 minutes after admission of the CO₂ and then the bomb is pumped for a further 30 minutes with heating, to remove any radon (V1 open, S11 open, 3W2 in the low vacuum position). The temperature of the vessel during this period is 750-800°C. The vessel is allowed to cool before hydrolysis of the carbide.

Freshly distilled water is slowly added to the cooled lithium carbide, and the pressure inside the reaction vessel rises with evolution of acetylene (reaction (vi)) and hydrogen, a product of the reaction of the excess lithium metal with water. The collection system is set up as follows. Trap T7 is cooled to -78°C by an acetone/solid CO₂ slush bath, traps T8 and T9 are cooled to -196°C with liquid nitrogen, stopcock 3W3 is in the low vacuum position and stopcocks S11, S12, S13, S14 and S15 are all in the open position. When the gas pressure inside the reaction vessel approaches 760 torr, valve V1 is carefully opened and the gases are admitted to the line, water vapour being condensed in T7, acetylene in T8 and T9 and the

hydrogen being pumped away. The maximum reading on the Bourdon gauge B2 is 20-25 torr, thus ensuring a flow rate such that virtually all the acetylene condenses in T8. Gas collection is continued until the pressure inside the reaction vessel has fallen to 200 torr, at which point V1 is shut and a further aliquot of water is added through V2. The process is repeated until no further gas is evolved, normally after addition of 3-4 litres of water. To collect the final traces of acetylene the pressure in the chamber is reduced to around 80 torr causing the reaction mixture to boil, and care is necessary to prevent quantities of water distilling into the main part of the collection system. When all the product gases have been collected the reaction vessel is closed off, stopcocks S11, S12, S13, S14 and S15 are turned to the off position and stopcock 3W3 is turned from low vacuum to high vacuum. The acetylene in traps T8 and T9 is pumped to better than 10^{-4} torr. The high vacuum pumping system on the acetylene and benzene sections of the vacuum line consists of an air-cooled oil diffusion pump backed by a high speed rotary pump, in contrast to the mercury diffusion pump assembly on the CO₂ section. This is a safeguard against the possible formation of explosive mercury acetylides.

Further purification of the acetylene is achieved by passing the gas through two scrubbing columns containing glass beads coated with orthophosphoric acid. The

sequence of operations is as follows. Stopcock 3W3 is in the closed position and traps T10, a water mist trap, and T11 are cooled to -78°C and -196°C respectively. With stopcocks S15, S16, S17, S18, S20, S21 and S22 open and S14, S19, S23 and S26 closed, the liquid nitrogen traps surrounding the acetylene collection traps T8 and T9 are removed and the gas slowly distils through the columns. The primary function of the orthophosphoric acid is to remove ammonia from the acetylene as ammonium phosphate. The ammonia is the hydrolysis product of lithium nitride formed from impurity nitrogen oxides in the carbon dioxide and from possible outgassing of atmospheric nitrogen adsorbed on the stainless steel. It is necessary to replace the scrubbing column with a fresh unit every two to three weeks, usually after treatment of 40 litres of acetylene, since the build-up of phosphate on the beads and discolouration of the orthophosphoric acid reduce the efficiency of the cleaning procedure.

When all the acetylene has been condensed in trap T11, stopcocks S15, S16, S17, S18, S20 and S21 are closed, S26 opened and 3W4 turned to the high vacuum position. The acetylene is again pumped to 10^{-4} torr. Once the required vacuum has been achieved, 3W4, S26 and S22 are closed, the gas is distilled into the storage system and the yield is measured. The storage system comprises three tanks with respective volumes 16l, 6l, and 5l again allowing flexibility in the storage conditions. The recorded yields for the conversion of carbon dioxide to acetylene are shown as a histogram in Fig. 2-5.

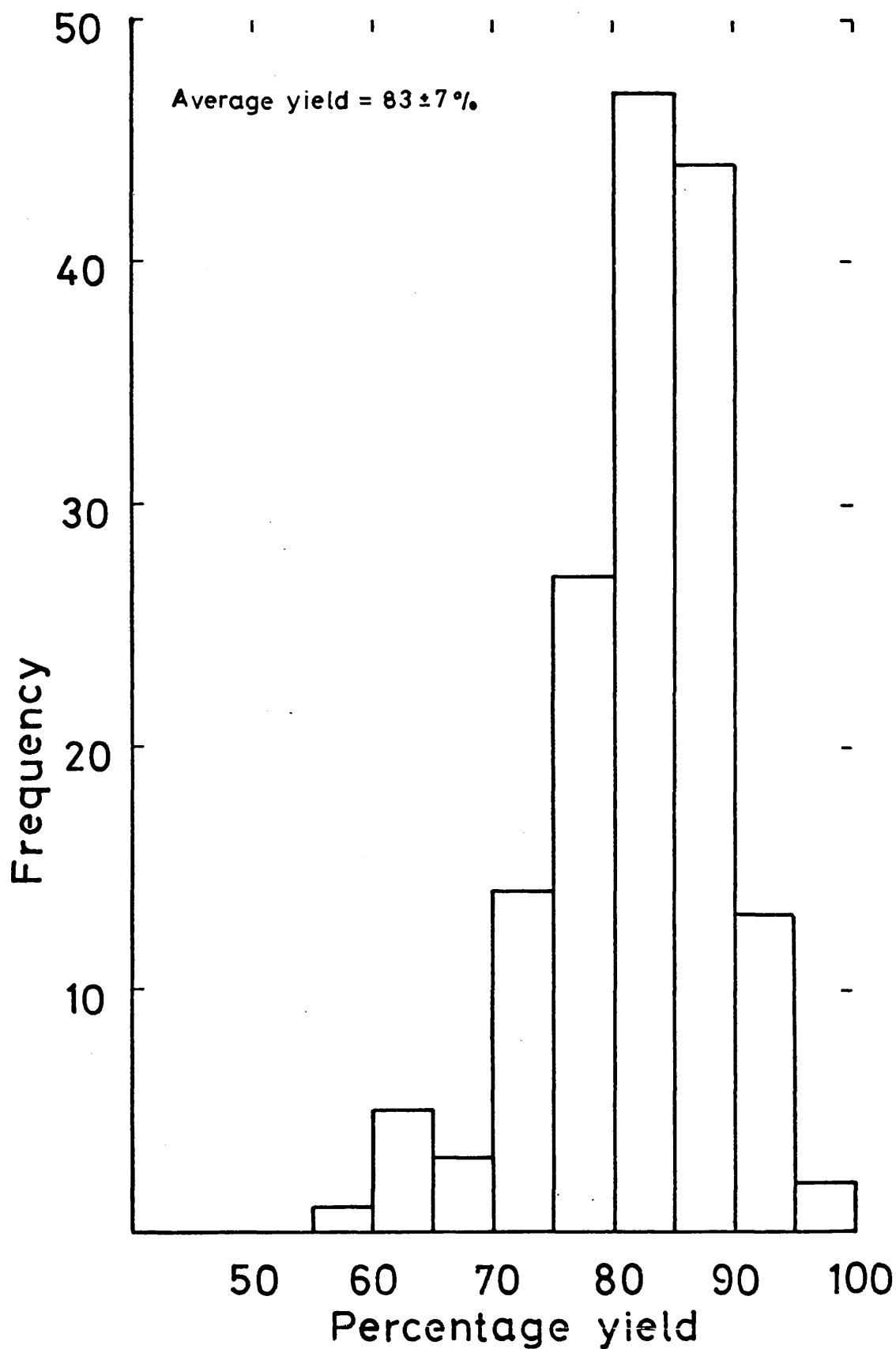
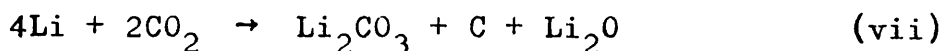


FIGURE 2-5: CO_2 to C_2H_2 conversion yields

Tamers (1975) has given a comprehensive analysis of the side reactions which may affect the eventual yield of acetylene. The main losses of carbon occur by the following pathways:



These losses of carbon may be reduced by heating the reaction mixture. The lithium carbonate decomposes to a significant extent at temperatures in excess of 600°C, which reverses reaction (viii). At the final temperature of 900°C the regenerated CO₂ is eventually converted to lithium carbide by reaction (v) and the carbon of (vii) by the reaction



Hydrolysis of the lithium carbide, cooled to room temperature, proceeds with a quantitative yield as shown in reaction (vi). The remaining solution should be clear after high yield reactions. A black suspension indicates the predominance of the secondary reaction (vii) and a grey suspension, reaction (viii). Lithium carbonate has low solubility in lithium hydroxide solution. Tamers' optimized acetylene yield is in excess of 95%, compared to 83 ± 7% for this research. It seems most likely that the deficiency in yield is due to the slightly lower reaction temperatures employed, resulting in competition of reaction (vii) with the desired pathway, namely reaction (v). Perhaps careful thermometric measurement of the reaction temperature and the use of an electrical furnace

to achieve a higher temperature might raise the average yield to a value consistent with the optimised yield quoted by Tamers.

2.2.4 Cyclotrimerisation of acetylene to benzene

The initial work on a practical synthesis of benzene for radiocarbon dating was again reported by Tamers (1960). The cyclotrimerisation reaction was performed by pyrolysis of acetylene at 650°C. Further developments were published a year later (Tamers et al., 1961; Starik et al., 1961), the latter workers using a Ziegler catalyst. In 1962 a diborane activated catalyst was introduced for acetylene cyclisation (Noakes et al., 1962). By 1965, most laboratories engaged in the liquid scintillation technique had switched to transition metal activated silica-alumina catalysts for acetylene cyclisation (Noakes et al., 1965; Tamers, 1965; Pietig and Scharpenseel, 1966).

The catalyst used for this study, KC Perlkatalysator neu, supplied by Kali Chemie, Hannover, Germany, is silica-alumina activated by Cr^{VI}. The catalyst is supplied in pellet form, the average pellet size being 2-3mm. The essential features of the acetylene to benzene system are shown in Fig. 2-6. Greaseless stopcocks and joints are used in the immediate vicinity of the catalyst vessel and collection finger since the high vacuum grease readily dissolves in benzene.

10g of catalyst per litre atmosphere of sample acetylene are placed in the catalyst vessel and the system is evacuated with G1, G2 open, G3, G4 and S26 shut and 3W4 in the low vacuum position. The catalyst is heated to

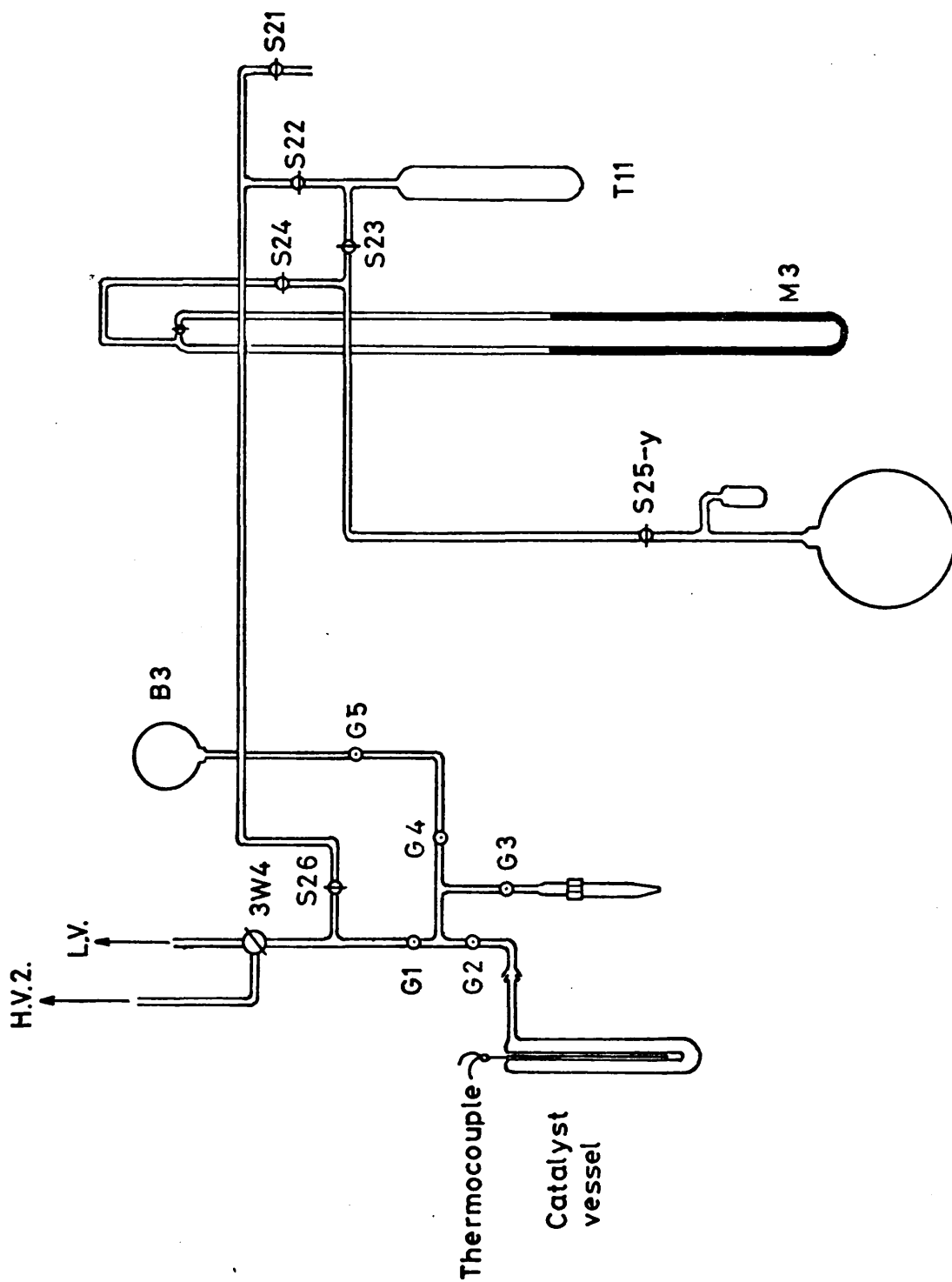


FIGURE 2-6 : Benzene synthesis system

450°C to remove all traces of moisture and adsorbed gas. When this temperature has been reached, 3W4 is turned to the high vacuum position and heating is continued until a pressure of 10^{-2} torr has been attained. The heating jacket is then removed and pumping continued while the catalyst cools, until better than 10^{-3} torr is registered. Stopcock G2 is now shut off and the acetylene expanded from its storage bulb 'y' into the manifold (with stopcocks S25-y, S23, S24, S22, S26, G1, G4 and G5 all open, 3W4 in the off position and S21 and G3 shut). The pressure of gas can be read on manometer M3 or on the 0-760 torr Bourdon gauge B3. This done, the main storage area is now closed off, S25-y shut, and the catalyst vessel is opened via G2. There is a steady drop in pressure as the acetylene is adsorbed on to the catalyst. The rise in temperature of the catalyst is monitored and further addition of acetylene is stopped when the temperature reaches 100°C. This "greaseless" section of the line is now shut off, G1 shut, and the small amount of acetylene remaining in this part of the system is quickly adsorbed on to the catalyst. When the pressure on the Bourdon gauge B3 is close to zero G3 is opened and the product benzene distilled from the catalyst into the demountable cold finger T12 cooled to -196°C. The catalyst is allowed to cool down and then the procedure is repeated. When all the acetylene in the storage bulb has been reacted and, after the benzene collection finger has been warmed up to release any

acetylene frozen out with the benzene and that small amount also reacted, the "greaseless" section is isolated with G1 shut. The catalyst is heated up to 200°C and all the product benzene is collected in cold finger T12. The collection vessel can then be warmed up and detached from the vacuum line. The sample is then accurately weighed and the conversion yield calculated. An amount of benzene, approximately 0.5-0.7ml, is removed for combustion to carbon dioxide and mass spectrometric assay.

The record of benzene yields is shown as a histogram in Fig. 2-7. The overall yield of $81 \pm 7\%$ is not truly representative of the performance of the catalyst. The catalyst was supplied in a large metal container. After the seal had been broken the drum could not be resealed and gradually the colour of the pretreated catalyst altered from yellow to greyish. This was identified as a poisoning effect and the catalyst was immediately repacked in glass storage bottles sealed with paraffin tape. After this precaution only traces of discoloured catalyst have been observed, presumably remnants of the surface layer which became mixed when the contents of the drum were redistributed. A more realistic value of the mean conversion yield based on 114 observations taken after the repacking is $83 \pm 6\%$. This value is, however, lower than that reported by many laboratories using similar benzene synthesis techniques. The paper by Tamers cited in Section 2.2.3 also gives details of side reactions in the cyclotrimerisation reaction and how these affect the

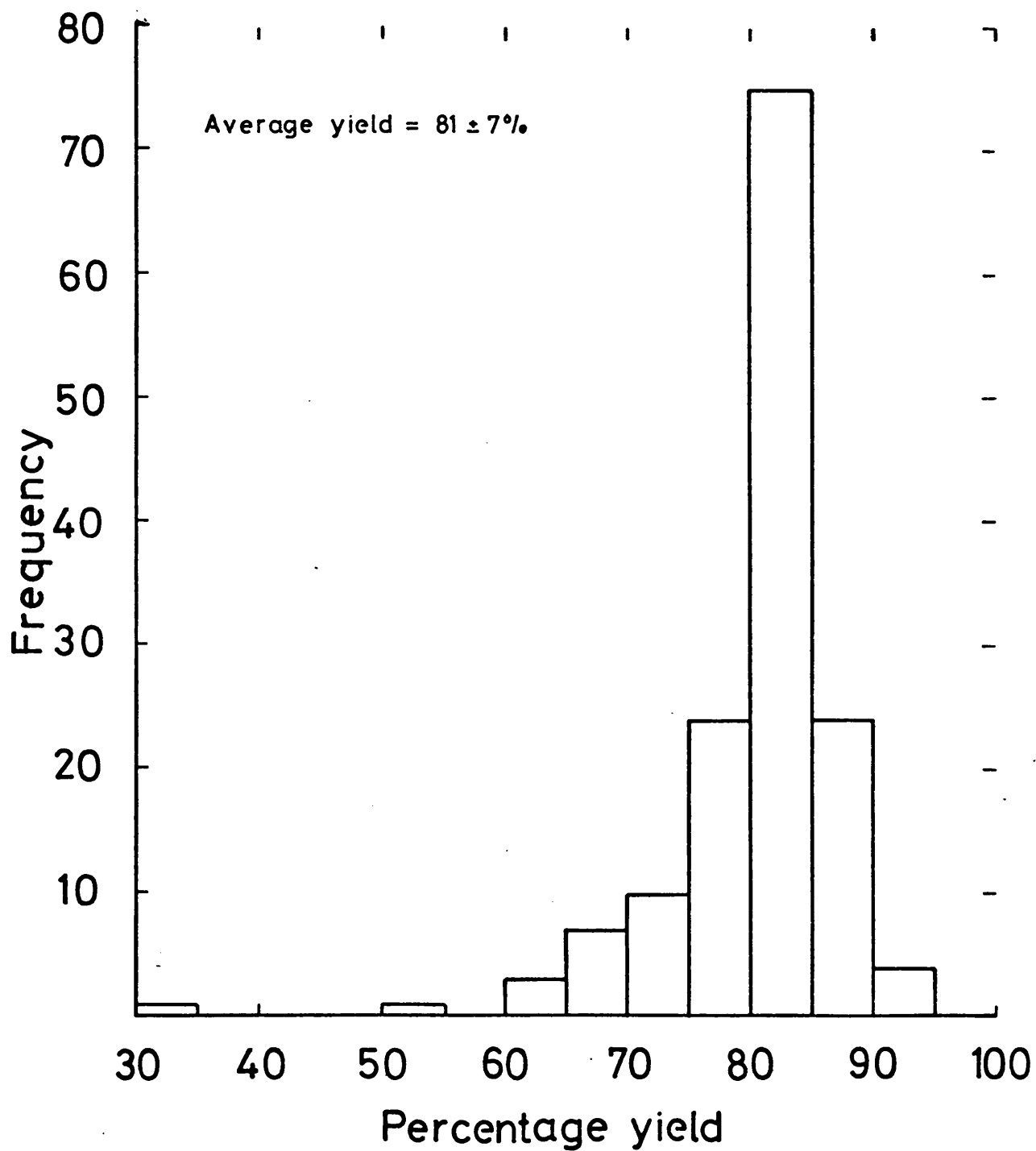
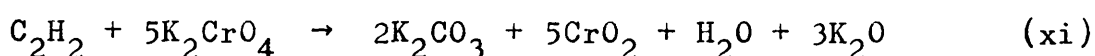
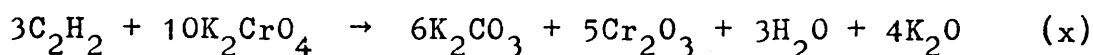


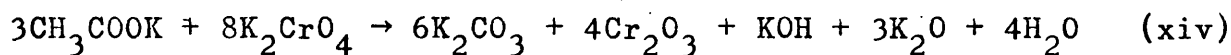
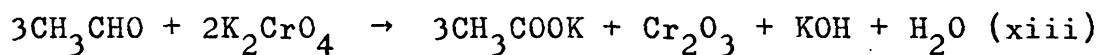
FIGURE 2-7: C_2H_2 to C_6H_6 conversion yields

overall yield of benzene. Tamers reports that under ideal conditions 99% conversion can be achieved.

The catalyst is deactivated to some degree during the reaction, as a result of the following acetylene oxidation reactions:



These two reactions can proceed directly especially at higher temperatures, i.e. at temperatures greater than 200°C. However mechanisms involving intermediates such as acetaldehyde and acetic acid would be more likely since it was observed that small amounts of moisture in acetylene caused rapid catalyst deactivation in addition to lower benzene yields. This would begin with a reaction of acetylene with water present in minimal amounts either in the gas or on the catalyst, reaction (xii). The reactions could stop with the formation of an acetate salt or proceed to potassium carbonate.



Tamers verified the presence of carbonates by acid attack and subsequent collection of evolved CO_2 in ammonium hydroxide solution and detected traces of carbonyl groups via infra-red spectrometry. Since acetaldehyde is very reactive, (xiii) would proceed rapidly at all temperatures and reaction (xiv) would be more significant at higher temperatures. The acetate could also of course react with

acetylene, forming vinyl acetate which readily undergoes polymerisation. The laboratory procedure as stated earlier aims to keep the catalyst temperature below 100°C, however the generation of "hot-spots" on the catalyst, perhaps due to the design of the catalyst vessel, may cause localised overheating. If the catalyst is heated to 400°C after collection of the benzene, a yellow oily substance distils to the top of the catalyst vessel. This is presumably a poly-acetylene compound formed by the mechanism proposed previously.

The colours of the deactivated catalyst provide an indication of the predominating reactions. The production of hydrogen, by high temperature (200°C) decomposition of acetylene, can occur causing reduction of the chromate and uncontrolled addition of acetylene, resulting in a rapid temperature increase, may result in deposition of elemental carbon on the catalyst. The brown colour, normally observed in this system, is due to CrO_2 and is generally produced when the reaction temperature is about 100°C. Of course $\text{Cr}_2^{\text{III}}\text{O}_3$ can be converted to $\text{Cr}^{\text{IV}}\text{O}_2$ by reaction with chromate, further deactivating the catalyst. It is possible to regenerate the catalyst by heating it in air to 450°C, oxidising the Cr^{IV} and Cr^{III} to Cr^{VI} , however because of the possibility of memory effects this is not done and used catalyst is discarded.

If the low average yield value obtained in this research is largely due to a humidity rather than a temperature effect then, according to Tamers, the samples of acetylene would contain up to 5% water vapour. This value seems to

be very high since overnight storage of the acetylene with the storage bulb cold finger cooled to -78°C had no effect on the yield of benzene obtained on the following day. The answer to the problem of low yields may well lie in the scrubbing procedure, outlined earlier, not being as effective as has been assumed, rather than in the retention of large quantities of water vapour in the sample.

The overall conversion yield from CO_2 to benzene is 66%. This value is very low compared to the figures quoted by laboratories utilising similar chemical procedures (e.g. Tamers, 1975; Harkness and Wilson, 1972) and may result in alteration of the isotopic composition of the sample by chemical fractionation. An assessment of fractionation effects will be given in Chapter 4.

The purity of the final benzene has been assessed by chromatographic analysis. For a series of samples benzene purity was 99+%, the impurities consisting of organic compounds resulting from the combination of four acetylene units, namely ethylbenzene and para-xylene. Some toluene was also present.

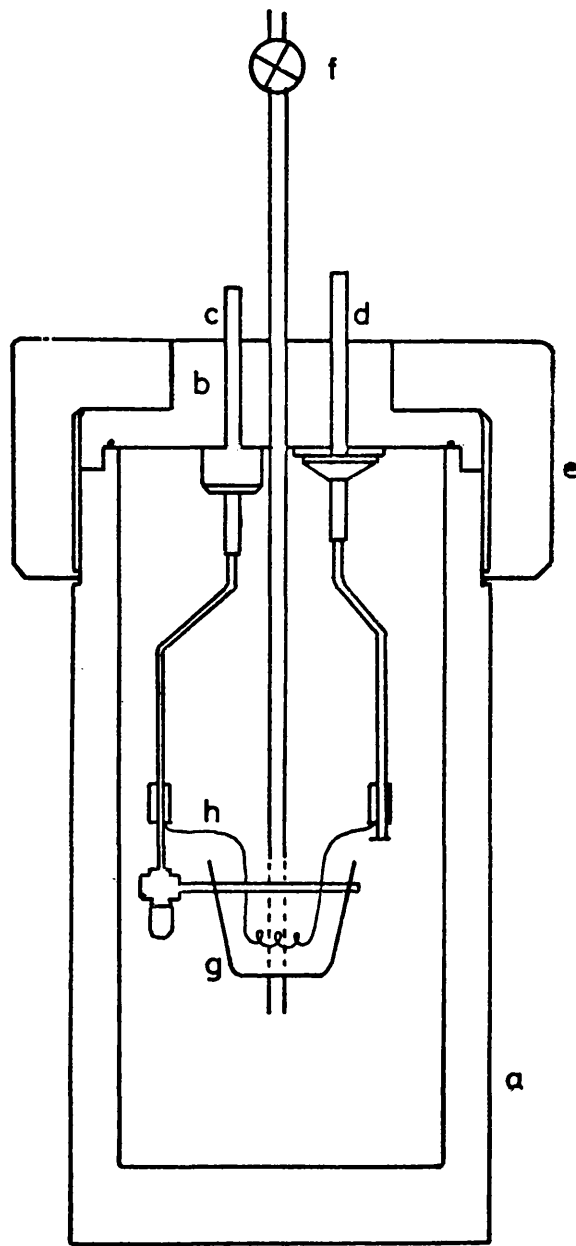
2.2.5 Combustion of benzene to carbon dioxide

The complex chemical procedures involved in the preparation of the appropriate counting substance, particularly in the synthesis of benzene for liquid scintillation counting may affect the isotopic integrity of the sample resulting in erroneous assay. Thus, to monitor any fractionation effect, a sample of product

benzene is oxidised to CO_2 and its stable carbon isotope ratio determined mass spectroscopically. This ratio can then be compared with the stable carbon ratio of CO_2 produced by the sample combustion. This latter ratio is assumed to reflect the fractionation produced in nature following photosynthesis.

Samples are combusted in a modified stainless steel calorimeter with an approximate volume of 300ml (Fig. 2-8). Modifications to the bomb were necessary since the original Schröder valve was unsuitable for bleeding the product gases into the collection system. A gas inlet-outlet tube with a metering valve has been added to the top plate of the bomb and connections to the collection system are completed by "swagelock" couplings. The ignition circuitry is analogous to that used in the large combustion vessel (Section 2.2.2). Samples of benzene, 0.1ml, are added from a syringe to the "vitreosil" crucible and the bomb is sealed and pressurised with oxygen. The firing connections are completed and the combustion effected.

A number of test combustions were carried out to determine optimum firing conditions and these indicated that the most reproducible conditions, in some ways unsatisfactory since high conversion yield could not be guaranteed, were obtained by an initial oxygen pressure of 15-17 atmospheres, a 3 times excess, and an ambient temperature of 50-60°C. The increase in temperature obtained by standing the combustion vessel in a hot water bath for 10 minutes prior to firing, increases the vapour



KEY : a: Main reaction chamber; b: Top plate with electrodes c&d; e: Toroidal sealing ring; f: Gas inlet-outlet valve; g: Sample crucible; h: Ignition wire

FIGURE 2-8 : Microcombustion bomb

pressure of benzene which is depressed at room temperature as a result of the increased pressure of oxygen. The gas collection system (Fig. 2-9) and the sequence of operations for collecting and purifying the sample are almost identical to those described in Section 2.2.2. The only differences are that only one throttling valve is used, instead of two as on the main system, an additional 0-100 torr Bourdon gauge has been introduced to measure the generally higher input pressure and there is no storage area since the time required for a combustion is only 45 minutes from setting up the bomb to removing the sample bottle of CO_2 .

2.2.6 Summary of laboratory procedure.

The laboratory routine, including approximate times for the individual processes, is presented as a flow chart in Fig. 2-10. The construction of the vacuum system for benzene synthesis and establishment of the procedures occupied the first ten months of the research project.

2.3 Measurement of isotopic fractionation

Isotopic fractionation, as a result of kinetic and thermodynamic factors, occurs in the transfer of carbon between different phases of the environment. For example, it was shown by Craig (1953) that terrestrial organic plants are depleted in ^{13}C by approximately 2% compared to the atmosphere from which they assimilate CO_2 . It is assumed that the fractionation effect for ^{14}C is twice as large as for ^{13}C (Craig, 1954). Before measured ^{14}C

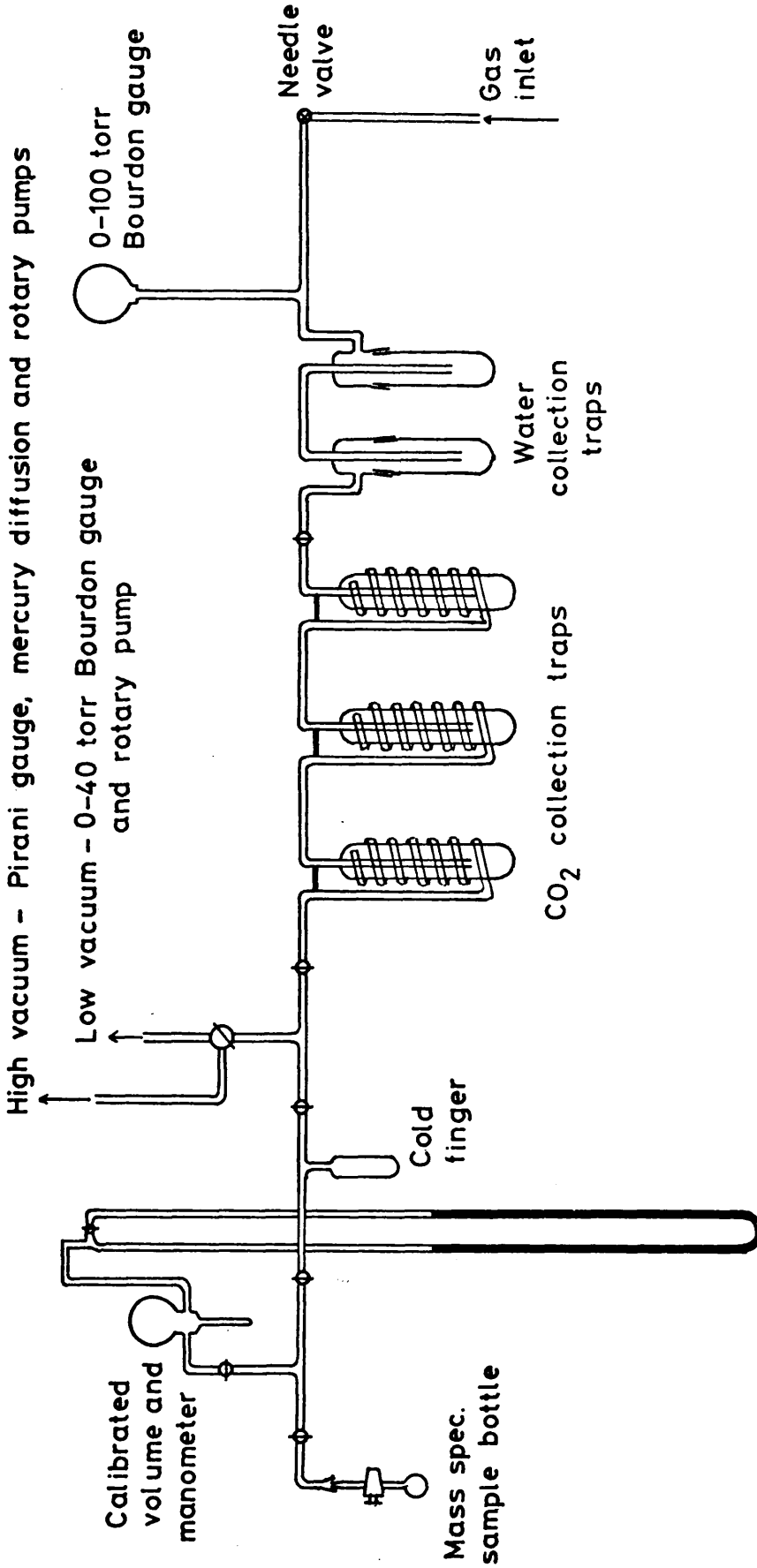


FIGURE 2-9 : Micro-combustion gas handling system

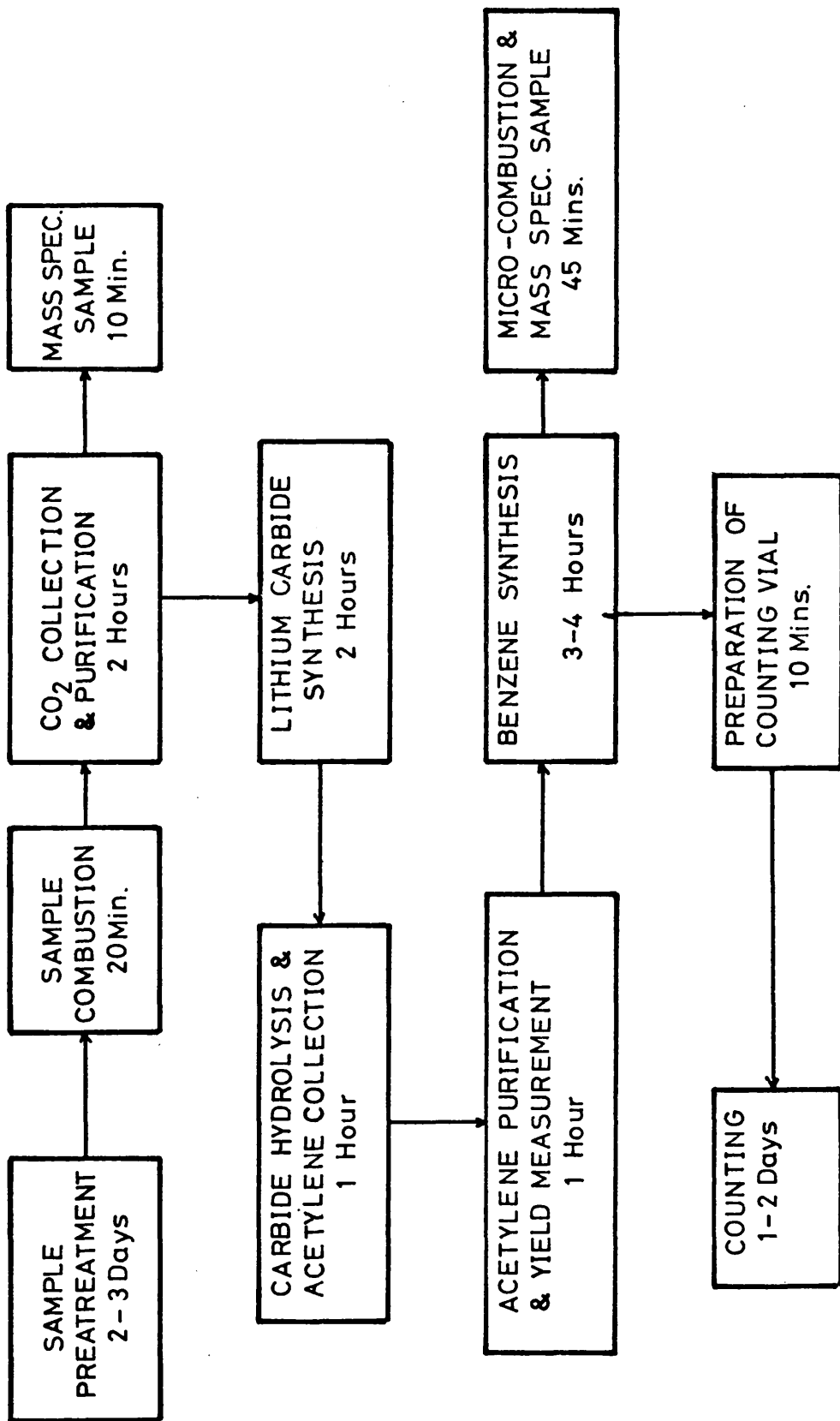


FIGURE 2-10: Flow diagram of laboratory procedure

concentrations can be compared to a standard activity , therefore, this fractionation correction must be applied.

Measurement of the $^{13}\text{C}/^{12}\text{C}$ ratio is generally performed on a sample of CO_2 removed after the sample combustion stage. The effects of further isotopic fractionation in the subsequent synthesis of benzene are not normally considered. (A discussion of possible variations in the carbon isotope composition of samples during benzene synthesis is given in Chapter 4). Sample $^{13}\text{C}/^{12}\text{C}$ ratios are measured using a V.G. Micromass 602B mass spectrometer. The observed ratio is represented by an enrichment relative to a primary standard based on the general formula (Craig, 1961):

$$\delta^{13}\text{C} = \frac{^{13}\text{C}/^{12}\text{C}_{\text{SAMPLE}} - ^{13}\text{C}/^{12}\text{C}_{\text{REFERENCE}}}{^{13}\text{C}/^{12}\text{C}_{\text{REFERENCE}}} \times 1000 \text{ ‰}$$

The primary standard is CO_2 produced from P.D.B. calcium carbonate by reaction with 100% orthophosphoric acid at 25.2°C . P.D.B. is a Cretaceous belemnite, Belemnitella Americana, from the Peedee formation of South Carolina. In practice a secondary standard (or standards), previously calibrated against the primary standard, is used. For this work the secondary standards used were:

1. carbon dioxide produced from Scots Pine wood cellulose
- and 2. carbon dioxide produced by combustion of a sample of human brain tissue

The per mille enrichments of these standards with respect to the P.D.B. standard are $-23.90 \pm 0.10 \text{ ‰}$ and $-26.10 \pm$

TABLE 2-2 ANALYSES OF BRAIN STANDARD AGAINST
TREE RING STANDARD

Date of analysis	$\delta^{13}\text{C}$ w.r.t. P.D.B.	Date of analysis	$\delta^{13}\text{C}$ w.r.t. P.D.B.
20.02.76	-26.13	12.11.76	-26.10
01.03.76	-26.23	12.11.76	-26.17
08.03.76	-26.07	04.02.77	-26.09
08.03.76	-26.14	16.03.77	-26.22
13.03.76	-26.13	02.04.77	-26.13
15.03.76	-26.11	05.04.77	-26.05
22.03.76	-26.18	19.04.77	-26.01
19.05.76	-26.08	20.04.77	-26.03
04.09.76	-25.71	23.04.77	-26.04
11.09.76	-26.14	24.04.77	-26.06
16.10.76	-26.15	29.04.77	-26.03
16.10.76	-26.01	02.05.77	-26.03
11.11.76	-26.04	03.05.77	-26.00

Mean value of $\delta^{13}\text{C} \pm 1\sigma = -26.08 \pm 0.09^{\circ}/\text{oo}$

0.10 ‰ respectively, the calibration being performed in the radiocarbon laboratory at the Scottish Universities Research and Reactor Centre, East Kilbride (Harkness, pers. comm.). The secondary standards are regularly compared and the results of these measurements are given in Table 2-2.

2.4 The Liquid Scintillation Technique

2.4.1 Introduction

In contrast to Geiger and proportional counting techniques, liquid scintillation counting utilises a system in which the sample is introduced into solution or into intimate contact with a scintillator medium which is itself usually a solution. A beta particle emitted by the sample raises the solvent molecules along its path of travel to an excited state. This energy is transferred from one solvent molecule to another, diffusing the original energy of the electron. Finally, the solvent molecule or molecules transfer their energy in the form of photons of light at their characteristic wavelength. When the light photons strike a secondary scintillator molecule, they are absorbed and re-emitted at a longer wavelength. Some energy is lost in each step of the process. Energy diffusion and loss plus quantum statistics reduce the overall resolution of the system both during the scintillation process and in the conversion of light energy to electrical energy in the photomultiplier itself. A schematic diagram of the scintillation process is given in Figure 2-11.

The detector is a scintillator used in conjunction with a photomultiplier tube to convert scintillation events,

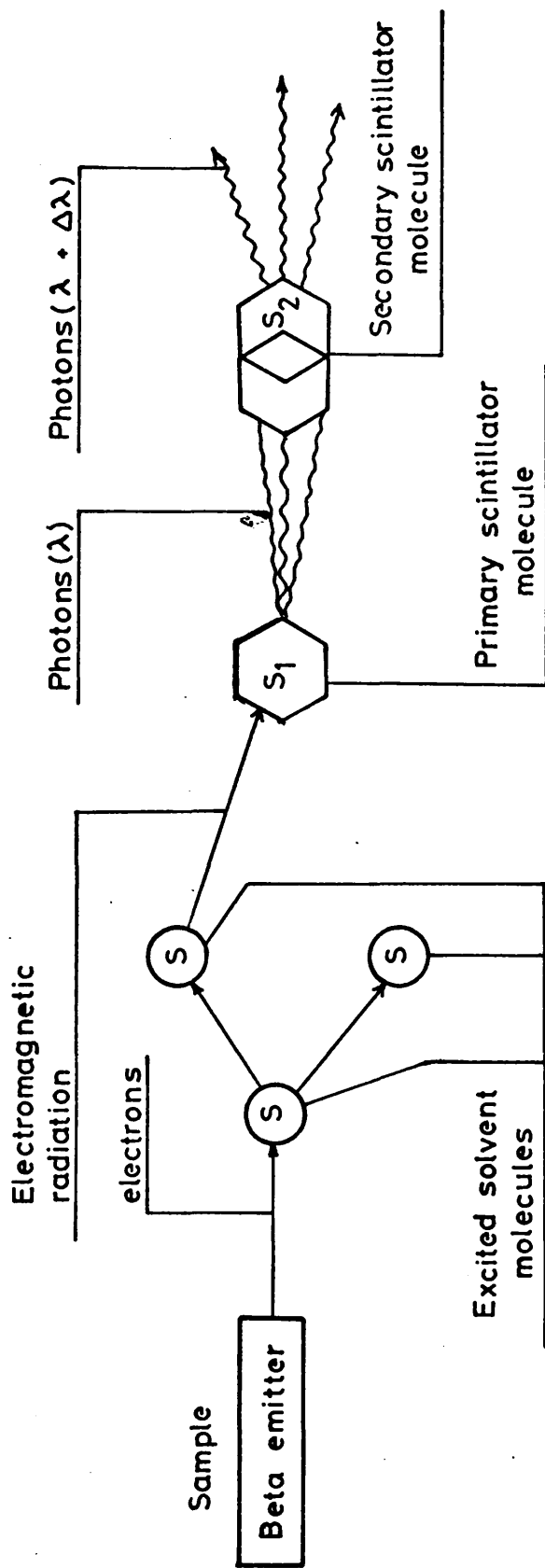


FIGURE 2-11: Energy transfer scheme in a liquid scintillator

photons of light, into an electrical pulse proportional to the magnitude of the event. The photon yield in a standard scintillation solution is approximately 5 photons/keV of beta energy. Thus as ^{14}C has a mean beta energy of 50 keV and a maximum of 156 keV, the photon yield per event would be respectively 250 and 780 photons.

2.4.2 The scintillation medium

Most liquid scintillation systems contain at least one type of scintillator. The prerequisites of a good scintillator are that it must give off photons at a wavelength compatible with the response of the photomultiplier tubes; that the photon yield be reasonably good and that it is soluble in solvents used for liquid scintillation counting. A list of common primary scintillants is given in Table 2-3. Of these primary scintillants PPO is the most widely used. However the wavelength of photon emission of this compound is too short for the best photomultiplier tube response.

It is, therefore, necessary to add a secondary scintillator to the "cocktail" to correct this condition. This secondary scintillator has the property of absorbing photons emitted by the primary scintillator and re-emitting photons of a longer wavelength where the photocathode response of the photomultiplier tubes is higher.

The most commonly used secondary scintillant is POPOP, 1,4bis[2-(5-phenyloxazolyl)]benzene, producing a shift in wavelength from 370nm to 425nm. One drawback of POPOP is its poor solubility in toluene. The derivative, dimethyl-POPOP emits at about the same wavelength but is about twice as soluble. (The structural formulae of the scintillation

TABLE 2-3 COMMON PRIMARY SCINTILLATORS

Primary scintillator	Relative photon yield	Wavelength at peak emission nm	Solubility in toluene
p-terphenyl	1.0	340	poor
PDB ¹	1.2	400	fair
PPO ²	0.95	370	good
Butyl-PDB ³	1.05	366	good

1 2-Phenyl-5-biphenyl-oxadiazole

2 2,5-diphenyloxazole

3 2-(4'-t-butylphenyl)-5-(4"-biphenyl)-oxadiazole

compounds is shown in Fig. 2-12).

A good solvent for liquid scintillation mixtures should possess the following properties: it must

1. dissolve the scintillants in sufficient concentration,
 2. be a good energy transfer agent,
 3. have a low freezing point ($< + 4^{\circ}\text{C}$)
- and 4. be safe to use (i.e., relatively non-toxic, high flash point).

Good solvents are found in the aromatic hydrocarbon group of which toluene is most popular.

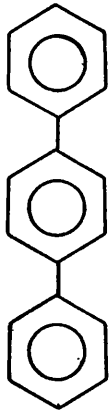
The sample container plays an important part in the liquid scintillation system. It must

1. be resistant to attack by solvents and additives,
 2. be transparent at the wavelength of common scintillators,
 3. have reproducible geometry
- and 4. contain little or no residual activity.

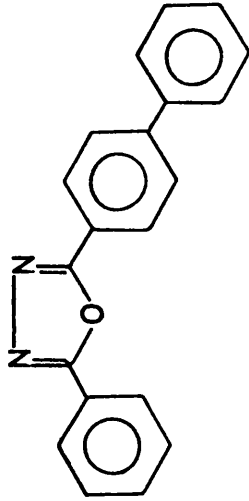
Glass vials of 22 ml capacity are the most commonly used sample containers. Glass meets all the requirements listed above except that all glass contains some ^{40}K , an energetic beta-gamma emitter. Special glass with a very low ^{40}K content is commercially available and is used in this research.

2.4.3 Counter electronics

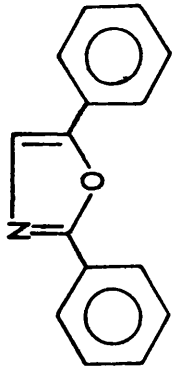
The second part of the detection system is the photomultiplier tube. Its basic function is to convert light into electrical energy proportional to the light output of the scintillator system. A photomultiplier tube



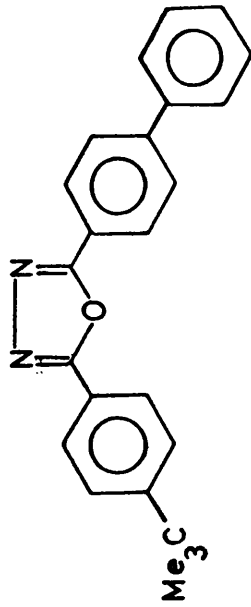
p-Terphenyl



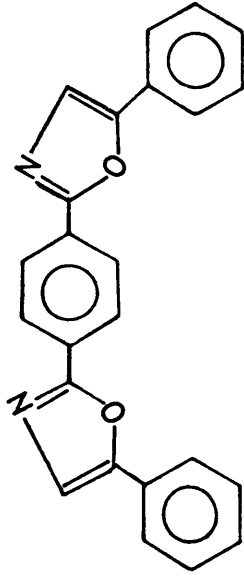
2-Phenyl-5-biphenyl-oxadiazole
(PDB)



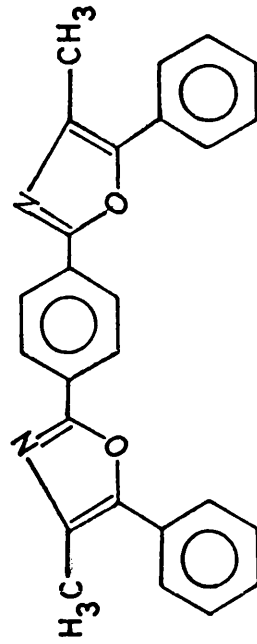
2,5-diphenyloxazole
(PPO)



2-(4'-t-butylphenyl)-5-(4''-biphenyl)-
oxadiazole (butyl-PDB)



1,4-Di[2-(5-phenyloxazolyl)]benzene
(POPOP)



1,4-Di[2-(4-methyl-5-phenyloxazolyl)]benzene
(di-methyl POPOP)

FIGURE 2-12 : Structural
formulae of common liquid
scintillators.

(Fig. 2-13) consists of a glass envelope with a glass or quartz face. A thin deposit of a low work function material such as CsSb is evaporated on the inside surface of the face (photocathode). When this surface is struck by light of a particular wavelength photoelectrons are emitted. A chain of "dynodes" is placed after the photocathode. The cathode is at ground potential while the dynodes and the anode have a positive voltage of from 800 - 2000 volts impressed over the dynode-anode series. Each dynode is electrically connected to the next through a resistance network such that the potential between dynodes is roughly equal. A potential is usually impressed between the last dynode and the anode. In this way, electrons emitted by the photocathode are accelerated from one dynode to the next and finally to the anode.

As the electrons strike each dynode, which is also coated with a low work function material, a process of secondary emission causes 1 to several new electrons to be emitted as a function of the high voltage for each electron striking the dynode. These electrons are in turn accelerated to the next dynode and so on down to the anode, the number of electrons increasing exponentially at each stage. There are usually 12 - 14 dynodes in modern phototubes. Thus, if one electron is emitted by the photocathode, typically 3^{12} electrons strike the anode causing sufficient amplification that a pulse may be detected by the electronics of the instrument. The current gain obtainable can be as high as 10^8 .

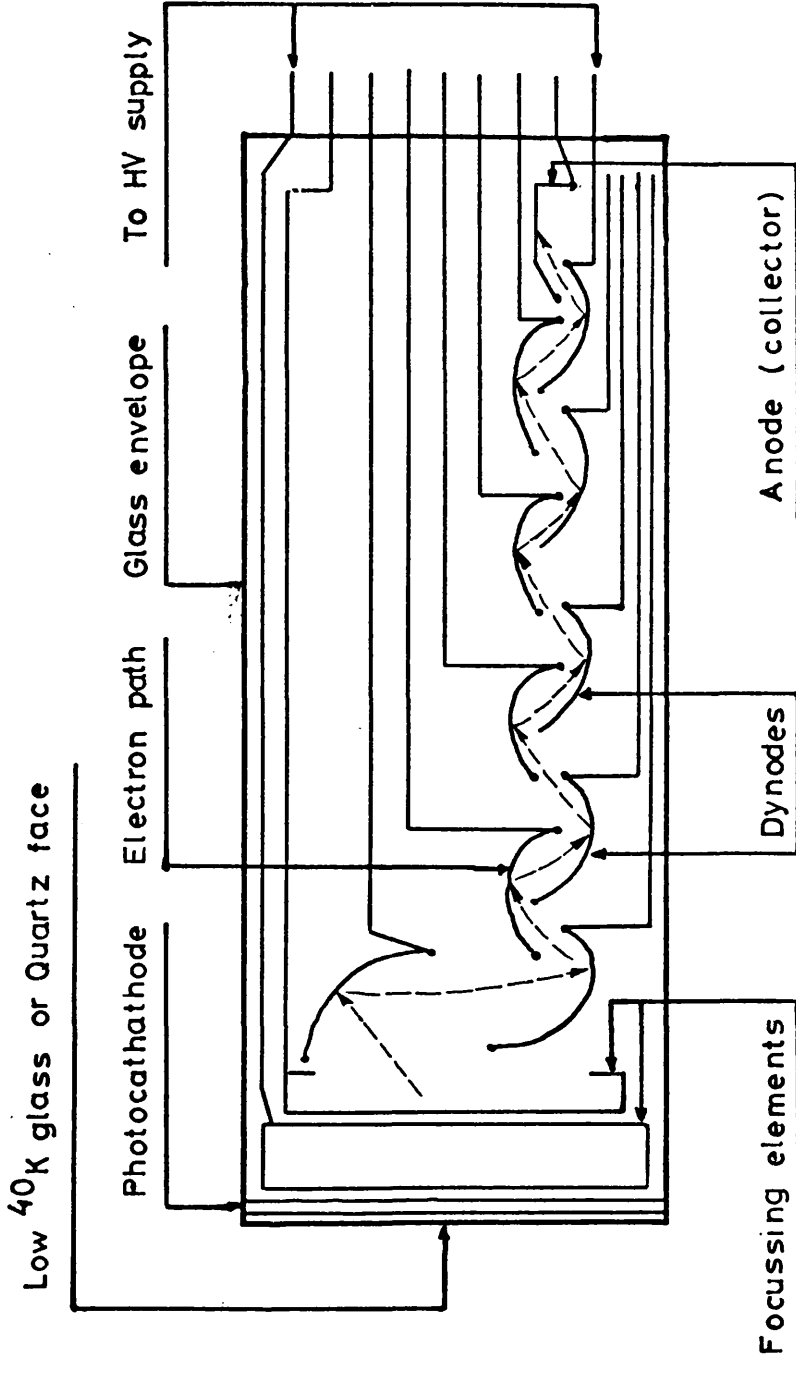


FIGURE 2-13: Schematic diagram of a photomultiplier tube

The output at the anode is proportional to the light input at the photocathode producing a pulse spectrum roughly equivalent to the energy spectrum of the isotope. This enables pulse height analysis on the pulse output with the aid of discriminatory circuitry.

However, the one drawback of photomultipliers arises as a consequence of the low work function of the photocathode. Spontaneous emission of electrons from the photocathode due to heat, produces "thermal noise" or "dark noise". This phenomenon is strongly temperature dependent and the pulses at the anode are indistinguishable from those due to radioactive disintegrations in the sample. It is therefore essential that the phototubes be operated in a refrigerated environment. Although cooling can reduce thermal noise by a factor of about 40, it still remains sufficiently high that further measures must be taken.

The most practical measure yet developed to reduce thermal noise contribution to the background is coincidence circuitry. With this system two photomultipliers are used instead of one. Thermal electrons are emitted one at a time and randomly in each phototube. Thus, it is unlikely that pulses due to two such electrons would be detected simultaneously at both outputs. A circuit is therefore installed such that if it receives a pulse simultaneously from each tube, the event is counted; if a pulse is received from only one tube, the event is not counted. However, when photons are given off from a radioactive decay event in the sample, a sufficient number is usually produced to cause photoelectrons to be emitted by the photocathode of each tube simultaneously. The resulting coincident pulses

will be accepted by the electronics.

The reduction in background arising from the coincidence circuitry greatly improves the figure of merit, E^2/B , of the detection system. (This quantity is defined in Section 2.5.2). The figure of merit is also enhanced by the technique of pulse summation. This configuration adds the pulse amplitudes of both photomultipliers before pulse height analysis improving the counting efficiency, increasing the energy resolution and improving the signal/noise ratio.

2.4.4 Quenching

Any process which interferes with the conversion of beta particle energy to scintillations or with light transmission reduces the amount of light which reaches the photomultiplier. As a result, fewer scintillations are detected and the pulses generated are of lower voltage. Consequently, efficiency is reduced and the whole pulse voltage spectrum is shifted to a lower voltage range. This interference (and the consequent reduction in efficiency) is called quenching. Unless quenching is known to be constant or the efficiency can be estimated (Section 2.5.5), the comparison of count rates derived from different samples is meaningless. Various causes of quenching are given below.

1. Interference with the transmission of energy from beta-particle to scintillator.

Some of the energy may be absorbed by an interfering substance and dissipated as heat. This is chemical quenching and is caused by aliphatic compounds such as ketones, amines and halogenated compounds. Alternatively

some of the energy may be prevented from reaching excitable molecules by the dilution effect - dilution quenching - of compounds such as ethers, alcohols and esters. The overall effect is the same in both cases, that is a reduction in the energy reaching the scintillator, but the result of chemical quenching is more marked. It is worth noting that oxygen, water, acids and alkalis are strong quenching agents. (The other two mechanisms of quenching are added for completeness although they are inapplicable to liquid scintillation counting of benzene;)

2. Interference with the transmission of light from scintillator to photomultiplier.

This happens most commonly when coloured materials in the solution to be counted absorb part of the light emitted by the scintillator - colour quenching. Red solutions are the most potent colour quenching agents since they absorb most strongly the wavelengths emitted by the scintillator. In contrast blue solutions cause little or no colour quenching.

3. Self quenching.

A radioactive material may itself cause quenching if it has the properties of a quencher. An obvious example is radioactive chloroform.

In liquid scintillation counting of benzene, therefore, chemical quenching, arising from impurities in the counting medium, is the sole causal factor producing distortion of the pulse voltage spectrum with resulting drop in counting efficiency.

2.5 The ^{14}C detection system

2.5.1 Description

The counting apparatus used in this research is a Model

3330 Automatic Tri-Carb Liquid Scintillation Spectrometer constructed by the Packard Instrument Company. The basic specifications are as follows. The complete shield assembly is mounted in an 11 cubic foot, temperature controlled chest type freezer, temperature being maintained within $\pm 0.5^{\circ}\text{C}$ over a range of approximately -5 to $+15^{\circ}\text{C}$. The optical chamber containing the two matched Bialkali photomultiplier tubes is screened from environmental radiation by a minimum of 2 inches of lead shielding in all directions. The 0-2400 V high voltage supply provided has a guaranteed stability of 0.01% per day. Output pulse from the photomultipliers are fed through high speed coincidence and pulse summation circuits. Three separate pulse height analysis channels are incorporated, each with a linear amplifier and a precision gain control. Three scalars record the contents of the channels. A simplified diagram of the electronics is given in Fig. 2-14. Samples are accommodated in a 300 position belt type chamber and automatic programming enables group counting, rejection and repeat counting modes. Complete light-tightness of the optical chamber is ensured by a "light-lock" consisting of an expanding rubber seal on the elevator and a five leaf shutter at the chamber entrance. At the end of a count the accumulated data are printed out via a teletype with a paper tape punch. The read-out lists position in sample belt, count time, counts in each channel and external standard counts. A radium-226 source with an activity of $20\mu\text{Ci}$ ($\pm 10\%$) is used in the system as an external standard. In the out position, the capsule is shielded by approximately

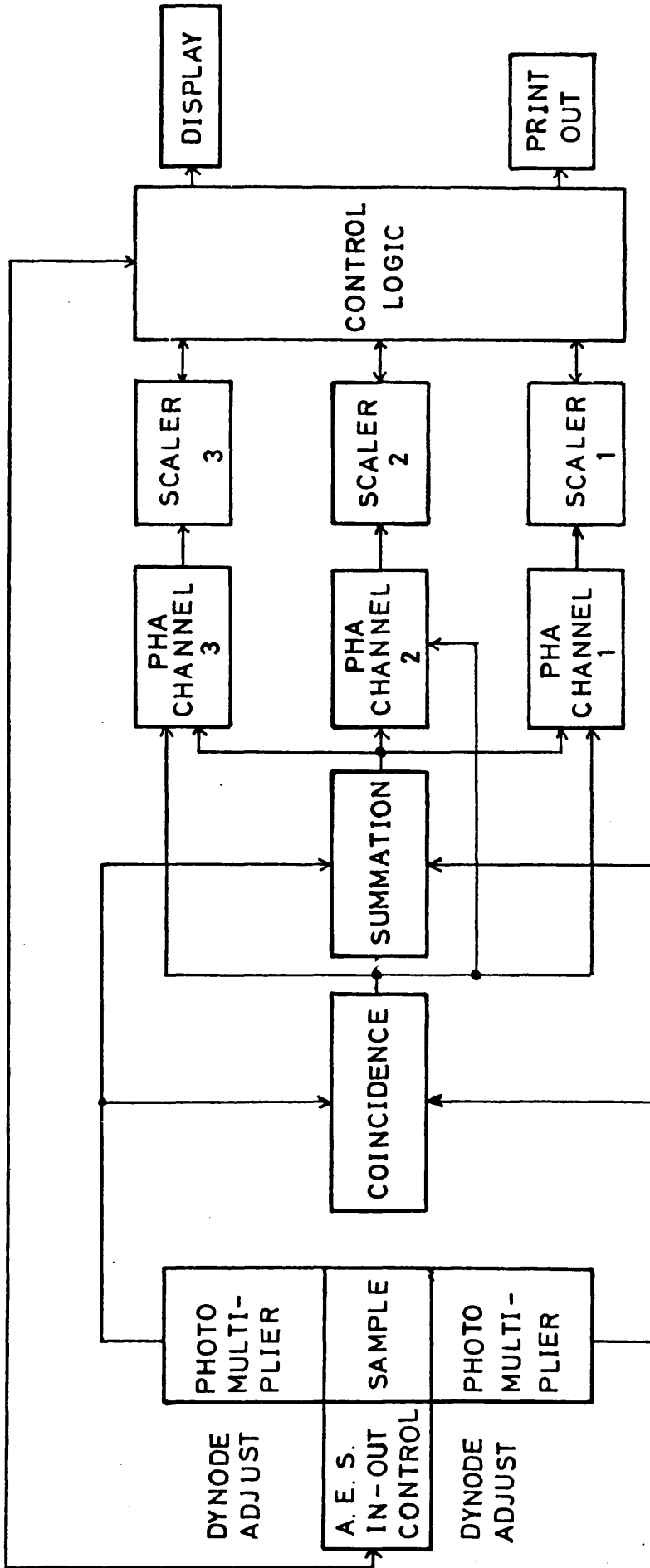


FIGURE 2-14: Schematic diagram of counting system electronics

12 inches of lead, and is driven into position by an electropneumatic pump.

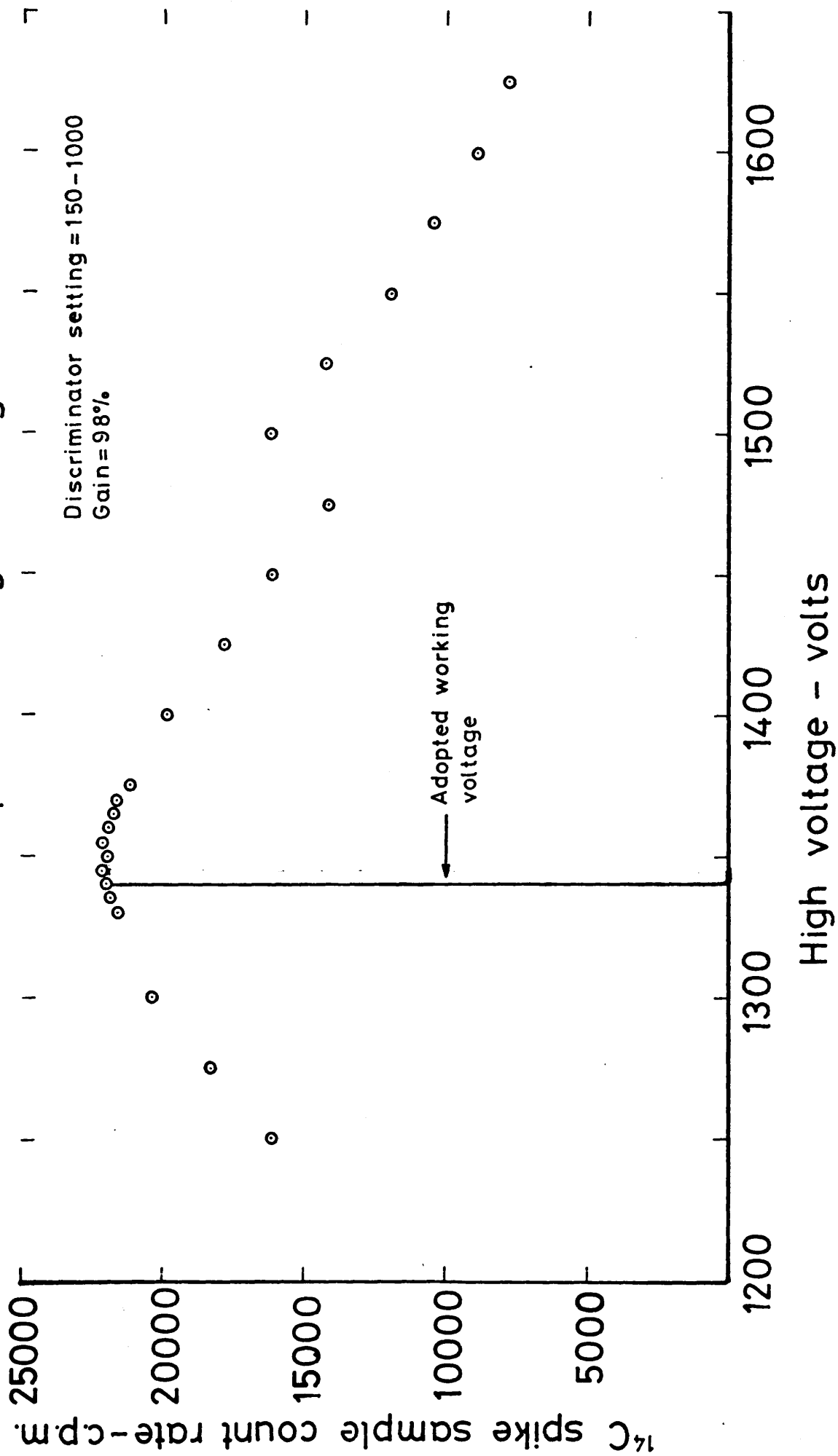
2.5.2 Optimisation of the counting system for low level ^{14}C assay

In determining the optimum conditions of the counting system one has to consider the balance of three parameters, namely the high voltage supply to the photomultiplier tubes, the discriminator positions of the three independent counting channels and the gain (or attenuation) setting for each channel. At the balance point, the figure of merit E^2/B , E being the absolute detection efficiency and B the background count rate, should be at maximum. If the sensitivity for a 95% accurate determination of ^{14}C by liquid scintillation counting is defined as that amount of ^{14}C required to raise the background count rate by twice its root mean square deviation (i.e. $2\sqrt{N}/T$, where N is the number of counts accumulated in time T), then decreasing the background count rate will decrease the detection efficiency and increase the time necessary to achieve the desired accuracy. For low level samples, the figure of merit is directly proportional to the number of samples counted per week to this given statistical accuracy. The first step in the optimisation process can, of course, be completed without modifying the electronics, that is by adjustment of the freezer temperature to reduce the "thermal noise" in the photomultipliers. The working temperature of the instrument is set at $0 \pm 0.5^\circ\text{C}$.

The photomultiplier tube optimum working voltage is determined before the instrument is despatched to the user and the value, in this case 1725v, will, with the appropriate

gain setting, produce the best pulse height spectrum for dual ^3H and ^{14}C counting. The recommended gain setting of $\sim 6\%$ means that the pulse height spectrum of ^{14}C has been altered to a large extent in order to accommodate the pulse height spectrum of ^3H . The maximum energy of the ^3H beta particle is 18 keV so that the degree of "energy overlap" of the beta spectra of ^{14}C and ^3H is 12%. Since the mean beta energy for ^{14}C , 50 keV, is higher than E_{max} for ^3H it should be possible to define a window for a slightly attenuated ^{14}C pulse height spectrum which, with appropriate discriminator settings, should have a very small tritium, and also background contribution. The gain setting for all three channels was set to 98%. At this value the detection efficiency is very much reduced since the H.V. potential on the photomultiplier tubes is now too high, placing the larger part of the pulse height spectrum above the upper discriminator level. It is therefore necessary to adjust the high voltage to compensate for the high gain (Fig. 2-15). The operating voltage adopted here is 1340 volts. The selected operating voltage lies to one side of an apparent "plateau" region since the background count rate at this setting is slightly lower than in the centre of this region. In addition the specified stability of the high voltage supply ensures that the overall detection efficiency does not vary significantly at this voltage. The graph shows an apparent discontinuity at 1500 volts. This voltage corresponds to a change in the "coarse" adjustment switch and probably reflects an irregularity in the H.V. wind up control. The pulse height spectra obtained at this gain and H.V. setting for ^{14}C , ^3H

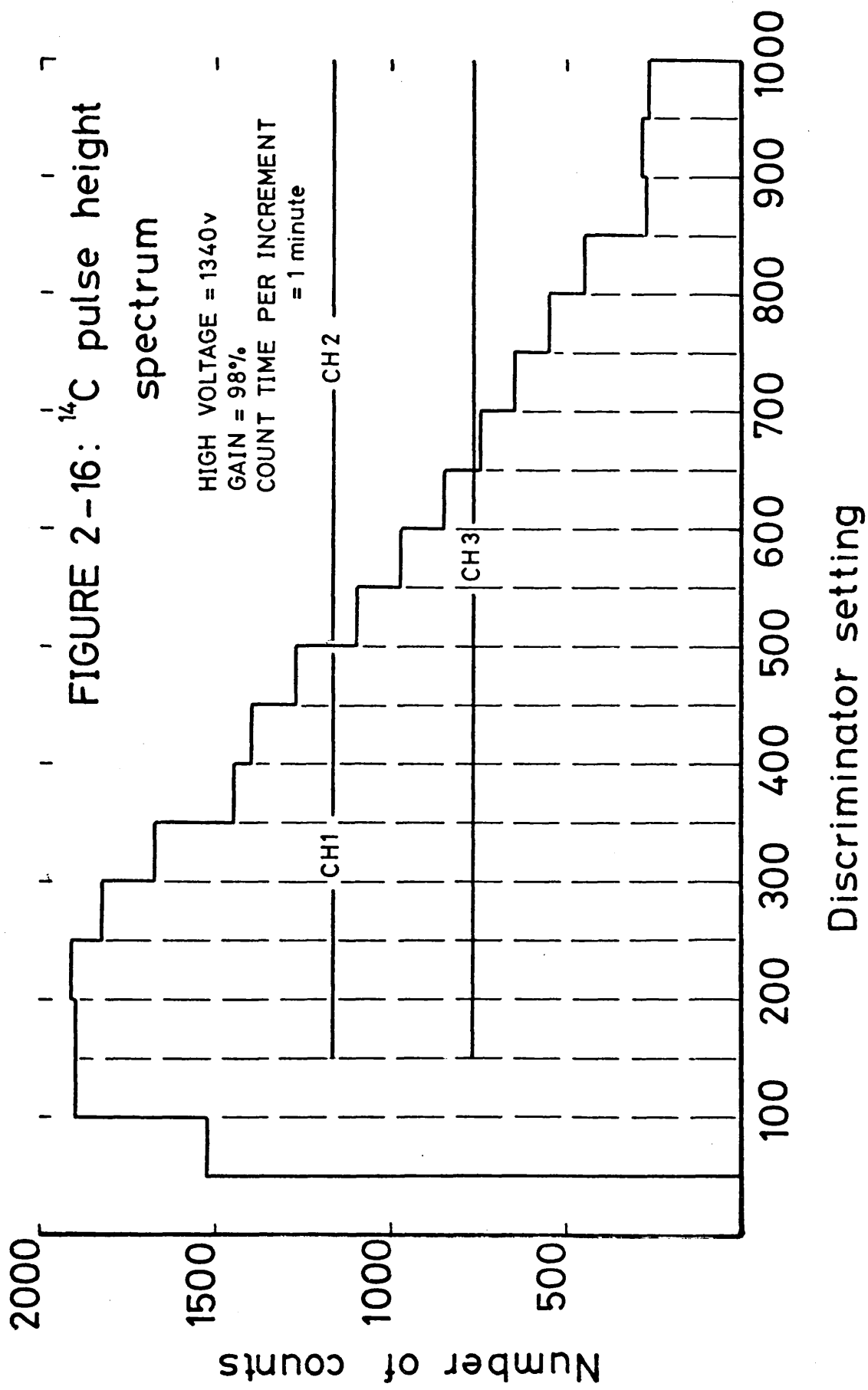
FIGURE 2-15 : Variation of the count rate of a ^{14}C spike sample with high voltage

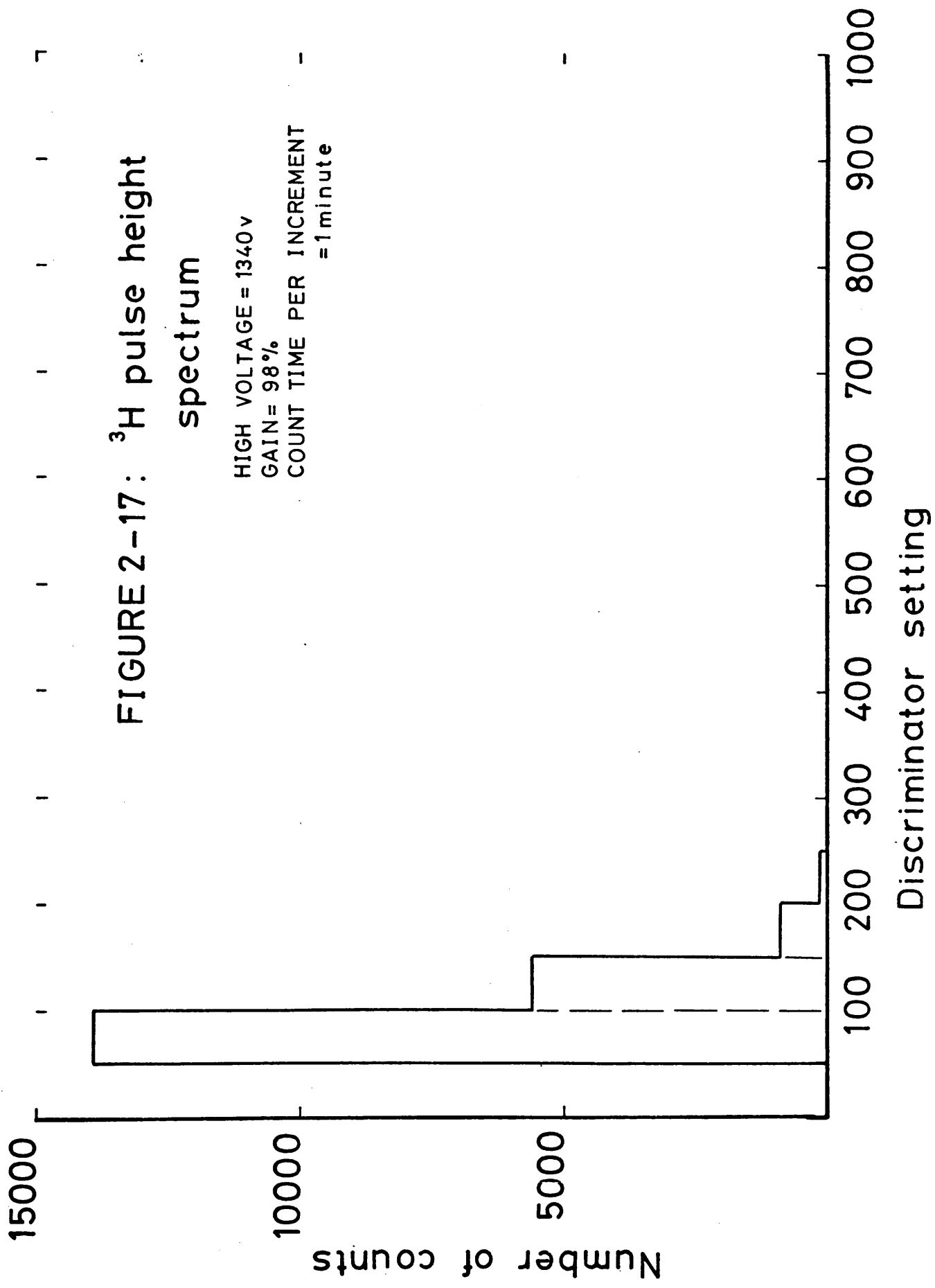


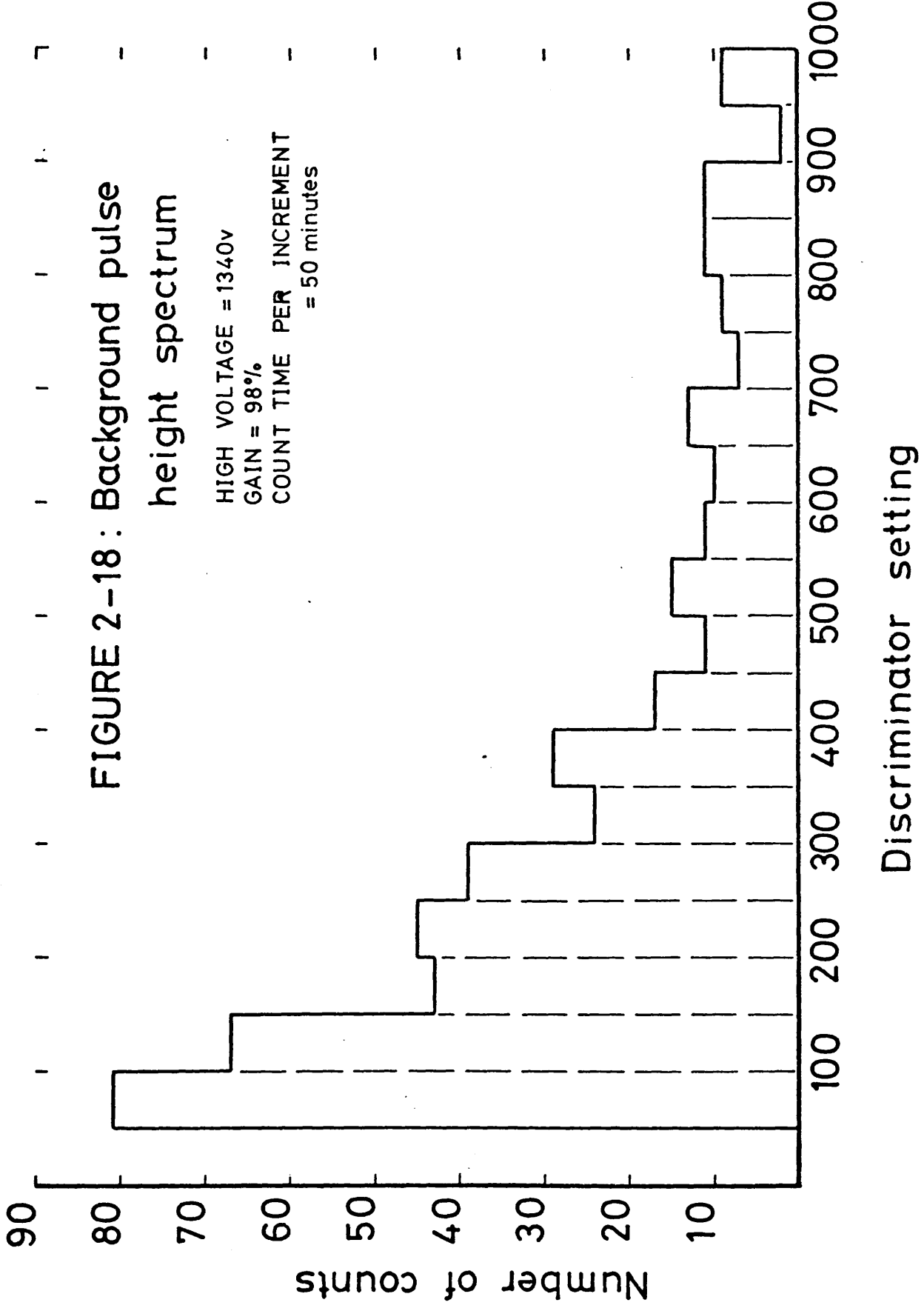
and background shown in Figs. 2-16, 2-17 and 2-18. The discriminators are now deployed to screen off the tritium and background contributions (Fig. 2-16). Channel 3 (CH3), 150-1000mV, monitors the whole ^{14}C spectrum, while channels 1 and 2 (CH1 and CH2) are set at 150-487mV and 487-1000mV respectively to monitor changes in the spectrum shape as a result of quench effects. The figure of merit for detection of ^{14}C for a 10 ml solution and with this set of conditions is ~ 600 ($E = 67\%$ and $B = 7.5$ c.p.m.) with the efficiency for $^3\text{H} < 0.01\%$. The corresponding data for a 5 ml solution is; efficiency = 62%, background = 4.5 c.p.m. and figure of merit = 860. The virtual exclusion of tritium from the ^{14}C window incidentally enables distilled tap water, rather than specially collected "aged" or "dead" water, to be used in the carbide hydrolysis reaction. Small, but significant (~ 0.5 c.p.m.), changes in the background count rate can be effected by adjustment of the platform height which alters the position of the vial between the photomultipliers in the optical chamber.

2.5.3 Preparation of the standard geometry vial

The intercomparison of modern standard and sample activities required to produce a radiocarbon date is simplified if one is working with identical quantities of carbon. After consideration of sample size and the quantities of benzene which could readily be synthesised, it was decided that a 10 ml geometry counting vial be adopted as the norm.







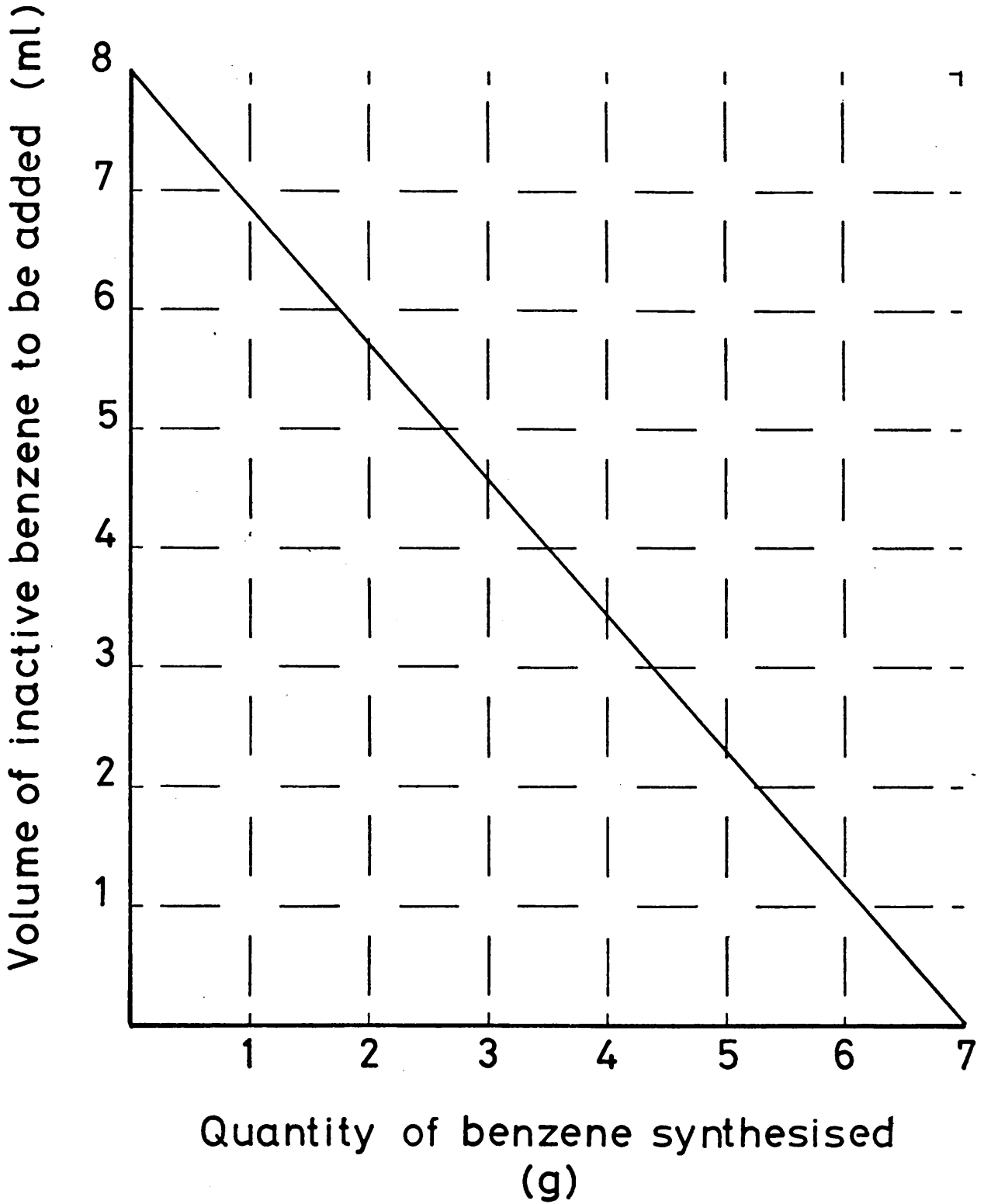
8 ml of sample benzene (7g) is placed in the vial, the empty volume of the vial having previously been blackened as a precaution against photomultiplier crosstalk (Appendix 1). Samples which do not yield sufficient benzene are diluted to the requisite volume with scintillation grade benzene. The quantity of benzene necessary is read off the nomogram shown in Fig. 2-19.

2 ml of the scintillation solution is then added to the benzene and the screw cap securely fitted. (For standards and backgrounds which are to be monitored over extended periods it is necessary to seal the cap with epoxy resin glue to eliminate evaporative losses). The concentrations of PPO, the primary scintillant and POPOP, the secondary scintillant are 20g/l^{-1} and 1.25g/l^{-1} respectively in toluene solvent. Some of the samples prepared were counted in 5 ml geometry vials. The scintillation cocktail contains 4 ml of sample benzene and 1 ml of scintillation solution. As for 10 ml geometry vials, certain samples require addition of "dead" benzene to make up the standard volume for counting, the quantity required being read off a graph similar to Fig. 2-19.

2.5.4 Background count rate (See Appendix 1)

The automatic cycling mode of the scintillation spectrometer enables assessment of the background and modern count rates concurrently with sample counting. The benzene for a background sample can be prepared from materials containing no radiocarbon, such as coal or marble chips, or is available directly as scintillation grade benzene. The

FIGURE 2-19: Nomogram for preparation of standard 10ml. counting vial



average counting time for an individual batch of six samples, plus background and standard vials, is 2500-3000 minutes per sample. Typical sets of results for marble and scintillation grade benzene background vials are given in Tables 2-4 and 2-5. Based on these data, the background count rates used in the calculation of the radiocarbon ages are therefore

CHANNEL 1 : 3.63 ± 0.01 c.p.m.

CHANNEL 2 : 3.93 ± 0.01 c.p.m.

CHANNEL 3 : 7.44 ± 0.01 c.p.m.

The background count rates in the three counting channels for 5 ml geometry samples have also been monitored. The results are as follows

CHANNEL 1 : 2.31 ± 0.01 c.p.m.

CHANNEL 2 : 2.36 ± 0.01 c.p.m.

CHANNEL 3 : 4.49 ± 0.01 c.p.m.

2.5.5 Quench-efficiency calibration

The distortion of the ^{14}C pulse height spectrum by impurities in the scintillation cocktail can, if uncorrected, lead to inaccurate radiocarbon dates. This distortion is, as will be described shortly, a fairly small effect but nevertheless requires correction so that only count rates from a "normalised" pulse height spectrum are compared.

There are two principal methods of quench-efficiency calibration, the external standard method and the sample channels ratio method. In the former a high activity source, in this case ^{226}Ra , is brought up close to the vial in the counting chamber. Compton electrons are produced in the scintillation medium and these produce light pulses

TABLE 2-4

BACKGROUND DATA 1 - MARBLE

Date of count	Channel 1 count rate c.p.m., $\pm 1\sigma$	Channel 2 count rate c.p.m., $\pm 1\sigma$	Channel 3 count rate c.p.m., $\pm 1\sigma$
09.07.75	3.58 \pm 0.03	3.80 \pm 0.03	7.25 \pm 0.04
16.09.75	3.66 \pm 0.04	3.93 \pm 0.04	7.48 \pm 0.06
30.09.75	3.63 \pm 0.04	3.94 \pm 0.04	7.50 \pm 0.06
14.10.75	3.60 \pm 0.04	3.93 \pm 0.04	7.42 \pm 0.06
28.10.75	3.59 \pm 0.03	3.87 \pm 0.03	7.36 \pm 0.05
18.11.75	3.68 \pm 0.04	3.90 \pm 0.04	7.44 \pm 0.06
03.12.75	3.61 \pm 0.04	3.93 \pm 0.03	7.38 \pm 0.04
23.12.75	3.71 \pm 0.03	3.93 \pm 0.03	7.49 \pm 0.04
05.01.76	3.61 \pm 0.04	4.02 \pm 0.04	7.47 \pm 0.06
09.01.76	3.65 \pm 0.03	3.96 \pm 0.03	7.50 \pm 0.04
23.01.76	3.63 \pm 0.03	3.99 \pm 0.03	7.49 \pm 0.04
05.02.76	3.63 \pm 0.04	3.88 \pm 0.04	7.40 \pm 0.06
19.02.76	3.63 \pm 0.04	3.88 \pm 0.04	7.38 \pm 0.06
05.03.76	3.67 \pm 0.04	3.95 \pm 0.04	7.50 \pm 0.06
19.03.76	3.72 \pm 0.04	3.99 \pm 0.04	7.59 \pm 0.05
29.03.76	3.65 \pm 0.04	3.87 \pm 0.04	7.41 \pm 0.05
12.04.76	3.68 \pm 0.05	3.92 \pm 0.05	7.44 \pm 0.07
15.04.76	3.56 \pm 0.04	3.99 \pm 0.04	7.52 \pm 0.06
Mean value	3.63 \pm 0.01	3.93 \pm 0.01	7.44 \pm 0.01

TABLE 2-5 BACKGROUND DATA 2 - SCINTILLATION GRADE

BENZENE

Date of Count	Channel 1 count rate c.p.m. $\pm 1\sigma$	Channel 2 count rate c.p.m. $\pm 1\sigma$	Channel 3 count rate c.p.m. $\pm 1\sigma$
18.02.77	3.61 \pm 0.04	3.95 \pm 0.04	7.47 \pm 0.05
05.03.77	3.61 \pm 0.04	3.88 \pm 0.04	7.41 \pm 0.05
24.03.77	3.65 \pm 0.04	3.92 \pm 0.04	7.49 \pm 0.05
08.04.77	3.68 \pm 0.04	3.95 \pm 0.04	7.54 \pm 0.05
26.04.77	3.65 \pm 0.04	3.94 \pm 0.04	7.48 \pm 0.05
11.05.77	3.58 \pm 0.04	3.87 \pm 0.04	7.36 \pm 0.05
Mean value	3.63 \pm 0.02	3.92 \pm 0.02	7.46 \pm 0.02

TABLE 2-6 QUENCH-EFFICIENCY CALIBRATION

Sample	Channel 1 count rate c.p.m. $\pm 1\sigma$	Channel 2 count rate c.p.m. $\pm 1\sigma$	Channel 3 count rate c.p.m. $\pm 1\sigma$	Ratio 1/2 $\pm 1\sigma$	Relative efficiency %
Standard	25.24 \pm 0.08	33.44 \pm 0.08	58.91 \pm 0.12	0.756 \pm 0.003	100
1	29.07 \pm 0.09	29.42 \pm 0.09	58.61 \pm 0.13	0.988 \pm 0.004	99.3
2	29.64 \pm 0.09	28.29 \pm 0.09	57.94 \pm 0.13	1.048 \pm 0.005	98.6
3	29.96 \pm 0.09	25.87 \pm 0.09	56.82 \pm 0.13	1.158 \pm 0.005	96.4
4	31.39 \pm 0.10	22.95 \pm 0.09	55.90 \pm 0.13	1.390 \pm 0.007	94.8
5	33.10 \pm 0.10	19.83 \pm 0.08	52.99 \pm 0.13	1.669 \pm 0.008	89.9
6	34.19 \pm 0.10	18.33 \pm 0.07	52.66 \pm 0.12	1.865 \pm 0.008	89.4
7	35.25 \pm 0.09	14.40 \pm 0.07	49.78 \pm 0.12	2.448 \pm 0.013	84.4
8	35.32 \pm 0.09	8.07 \pm 0.05	43.28 \pm 0.12	4.377 \pm 0.029	73.4
9	31.32 \pm 0.09	4.18 \pm 0.05	36.39 \pm 0.10	7.492 \pm 0.092	61.9
10	31.95 \pm 0.09	4.00 \pm 0.05	35.61 \pm 0.10	7.988 \pm 0.102	60.4
11	30.75 \pm 0.09	3.49 \pm 0.04	34.68 \pm 0.10	8.811 \pm 0.104	59.0

which are detected and registered. The pulse height spectrum of the high activity Compton electron source will also be affected by the quench material and thus, depending on the amount of quencher present in the sample, the ratio of the number of counts registered in two channels will vary and since the source producing the Compton electrons is of high activity the statistical uncertainty on the ratio is very small. It was, however, found that the effects of quenching agents, present in virtually all the samples analysed, were too small to have any influence on the external standard ratio.

The sample channels ratio method used in this work was based on the ratio of the count rates for the two narrow channels, that is channel 1 to channel 2, and was therefore a direct measure of the influence of quenching agents on the ^{14}C pulse height spectrum.

A solution of known activity, 9.82 d.p.m./ml, was prepared from a ^{14}C -toluene spike of initial activity 5.61×10^5 d.p.m./g and freshly opened scintillation grade benzene. Acetone was selected as the quenching agent. A series of samples of 10 ml counting geometry, containing increasing amounts of quencher was made up and along with an unquenched sample, the batch was counted for >4000 minutes. It was assumed that the channel 1 to channel 2 ratio and the channel 3 total sample count rate corresponded to ideal counting conditions ($E = 100\%$). The results are given in Table 2-6.

The calibration line adopted for quench correction is a polynomial function derived using a NAGLIB subroutine programme available on the NUMAC computing network. This

programme will select the best fitting polynomial function for n pairs of observations, of maximum order $n-1$. The resultant polynomial is of the general form

$$f(x) = a_1 + a_2x + a_3x^2 + \dots + a_mx^{m-1}$$

It is found that the best fitting function is

$$E = 109.78 - 12.80R + 1.20R^2$$

where E is the efficiency relative to the unquenched standard and R is the channels ratio. A graph of this function is given in Fig. 2-20. In practice, however, very few samples give a channels ratio of >1.0 and since over the range $0.8 \leq R \leq 2.0$ the quench calibration can be expressed more precisely as a straight line, of correlation coefficient $r = -0.987$, the function employed for the normalisation of sample count rates is:

$$E = 108.30 - 10.04R$$

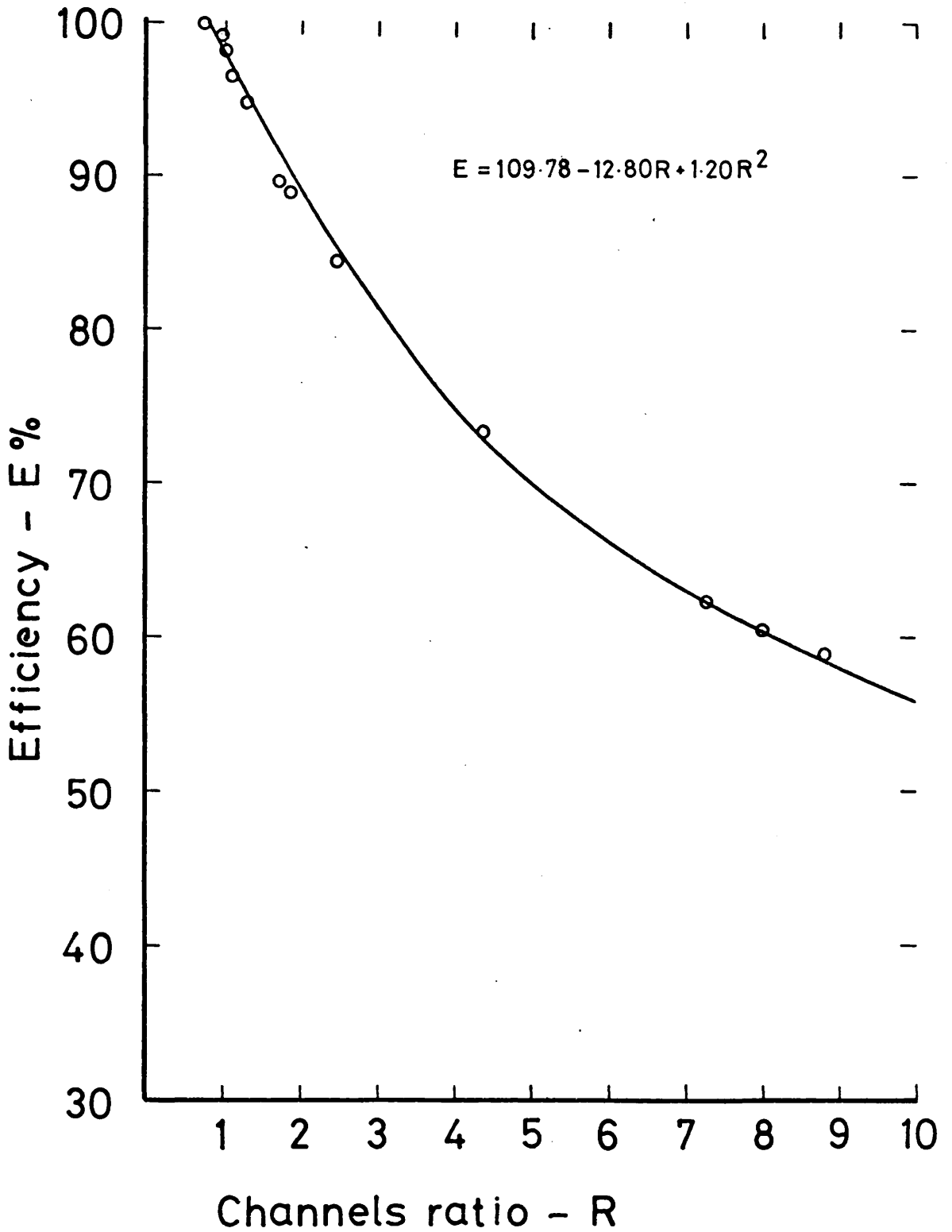
This function is shown in Fig. 2-21.

2.5.6 Modern standard count rates

The standard used for radiocarbon dating is oxalic acid distributed by the National Bureau of Standards (N.B.S.) in Washington. The primary dating standard, 1890 wood, is assumed to have a "natural level" of ^{14}C activity. It has been observed that 95% of the N.B.S. standard activity in 1958 equals the decays corrected ^{14}C activity of the primary standard (Broecker and Olson, 1959).

The oxalic acid may be prepared for counting in one of two ways; firstly by direct combustion, or secondly by wet oxidation with acidified saturated potassium permanganate solution. The latter method is the one used in this research.

FIGURE 2-20: Quench calibration curve



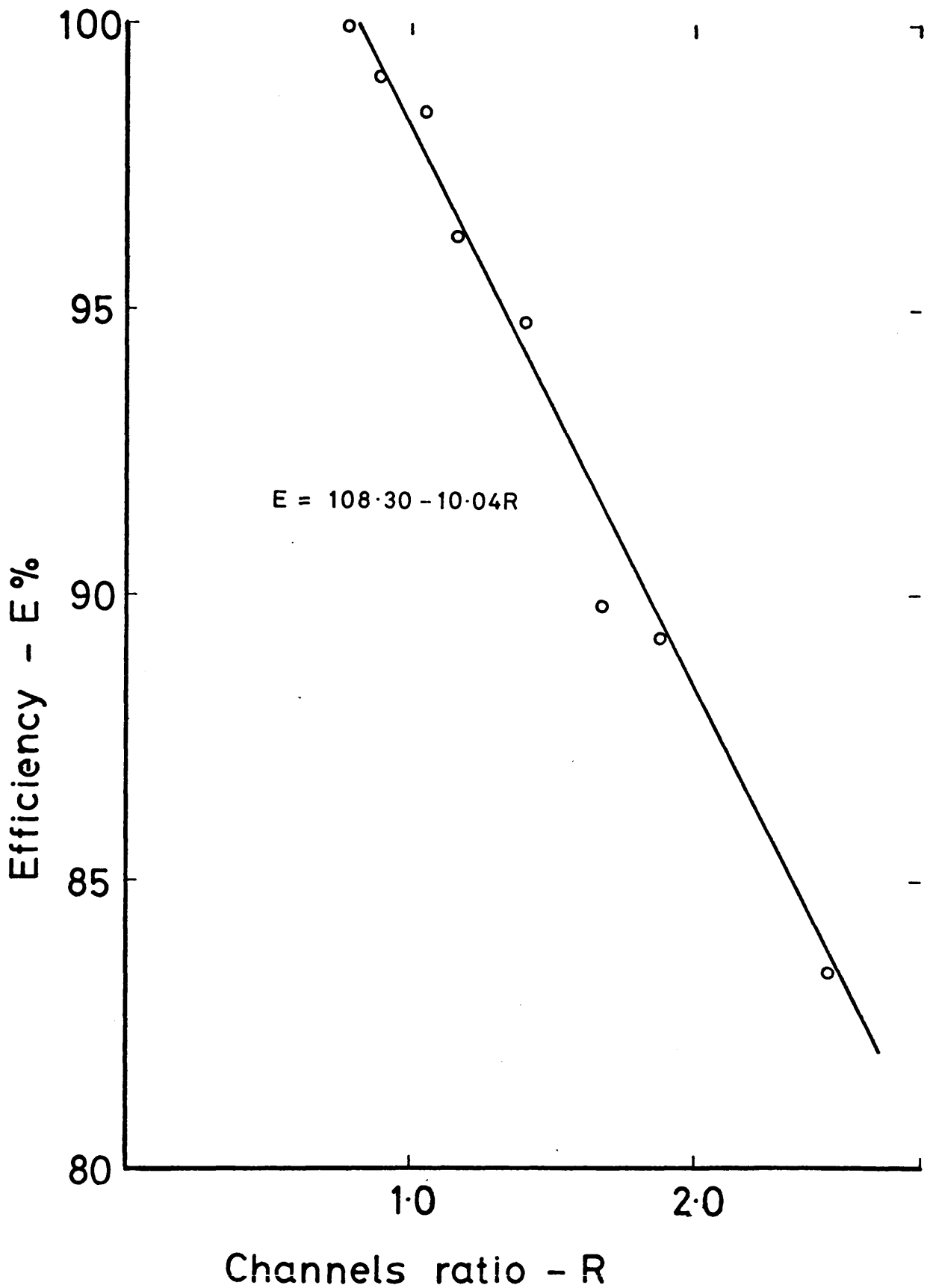


FIGURE 2-21 : Quench calibration line
(for samples with $R > 2.5$
i.e. small quench effect)

Saturated acidified potassium permanganate (5ml conc. HNO_3 per litre of solution) is slowly added to the reaction flask containing a weighed quantity of standard oxalic acid ($\text{C}_2\text{O}_4\text{H}_2 \cdot 5\text{H}_2\text{O}$). The oxidation apparatus is shown in Fig. 2-22. Prior to addition of the oxidising solution the reaction flask and CO_2 collection system is pumped on low vacuum to better than 10^{-1} torr. The reaction mixture is stirred continuously and product CO_2 collected in the traps on the main CO_2 collection system. One difference in the collection of CO_2 from the oxidation is that there is not continuous pumping as this would increase the quantity of water which distils into the collection system, resulting in blockage of the water traps. Addition of permanganate solution is continued until the reaction mixture becomes brown due to the precipitation of manganese dioxide.

The modern standard counting vial is included in each batch of samples prepared for counting. After the observed count rate has been corrected for background, quench effects and dilution the following additional corrections are made for isotopic fractionation and radioactive decay.

(1) the isotopic fractionation correction is

based on the mean value obtained for standard oxalic acid derived CO_2 , namely -19.0‰ with respect to P.D.B. All modern standard activities are therefore corrected for fractionation relative to -19.0‰ . Thus

$$A' = A \left[1 - \frac{2(\delta^{13}\text{C} + 19)}{1000} \right]$$

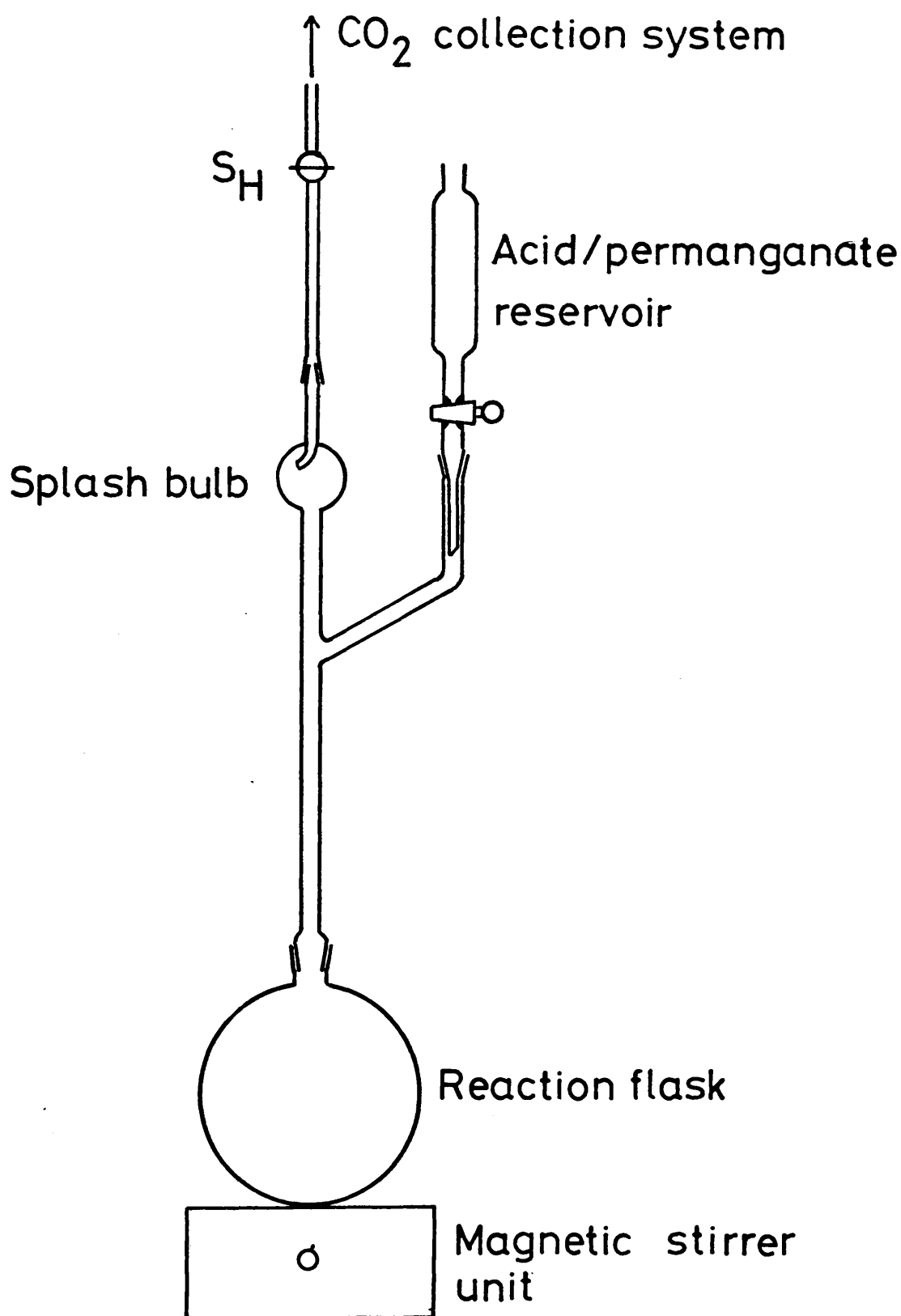


FIGURE 2-22: Sample hydrolysis/wet oxidation system

where A is the observed modern standard activity corrected for quench effects and dilution, and $\delta^{13}\text{C}$ is the $^{13}\text{C}/^{12}\text{C}$ ratio in the CO_2 relative to P.D.B.

- (2) The international standard activity is taken as 95% of the activity at 1st January, 1958. Thus present day activities must be corrected for decay since that time. The decay rate is $0.12^0/00$ per year. So

$$A^0 = A' \left[1 + \frac{0.12(t-t_0)}{1000} \right]$$

where $t-t_0$ is the number of years between the date of measurement, t , and 1958, t_0 .

A typical set of count rates for a particular modern standard obtained over a period of 12 months is presented in Table 2-7. From these data, it is obvious that the detection system has a high degree of long-term stability. The gradual increase in the channels ratio is most probably due to increased quenching by oxygen in the counting vial. Williams (1977) has suggested that this effect may be minimised by sealing the sample with an internal argon atmosphere. It may also be noted that evaporative loss of sample is not evident from these data. A number of modern standard samples were prepared during this research and the appropriate results are given in Table 2-8. (The count rate for sample 426/B was determined under slightly different conditions and is thus not representative of the established modern standard count rate).

TABLE 2-7

MODERN STANDARD - M6

Date of count	Net count rate c.p.m. $\pm 1\sigma$	Channels Ratio
28.10.75	63.70 \pm 0.14	0.806
18.11.75	63.42 \pm 0.17	0.815
03.12.75	63.28 \pm 0.11	0.828
23.12.75	63.30 \pm 0.13	0.820
05.01.76	63.12 \pm 0.19	0.816
09.01.76	63.05 \pm 0.12	0.811
23.01.76	63.41 \pm 0.12	0.832
05.02.76	63.23 \pm 0.17	0.823
19.02.76	63.35 \pm 0.16	0.834
05.03.76	63.10 \pm 0.16	0.833
19.03.76	63.34 \pm 0.18	0.833
25.03.76	63.19 \pm 0.21	0.840
29.03.76	63.19 \pm 0.17	0.835
15.04.76	63.30 \pm 0.16	0.856
03.05.76	63.14 \pm 0.15	0.851
20.09.76	63.28 \pm 0.17	0.844
Mean value	63.28 \pm 0.04	0.830

TABLE 2-8

N. B. S. OXALIC ACID STANDARDS

Sample	$\delta^{13}\text{C}$ ‰ w.r.t. P.D.B.	Count rate c.p.m. $\pm 1\sigma$
426/B	-23.0	63.96 \pm 0.08
M6	-19.8	63.34 \pm 0.04
G99	-28.3	63.48 \pm 0.15
G194	-26.4	63.54 \pm 0.04
25.4.75*	-17.7	33.22 \pm 0.08

* 5 ml geometry standard

2.6 Calculation of results

^{14}C enrichments are calculated relative to 95% of the activity of the secondary dating standard, N.B.S. oxalic acid, and are expressed in terms of $\delta^{14}\text{C}$ and $\Delta^{14}\text{C}$. The former term refers to the concentration of ^{14}C , with respect to the standard, prior to correction for isotopic fractionation. The calculation is as follows:

$$\delta^{14}\text{C} = \left[\frac{\alpha \cdot A_s - 0.95A^0}{0.95A^0} \right] \times 1000 \text{ } \text{‰}$$

where α is the dilution factor (usually >1)

A_s is the mean sample count rate in counts per minute and A^0 is the mean modern standard count rate in counts per minute.

The adjustment for isotopic fractionation is performed using the formula of Broecker and Olson (1961):

$$\Delta^{14}\text{C} = \delta^{14}\text{C} - (2\delta^{13}\text{C} + 50) \left(1 + \frac{\delta^{14}\text{C}}{1000} \right) \text{ } \text{‰}$$

$$\text{where } \delta^{13}\text{C} = \frac{{}^{13}\text{C}/{}^{12}\text{C}_{\text{SAMPLE}} - {}^{13}\text{C}/{}^{12}\text{C}_{\text{P.D.B.}}}{{}^{13}\text{C}/{}^{12}\text{C}_{\text{P.D.B.}}}$$

$\delta^{14}\text{C}$ and $\Delta^{14}\text{C}$ are usually quoted to $\pm 1\sigma$ related solely to the random uncertainties associated with the sample, modern and background rates, and with mass spectrometric measurements. The error on $\delta^{14}\text{C}$ is calculated using the formula of Callow et al., (1965).

$$\pm 1\sigma (\delta^{14}\text{C}) = \pm \frac{1000 \cdot \alpha \cdot A_s}{0.95A^0} \left[\left(\frac{\sigma_{A_s}}{A_s} \right)^2 + \left(\frac{\sigma_{A^0}}{A^0} \right)^2 \right]^{\frac{1}{2}}$$

The error on $\Delta^{14}\text{C}$, from the same source is calculated from the relationship

$$\pm 1\sigma (\Delta^{14}\text{C}) = \pm \left\{ \frac{1}{4} \left[\left(1 - \frac{(2\delta^{13}\text{C} + 50)}{1000} \right)^2 \cdot \sigma^2(\delta^{14}\text{C}) + \left(1 + \frac{\delta^{14}\text{C}}{1000} \right)^2 \cdot \sigma^2(\delta^{13}\text{C}) \right] \right\}^{\frac{1}{2}}$$

The 1962 conference on radiocarbon dating at Cambridge resolved to maintain the practice of using the 5568 year half life, despite improved measurements giving a mean value of 5730 years (Godwin, 1962). The reason for this decision, which is still being followed, was to avoid the confusion which would arise if the volumes of data published required revision. The conversion of ages based on the short half life to those based on the 5730 year half life is achieved by multiplication by 1.03. It is also customary to report radiocarbon age determinations in years B.P. (before present), where "present" is taken as 1950.

Therefore the age T yrs B.P. of a sample is given by

$$T = \frac{1}{\lambda} \ln \left[\frac{1}{1 + (\Delta^{14}\text{C} \cdot 10^{-3})} \right]$$

where λ is the decay constant given by $\lambda = \frac{\ln 2}{t_{\frac{1}{2}}}$

$1/\lambda$ is often called the mean life time of radiocarbon and has a value of 8033 years. The limits of the age at $\pm 1\sigma$ level are given by

$$(T + t_1, T - t_2) = \frac{1}{\lambda} \ln \left[\frac{1}{1 + \left(\frac{\Delta^{14}\text{C} + \sigma(\Delta^{14}\text{C})}{1000} \right)} \right]$$

A Fortran IV computer programme has been written to perform the above calculations. The programme is presented in Appendix 2.

CHAPTER 3

RESULTS

The samples analysed in this research can be classified in three ways: firstly, intercalibration and replicate samples aimed at assessing the accuracy and reproducibility of the laboratory procedures, secondly archaeological samples and finally geochemical samples. In the tables and graphs which follow, the error ($\pm 1\sigma$) quoted on individual radiocarbon determinations is that uncertainty arising solely from counting statistics.

3.1 Intercalibration samples and replicate analyses

A series of intercalibration samples has been analysed during the course of this research work. Samples for analysis have been supplied by the Scottish Universities Research and Reactor Centre radiocarbon laboratory (SRR) and by the La Jolla radiocarbon laboratory (LJ). In addition, SRR has performed "check" analyses on some of the geochemical samples. Several samples have also been analysed in the gas counting radiocarbon laboratory at Glasgow (GU1). The results of the intercalibration samples are given in Table 3-1-1. In general, there is good agreement between laboratories. There is, however, one notable exception, namely West Runton 6. Four analyses on this sample by SSR and a further three by the Groningen laboratory all indicate a "minimum age" for this sample. The fact that both Glasgow laboratories have independently produced a considerably younger age suggests that some

contaminant has been incorporated into the sample. The difference in age between SRR and Glasgow corresponds to a ~4% contamination with modern carbon.

The assessment of laboratory reproducibility was performed by replicate analysis. A section of wood, Ynyslas 1, which had previously undergone sequential growth increment analysis was selected as the replicate "standard". The pine wood section was chopped up manually and then ground in a mill producing a roughly homogeneous sample. Replicate analyses, including chemical pretreatment, were then performed on this material. The results are presented in Table 3-1-2. A second set of replicate analyses was performed using rice as the replicate standard. The results of these measurements are given in Table 3-1-3. In addition to the normal mass spectrometric measurement of the carbon isotope enrichment, samples of CO_2 and benzene were submitted for $^{13}\text{C}/^{12}\text{C}$ ratio measurement using an AEI 902S mass spectrometer. The abundance ratios are listed in columns 5 and 6 of Table 3-1-3.

A more accurate determination of the stable carbon isotope ratio for benzene may be obtained if the benzene can be quantitatively converted to CO_2 . The benzene derived CO_2 can then be analysed using a double collector instrument and the result, $\delta^{13}\text{C}_{\text{BE}}$, when compared with the enrichment obtained from sample-derived CO_2 , $\delta^{13}\text{C}_{\text{CE}}$, should indicate whether there is any fractionation during benzene synthesis. The micro-combustion system constructed for conversion of benzene to CO_2 was calibrated

by replicate analyses of scintillation grade benzene and wood cellulose. Table 3-1-4 gives the results of 30 complete analyses on scintillation grade benzene. The data for wood cellulose are given in Table 3-1-5.

The extent of possible fractionation effects in the benzene synthesis procedure was investigated during routine analysis of tree-ring sections Stolford 4 and Stolford 5. The stable isotope data for these sections are presented in Tables 3-1-6 and Tables 3-1-7. For Stolford 4 samples, both single and double collector mass spectrometric measurements were recorded. (These results are presented in isolation from the corresponding ^{14}C data since the implications of the findings are particularly relevant to the interpretation of the replicate analysis data).

3.2 Archaeological samples

Archaeological samples have been submitted to the laboratory during the period of research. The results of the age determinations are given in Table 3-2-1. The samples from excavations at South Cadbury (GU 645 - GU 651) were submitted by L. Alcock and formed the basis of an intercalibration exercise with SRR. Accordingly these data are discussed in detail in Chapter 6. Samples GU 652, GU 653, GU 654 and GU 793 were collected personally during the 1976 British-Ecuadorean expedition to the Los Tayos Caves and the background information to these samples is also discussed in Chapter 6.

3.3 Geochemical samples

^{14}C assay of seven "floating" chronologies was performed during this research, six of which were from submerged forest sites along the west coast of the United Kingdom, the other section being recovered from an archaeological site in North East Scotland. Before sequential growth-increment analysis was carried out, however, wood samples, collected from a number of submerged forest sites, were dated to yield an indication of the range of ages which could be expected from this source. The results of these analyses are given in Table 3-3-1. Also included in this table are dates for two oak wood samples Newtown 1 and Rheidol 1. These tree stumps were collected from river bed gravel and their estimated age was pre-glacial!

The results of the sequential growth-ring analyses for tree-ring sections Borth 1 (BH 1), Borth 4 (BH 4), Borth 6 (BH 6), Ynyslas 1 (YS 1), Stolford 4 (SD 4), Stolford 5 (SD 5) and Cullykhan 1 (CK 1) are presented in Tables 3-3-2 - 3-3-8. The analysis of Cullykhan 1 and Borth 1 was shared between the Glasgow laboratory and the East Kilbride laboratory (SRR). In the former, pretreatment, benzene synthesis and mass spectrometric assay were performed at SRR whilst samples were counted at the Glasgow laboratory. In the latter, pretreatment and counting were carried out at Glasgow, the benzene synthesis and mass spectrometric assay being performed at SRR. The data are also presented graphically in Figs. 3-3-1 - 3-3-7. In each graph the conventional radio-carbon age is plotted against growth-ring number, the

- growth-rings being counted from a marker pin, at or near the centre of the tree section, inserted at the time of dendrochronological measurement. Thus, on the axis of abscissae, time increases to the right. The horizontal error bars depict the number of annual growth increments in the sample, the vertical error bars expressing the one sigma counting error associated with each measurement.

TABLE 3-1-1

INTERCALIBRATION SAMPLES

Sample description	Conventional ^{14}C age $\pm 1\sigma$ (or $\Delta^{14}\text{C} \pm 1\sigma$)	
	This laboratory	Other laboratory
Hitchcock wood	GU 656 : 166 ± 42	LJ 3451 : 142 ± 68
		LJ 3471 : 221 ± 89
Charcoal	GU 657 : $\Delta^{14}\text{C} = 5.01 \pm 5.62\text{‰}$	LJ 3448 : $\Delta^{14}\text{C} = -3.8 \pm 6.1\text{‰}$
Wood	GU 658 : 3505 ± 58	LJ 3453 : 3793 ± 61
		GU1 : 3551 ± 64
West Runton 6 wood	GU 660 : $26,450 \pm 420$	SRR 225-228 : $>47,500$
	GU 661 : $26,000 \pm 480$	GrN 6819 : $>54,200$
		GrN 6892 : $>47,400$
		GU1 : 21723 ± 532
Penzance Wood	GU 659 : 4093 ± 50	SRR 714 : 4278 ± 50
		GU1 : 4025 ± 67
Ynyslas 1 wood replicate standard	Mean of 24 analyses : 4875 ± 86	SRR : 4926 ± 52
		GU1 (mean) 4890 ± 260
Clarach 1 wood	GU 660 : 5592 ± 143	GU1 (mean) 5472 ± 260
Borth 4 wood rings 51 - 60	GU 746 : 3798 ± 30	SRR : 3796 ± 51
Borth 6 wood rings 141-150	GU 730 : 3960 ± 46	SRR : 4016 ± 53
Borth 6 wood rings 151-160	GU 731 : 3738 ± 43	SRR : 3958 ± 52

TABLE 3-1-2

YNYSLAS 1 REPLICATE ANALYSES

Sample Number	$\delta^{14}\text{C} \pm 1\sigma$ ‰	$\Delta^{14}\text{C} \pm 1\sigma$ ‰	$\delta^{13}\text{C} \pm 1\sigma$ ‰ w.r.t. P.D.B.	Age $\pm 1\sigma$ years B.P. $t_{1/2} = 5568\text{y}$	Age years B.P. $t_{1/2} = 5730\text{y}$
GU 669	-452.20 \pm 3.49	-453.29 \pm 3.50	-24.00 \pm 0.05	4825 \pm 52	4969
GU 670	-465.29 \pm 2.72	-465.92 \pm 2.72	-24.40 \pm 0.05	5012 \pm 41	5163
GU 671	-457.83 \pm 2.61	-458.69 \pm 2.61	-24.20 \pm 0.05	4904 \pm 39	5052
GU 672	-463.97 \pm 2.56	-465.36 \pm 2.57	-23.70 \pm 0.05	5004 \pm 39	5154
GU 673	-451.93 \pm 3.06	-452.91 \pm 3.06	-24.10 \pm 0.05	4819 \pm 45	4964
GU 674	-464.43 \pm 2.44	-465.29 \pm 2.45	-24.20 \pm 0.05	5003 \pm 37	5152
GU 675	-451.85 \pm 2.87	-453.17 \pm 2.87	-23.80 \pm 0.05	4823 \pm 42	4967
GU 676	-450.01 \pm 2.69	-451.00 \pm 2.70	-24.10 \pm 0.05	4791 \pm 40	4934
GU 677	-447.24 \pm 2.26	-448.35 \pm 2.26	-24.00 \pm 0.05	4752 \pm 33	4895
GU 678	-459.25 \pm 2.49	-460.44 \pm 2.47	-23.90 \pm 0.05	4930 \pm 37	5078
GU 679	-455.13 \pm 2.23	-456.55 \pm 2.23	-23.70 \pm 0.05	4873 \pm 33	5019
GU 680	-448.01 \pm 2.35	-449.23 \pm 2.35	-23.90 \pm 0.05	4765 \pm 35	4908

TABLE 3-1-2

XNYSLAS 1 REPLICATE ANALYSES (cont'd)

Sample Number	$\delta^{14}\text{C} \pm 1\sigma$ ‰	$\Delta^{14}\text{C} \pm 1\sigma$ ‰	$\delta^{13}\text{C} \pm 1\sigma$ ‰ w.r.t. P.D.B.	Age $\pm 1\sigma$ years BP $t_1 = 5568\text{y}$ t_2	Age years B.P. $t_1 = 5730\text{y}$ t_2
GU 681	-454.50 \pm 2.45	-455.92 \pm 2.46	-23.70 \pm 0.05	4863 \pm 36	5009
GU 682	-456.91 \pm 2.29	-458.32 \pm 2.29	-23.70 \pm 0.05	4899 \pm 34	5046
GU 683	-448.32 \pm 2.54	-449.53 \pm 2.55	-23.90 \pm 0.05	4770 \pm 37	4912
GU 684	-454.81 \pm 2.38	-456.12 \pm 2.38	-23.80 \pm 0.05	4866 \pm 35	5012
GU 685	-446.75 \pm 2.84	-447.96 \pm 2.85	-23.90 \pm 0.05	4747 \pm 42	4889
GU 686	-456.46 \pm 2.05	-457.55 \pm 2.05	-24.00 \pm 0.05	4887 \pm 30	5034
GU 687	-448.51 \pm 2.38	-449.61 \pm 2.38	-24.00 \pm 0.05	4771 \pm 35	4914
GU 688	-461.98 \pm 1.95	-462.95 \pm 1.95	-24.10 \pm 0.05	4968 \pm 29	5117
GU 689	-450.11 \pm 1.91	-450.77 \pm 1.92	-24.40 \pm 0.05	4788 \pm 28	4931
GU 690	-461.78 \pm 1.94	-460.59 \pm 1.94	-26.10 \pm 0.05	4933 \pm 29	5081
GU 691	-453.05 \pm 1.91	-454.25 \pm 1.92	-23.90 \pm 0.05	4839 \pm 28	4984
GU 692	-446.57 \pm 2.26	-447.46 \pm 2.26	-24.20 \pm 0.05	4739 \pm 33	4881

TABLE 3-1-3

RICE STANDARD REPLICATE ANALYSES

Sample Number	$\delta^{14}\text{C} \pm 1\sigma$ ‰	$\Delta^{14}\text{C} \pm 1\sigma$ ‰	$\delta^{13}\text{C} \pm 1\sigma$ ‰ w.r.t. P.D.B.	$^{13}\text{C}/^{12}\text{C}$ ‰ CO_2	$^{13}\text{C}/^{12}\text{C}$ ‰ C_6H_6
GU 693	416.44 ± 3.41	413.32 ± 3.42	-23.90 ± 0.05		
GU 694	397.40 ± 3.36	394.61 ± 3.36	-24.00 ± 0.05		
GU 695	415.39 ± 3.36	413.41 ± 3.36	-24.30 ± 0.05		1.07
GU 696	418.22 ± 3.51	419.36 ± 3.50	-25.40 ± 0.05		1.08
GU 697	401.96 ± 3.42	401.96 ± 3.42	-25.00 ± 0.05	1.14	1.08
GU 698	422.33 ± 3.60	418.92 ± 3.61	-23.80 ± 0.05	1.07	1.09
GU 699	404.38 ± 3.42	398.20 ± 3.44	-22.80 ± 0.05	1.13	
GU 700	391.52 ± 3.63	389.02 ± 3.64	-24.10 ± 0.05	1.14	
GU 701	397.24 ± 3.42	394.45 ± 3.43	-24.00 ± 0.05		
GU 702	400.79 ± 3.39	397.43 ± 3.40	-23.80 ± 0.05		

TABLE 3-1-4

CALIBRATION OF MICRO-COMBUSTION SYSTEM -
 REPLICATE MEASUREMENTS ON SCINTILLATION

GRADE BENZENE

Analysis Number	Yield %	$\delta^{13}\text{C} + 1\sigma$ o/oo w.r.t. P.D.B.	Analysis Number	Yield %	$\delta^{13}\text{C} + 1\sigma$ o/oo w.r.t. P.D.B.
1	33	-24.81 ± 0.05	16	67	-24.63 ± 0.05
2	99	-25.27 ± 0.05	17	64	-24.75 ± 0.05
3	50	-25.02 ± 0.05	18	68	-24.72 ± 0.05
4	42	-24.73 ± 0.05	19	67	-24.48 ± 0.05
5	58	-24.67 ± 0.05	20	63	-24.69 ± 0.05
6	67	-24.51 ± 0.05	21	56	-24.29 ± 0.05
7	79	-24.35 ± 0.05	22	53	-24.52 ± 0.05
8	40	-24.59 ± 0.05	23	30	-24.44 ± 0.05
9	60	-24.45 ± 0.05	24	48	-24.55 ± 0.05
10	58	-24.60 ± 0.05	25	61	-24.36 ± 0.05
11	73	-24.51 ± 0.05	26	61	-24.81 ± 0.05
12	74	-24.65 ± 0.05	27	63	-24.51 ± 0.05
13	90	-24.60 ± 0.05	28	43	-24.20 ± 0.05
14	60	-24.72 ± 0.05	29	67	-24.35 ± 0.05
15	65	-24.76 ± 0.05	30	34	-24.03 ± 0.05

TABLE 3-1-5 CALIBRATION OF MICRO-COMBUSTION SYSTEM -
REPLICATE ANALYSES ON WOOD CELLULOSE

Analysis Number	$\delta^{13}\text{C} \pm 1\sigma$ ‰ w.r.t. P.D.B.
1	-24.57 ± 0.05
2	-24.57 ± 0.05
3	-24.62 ± 0.05
4	-24.80 ± 0.05
5	-24.77 ± 0.05
6	-24.51 ± 0.05
7	-24.59 ± 0.05
8	-24.65 ± 0.05

TABLE 3-1-6

STABLE CARBON ISOTOPE DATA FOR STOLFORD 4

Sample Number	CO ₂ %	Chemical Yield C ₂ H ₂ : C ₂ H ₂ → C ₆ H ₆ %	Micro-combustion yield, C ₆ H ₆ → CO ₂ %	¹³ C/ ¹² C Ratio C ₆ H ₆ %	Cellulose/CO ₂ ^δ ¹³ CCE o/oo wrt PDB	Benzene/CO ₂ ^δ ¹³ CBE o/oo wrt PDB	Difference ^δ ¹³ CBE- ^δ ¹³ CCE o/oo
GU 755	89	79	46	1.10	-24.06	-23.96	+0.10
GU 756	90	83	48	1.06	-23.98	-23.87	+0.11
GU 757	90	87	73	1.01	-24.41	-24.28	+0.13
GU 758	88	84	88	1.05	-24.20	-23.92	+0.28
GU 759	85	81	80	1.07	-23.94	-24.20	-0.26
GU 760	82	79	66	1.04	-24.06	-23.85	+0.21
GU 761	85	78	83	1.10	-23.10	-23.24	-0.14
GU 762	85	86	70	1.02	-22.79	-23.15	-0.36

TABLE 3-1-7

STABLE CARBON ISOTOPE DATA FOR STOLFORD 5

Sample Number	Chemical Yield		Micro-combustion yield $C_6H_6 \rightarrow CO_2$ %	$\delta^{13}C$ value		Difference $\delta^{13}C_{BE} - \delta^{13}C_{CE}$ ‰
	$CO_2 \rightarrow C_2H_2$ %	$C_2H_2 \rightarrow C_6H_6$ %		$\delta^{13}C_{CE}$ ‰ w.r.t. P.D.B.	$\delta^{13}C_{BE}$ ‰	
GU 763	93	77		-23.91		
GU 764	82	85	75	-23.76	-24.16	-0.40
GU 765	89	78	62	-23.56	-23.84	-0.28
GU 766	86	88	64	-23.57	-22.57	+1.00
GU 767	86	73	53	-23.32	-23.90	-0.58
GU 768	83	86	68	-23.05	-23.35	-0.30
GU 769	96	95	88	-23.16	-23.62	-0.46
GU 770	83	73	60	-22.86	-23.81	-0.95
GU 771	89	83	66	-23.04	-23.61	-0.57
GU 772	91	79	54	-23.35	-23.84	-0.49
GU 773	85	84	45	-23.64	-23.78	-0.14
GU 774	88	65	67	-23.90	-24.37	-0.47
GU 775	82	84	87	-23.68	-23.87	-0.19
GU 776	89	80	78	-23.69	-23.97	-0.58

TABLE 3-1-7 STABLE CARBON ISOTOPE DATA FOR STOLFORD 5 (cont'd)

Sample Number	Chemical Yield CO ₂ → C ₂ H ₂ : C ₂ H ₂ → C ₆ H ₆ %	Micro-Combustion yield C ₆ H ₆ → CO ₂ %	¹³ C value δ ¹³ C _{CE} - δ ¹³ C _{BE} o/oo w.r.t. P.D.B.	Difference δ ¹³ C _{BE} - δ ¹³ C _{CE} o/oo
GU 777	89	76	-23.95	-0.42
GU 778	88	95	-23.77	-0.38
GU 779	89	63	-23.50	-0.42
GU 780	88	63	-24.05	-0.42
GU 781	88	77	-23.70	-0.12
GU 782	77	66	-23.57	-0.07
GU 784	80	65	-23.62	-0.29
GU 785	77	23	-23.42	-0.46
GU 786	61	53	-23.77	-0.04
GU 787	84	71	-23.78	-0.94
GU 788	87	67	-24.25	-0.22
GU 789	86		-29.94	
GU 790	74	75	-23.40	-0.36
GU 791	94	55	-24.69	+0.18

TABLE 3-2-1

ARCHAEOLOGICAL SAMPLES

Sample Number	Sample Code	Location	Material	years	Age $\pm 1\sigma$ B.P. (A.D. - B.C.)	$\delta^{13}\text{C} \pm 1\sigma$ ‰ w.r.t. P.D.B.
GU 645	SC/K 659 (i)	South Cadbury England (51°01'N, 2°32'W)	Carbonised wood	1814 \pm 31	(A.D. 136)	-24.60 \pm 0.05
GU 646	SC/K 659 (ii)	South Cadbury	Carbonised wood	1961 \pm 27	(11 B.C.)	-25.80 \pm 0.05
GU 647	SC/K 659(iii)	South Cadbury	Carbonised wood	1839 \pm 26	(A.D. 111)	-25.20 \pm 0.05
GU 648	SC/K 659 (iv)	South Cadbury	Carbonised wood	2214 \pm 43	(264 B.C.)	-24.80 \pm 0.05
GU 649	SC/K 659 (v)	South Cadbury	Carbonised grain	1949 \pm 26	(A.D. 1)	-24.10 \pm 0.05
GU 650	SC/K 659 (vi)	South Cadbury	Carbonised grain	1765 \pm 47	(A.D. 185)	-24.30 \pm 0.05
GU 651	SC/K 747(vii)	South Cadbury	Carbonised wood	1825 \pm 48	(A.D. 125)	-23.70 \pm 0.05

TABLE 3-2-1: ARCHAEOLOGICAL SAMPLES (cont'd)

Sample Number	Sample Code	Location	Material	Age ± 1σ years B.P. (A.D. - B.C.)	δ ¹³ C ± 1σ ‰ w.r.t. P.D.B.
GU 652	OM-S6	Teniente Ortiz Morona Santiago Ecuador (3°3'S, 78°2'W)	Carbonised wood	1012 ± 66 (A.D. 938)	-28.64 ± 0.05
GU 653	OMST 1-4	Teniente Ortiz Ecuador	Carbonised wood	235 ± 36 (A.D. 1714)	-26.70 ± 0.05
GU 654	OMST 1-5	Teniente Ortiz Ecuador	Carbonised wood	125 ± 60 (A.D. 1825)	-27.60 ± 0.05
GU 792	CK 3	Castle Point, Troup, Banffshire (57°41'7"N 2°17'26"W)	Wood	3107 ± 303 (1157 B.C.)	-25.10 ± 0.05
GU 793	MS-LT-1	Los Tayos Cave (3°19'S, 78°14'W)	Soil	δ ¹⁴ C = 2.58 ± 1.38‰	

TABLE 3-3-1 : RADIOCARBON DATES FOR SUBMERGED
FOREST SITES

Sample Number	Location	Age $\pm 1\sigma$ years B.P.
GU 662	Clarach-1	5592 \pm 143
GU 663	Stolford-1	4443 \pm 199
GU 664	Morecambe-1	7544 \pm 306
GU 665	Llanaber-1	734 \pm 52
GU 666	Alt Mouth-1	4351 \pm 46
GU 667	Newtown-1	885 \pm 83
GU 668	Rheidol-1	647 \pm 136

TABLE 3-3-2 BORTH 1 PINE - TREE-RING/RADIOCARBON ANALYSES

Sample Number	Growth rings	$\delta^{14}\text{C} + 1\sigma$ ‰	$\Delta^{14}\text{C} + 1\sigma$ ‰	$\delta^{13}\text{C} + 1\sigma$ ‰ w.r.t. P.D.B.	Age $\pm 1\sigma$ years B.P. $t_{1/2} = 5568\text{y}$	Age years B.P. $t_{1/2} = 5730\text{y}$
GU 703	0 - 20	-475.19 \pm 2.75	-476.13 \pm 2.76	-24.10 \pm 0.05	5167 \pm 42	5322
GU 704	21 - 30	-480.47 \pm 2.31	-481.41 \pm 2.31	-24.10 \pm 0.05	5249 \pm 36	5406
GU 705	31 - 40	-482.53 \pm 2.37	-483.26 \pm 2.37	-24.30 \pm 0.05	5277 \pm 37	5436
GU 706	41 - 50	-498.79 \pm 2.27	-499.89 \pm 2.27	-23.90 \pm 0.05	5540 \pm 37	5706
GU 707	51 - 60	-479.75 \pm 2.30	-480.89 \pm 2.31	-23.90 \pm 0.05	5240 \pm 36	5398
GU 708	61 - 70	-484.49 \pm 2.54	-485.63 \pm 2.55	-23.90 \pm 0.05	5314 \pm 40	5474
GU 709	71 - 80	-471.78 \pm 2.35	-473.26 \pm 2.36	-23.60 \pm 0.05	5124 \pm 36	5277
GU 710	81 - 90	-475.39 \pm 3.40	-476.54 \pm 5.42	-23.90 \pm 0.05	5174 \pm 84	5329

TABLE 3-3-3 BORTH 4 OAK - TREE-RING/RADIOCARBON ANALYSES

Sample Number	Growth rings	$\delta^{14}\text{C} + 1\sigma$ ‰	$\Delta^{14}\text{C} + 1\sigma$ ‰	$\delta^{13}\text{C} + 1\sigma$ ‰	Age $\pm 1\sigma$ years B.P. $t_{1/2} = 5568\text{y}$	Age years B.P. $t_{1/2} = 5730\text{y}$
GU 742	-15 - +10	-389.26 \pm 6.37	-387.92 \pm 6.35	-26.10 \pm 0.05	3917 \pm 84	4035
GU 743	11 - 30	-378.33 \pm 7.31	-377.46 \pm 7.30	-25.70 \pm 0.05	3781 \pm 95	3895
GU 744	31 - 40	-380.04 \pm 4.52	-377.56 \pm 4.50	-27.00 \pm 0.05	3783 \pm 58	3896
GU 745	41 - 50	-398.74 \pm 2.66	-396.21 \pm 2.65	-27.10 \pm 0.05	4027 \pm 35	4148
GU 746	51 - 60	-379.41 \pm 2.36	-378.79 \pm 2.35	-25.50 \pm 0.05	3798 \pm 30	3912
GU 747	61 - 70	-380.38 \pm 2.37	-381.37 \pm 2.38	-24.20 \pm 0.05	3832 \pm 31	3947
GU 748	71 - 80	-371.24 \pm 2.87	-371.49 \pm 2.87	-24.80 \pm 0.05	3705 \pm 37	3816
GU 749	81 - 90	-376.50 \pm 4.77	-375.13 \pm 4.76	-26.10 \pm 0.05	3751 \pm 61	3864
GU 750	91 - 100	-380.99 \pm 2.20	-381.61 \pm 2.20	-24.50 \pm 0.05	3835 \pm 29	3950
GU 751	101 - 110	-381.69 \pm 3.52	-381.81 \pm 3.52	-24.90 \pm 0.05	3838 \pm 46	3953
GU 752	111 - 120	-382.88 \pm 2.58	-383.25 \pm 2.58	-24.70 \pm 0.05	3856 \pm 33	3971
GU 753	121 - 130	-379.32 \pm 2.41	-379.82 \pm 2.41	-24.60 \pm 0.05	3812 \pm 31	3926
GU 754	131 - 140	-380.48 \pm 2.42	-381.10 \pm 2.42	-24.50 \pm 0.05	3828 \pm 32	3943

TABLE 3-3-4 BORTH 6 OAK - TREE-RING/RADIOCARBON ANALYSES

Sample Number	Growth Rings	$\delta^{14}\text{C} \pm 1\sigma$ ‰	$\Delta^{14}\text{C} \pm 1\sigma$ ‰	$\delta^{13}\text{C} \pm 1\sigma$ ‰ w.r.t. P.D.B.	Age $\pm 1\sigma$ years B.P. $t_{1/2} = 5568\text{y}$	Age years B.P. $t_{1/2} = 5730\text{y}$
GU 719	1 - 10	-425.80 \pm 3.50	-424.99 \pm 3.49	-25.70 \pm 0.05	4419 \pm 49	4552
GU 720	11 - 22	-415.55 \pm 3.39	-415.20 \pm 3.38	-25.30 \pm 0.05	4284 \pm 47	4412
GU 721	23 - 40	-396.41 \pm 7.77	-396.41 \pm 7.77	-25.00 \pm 0.05	4029 \pm 104	4150
GU 722	41 - 69	-397.12 \pm 2.58	-398.09 \pm 2.59	-24.20 \pm 0.05	4052 \pm 35	4173
GU 723	70 - 80	-409.42 \pm 3.33	-410.49 \pm 3.33	-24.10 \pm 0.05	4219 \pm 46	4345
GU 724	81 - 90	-391.27 \pm 2.73	-391.02 \pm 2.73	-25.20 \pm 0.05	3958 \pm 36	4077
GU 725	91 - 100	-382.19 \pm 5.33	-380.83 \pm 5.32	-26.10 \pm 0.05	3825 \pm 69	3940
GU 726	101 - 112	-377.34 \pm 4.15	-375.97 \pm 4.14	-26.10 \pm 0.05	3762 \pm 54	3874
GU 727	113 - 120	-390.33 \pm 3.04	-392.64 \pm 3.05	-23.10 \pm 0.05	3968 \pm 40	4099
GU 728	121 - 130	-384.35 \pm 3.18	-384.47 \pm 3.18	-24.90 \pm 0.05	3872 \pm 42	3988
GU 729	131 - 140	-408.85 \pm 2.70	-408.38 \pm 2.70	-25.40 \pm 0.05	4190 \pm 37	4316
GU 730	141 - 150	-390.33 \pm 3.48	-391.18 \pm 3.49	-24.30 \pm 0.05	3960 \pm 46	4079

TABLE 3-3-4

BORTH 6 OAK - TREE-RING/RADIOCARBON ANALYSES (cont'd)

Sample Number	Growth Rings	$\delta^{14}\text{C} \pm 1\sigma$ ‰	$\Delta^{14}\text{C} \pm 1\sigma$ ‰	$\delta^{13}\text{C} \pm 1\sigma$ ‰ w.r.t. P.D.B.	Age $\pm 1\sigma$ years B.P. $t_{1/2} = 5568\text{y}$	Age years B.P. $t_{1/2} = 5730\text{y}$
GU 731	151 - 160	-372.98 \pm 3.34	-372.08 \pm 3.34	-25.70 \pm 0.05	3738 \pm 43	3850
GU 732	161 - 170	-403.56 \pm 3.36	-403.20 \pm 3.36	-25.30 \pm 0.05	4120 \pm 45	4244
GU 733	171 - 180	-407.57 \pm 6.39	-408.28 \pm 6.40	-24.40 \pm 0.05	4189 \pm 87	4315
GU 734	181 - 190	-390.03 \pm 3.54	-391.25 \pm 3.55	-24.00 \pm 0.05	3961 \pm 47	4080
GU 735	191 - 200	-393.44 \pm 2.47	-394.66 \pm 2.47	-24.00 \pm 0.05	4006 \pm 33	4126
GU 736	201 - 210	-392.02 \pm 4.49	-392.99 \pm 4.50	-24.20 \pm 0.05	3984 \pm 60	4104
GU 737	211 - 220	-393.30 \pm 1.96	-394.15 \pm 1.96	-24.30 \pm 0.05	3999 \pm 26	4119
GU 738	221 - 230	-408.09 \pm 3.22	-408.92 \pm 3.23	-24.30 \pm 0.05	4198 \pm 44	4323
GU 739	231 - 240	-397.56 \pm 3.38	-396.72 \pm 3.37	-25.70 \pm 0.05	4034 \pm 45	4155
GU 740	241 - 250	-399.30 \pm 2.21	-399.30 \pm 2.21	-25.00 \pm 0.05	4068 \pm 45	4190
GU 741	251 - 270	-387.77 \pm 4.79	-388.99 \pm 4.79	-24.00 \pm 0.05	3957 \pm 64	4076

TABLE 3-3-5 YNYSLAS 1 PINE - TREE-RING/RADIOCARBON ANALYSES

Sample Number	Growth Rings	$\delta^{14}\text{C} \pm 1\sigma$ ‰	$\Delta^{14}\text{C} \pm 1\sigma$ ‰	$\delta^{13}\text{C} \pm 1\sigma$ ‰	Age $\pm 1\sigma$ years B.P. $t_{1/2} = 5568\text{y}$	Age years B.P. $t_{1/2} = 5730\text{y}$
GU 711	-10 - +10	-471.56 \pm 3.11	-472.09 \pm 3.12	-24.50 \pm 0.05	5106 \pm 48	5259
GU 712	0 - 10	-460.41 \pm 5.91	-460.74 \pm 5.91	-24.70 \pm 0.05	4935 \pm 89	5082
GU 713	11 - 20	-464.52 \pm 3.42	-465.70 \pm 3.43	-23.90 \pm 0.05	5009 \pm 52	5159
GU 714	21 - 30	-462.40 \pm 2.62	-463.37 \pm 2.63	-24.10 \pm 0.05	4974 \pm 39	5123
GU 715	31 - 40	-460.74 \pm 3.06	-461.50 \pm 3.07	-24.30 \pm 0.05	4946 \pm 46	5094
GU 716	41 - 50	-466.56 \pm 3.01	-467.42 \pm 3.01	-24.20 \pm 0.05	5035 \pm 46	5186
GU 717	51 - 60	-458.46 \pm 2.66	-459.98 \pm 2.67	-23.60 \pm 0.05	4924 \pm 40	5071
GU 718	61 - 70	-458.60 \pm 3.21	-460.44 \pm 3.22	-23.30 \pm 0.05	4930 \pm 48	5078

TABLE 3-3-6 STOLFORD 4 OAK - TREE-RING/RADIOCARBON ANALYSES

Sample Number	Growth Rings	$\delta^{14}\text{C} \pm 1\sigma$ ‰	$\Delta^{14}\text{C} \pm 1\sigma$ ‰	$\delta^{13}\text{C} \pm 1\sigma$ ‰ w.r.t. P.D.B.	Age $\pm 1\sigma$ years B.P. $t_{1/2} = 5568\text{y}$	Age years B.P. $t_{1/2} = 5730\text{y}$
GU 755	1 - 10	-445.96 \pm 2.34	-447.00 \pm 2.34	-24.06 \pm 0.05	4733 \pm 34	4875
GU 756	11 - 20	-450.72 \pm 2.42	-451.84 \pm 2.43	-23.98 \pm 0.05	4803 \pm 36	4977
GU 757	21 - 30	-445.34 \pm 2.12	-445.99 \pm 2.12	-24.41 \pm 0.05	4718 \pm 31	4860
GU 758	31 - 40	-440.02 \pm 2.81	-440.92 \pm 2.82	-24.20 \pm 0.05	4645 \pm 41	4784
GU 759	41 - 50	-428.83 \pm 3.35	-430.04 \pm 3.36	-23.94 \pm 0.05	4490 \pm 47	4625
GU 760	51 - 60	-444.73 \pm 2.12	-445.77 \pm 2.13	-24.06 \pm 0.05	4715 \pm 31	4856
GU 761	61 - 70	-447.99 \pm 2.86	-450.09 \pm 2.87	-23.10 \pm 0.05	4778 \pm 42	4921
GU 762	71 - 80	-442.78 \pm 2.21	-445.25 \pm 2.22	-22.79 \pm 0.05	4707 \pm 32	4848

TABLE 3-3-7 STOLFORD 5 OAK - TREE-RING/RADIOCARBON ANALYSES

Sample Number	Growth rings	$\delta^{14}\text{C} \pm 1\sigma$ ‰	$\Delta^{14}\text{C} \pm 1\sigma$ ‰	$\delta^{13}\text{C} \pm 1\sigma$ ‰ w.r.t. P.D.B.	Age $\pm 1\sigma$ years B.P. $t_1 = 5568\text{y}$	Age years B.P. $t_1 = 5730\text{y}$
GU 763	-12 - +10	-489.82 \pm 5.00	-490.93 \pm 5.01	-23.91 \pm 0.05	5398 \pm 79	5560
GU 764	11 - 20	-483.30 \pm 4.23	-484.58 \pm 4.24	-23.76 \pm 0.05	5298 \pm 66	5457
GU 765	21 - 30	-476.79 \pm 3.57	-478.30 \pm 3.59	-23.56 \pm 0.05	5201 \pm 55	5357
GU 766	31 - 40	-482.23 \pm 2.90	-483.72 \pm 2.90	-23.57 \pm 0.05	5285 \pm 45	5443
GU 767	41 - 50	-489.31 \pm 2.51	-491.03 \pm 2.52	-23.32 \pm 0.05	5399 \pm 40	5561
GU 768	51 - 60	-480.70 \pm 2.54	-482.72 \pm 2.55	-23.05 \pm 0.05	5269 \pm 40	5427
GU 769	61 - 70	-480.07 \pm 3.81	-481.98 \pm 3.82	-23.16 \pm 0.05	5258 \pm 60	5415
GU 770	71 - 80	-475.06 \pm 2.93	-477.31 \pm 2.95	-22.86 \pm 0.05	5186. \pm 45	5341
GU 771	81 - 90	-487.93 \pm 2.69	-489.94 \pm 2.71	-23.04 \pm 0.05	5382 \pm 43	5543
GU 772	91 - 100	-487.91 \pm 2.57	-489.60 \pm 2.58	-23.35 \pm 0.05	5377 \pm 41	5538
GU 773	101 - 110	-478.15 \pm 2.50	-479.57 \pm 2.51	-23.64 \pm 0.05	5220 \pm 39	5377
GU 774	111 - 120	-475.10 \pm 3.46	-476.26 \pm 3.47	-23.90 \pm 0.05	5169 \pm 53	5324
GU 775	121 - 130	-477.11 \pm 4.63	-478.49 \pm 4.62	-23.68 \pm 0.05	5204 \pm 72	5540
GU 776	131 - 140	-469.63 \pm 3.36	-471.34 \pm 3.37	-23.39 \pm 0.05	5094 \pm 51	5247
GU 777	141 - 150	-468.55 \pm 5.31	-469.67 \pm 5.32	-23.95 \pm 0.05	5067 \pm 81	5221

TABLE 3-3-7 STOLFORD 5 OAK - TREE-RING/RADIOCARBON ANALYSES (cont'd)

Sample Number	Growth rings	$\delta^{14}\text{C} \pm 1\sigma$ ‰	$\Delta^{14}\text{C} \pm 1\sigma$ ‰	$\delta^{13}\text{C} \pm 1\sigma$ ‰	w.r.t. P.D.B.	Age $\pm 1\sigma$ years B.P. $t_{1/2} = 5568\text{y}$	Age years B.P. $t_{1/2} = 5730\text{y}$
GU 778	151 - 160	-469.86 \pm 3.99	-471.16 \pm 4.00	-23.77 \pm 0.05		5092 \pm 70	5244
GU 779	161 - 170	-452.73 \pm 8.56	-454.37 \pm 8.59	-23.50 \pm 0.05		4840 \pm 127	4986
GU 780	171 - 180	-465.43 \pm 6.87	-466.45 \pm 6.88	-24.05 \pm 0.05		5020 \pm 104	5171
GU 781	181 - 190	-466.29 \pm 4.01	-467.68 \pm 4.02	-23.70 \pm 0.05		5039 \pm 61	5190
GU 782	191 - 200	-469.70 \pm 4.38	-471.21 \pm 4.39	-23.57 \pm 0.05		5092 \pm 67	5245
GU 784	211 - 220	-464.08 \pm 4.03	-465.56 \pm 4.04	-23.62 \pm 0.05		5007 \pm 61	5157
GU 785	221 - 230	-464.40 \pm 4.46	-466.09 \pm 4.47	-23.42 \pm 0.05		5015 \pm 68	5165
GU 786	231 - 240	-453.26 \pm 6.53	-454.61 \pm 6.55	-23.77 \pm 0.05		4844 \pm 97	4989
GU 787	241 - 250	-460.99 \pm 3.59	-462.31 \pm 3.60	-23.78 \pm 0.05		4958 \pm 54	5107
GU 788	251 - 260	-449.63 \pm 4.57	-450.45 \pm 4.58	-24.25 \pm 0.05		4783 \pm 67	4926
GU 789	261 - 270	-445.30 \pm 8.52	-449.92 \pm 8.43	-29.94 \pm 0.05		4775 \pm 124	4919
GU 790	271 - 280	-457.22 \pm 4.53	-458.95 \pm 4.55	-23.40 \pm 0.05		4908 \pm 68	5056
GU 791	281 - 290	-453.40 \pm 4.56	-453.74 \pm 4.57	-24.69 \pm 0.05		4831 \pm 67	4976

TABLE 3-3-8 CULLYKHAN 1 OAK - TREE-RING/RADIOCARBON ANALYSES

Sample Number	Growth Rings	$\delta^{14}\text{C} + 1\sigma$ ‰	$\Delta^{14}\text{C} + 1\sigma$ ‰	$\delta^{13}\text{C} + 1\sigma$ ‰ w.r.t. P.D.B.	Age $\pm 1\sigma$ years B.P. $t_{1/2} = 5568\text{y}$	Age years B.P. $t_{1/2} = 5730\text{y}$
SRR 844	8 - 18	-249.43 \pm 4.24	-250.48 \pm 4.24	-24.30 \pm 0.05	2317 \pm 45	2387
SRR 845	19 - 28	-260.10 \pm 4.36	-260.54 \pm 4.37	-24.70 \pm 0.05	2425 \pm 47	2498
SRR 846	29 - 38	-255.61 \pm 4.50	-256.05 \pm 4.50	-24.70 \pm 0.05	2377 \pm 49	2448
SRR 847	39 - 48	-218.18 \pm 5.06	-218.49 \pm 5.06	-24.80 \pm 0.05	1981 \pm 52	2040
SRR 848	49 - 58	-250.21 \pm 4.29	-249.46 \pm 4.28	-25.50 \pm 0.05	2305 \pm 46	2374
SRR 849	59 - 78	-244.45 \pm 4.87	-243.99 \pm 4.87	-25.30 \pm 0.05	2247 \pm 52	2314
SRR 850	79 - 88	-246.89 \pm 4.93	-246.74 \pm 4.93	-25.10 \pm 0.05	2276 \pm 52	2344
SRR 851	89 - 98	-261.60 \pm 3.06	-261.45 \pm 3.06	-25.10 \pm 0.05	2435 \pm 33	2508
SRR 852	99 - 108	-260.72 \pm 3.65	-260.43 \pm 3.65	-25.20 \pm 0.05	2423 \pm 40	2496
SRR 853	109 - 118	-250.51 \pm 3.27	-250.21 \pm 3.27	-25.20 \pm 0.05	2313 \pm 35	2382

TABLE 3-3-8

CULLYKHAN 1 OAK - TREE-RING/RADIOCARBON ANALYSES (cont'd)

Sample Number	Growth rings	$\delta^{14}\text{C} \pm 1\sigma$ ‰	$\Delta^{14}\text{C} \pm 1\sigma$ ‰	$\delta^{13}\text{C} \pm 1\sigma$ ‰ w.r.t. P.D.B.	Age $\pm 1\sigma$ years B.P. $t_{1/2} = 5568\text{y}$	Age years B.P. $t_{1/2} = 5730\text{y}$
SRR 854	119 - 128	-252.02 \pm 3.24	-251.74 \pm 3.24	-25.20 \pm 0.05	2329 \pm 35	2399
SRR 855	129 - 138	-252.28 \pm 2.79	-252.28 \pm 2.79	-25.00 \pm 0.05	2336 \pm 30	2406
SRR 856	139 - 148	-256.09 \pm 3.51	-255.64 \pm 3.51	-25.30 \pm 0.05	2371 \pm 38	2442
SRR 857	149 - 158	-252.78 \pm 2.51	-252.78 \pm 2.51	-25.00 \pm 0.05	2341 \pm 27	2411
SRR 858	159 - 168	-246.88 \pm 2.75	-245.37 \pm 2.74	-26.00 \pm 0.05	2262 \pm 29	2330
SRR 859	169 - 188	-250.56 \pm 2.64	-248.76 \pm 2.63	-26.20 \pm 0.05	2298 \pm 28	2367
SRR 860	189 - 208	-254.98 \pm 2.60	-253.64 \pm 2.60	-25.90 \pm 0.05	2350 \pm 28	2420
SRR 861	209 - 228	-239.74 \pm 3.18	-238.68 \pm 3.17	-25.70 \pm 0.05	2191 \pm 33	2257
SRR 862	219 - 238	-252.09 \pm 3.71	-250.89 \pm 3.71	-25.80 \pm 0.05	2321 \pm 40	2391
SRR 863	239 - 258	-268.72 \pm 4.44	-268.86 \pm 4.44	-24.90 \pm 0.05	2516 \pm 49	2591

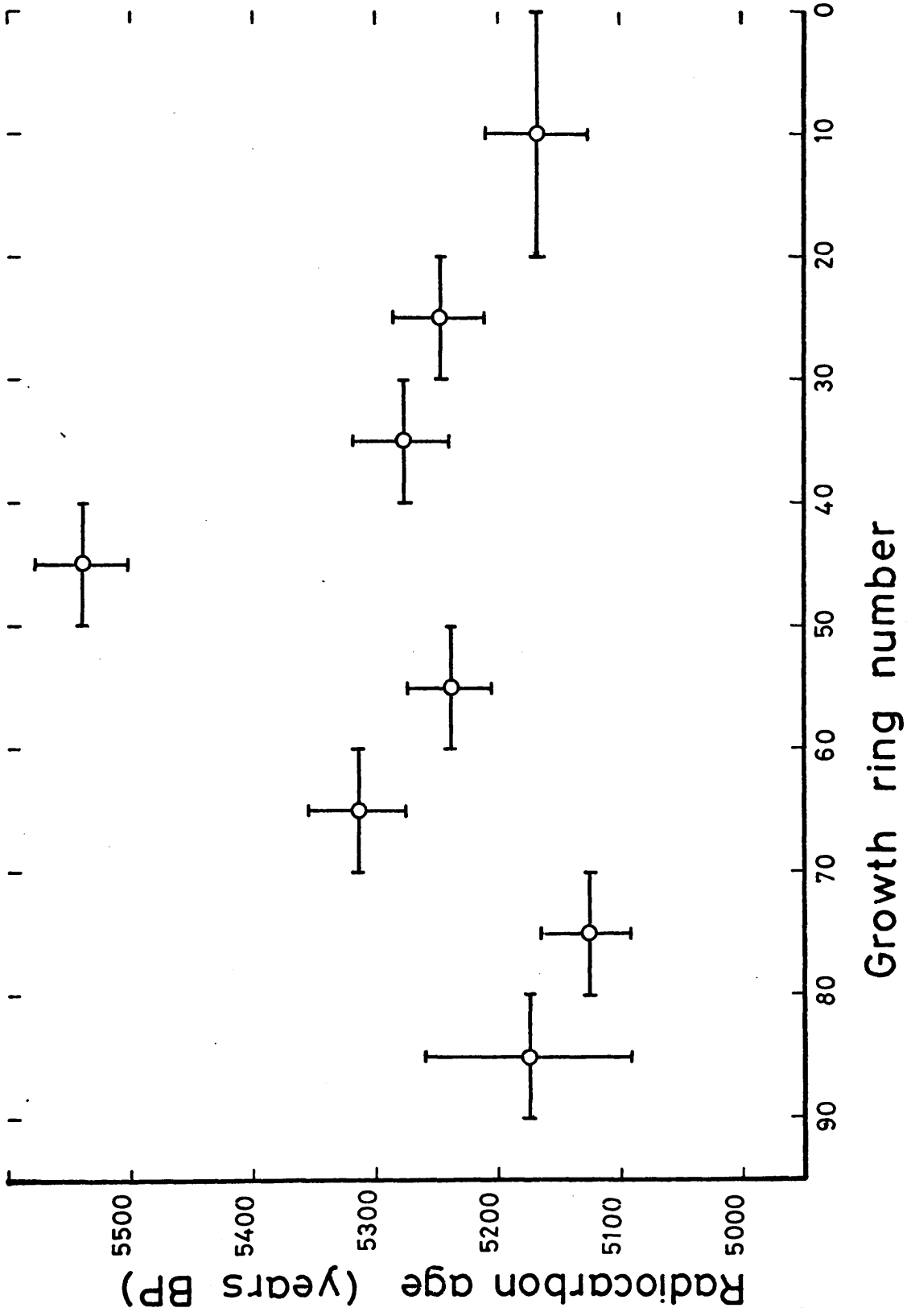


FIGURE3-1 : Borth 1 - Radiocarbon analyses

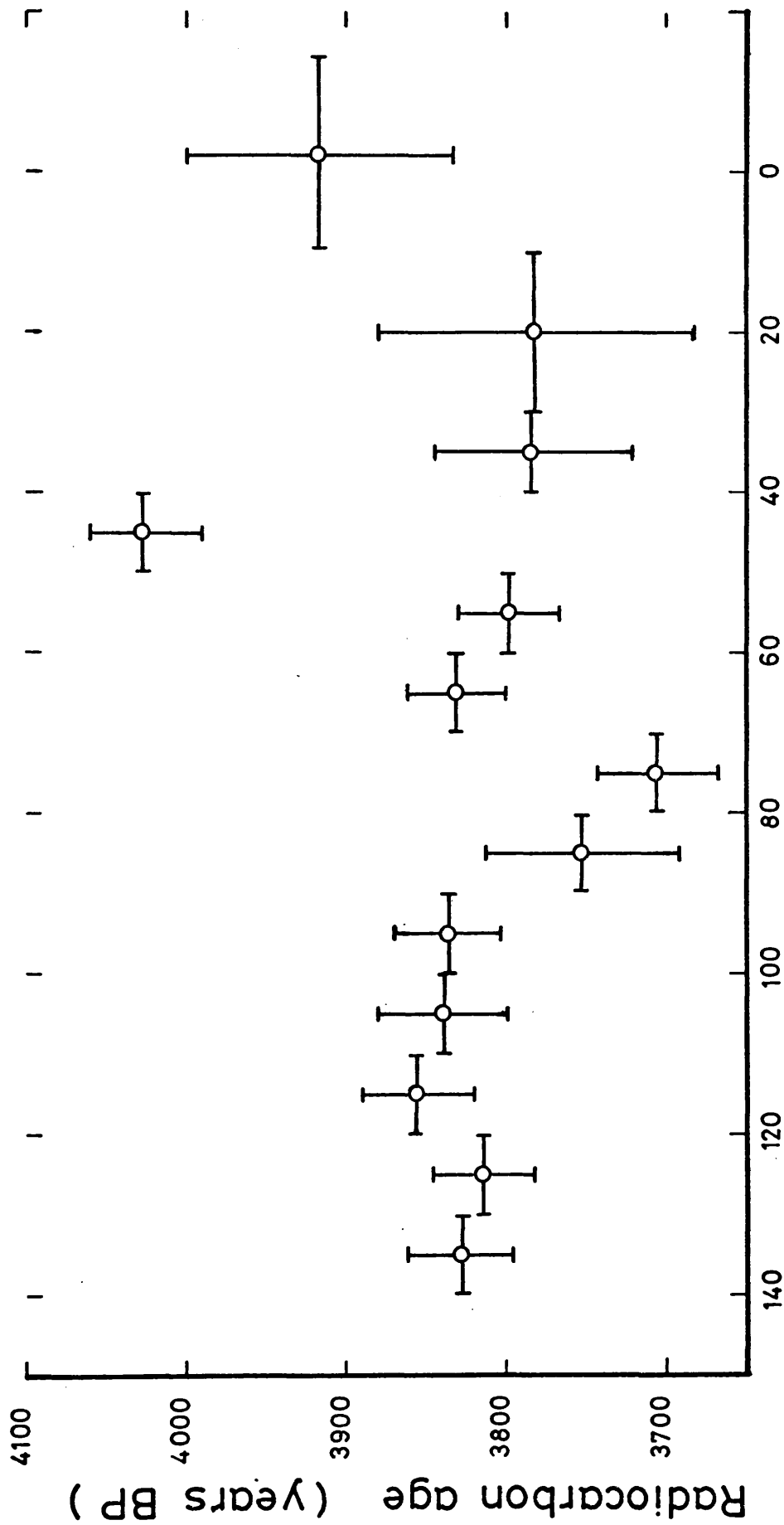
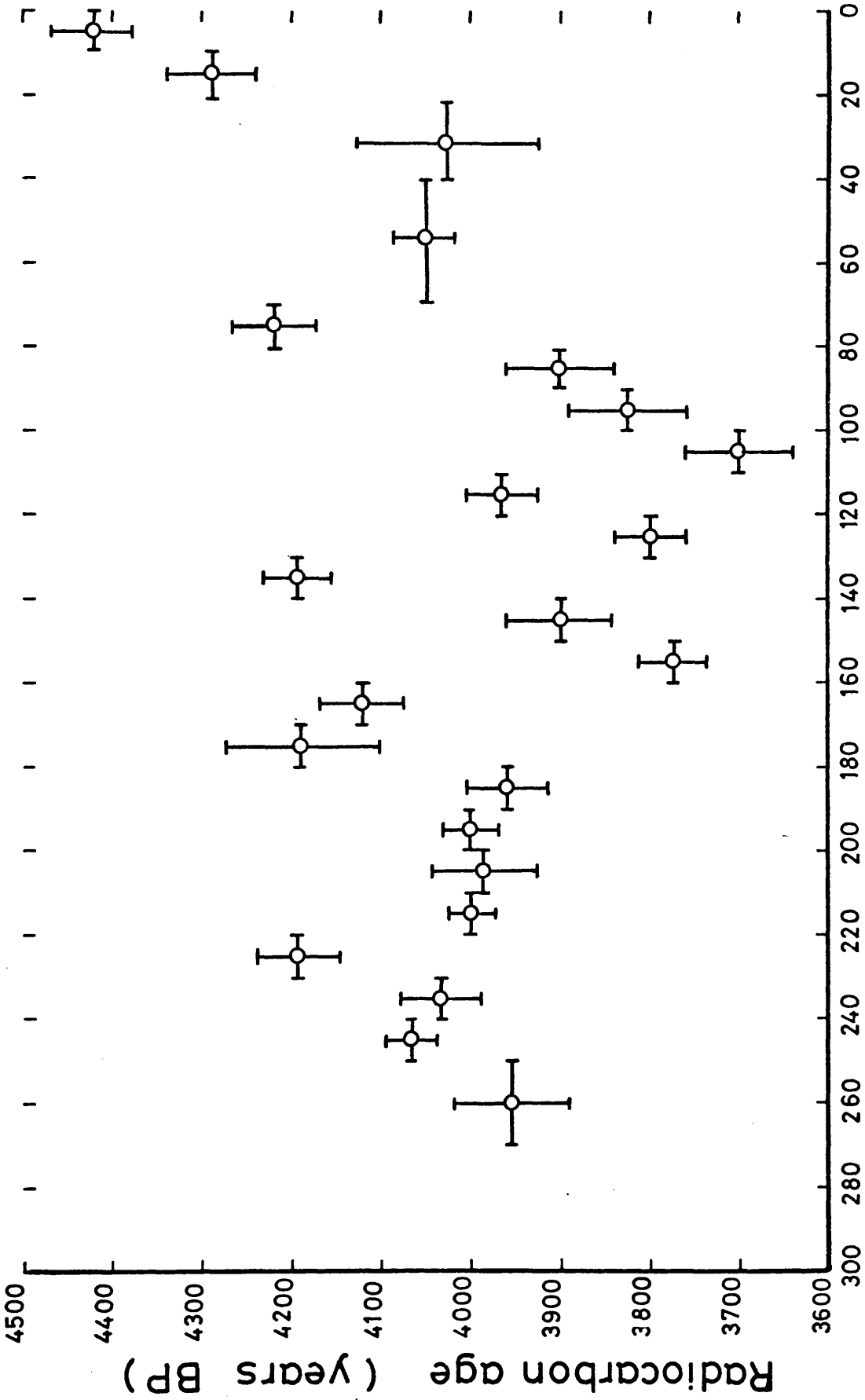


FIGURE 3-2: Borth 4 - Radiocarbon analyses



Growth ring number
FIGURE 3-3: Borth 6 - Radiocarbon analyses

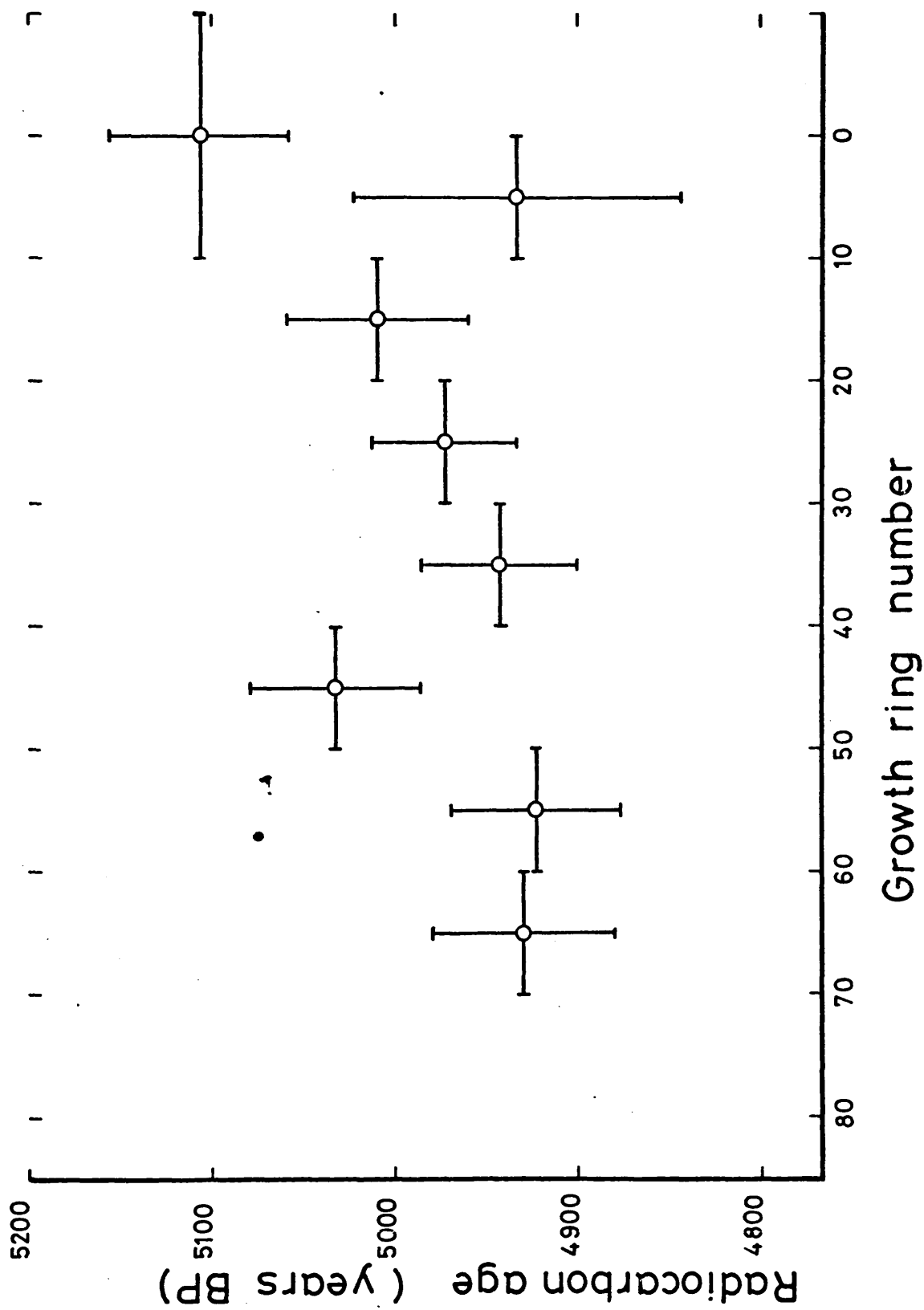
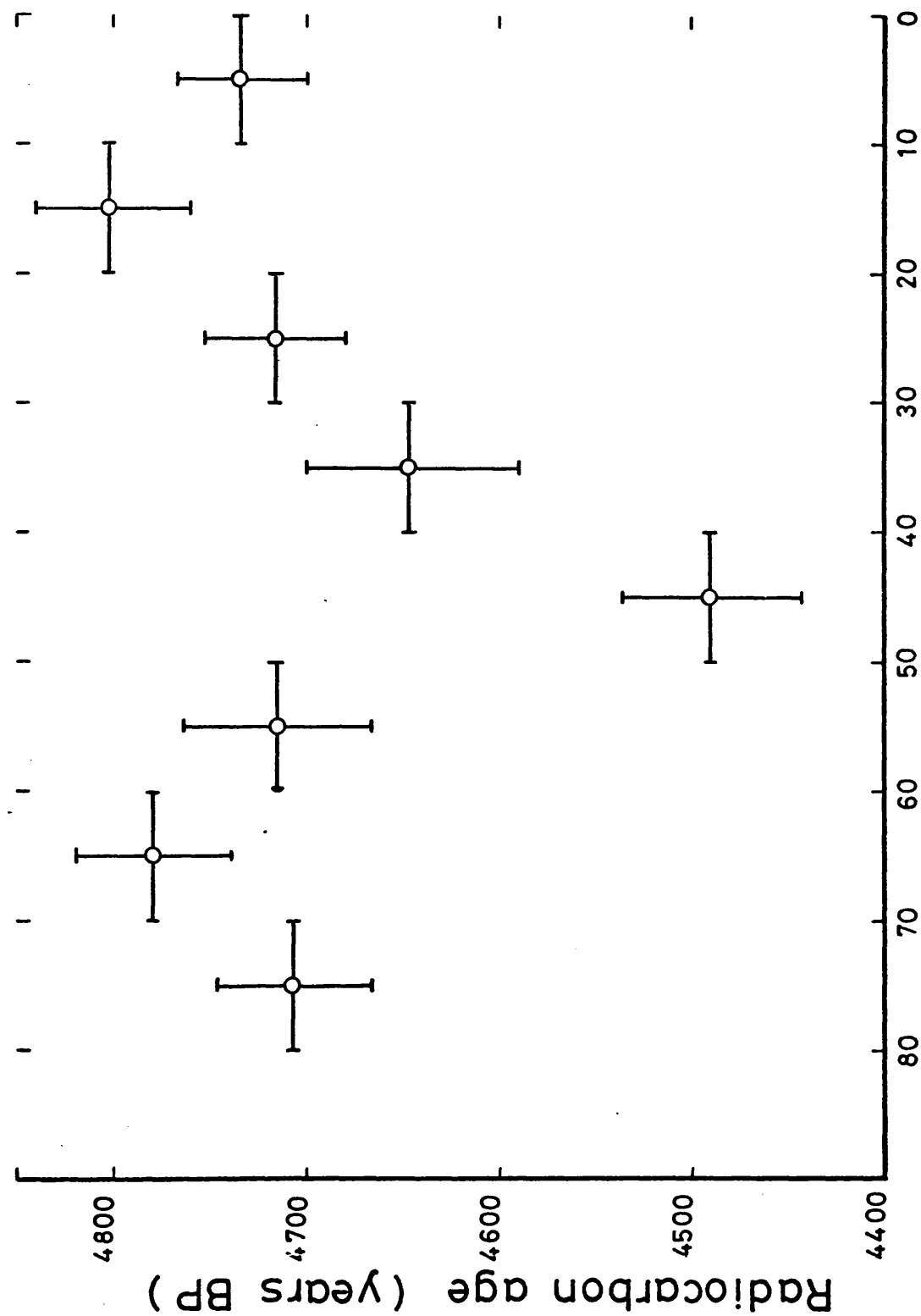


FIGURE 3-4 : Ynyslas 1 - Radiocarbon analyses



Growth ring number
FIGURE 3-5: Stolford 4 - Radiocarbon analyses

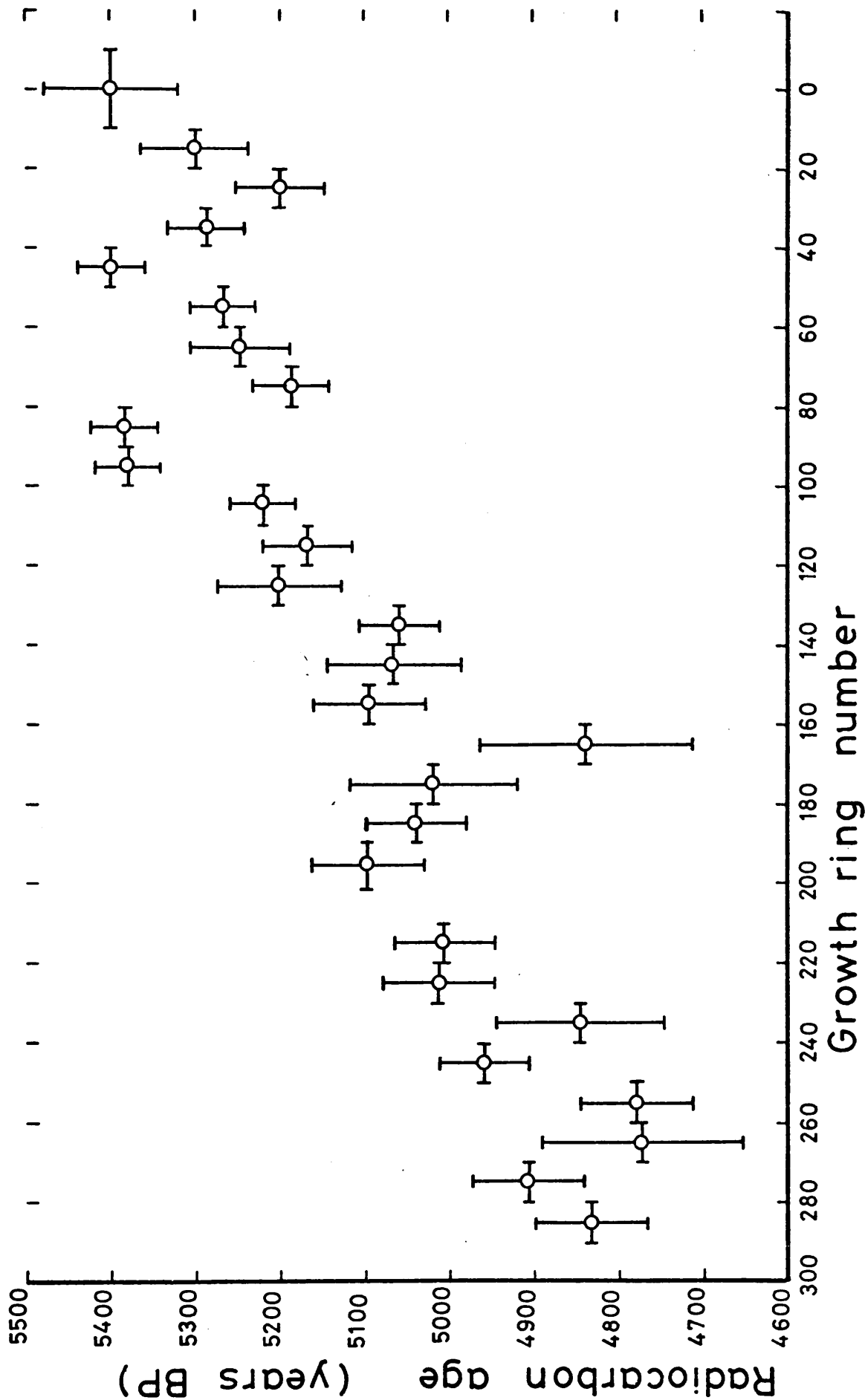


FIGURE 3-6 : Stolford 5 - Radiocarbon analyses

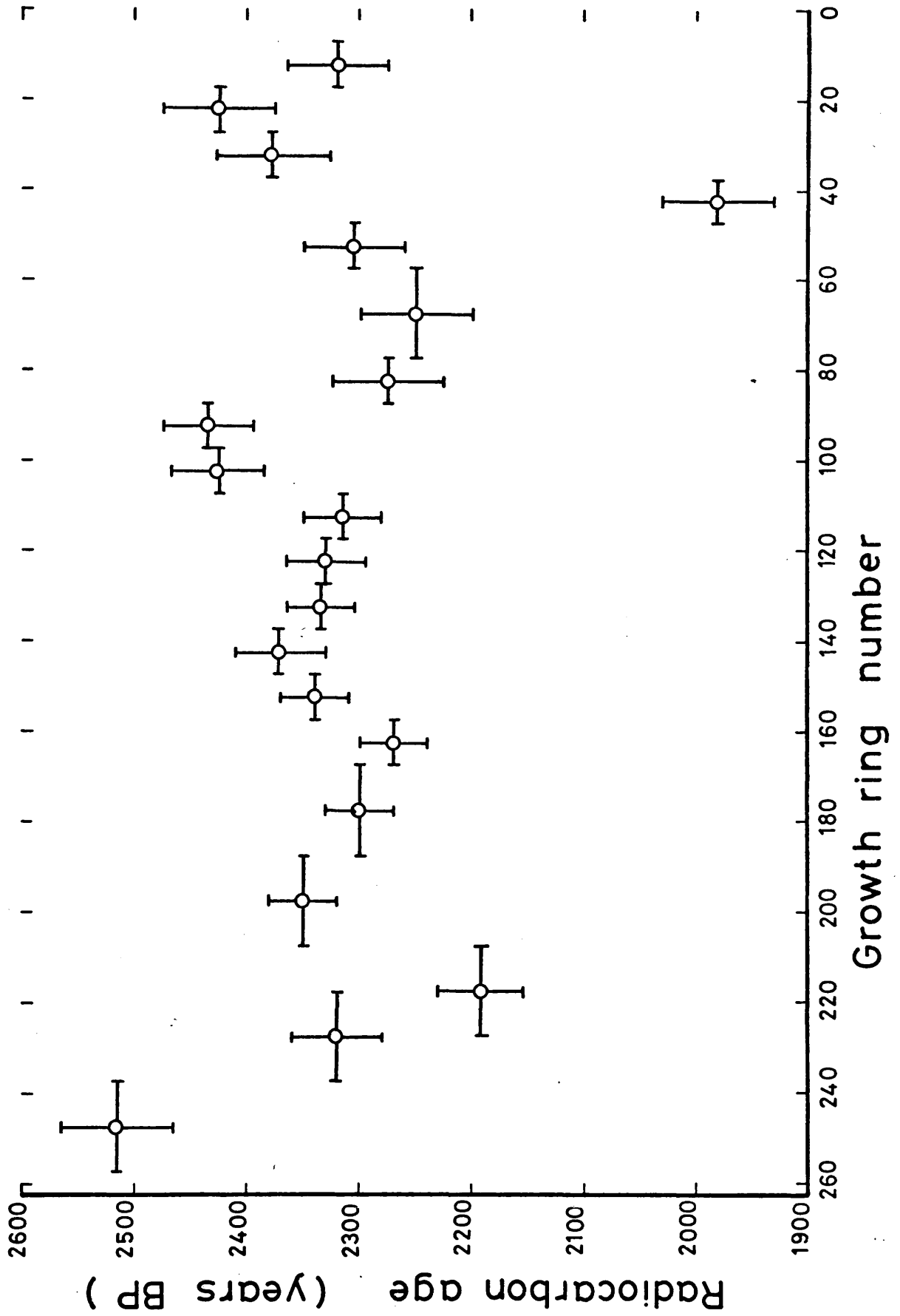


FIGURE 3-7 : Cullykhan 1 - Radiocarbon analyses

CHAPTER 4

ASSESSMENT OF LABORATORY PROCEDURES

Interpretation of the results of any measurement process requires an understanding of the random errors inherent in the particular method of assay. Radiocarbon age determinations are conventionally reported in the form $\text{Age} \pm \epsilon$ in units of years before present (B.P.), present being taken as 1950. In general, the error ϵ , quoted at the one sigma level, is based solely on the variability due to "counting statistics" and many laboratories suggest that non-counting errors are negligible. Interlaboratory calibration exercises, however, allow the calculation of an independent estimate of the standard error for an intercalibration sample series and this quantity can be compared with the standard error quoted by the participating laboratories. Intercalibration samples are usually not used for this purpose but rather the results of the analysis are taken as an indication that a new laboratory is "getting the same answer" as an established dating system.

Clark and Renfrew (1973) analysed the differences in radiocarbon ages (Berger, 1970; Edwards, 1970) of 25 samples divided and assayed by two laboratories (BM and UCLA). The outcome of the analysis throws considerable doubt upon the assumption that non-counting errors are negligible. It was shown that, although there was no systematic difference between these laboratories with this series of samples, the true standard errors of the radiocarbon dates were possibly 40% greater than the quoted values.

In the preparation of his version of the bristlecone pine calibration curve, Clark (1975) has performed a similar analysis on the bristlecone pine data produced by La Jolla, Pennsylvania and Arizona radiocarbon laboratories. The results imply that there are no systematic differences between these three laboratories but that there is very significant between laboratories variability. In other words, the measurements from these three laboratories agree on average, but sometimes one laboratory produces a date say 200 years below the other and then sometimes 200 years or so above. Further, Clark has demonstrated that on average the variability between replicate observations is far in excess of the variability expected in terms of the quoted standard errors and that each of the laboratories contributing data to the study underestimate this variability by the same amount.

In the early stages of this research programme, the results obtained from sequential growth-increment analysis of "floating" chronologies produced differences between adjacent samples far in excess of previously reported or considered fluctuations. It was, therefore, decided to instigate a study by which the total error associated with each age determination could be assessed, thus testing the veracity of the previously and subsequently produced results.

The total error associated with a single radiocarbon measurement will consist of contributions arising from counting statistics and any non-counting error, thus

$$\epsilon_{\text{TOTAL}} = [\epsilon_{\text{C}}^2 + \epsilon_{\text{UC}}^2]^{\frac{1}{2}}$$

where ϵ_{TOTAL} is the total error associated with a single assay ($\pm 1\sigma$),

ϵ_{C} is the counting statistics error

and ϵ_{UC} is the non-counting error.

For a series of replicate analyses it is possible to obtain an estimate of the total variability ϵ_{TOTAL} , arising from ϵ_{C} and ϵ_{UC} , the former being directly calculable.

The counting error, ϵ_{C} , is based on the accumulated ^{14}C counts for each sample and is further influenced by the data from repeated measurements of modern standard and background samples, prepared at regular intervals. The "counting statistics" error also includes the uncertainty associated with the measurement of $\delta^{13}\text{C}$.

The long-term stability of the Glasgow counting system is excellent. Figs. 4-1 and 4-2 reproduce graphically the data presented in Tables 2-7 and 2-4, and show oxalic acid and background activities as recorded over periods of 11 and 10 months respectively. For oxalic acid, the standard deviation about the mean is $2.2^{\circ}/\text{oo}$ for a total of 16 determinations. The standard deviation in the number of counts of a single determination is $2.4^{\circ}/\text{oo}$. The scatter of the values around the mean and the variability of a single measurement evidently are nearly equal. Thus only statistical variability in the number of counts plays a role in the oxalic acid determinations and the error associated with the modern standard count rate is given by

$$\text{Error } (\pm 1\sigma) = \frac{[\text{Total number of counts accumulated}]^{\frac{1}{2}}}{\text{Total count time}}$$

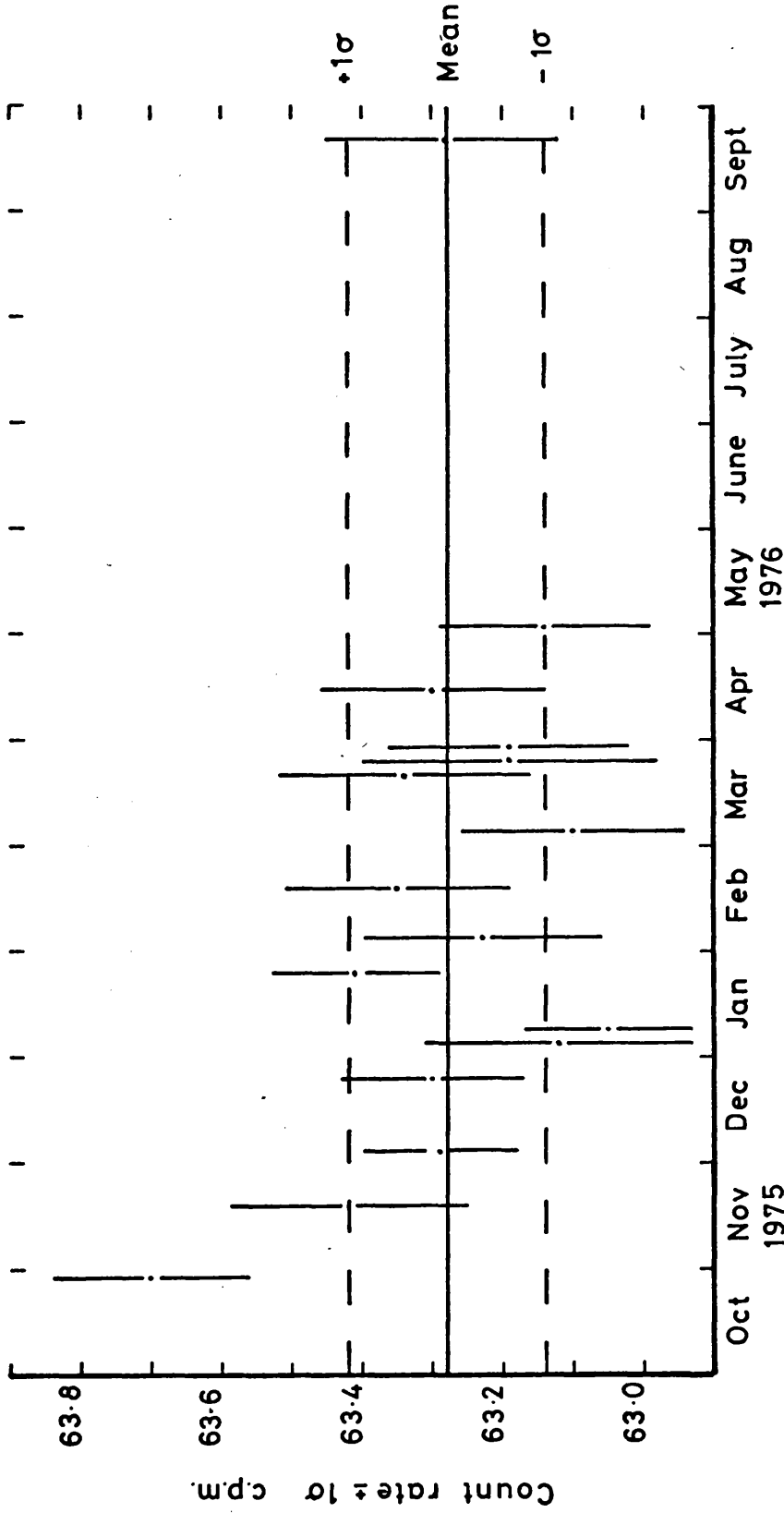


FIGURE 4-1: NBS oxalic acid standard M6 -
count rate versus time
October 1975 - September 1976

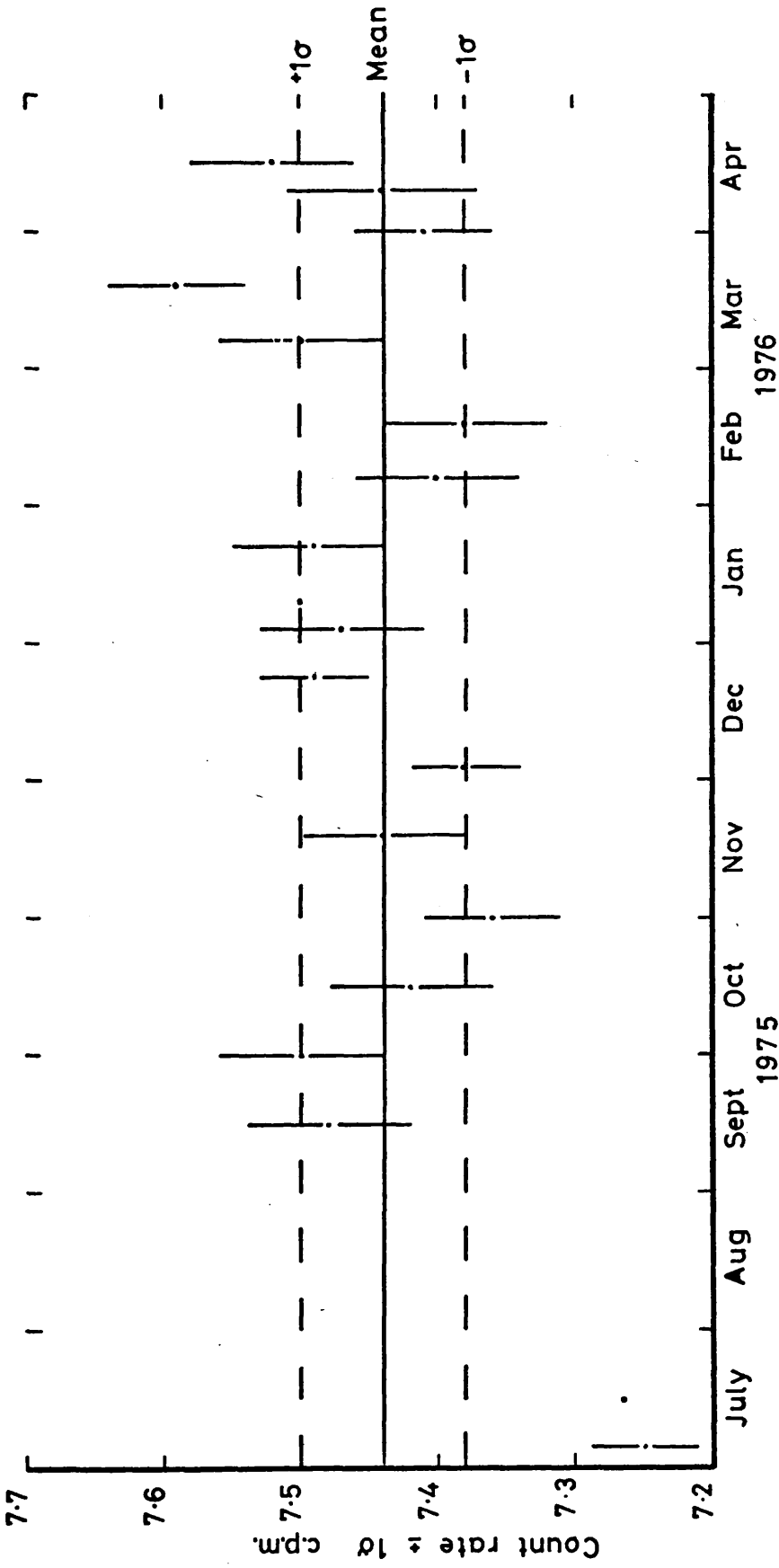


FIGURE 4-2: Background count rate versus time
July 1975 - April 1976

The background count rate data are treated in exactly the same fashion yielding the standard error quoted in Table 2-4. Regular assay of the N.B.S. oxalic acid standard, however, does not give a true indication of laboratory reproducibility, since it requires non-routine chemical procedures (i.e. no pretreatment, wet oxidation) in converting the oxalic acid to the adopted counting substance. Most laboratories, particularly those with gas counting procedures, will accumulate N.B.S. oxalic acid data on the same gas (or benzene) sample and thus the data record does not assess any non-counting errors whatsoever.

The wood sample selected for the replicate analysis standard, the homogenisation process and the methods used in ^{14}C assay have been described in the preceding chapters. The results of the 24 replicate analyses are presented in Table 3-1-2. From these data, the mean value of $\Delta^{14}\text{C}$ for the replicate standard and the standard error are calculated to be

$$\overline{\Delta^{14}\text{C}} \pm 1\sigma = -455.09 \pm 5.82^{\circ}/\text{oo} \text{ (4875} \pm 86 \text{ years B.P.)}$$

As can be seen from Table 3-1-1, this value is in excellent agreement with the single analysis result obtained by SRR (4926 \pm 52 years B.P.) and the mean of a series of analyses performed by the other Glasgow ^{14}C laboratory (4890 \pm 260 years B.P., Drndarski pers. comm.) . It is interesting to note that the standard error reported by this latter laboratory, based on a comparable number of analyses, is much greater than reported for this research. The average counting error for the replicate data in this study, however, is $\pm 2.45^{\circ}/\text{oo}$ (± 36 years) and thus there is a non-counting

error contribution to the overall variability amounting to $\pm 5.28^0/00$ (± 79 years). This corresponds to a relative error $\pm 1.16\%$.

In determining the source, or sources, of this non-counting error, all stages of the assay procedure must be considered. Additional variability may arise during sample pretreatment, in the conversion of sample to benzene through chemical fractionation, as a result of a non-negligible "blank" or memory effect, through gravimetric and volumetric errors in preparation of the scintillation cocktail or from some further, previously unconsidered counting effect, such as non-reproducible geometry.

The possible influence of variability in the pretreatment procedures was investigated by a second series of replicate analyses using rice grain as the "standard". Clearly if there is some contribution to the non-counting error arising from the sample pretreatment, through contamination, then the results of these analyses performed on a sample, which, it was deemed, did not require pretreatment should yield an overall non-counting error smaller than that obtained from the wood replicate series. The results of this second replicate set are presented in Table 3-1-3.

The mean value of $\Delta^{14}\text{C}$ and the error on the mean are calculated to be

$$\overline{\Delta^{14}\text{C}} \pm 1\sigma = 404.07 \pm 11.14^0/00$$

corresponding to a relative error of $\pm 2.76\%$ which is considerably greater than the total error of the wood replicate series. Elimination of the counting error leaves a non-counting uncertainty of $\pm 2.62\%$.

The possible reasons for the large error on the rice replicate series may be considered in three ways. Firstly, the standard error calculated for these samples may represent the true uncertainty for this laboratory, secondly the sample may have been contaminated and thirdly the carbon isotope composition of the rice grain may not have been homogeneous. In the first case, it has already been shown that for a series of complete replicate analyses the non-counting error, $\pm 1.16\%$, is much smaller than for the rice series. Furthermore, this excess error may indicate the presence of contaminating material, such as dust or small quantities of other grains, accumulated before the batch of rice was purchased from the retailer. Therefore, it is unlikely that the non-counting error indicated by these replicate analyses is representative of the true uncertainty.

The citation of chemical inhomogeneity as a cause of the large uncertainty raises several interesting points. The rice sample, of unknown origin but purchased locally, was presumably grown in 1975 since $\overline{\Delta^{14}\text{C}}$ for the replicate analyses is in agreement with the average $\Delta^{14}\text{C}$ of the atmosphere for that year (Stenhouse, pers. comm.). In many of the world's rice producing regions two crops are harvested each year and since the atmospheric radiocarbon concentration is at present decreasing at a rate estimated to be 2% per year, due to the dispersal of "bomb" ^{14}C throughout the carbon cycle, it is reasonable to assume that the atmospheric $^{14}\text{CO}_2$ concentration was different whilst the separate rice crops were being cultivated. The possible source of artificial variability therefore suggests, that,

in retrospect, the choice of rice as a replicate standard, or indeed the choice of any "bomb-era" cereal, may lead to an unrealistic assessment of the laboratory procedures, unless the sample can be subjected to some homogenisation procedure, such as milling to yield flour. With the sample in this form, however, one has to contend with the problems of sample handling particularly in the sample combustion stage.

Before discussing any uncertainty which may be introduced during the chemical reactions involved in the synthesis of benzene, one must consider the possibility of a contribution to the non-counting error as a result of what may be termed a "memory effect". Such an effect would arise from non-scrupulous cleaning of the stainless steel reaction vessels and glassware, poor vacuum conditions resulting in the retention of sample carbon as adsorbed gas on the walls of the storage vessels and also from a non-negligible "blank" value which may arise due to the emanation of gas from the stainless steel of reaction vessels.

The "blank" value was assessed by simulating a combustion but with no sample present. When the combustion had been completed and the exhaust gases passed through the collection traps, any condensible products were distilled into the micro-combustion vacuum line and allowed to expand into the high vacuum manifold which had previously been pumped to 10^{-3} torr. No increase in pressure was observed and it was concluded that no extraneous CO_2 was being introduced to the vacuum system, either from emanation from the bomb or as a result of impurity CO_2 in the tank oxygen supply.

Any memory effects caused by insufficient pumping of storage bulbs or gas collection traps would most likely be detected when a background or "minimum age" sample was being processed in the course of routine, more active, sample preparation. The inter-laboratory discrepancy for the West Runton wood intercalibration samples GU 660, GU 661, may well have been attributed to such an effect, were it not for the fact that the two analyses were in broad agreement with the analysis performed in the other Glasgow ^{14}C laboratory. The agreement of the count rates recorded on background samples prepared from marble and scintillation grade benzene (Tables 2-4 and 2-5) indicates that there are no memory effects incurred during routine benzene synthesis.

The chemical procedures used in the preparation of benzene may introduce a non-counting error through chemical fractionation. Mass spectrometric assay of a CO_2 sample removed after sample combustion is normally assumed to enable correction of the observed ^{14}C enrichment for fractionation of carbon isotopes in nature, although in fact it may also be correcting for fractionation induced during sample combustion, which is taken to be quantitative. As noted in Chapter 2, however, the chemical yields for the conversion of CO_2 to acetylene and conversion of acetylene to benzene are lower than those reported by other workers. These lower yields may produce changes in the carbon isotope composition of the CO_2 and therefore the initial mass spectrometric assay may not be the value appropriate to the correction of the radiometrically determined $\delta^{14}\text{C}$ enrichment. The fractionation effect of low yield reactions was investigated by Tamers and Pearson (1965) by replicate analyses or, more correctly, inter-

calibration measurements. Possible fractionation effects were evaluated in terms of a non-quantified error arising from discrepancies between ^{14}C assays. Although the benzene yields at that time were $\sim 50\%$, the authors reported that any fractionation effect would contribute a maximum of ± 80 years but probably less than ± 40 years to the non-quantified error.

For the second replicate series, of rice samples, aliquots of CO_2 and benzene were submitted for $^{13}\text{C}/^{12}\text{C}$ ratio measurement, as well as for normal $\delta^{13}\text{C}$ assay on CO_2 . The single collector mass spectrometer results showed, in general, that the $^{13}\text{C}/^{12}\text{C}$ ratio for benzene was lower than the ratio for carbon dioxide. (Table 3-1-3). It will, however, be shown that this result is not significant as the measurements are not sufficiently sensitive to detect small changes in isotopic composition of the order of $1^\circ/\text{oo}$.

A more accurate determination of the stable carbon isotope enrichment in synthesised benzene can be obtained if the benzene is quantitatively converted to carbon dioxide for analysis by a double collector mass spectrometer. The micro-combustion system designed for this purpose is described in Chapter 2. Assessment of the reproducibility of this system was performed by series of replicate analyses. One set used wood cellulose as standard and the eight measurements performed yielded the following mean value and standard deviation

$$\overline{\delta^{13}\text{C}_{\text{CE}}} = -24.64 \pm 0.10^\circ/\text{oo w.r.t. P.D.B.}$$

It is assumed that the cellulose is quantitatively converted to CO_2 and therefore this standard deviation is taken as the minimum error associated with a single analysis (assuming 100%

sample combustion yield). As stated earlier, however, it proved difficult to attain high benzene to carbon dioxide conversion yields. A second replicate series, using scintillation grade benzene as the replicate standard was performed (Table 3-1-4). The conversion yields for these analyses vary considerably about the average value of 57% but it can readily be verified by a standard chi squared test that the $\delta^{13}\text{C}_{\text{BE}}$ data are normally distributed with mean value $\delta^{13}\text{C}_{\text{BE}} = -24.59\text{‰}$ (w.r.t. P.D.B.) and standard deviation $\pm 0.24\text{‰}$. Further, it can be shown that there is no correlation between the carbon isotope enrichments and the benzene to carbon dioxide yields, an essential factor in interpretation of the subsequent data. The lower limit for the detection of any fractionation effect is taken as $\pm 0.24\text{‰}$.

Routine investigation of differences in isotopic composition of benzene-derived and sample-derived CO_2 was carried out during the ^{14}C assay of the tree-ring sections Stolford 4 and Stolford 5 (SD4 and SD5). The data are presented in Tables 3-1-6 and 3-1-7. For section SD4, stable carbon isotope analysis was performed on CO_2 and benzene, using the single collector spectrometer and on CO_2 from sample and synthesised benzene, using the double collector mass spectrometer. In general, there is no significant difference between the $\delta^{13}\text{C}$ values of sample-derived CO_2 . In addition, there is no apparent correlation between the recorded yields of the chemical procedures, including micro-combustion, and the measured differences in isotope enrichment. The large variations in the absolute $^{13}\text{C}/^{12}\text{C}$

ratios of carbon dioxide and benzene, up to 5%, do not always occur in the same sense as the differences in $\delta^{13}\text{C}$, $<0.3^{\circ}/\text{oo}$, indicating the relative insensitivity of the single collector spectrometer measurements and, thus, precluding any definitive interpretation of these particular results.

For wood section SD5, only double collector measurements were performed. In this case, the majority of $\delta^{13}\text{C}_{\text{BE}}$ values were smaller (more negative) than the corresponding $\delta^{13}\text{C}_{\text{CE}}$ values and in many cases the differences exceeded the replicate error for combustion of benzene, $\pm 0.24^{\circ}/\text{oo}$. Since the $\delta^{13}\text{C}_{\text{BE}}$ values are smaller than corresponding $\delta^{13}\text{C}_{\text{CE}}$ enrichments, the ^{13}C (and ^{14}C) content of the synthesised benzene is obviously lower compared to the ^{13}C (and ^{14}C) content of CO_2 produced by sample combustion. This may be the result of a chemical fractionation effect. As in the case of SD4, however, there is no correlation between recorded chemical yields and the differences in $\delta^{13}\text{C}$ values.

As a result of the non-quantitative conversion of benzene to CO_2 in the micro-combustion system it is only possible to make tentative conclusions from these data. There is no apparent correlation between chemical yield and differences in the stable carbon content of benzene-derived and sample-derived CO_2 , yet there appears to be a systematic-decrease in $\delta^{13}\text{C}$ values throughout the SD5 series. Thus any fractionation effect in the benzene synthesis is most probably a small one, certainly less than $1^{\circ}/\text{oo}$ and probably less than $0.5^{\circ}/\text{oo}$, leading to lower $\delta^{13}\text{C}$ values. Consequently, any fractionation effect contributes only a very small amount to the non-counting error.

Further sources of potential error, which in this treatment are being assessed as non-counting errors may actually be ascribed as counting errors. Such factors as radon in the scintillation cocktail and variable counting geometry will have a direct influence on the counting procedure and will therefore contribute to the overall counting error. These errors are basically not observable in the data producing the counting error since they are a function of sample preparation and storage time prior to counting, and also of the possibility of non-reproducibility in individual counting vials.

In the final stages of synthesis of lithium carbide after addition of CO_2 , heating of the reaction vessel is continued. This procedure enables decomposition of any lithium carbonate to lithium oxide and carbon dioxide, with subsequent CO_2/Li reaction producing the carbide, but it also facilitates outgassing of radon from the reaction vessel, any radon subsequently being pumped away. The generally lower reaction yields for this research have been attributed to insufficient heating of the reaction vessel and this may result in incomplete degassing of radon from the sample.

The amount of radon in any sample which will contribute to the observed count rate will depend not only on the size of the contribution from the benzene synthesis but also on the length of time the samples are stored prior to counting. A batch of samples for counting is generally prepared over 12 - 16 days, with a subsequent delay of 5 to 7 days before this batch is counted. Consequently, since the half-life of radon-222 is 3.82 days, only the most recently synthesised samples should contain any appreciable quantity of radon.

Figs. 4-3, 4-4 and 4-5 show the number of counts obtained in successive 100 minute counting increments for samples GU 760 (SD4, sample 6), GU 676 and GU 689 (Ynyslas replicate samples 8 and 21), the 100 minute increments being separated by 700 minutes in the automatic counting cycle. The time lapse between preparation of sample and counting is 0 days, 7 days and 11 days respectively. It can be seen from Fig. 4-3 that there is no evidence of any exponential trend in the number of counts accumulated in successive 100 minute increments for sample GU 760, which is more likely to contain radon than the other two samples. Indeed, it can be seen from all three figures that the number of counts per increment is constant for the total period, and it is concluded that contamination of samples by radon is not detected and therefore does not contribute to the observed non-counting error. Furthermore, since the expected number of counts for successive counting increments is constant, one can eliminate evaporative loss of benzene during storage and counting as a source of error. It may be that over longer periods of time this loss becomes significant if the vial cap is not secured with an adhesive or some other permanent seal. It has previously been shown that there is no noticeable evaporative loss over a period of eleven months for a sealed vial containing a modern standard sample. (Fig. 4-1).

The term "counting geometry" refers to the presentation of the samples to the ^{14}C detection system and for the liquid scintillation method will be determined by the position of the vial between the photomultiplier tubes, the quantity of scintillation cocktail in the vial and the counting vials themselves. Any variability in these parameters will have

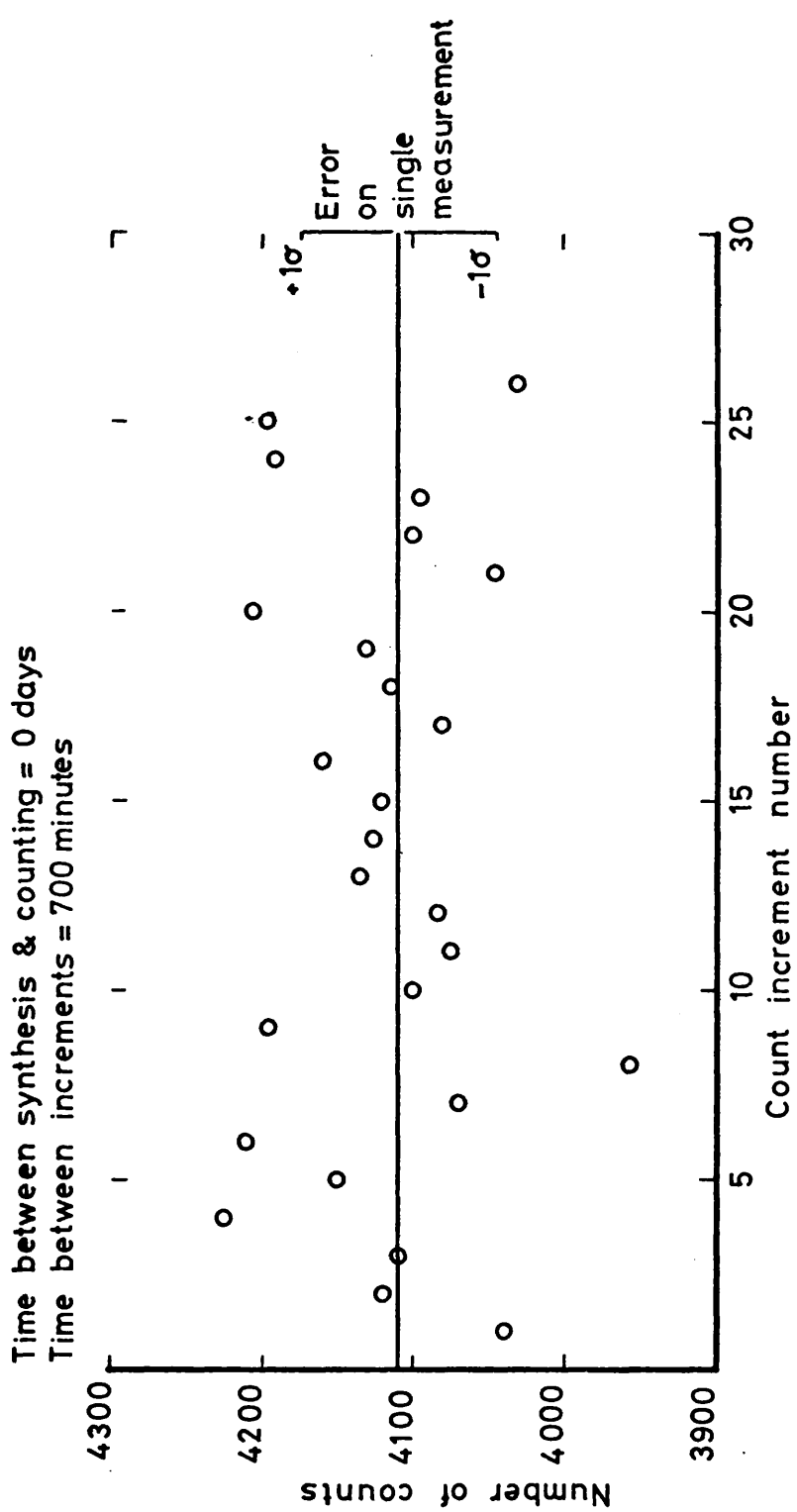


FIGURE 4-3: Stolford 4/6 (GU 760) - Number of counts accumulated in successive 100 minute counts.

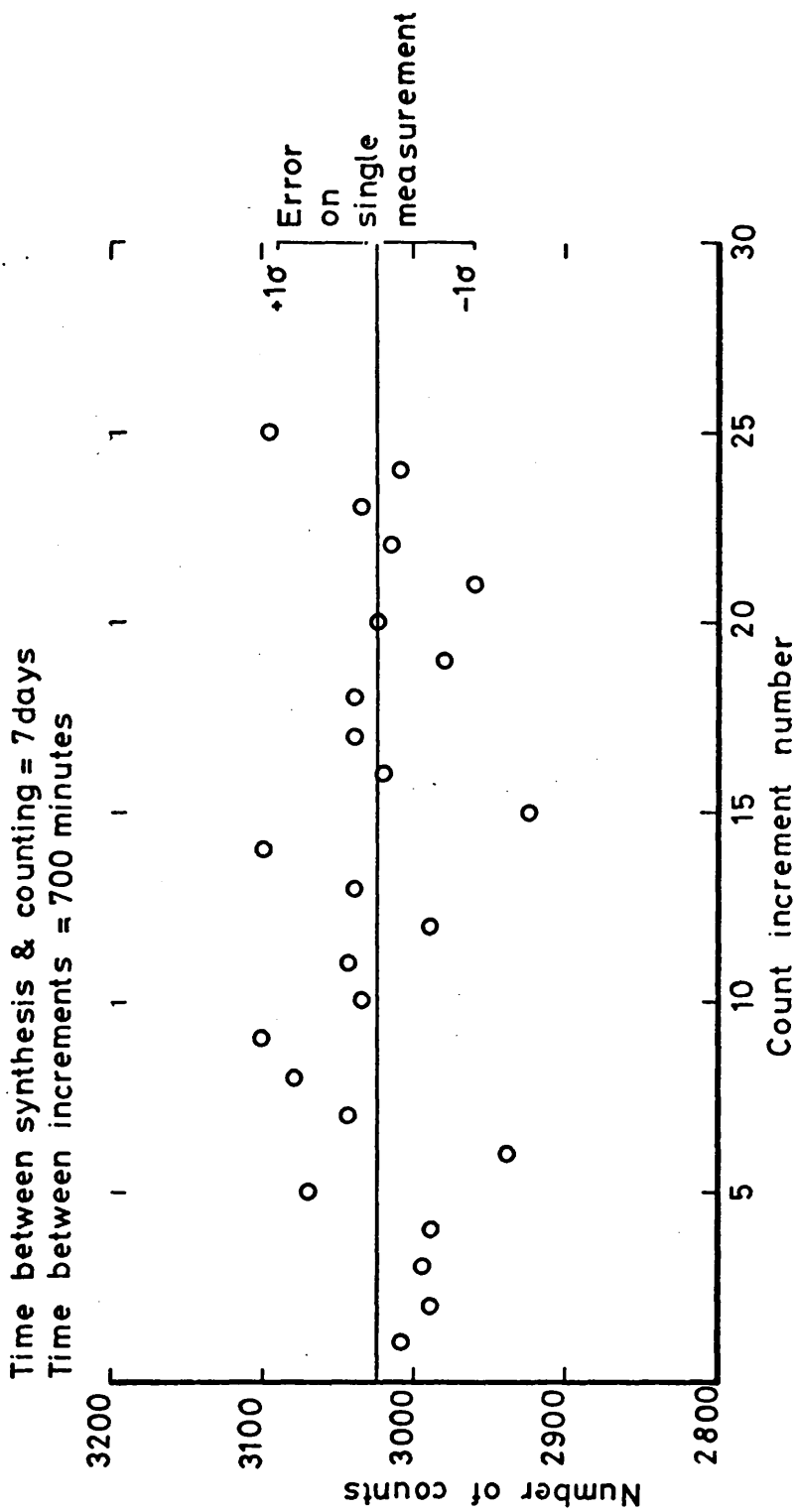


FIGURE 4-4 : Wood replicate 8 (GU 676) - Number
 of counts accumulated in successive
 100 minute counts

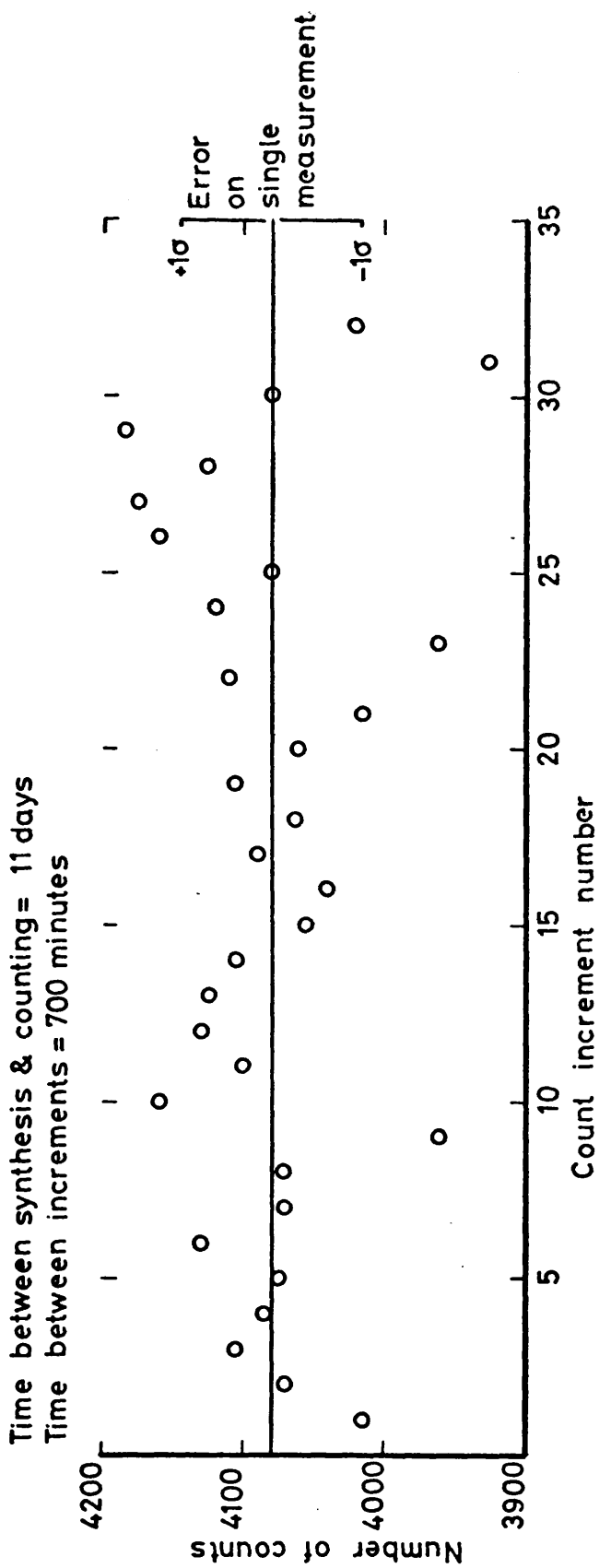


FIGURE 4-5: Wood replicate 21 (GU 689) - Number of counts accumulated in successive 100 minute counts

an effect on either or both the efficiency or the background. The position of the vial between the photomultiplier tubes is determined electrically by a micro-switch on the sample elevator which carries vials from the sample tray to the counting chamber, this position being assumed to be constant.

At the outset of this research project, a 10 ml counting geometry was adopted. The preparation of the standard geometry vial, described in Chapter 2, requires accurate weighing and use of volumetric apparatus such as burettes and pipettes. Errors associated with the use of gravimetric and volumetric apparatus have been assessed. Repeated weighing of a scintillation vial using different balances, accurate to the 4th or 5th decimal place showed that these determinations were consistent to the 4th decimal place and that there were no systematic differences between the balances used. The volumetric error was then assessed by adding standard amounts of benzene or scintillation solution to pre-weighed vials. These experiments have shown that the standard 10 ml counting solution is prepared to within less than 0.01 ml and, as is shown in Appendix 1, this variability will have a negligible effect on the background count rate and also on the ^{14}C detection efficiency since the primary and secondary scintillators, PPO and POPOP, are present in excess.

The conclusion to be drawn from the close scrutiny of the experimental procedures outlined above is that, apart from a possible fractionation effect of $<1^0/00$, there is no evidence of any major source of variability giving rise to the non-counting error calculated from the wood replicate

series. The fractionation effect may be corrected for by measuring the stable carbon isotope enrichment on benzene-derived CO_2 rather than on sample-derived CO_2 , the uncertainty on this measurement which will contribute to the counting error, being based on the series of micro-combustion-mass spectrometry measurements performed using scintillation grade benzene.

Since it has been shown that the non-counting error does not arise from uncertainties in the sample preparation procedures, the replicate material itself must be reconsidered. Before this wood was selected as a replicate standard, a sequential growth-increment analysis was performed. Comparison of these dates (Table 3-3-5) with those obtained in the replicate series shows that there is a systematic difference between the two sets of results, the replicate analysis generally being younger. This discrepancy may be the consequence of contamination of the replicate sample with modern carbon during the homogenisation process, the source of the contaminant being the plant tissue normally processed in the mill. Although cleaned as thoroughly as possible, the geometry of the mill may have prevented total removal of residual plant debris. It seems probable that this contaminating organic carbon would, at least to a certain extent, survive the pretreatment process (cellulose extraction) thus giving an erroneous assay. Moreover, it is unlikely that this contamination would be distributed uniformly through the sample for the following reasons. Firstly, the bulk replicate sample is not itself homogeneous, i.e. not totally reduced to sawdust. Secondly, most of the very finely divided contaminant would be incorporated into

the first pieces of chopped wood introduced to the mill and would, most probably, remain in contact with this wood as a result of the electrostatic charges induced during grinding.

The results of the sequential growth-increment analysis of this wood section, Ynyslas 1, are discussed in detail in Chapter 5. The data show that during the growth span of the tree the radiocarbon concentration in the atmosphere was virtually constant, and hence these eight analyses may be considered as further replicate samples. The mean value and standard error for the additional replicate analyses are calculated to be

$$\overline{\Delta^{14}\text{C}} \pm 1\sigma = -463.91 \pm 3.97^{\circ}/\text{oo} \quad (5008 \pm 59 \text{ years B.P.})$$

After subtraction of the average counting error, the non-counting error is found to be $\pm 2.08^{\circ}/\text{oo}$ (± 51 years), corresponding to a relative error of 0.4% which is considerably less than that for the 24 replicate analyses on the homogenised sample ($\pm 1.16\%$). It seems likely, therefore, that the variability induced in the homogenisation process through contamination largely accounts for the overall replicate error and that the true total error for a single analysis is close to the counting error.

Summary and conclusions

The series of replicate analyses has indicated that there is a considerable non-counting error associated with a single radiocarbon analysis. Subsequent counting of the experimental procedures has, however, led to the conclusion that this extra variability is most probably a consequence of contamination introduced during preparation of the bulk standard. The

possibility of there being a non-counting error should be included in the reported error on a single radiocarbon age determination. Thus for a sample analysis yielding the fractionation corrected ^{14}C enrichment $\Delta^{14}\text{C}_{\text{SAM}}$ and counting statistics error ϵ_c , the total error ϵ_{TOTAL} is given by

$$\epsilon_{\text{TOTAL}} = \left[\epsilon_c^2 + \left(\frac{k}{100} \times \Delta^{14}\text{C}_{\text{SAM}} \right)^2 \right]^{\frac{1}{2}}$$

k is the relative error (%) indicated by replicate analyses, for this research $k = 1.16\%$. It is, however, stressed that in the light of the above analysis, ϵ_{TOTAL} is the maximum uncertainty of the assay, the true uncertainty more probably being a value close to the counting error, and consequently, the analysis of data produced in this research is based on the counting error alone.

From this work, several recommendations can be put forward concerning the selection of replicate analysis working standards.

1. The working standard should, if possible, be aged and of a material which is typically analysed by the laboratory, e.g. wood,
2. the bulk sample should be homogenised to a consistent texture and if possible, a part of the original sample should be sacrificed as a safeguard against inclusion of contamination during the early stages of the homogenisation procedure,
3. as a precaution against violent combustion of finely divided material, pretreated samples should be "pelletized",
4. after running an initial batch of samples (say 20 - 30), aliquots of the replicate sample should be routinely analysed,
5. the error which is obtained from the distribution of

results should be quoted with the counting error when reporting ^{14}C dates.

The distribution of such working standards to other ^{14}C laboratories, on an intercalibration basis may lead to the introduction of a set of secondary ^{14}C standards which would provide a more satisfactory means of assessing laboratory reproducibility than is available with present standards.

CHAPTER 5

DISCUSSION OF TREE-RING/RADIOCARBON RESULTS5.1 Preliminary results

Previously accumulated ^{14}C data on samples recovered from submerged forest sites around the coast of the U.K. (Fig. 1-6) have proved the availability of a wide age range of material suitable for dendrochronological and radiocarbon studies. This research has concentrated on samples recovered from exposures along the west coast of England and Wales. Exploratory ^{14}C analyses (Table 3-3-1) have shown that, while many submerged forest sites date from the period of optimum development, that is 4,000 to 5,500 years B.P. (e.g. Borth (Tables 3-3-2, 3-3-3 and 3-3-4), Stolford, Clarach, Alt Mouth), there are areas yielding older and younger trees, such as Morecambe (GU 664: 7544 \pm 306 years B.P.) and Llanaber (GU 665: 732 \pm 52 years B.P.). It is interesting to note that the submerged forests only a few miles to the south of Llanaber, namely Clarach, Ynyslas and Borth, yield wood of a considerably older age, reflecting a wide difference in the history of formation of these exposures.

Comparison of previous data with those produced in this research yields information on the time interval during which forests were established. For example, samples from the earliest trees from the Ynyslas forest give a ^{14}C date of 6026 \pm 135 years B.P. (Q 380 - Godwin and Willis, 1961). Pine wood from the same site, dated at 5,000 years B.P. in sequential growth-increment analysis and replicate studies,

shows that this forest was in existence for approximately one millenium. A similar comparison shows that forests in Bridgewater Bay, Somerset at Burnham-on-Sea (Q 134 - Godwin and Willis, 1959; NPL 147, 148 - Callow and Hassal, 1968) and Stolford (this research) were established for almost 1500 to 2000 years.

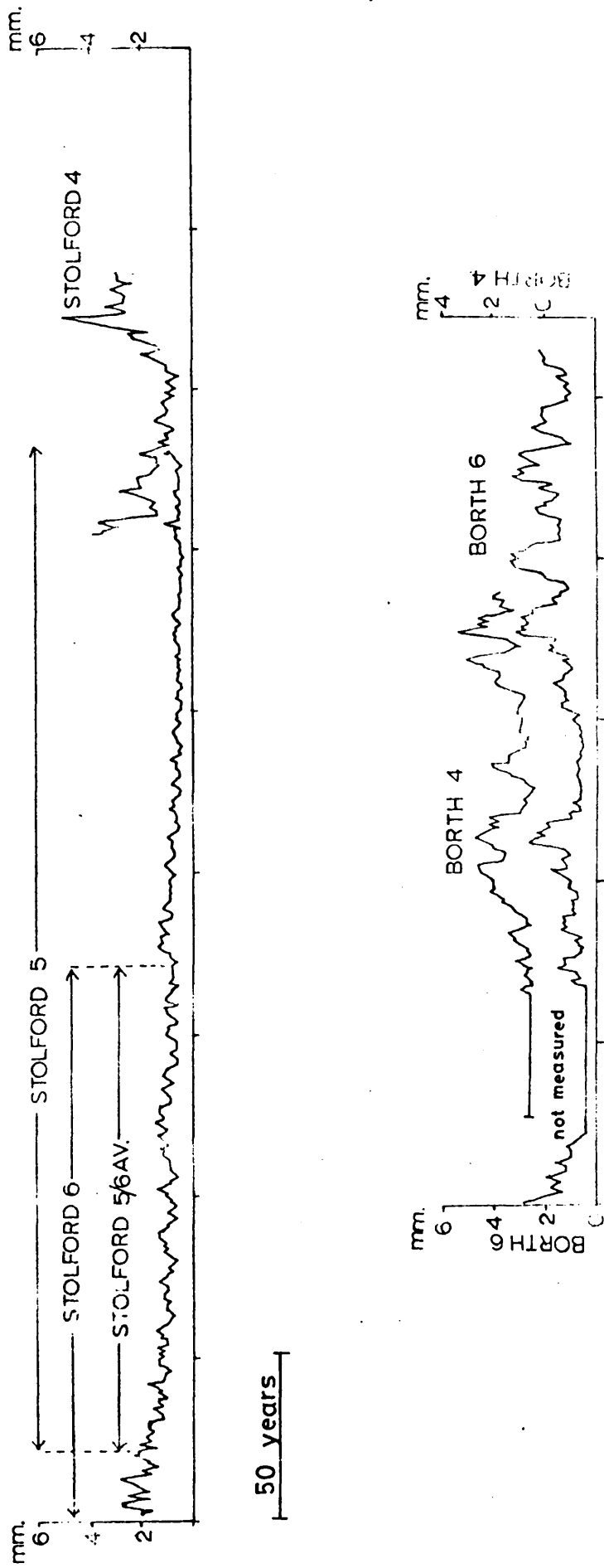
Samples from Newtown (GU 667: 885 ± 83 years B.P.) and Rheidol (GU 668: 647 ± 136 years B.P.), supposedly interglacial, were collected from very similar situations. In both cases, the trees were found under thick gravel, approximately 5m, near to a river, namely the Severn and the Rheidol. It was the opinion of hydrologists and geomorphologists that such a large quantity of gravel was of glacial or late-glacial origin, as the river flow had not, subsequently, been sufficient to transport such quantities. The trees, therefore, as there were no large oaks around in the full or late-glacial, must have been reworked from older, that is, interglacial deposits. ^{14}C analysis of the trees has shown that this is not so and a reappraisal of the situation has yielded the correct geomorphological interpretation. Both sites are on the inside of a bend in the river (or they were when the gravels were deposited). As the river meandered, it cut through the glacial gravels forming a cliff and removing them from the outside of the bend, redepositing them on the inside. The oaks were growing on the outside bank, were undercut, fell into the river, and were incorporated into the gravel. Since that time, the channel has subsequently moved and left the thick gravels apparently undisturbed.

5.2 Dendrochronology

Tree-ring/radiocarbon studies, based on submerged forest wood, have been concentrated on two major exposures in Bridgewater Bay, Somerset at Stolford ($51^{\circ} 12' 30''$ N., $3^{\circ} 6' 30''$ W.) and in Cardigan Bay, Wales at Borth-Ynyslas ($52^{\circ} 29' N.$, $4^{\circ} 4' W.$). From the former site an oak chronology spanning 360 years has been constructed and samples from sections Stolford 4 and Stolford 5 analysed. The tree-ring curve for this "floating" chronology is presented in Fig. 5-1. At the latter site, forests of both oak and pine had been established and a separate chronology for each species has been examined. It is in some ways unfortunate that the oak tree-ring record and ^{14}C growth-increment analysis were developed concurrently, since, after ^{14}C analysis of the oak section Borth 4, it was found that the Borth 6 section overlapped it completely. Thus the maximum range of the dendrochronology for this site is determined solely by Borth 6. The dendro-curve for this site is also presented in Fig. 5-1.

The pine forest at Borth-Ynyslas has also been investigated although it has not yet been possible to relate the two pine sections analysed Borth 1 and Ynyslas 1. One of the main problems with pine wood is that growth rings may occasionally be absent. Consequently, statistical construction of long sequences of tree rings, and inter-species overlap, i.e. oak-pine, is rendered difficult. Furthermore, pine tree-ring sequences from these exposures have tended not to follow the type of growth pattern recorded in the oak wood related to climate or water-table variations.

FIGURE 5-1: Tree-ring width curves for Stolford & Borth oak chronologies



The tree-ring curves in Fig. 5-1 are drawn according to the convention of time increasing to the left. Consequently, all subsequent radiocarbon/tree-ring diagrams have been plotted in accordance with this convention.

A further sample of oak wood has been recovered from an Iron Age site at Castle Point, Troup, Banffshire (57° 41' N., 2° 17' W). A comprehensive account of the archaeology of this multioccupational site has been produced by Greig (1970; 1971), and timber excavated from the gate structure dated at 2347 ± 59 years B.P. (BM 639 - Barker et al., 1971). This analysis, performed on the outermost rings of the timber, is in excellent agreement with the results obtained here (Table 3-3-8; SRR 861, 862, 863). The dendrochronological examination of the two timbers collected for this study was carried out at the Palaeoecology laboratory, Queen's University, Belfast, and results show that although the ring width pattern for both timbers correlated almost completely, this record could not be matched with established sections of the Irish bog oak chronology (Baillie, pers. comm.). The longer-lived stump, containing 258 growth rings, has been analysed.

5.3 Analysis of tree-ring/radiocarbon data

Analysis of tree-ring/radiocarbon data, in terms of variations in the natural ¹⁴C content of the atmosphere, requires a certain unavoidable level of subjectivity in the selection of a relationship between the two timescales.

Since a wide range of mathematical functions can be fitted to this type of data, for instance, by classical least squares techniques, there is, really, little to choose between statistical fitting and free-hand drawing, different workers accentuating the features which they consider important. The adoption of some form of statistical model is, however, desirable when data from different sources, such as in this case, submerged forest and bristlecone pine wood, are to be compared. Such a treatment has been applied to "floating" chronologies from Europe by Clark and Renfrew (1972) and Clark and Sowray (1974), assuming a common model for "floating" and absolute chronologies. The results obtained from these studies were in broad agreement with previous work by Ferguson et al. (1966) and Suess and Strahm (1970), which essentially fitted "wiggles" in the Suess calibration (Suess and Stuiver, 1966; Suess 1970a) to wiggles in the "floating" chronologies. This particular statistical method of analysis has been applied to the data obtained in this research and the results are discussed later. Of course, the exact form of the relationship between the radiocarbon and sidereal time-scales is not known. Over the relatively short time spans studied in this project, therefore, it is considered most appropriate to evaluate only a simple least squares model and further to discuss non-random variability about this "trend" line.

Linear least squares analysis has been performed on the oak and pine "floating" chronologies. The results are presented in Table 5-1. If the linear model is to be a good approximation to the data, then the mean square

TABLE 5-1 : LINEAR LEAST SQUARES ANALYSIS OF SUBMERGED FOREST FLOATING CHRONOLOGIES

Chronology	L.S.E. of gradient		^{14}C trend parallel to growth % per century	Expected $\frac{-2}{\epsilon_c}$	Variability $\frac{-2}{\epsilon}$ TOTAL	observed M.S.D.R.
	Unnormalised	normalised				
Cullykhan 1	+ 0.28 ± 0.35	+ 1.28 ± 0.35	-1.5	1399	2522	12030
Borth 4 and 6 (oak)	- 0.15 ± 0.44	+ 0.85 ± 0.44	-1.0	2312	6665	29856
Stolford 4 and 5	- 2.18 ± 0.15	- 1.18 ± 0.15	+1.5	3448	9355	8455
Borth 1 pine	- 0.73 ± 2.03	+ 0.27 ± 2.03	-0.3	1892	9385	19027
Inyslas 1 pine	- 1.44 ± 0.94	- 0.44 ± 0.94	+0.5	2601	9336	3424

deviation about the regression line (M.S.D.R.) should only reflect the variability arising from experimental factors. In Chapter 4, replicate ^{14}C measurements have indicated that the maximum variability on the set of analyses was $\pm 1.16\%$, although this value is most probably a large overestimate, the true value being close to the counting uncertainty. For each of the "floating" chronologies analysed, therefore, it is possible to estimate the expected M.S.D.R. for a good linear fit, based on $\bar{\epsilon}_{\text{TOTAL}}^2$ and $\bar{\epsilon}_{\text{C}}^2$. From Table 5-1, it is seen that for the Cullykhan and Borth oak chronologies and the Borth pine chronology, the observed M.S.D.R. exceeds the predicted value based on $\bar{\epsilon}_{\text{TOTAL}}^2$. For the Stolford oak and Ynyslas pine chronologies, the observed M.S.D.R. is less than the predicted value based on the maximum error, but exceeds that predicted purely from counting statistics, namely $\bar{\epsilon}_{\text{C}}^2$, thus enhancing the assertion that the maximum replicate error is indeed an overestimate of the true laboratory variability, the spurious uncertainty arising from extraneous contamination and not from experimental error. The results of the simple linear least squares analysis of the "floating" chronologies, therefore, show that, with the exception of the Ynyslas pine section, there are additional sources of variability in the data over and above experimental uncertainty.

This initial model, however, does not take account of the different uncertainty associated with individual measurements. A weighted least squares model has been

applied to the "floating" chronologies, the "weight" associated with an individual analysis being in inverse proportion to the variance of that measurement. The results of these calculations are given in Table 5-2. It is found that the overall trend in ^{14}C levels during the separate time spans is not markedly different from those calculated by the unweighted linear least squares method. As in the previous treatment, however, the variability about the least squares line exceeds that expected for a linear model.

These analyses have shown that the relationship between radiocarbon age and growth-ring index is, in virtually every case, Ynyslas being the exception, non-linear and accordingly an alternative situation involving "wiggles" must be considered. cursory visual inspection of the various tree-ring chronologies clearly indicates non-linear trends in the ^{14}C age-profile. Fluctuations, such as are apparent, have not generally been observed in bristlecone pine/radiocarbon data. This may well be due, however, to a "damping" effect arising from the lower sampling frequency of the American work. In Fig. 5-2, the sampling frequencies, expressed as an interval distribution for this research and bristlecone pine measurements (from Houtermans, 1971), are compared. The American data comprise analyses of samples, each consisting of ten growth increments, but at a much lower frequency than that employed here, adjacent samples being, on average, 21 - 22 years apart in contrast to 11 - 12 for this project.

TABLE 5-2 : WEIGHTED LINEAR LEAST SQUARES ANALYSIS OF SUBMERGED FOREST FLOATING CHRONOLOGIES

Chronology	L.S.E. of gradient Unnormalised	normalised	¹⁴ C trend parallel to growth % per century	Sigma-squared value*
Cullykhan (oak)	0.0	+ 1.0	- 1.2	6.12
Borth (oak)	- 0.06	+ 0.94	- 1.2	15.44
Stolford(oak)	- 2.24	- 1.24	+ 1.5	3.20
Borth (pine)	- 0.56	+ 0.44	- 0.5	13.09
Ynyslas (pine)	- 1.95	- 0.95	+ 1.2	1.12

* The expected variance, $v(y_i | x_i) = \sigma^2 w_i$ where w_i is inversely proportional to the square of the counting error.
For a good fit $\sigma^2 \approx 1$

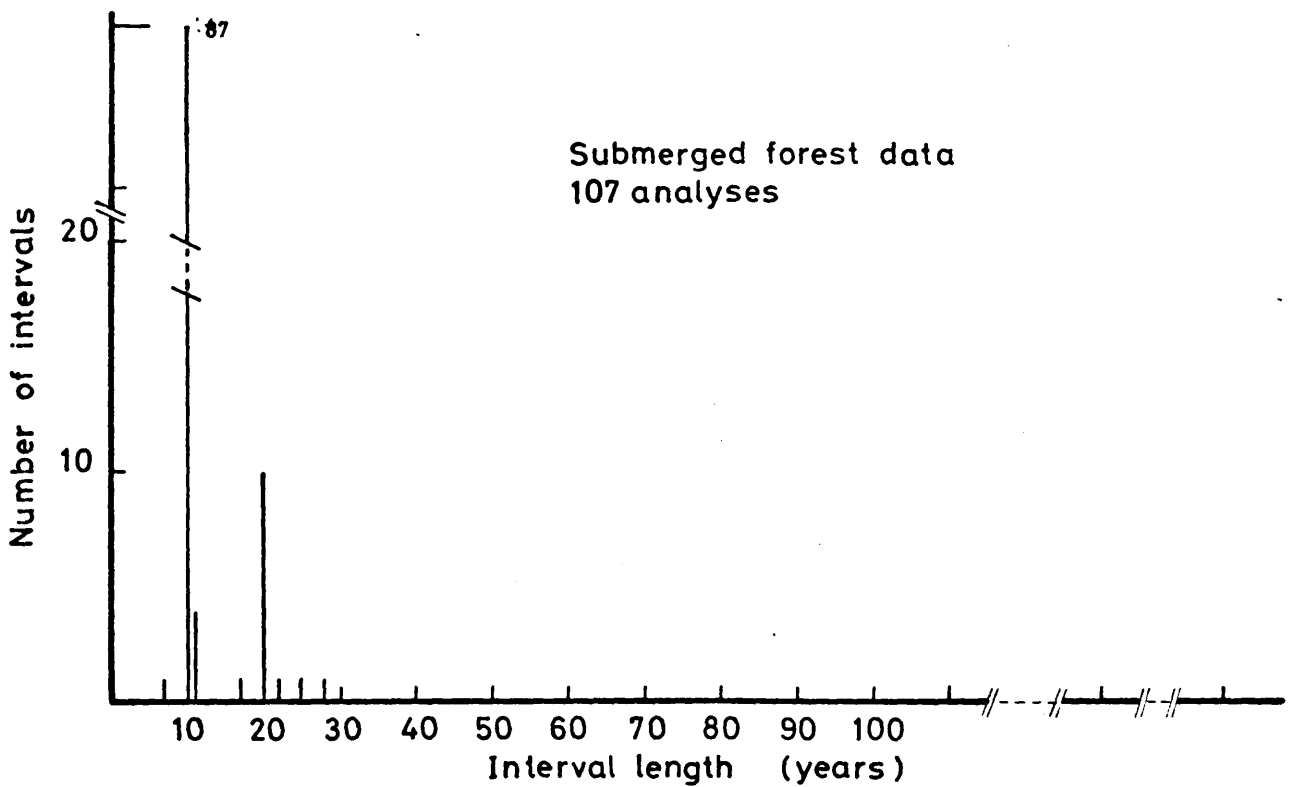
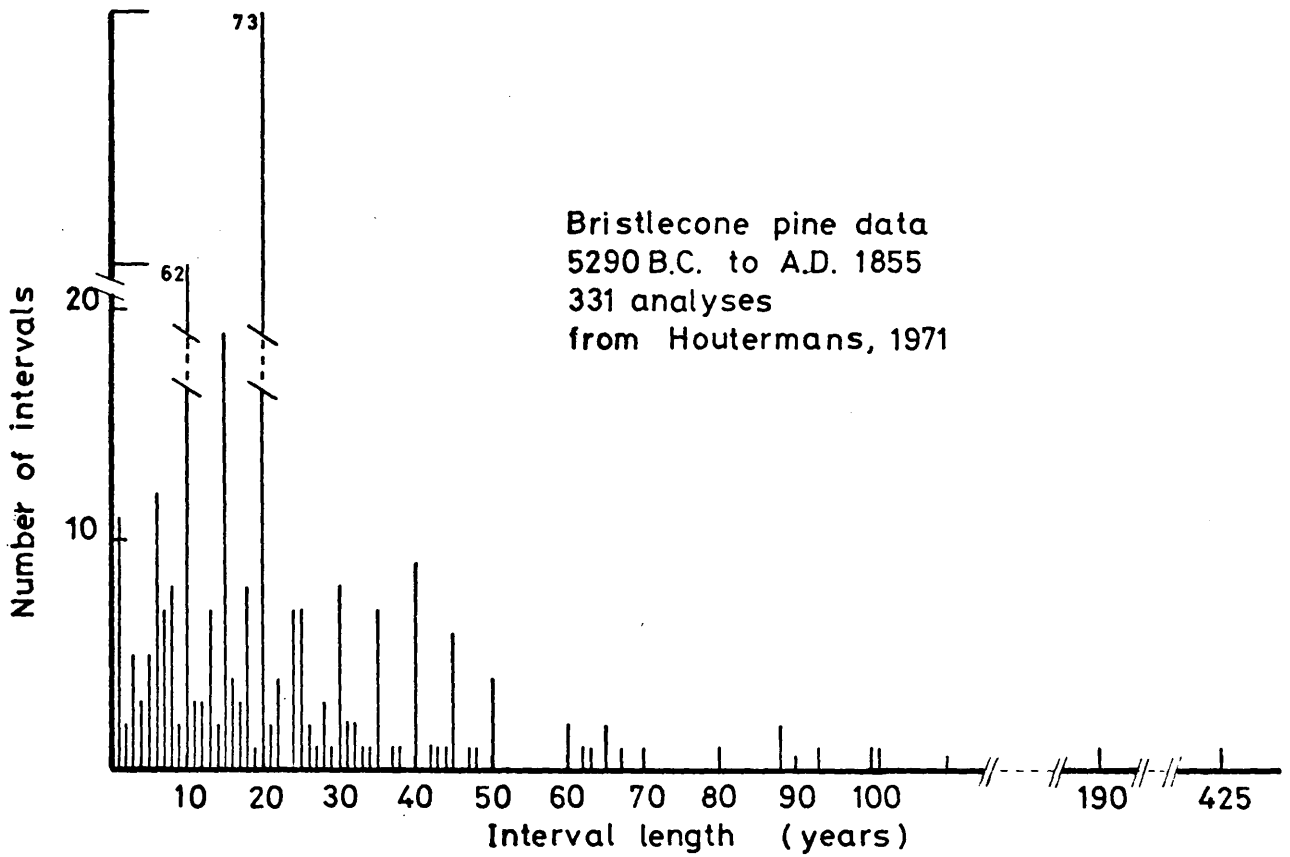


FIGURE 5-2 : Comparison of sampling frequencies

Furthermore, for the age interval of the U.K. wood studied, the sampling frequency for the bristlecone pine chronology is considerably reduced (3 - 4 samples per century). Indeed in Suess' interpretation of the calibration curve (Suess, 1970a), the calibration line is not continuous in the region of 5500 - 6500 tree-ring years B.P. ($\sim 5,000$ ^{14}C years B.P.).

Fig. 5-3A, B and C show the effect of a reduction in sampling frequency for the Stolford 5 section (Table 3-3-7). Three cases are considered.

A and B : the two possible profiles for 5 x 10
year samples per century

and C : profile for averaged adjacent analyses.

For A and C, the scatter about the least squares straight line has been reduced, indeed case C is a close approximation to a straight line if the counting errors in this latter case are considered to be comparable with those for the total chronology. The averaging process producing 5 x 20 year samples per century may, however, be considered as effectively doubling the counting time on individual ^{14}C assays, with a decrease in the expected M.S.D.R. to ~ 0.7 of the value expected as a result of the longer count time. In case C, however, the reduction in M.S.D.R. is greater than expected, therefore the averaging process appears to have "smoothed" the data. For each of the conditions, the scatter, in terms of smoothness of the radiocarbon/growth increment relationship, has been reduced to a level comparable with that observed in the bristlecone pine data. It is, however, important to note that the interpretation involved in each case will differ with

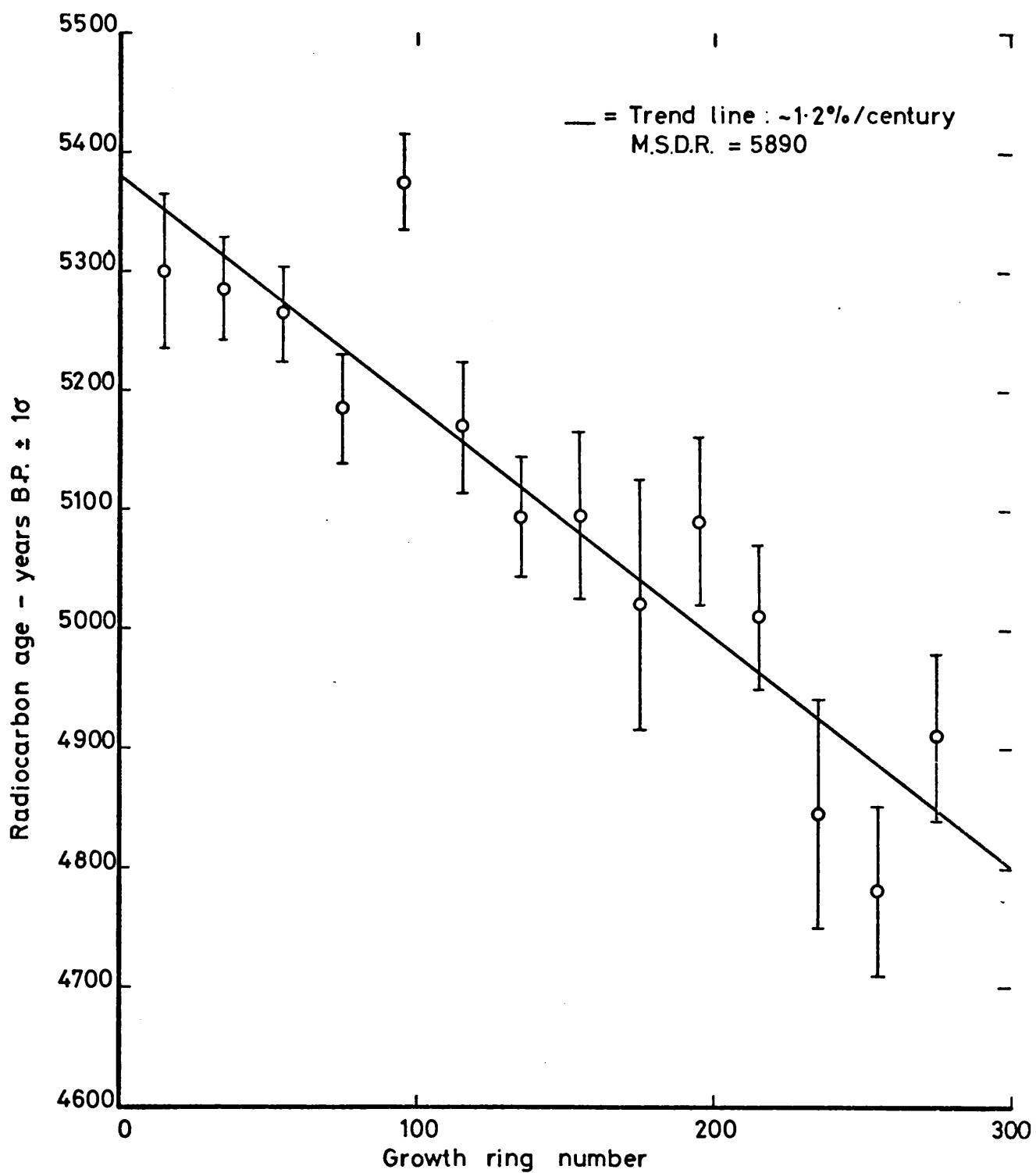


FIGURE 5-3A : Stolford 5 - 5x10 samples per century, alternate analyses Case A.

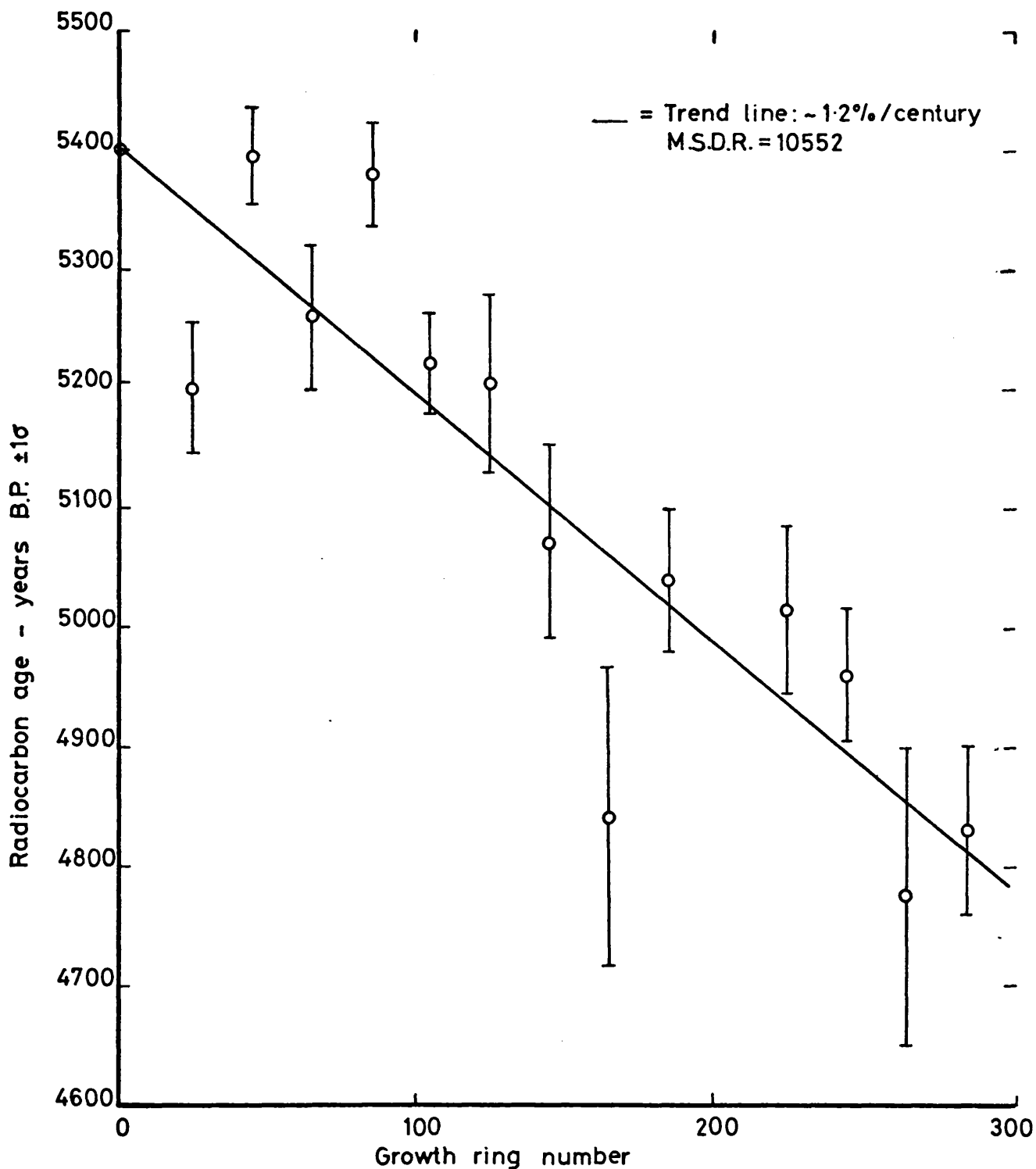


FIGURE 5 - 3B : Stolford 5 - 5x10 samples per century, alternate analyses Case B

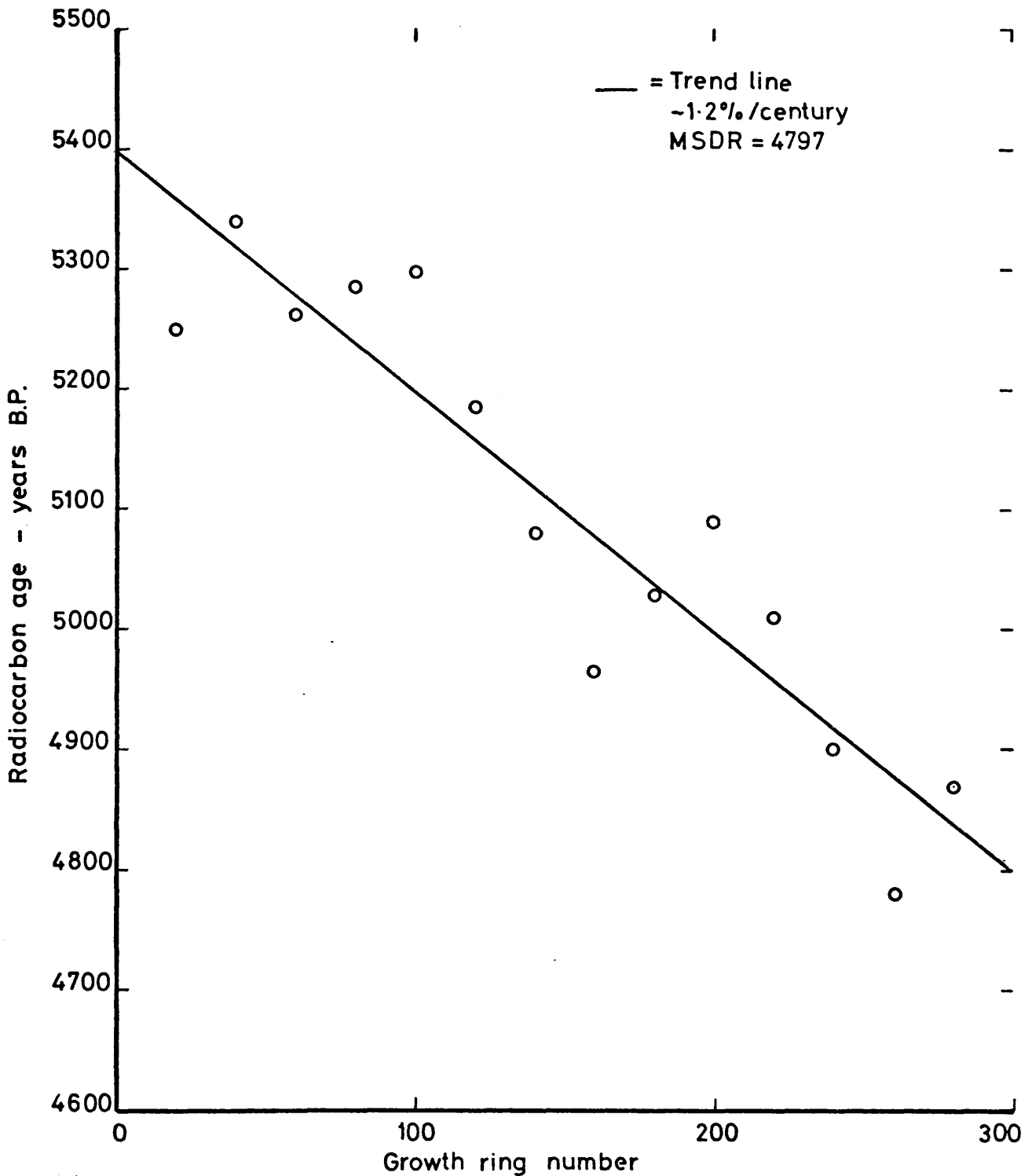


FIGURE 5-3C: Stolford 5 - 5x20 samples per century, adjacent averaged analyses Case C

regard to the overall trend of atmospheric ^{14}C concentrations, and, possibly of more importance, with regard to the frequency and magnitude of observed short-term fluctuations.

Any attempt at a semi-quantitative evaluation of the radiocarbon/calendar age relationship will, naturally, involve a degree of subjectivity and, as has been stated earlier, in this respect there is possibly little to be gained by searching for the mathematical equation which best represents the data, when a free-hand curve will, probably, give as reliable an account of the varying atmospheric ^{14}C concentration.

In the case of Cullykhan 1 (Table 3-3-8), various degrees of polynomial function have, however, been fitted to the data. The best fitting polynomial, namely the function minimising the M.S.D.R., is found to be fourth order, but the residual in this case is still in excess of the established random variability in ^{14}C assay. This function is plotted in Fig. 5-4 along with the weighted and unweighted least squares trend lines. Of particular interest is the sample at ring number 43 (SRR 847). This analysis gives a ^{14}C age 300 years younger than the samples adjacent to it, representing an increase in the ^{14}C concentration of almost 4% in ten years. Short-term variations of this magnitude have not previously been observed and it is difficult to arrive at an explanation for such an occurrence. The existence of such large fluctuations has significant implications with respect to archaeological dating and radiocarbon/calendar age calibration. In general, rates of change of the atmos-

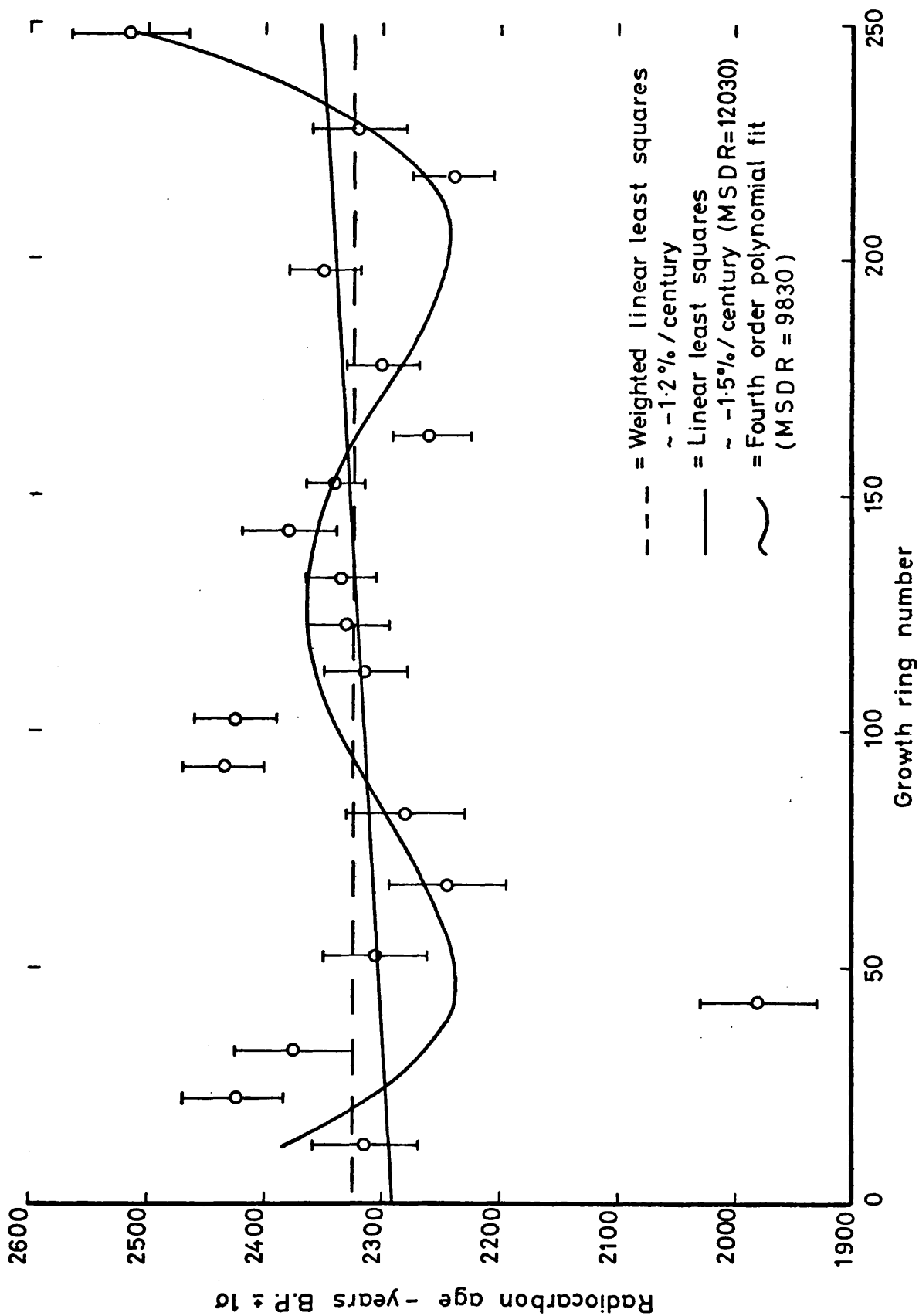


FIGURE 5-4 : Least squares approximations for Cullykhan data

pheric ^{14}C concentration during the Cullykhan 1 time span have been lower than this, although persistent. The maximum time derivative of ^{14}C is of the order of 3 - 4% in 30 years during the growth of the outer rings of the section.

The best fitting polynomial function for the Stolford oak chronology is a very smooth, featureless, cubic relationship. The marked fluctuation at the old end of the chronology, GU 763 - GU 767 (Table 3-3-7), a variation of $\sim 3\%$ in 50 years, has not been taken into account using this model, but is clearly a non-random event. Similarly, at the recent end of the chronology, samples GU 757 - GU 762 (Table 3-3-6) show a distinct variation of the same order of magnitude. The approximating functions for this "floating" chronology are illustrated in Fig. 5-5.

Of all the chronologies measured, the Borth oak sequence shows the greatest variability (Tables 3-3-3, 3-3-4). The agreement between the individual sections, Borth 4 and Borth 6, is fair, although the Borth 6 analyses are generally older than those for corresponding samples in Borth 4. In view of the replicate analysis study, it does not seem feasible that this variability should be related to experimental instability. The ^{14}C profile during this period shows distinct non-linear trends. For example, there is a rapid increase in atmospheric ^{14}C concentration, by as much as 5 - 6% during the first century of the chronology. Again polynomial regression techniques have been applied to the data, and the best fitting curve, plus the linear models for weighted and unweighted least squares analysis, are displayed in Fig. 5-6.

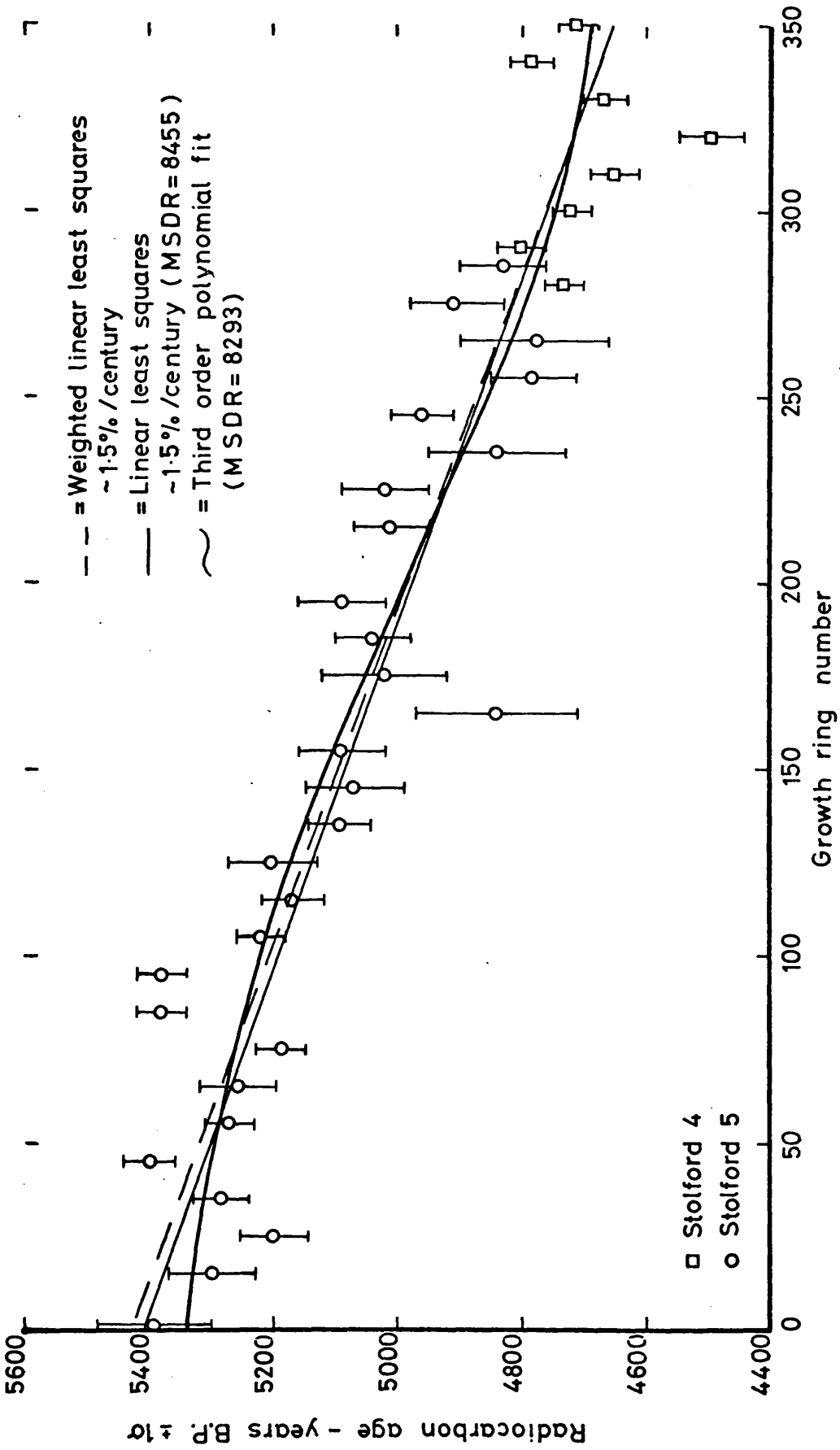


FIGURE 5-5: Least squares approximations for Stolford data

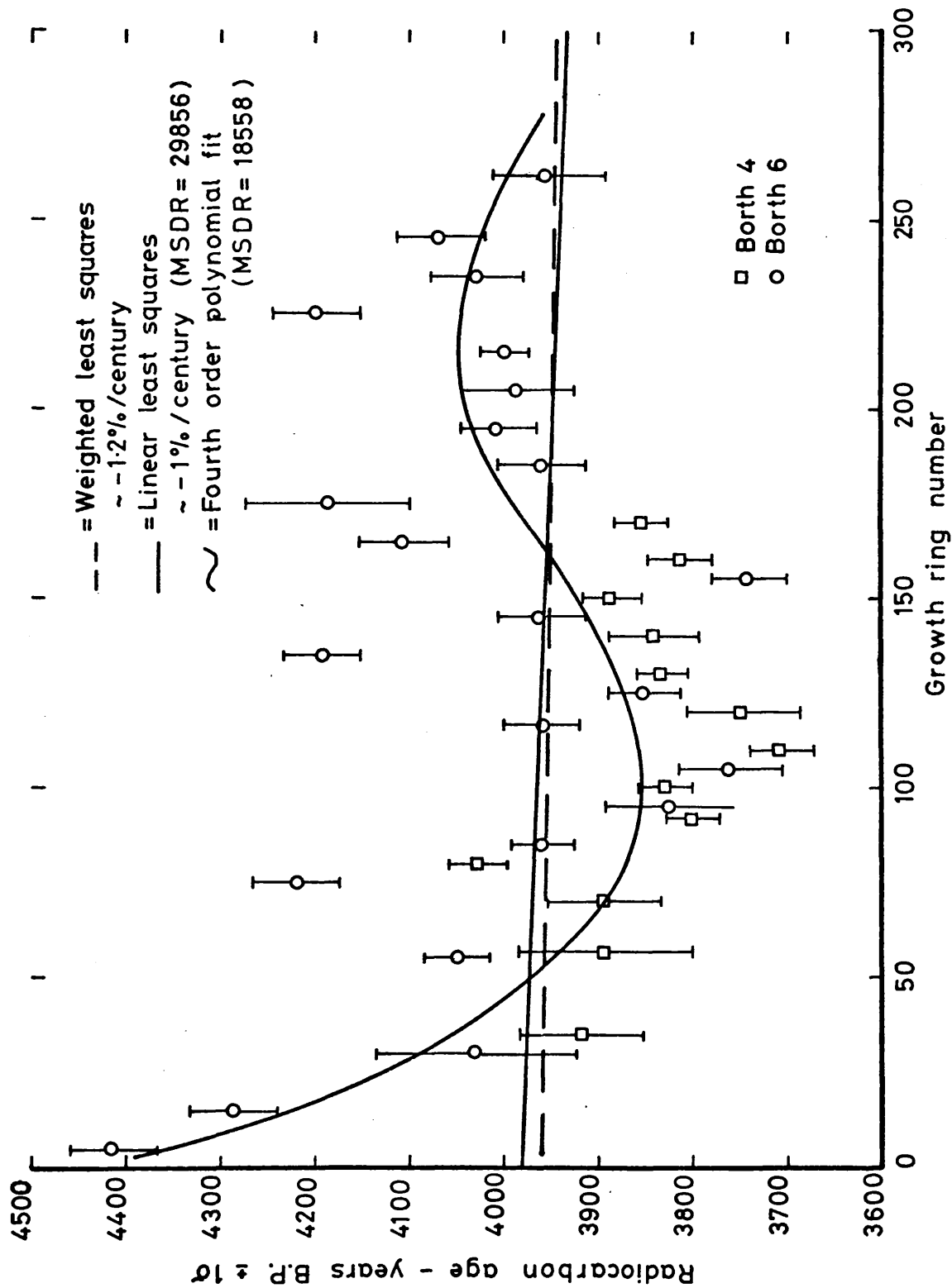


FIGURE 5-6 : Least squares approximations for Borth (oak) data

For the short pine tree-ring sequences analysed, it has been shown that the linear model is a reasonable fit in the case of Ynyslas 1 (Table 3-3-5). Borth 1, on the other hand, (Table 3-3-2) shows a distinct variation from linearity, amounting to a 3% decrease in atmospheric radiocarbon in 10 years, with an immediate increase of the same magnitude. No polynomial regression has been applied to this data set, since the small number of analyses precludes any degree of flexibility in the analysis. The weighted and unweighted least squares trend lines for these two chronologies are shown in Figs. 5-7 and 5-8.

In general, the radiocarbon data produced for the "floating" chronologies show clearly that short-term variations in atmospheric ^{14}C concentrations during the past millenia do exist. These perturbations, of the order of 2-3% over several decades, detected as a consequence of the increased sampling frequency employed in this study, have not previously been recognized in similar studies on bristlecone pine wood. Theoretical calculations on the natural radiocarbon cycle (Houtermans, 1966; Houtermans et al., 1973) have predicted that such short-term fluctuations, arising from variable ^{14}C production rates, tend to have a high attenuation and should, therefore, not be detected. The non-random variations observed here, if related to production-rate changes, apparently contradict the findings of these box model analogues.

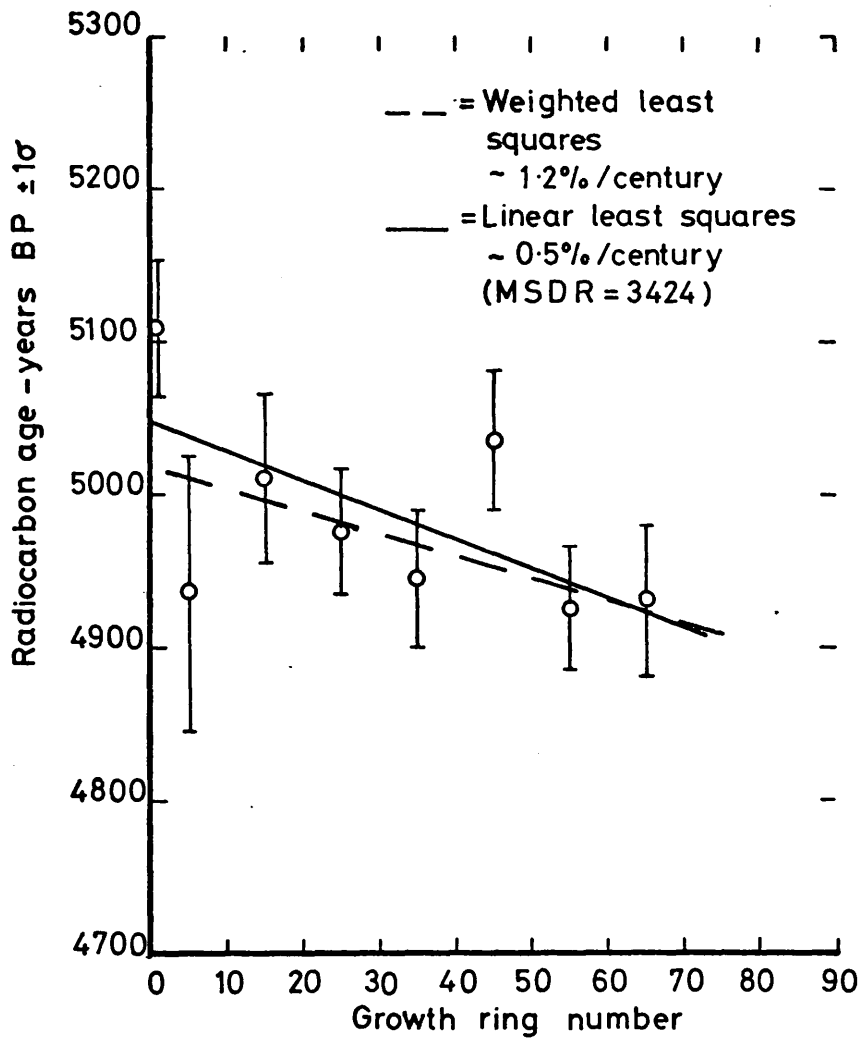


FIGURE 5-7: Least squares approximations for Ynyslas (pine) data

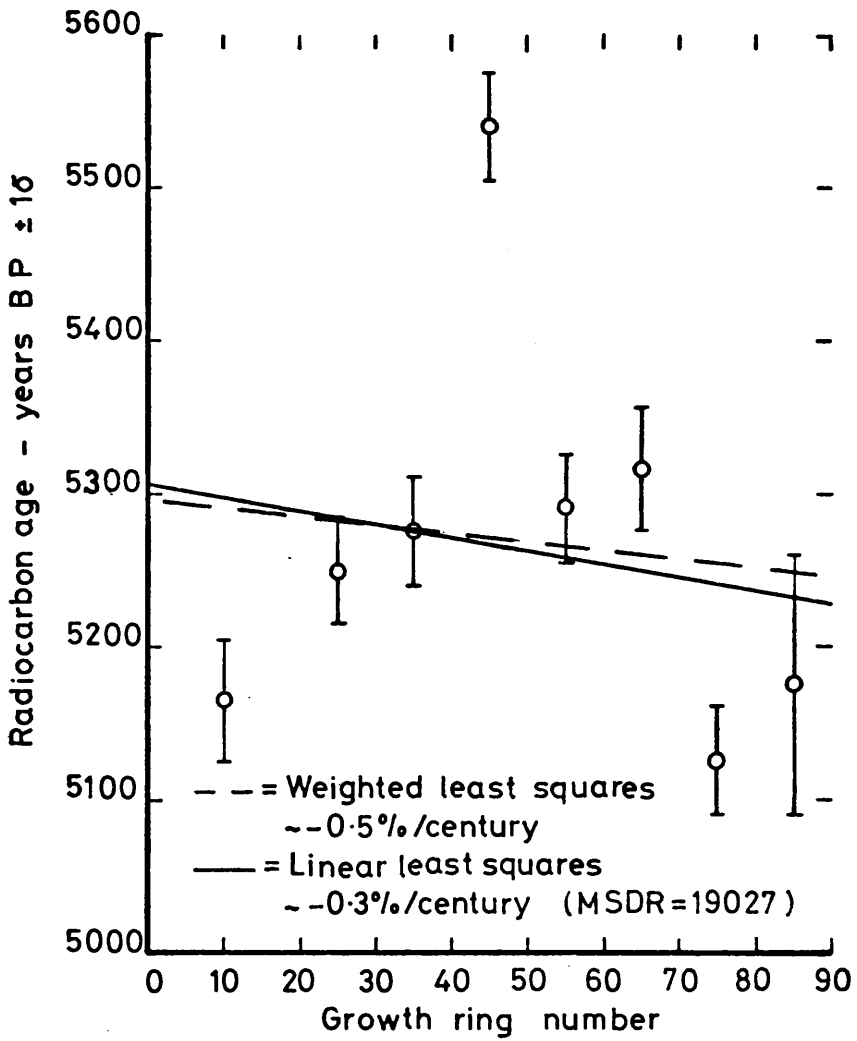


FIGURE 5 - 8 : Least squares approximations
for Borth (pine) data

The magnitude of these fluctuations is comparable with those discovered by other workers. For example, single tree-ring analyses by Baxter and Farmer (1973), Lavrukhina et al. (1974), Alexeev et al. (1975) and Drndarski (1977), show short-term fluctuations, of up to 3%, correlated with solar activity. Furthermore, Burleigh and Hewson (1976) have reported short-term fluctuations around 4,000 B.P. from measurements on deer antlers recovered from a Neolithic site in south eastern England. Although it is not possible to match this latter variation with the contemporary Borth chronology, the tree-ring analyses of this study corroborate the findings of these authors.

A possible explanation for the perturbations may be the existence of local effects. Lerman et al. (1970) have reported differences in ^{14}C specific activity for tree-rings from different locations. Furthermore, the work of Young and Fairhall (1968), on the distribution of "bomb"-produced ^{14}C , has shown latitudinal and meridional variation in the input of radiocarbon from the stratosphere to the troposphere. Thus, the temporal relationship between the tree-ring growth and the period of maximum tropopause instability is likely to be important in the incorporation of local effects. Very rapid growth during this time of maximal stratosphere-troposphere incursion should lead to a high sensitivity to short-term fluctuations in cosmic-ray-produced ^{14}C . On the other hand, the very slow growth of bristlecone pine wood may give rise to a

much slower response through a longer storage of nutrients. Clearly, ^{14}C measurements on single rings from the same growth year should show some correlation with ring width if this is a true source of local effects. Reiter (1973) has shown that influxes of stratospheric air into the troposphere can be triggered by solar flares. Measurements of ground-level concentrations of the cosmogenic radionuclides ^7Be and ^{32}P following such events, have shown increases of 50 - 100%, which are clearly not related to production rate changes. Moreover, the elevated levels of these radionuclides persist for several days. Similar short-term increases in ^{14}C , allied to rapid tree-ring growth could well represent a potential source of local effects.

Prevailing climatic effects may further affect the growth of a tree. There is, unfortunately, no evidence, either from the submerged forest tree-rings or associated pollen analysis, that, during the periods studied, the climate was any different from the present day. It is difficult, in the submerged forest dendrochronology, to distinguish rainfall effects from those due to sea-level-determined water-table variations. It therefore appears unlikely that observed short-term fluctuations in natural ^{14}C levels can be linked with palaeoclimatic events.

As for any "floating" tree-ring sequence, the full value of the data can only be assessed when it becomes fixed on an absolute scale. As stated earlier, the Cullykhan sequence will, most probably, remain "floating".

It is anticipated, however, that, in the course of future research, the submerged forest wood will be extended into an absolute chronology. Statistical comparison of the U.K. "floating" chronologies to the absolute bristlecone pine chronology has, in this study, been performed using the method developed by Clark and Renfrew (1972).

Although the procedure outlined here is for the simple case of positioning one floating chronology with respect to a master chronology, it is easily extended to deal with any number of floating chronologies. The relevant portion of the master chronology, represented by m pairs of observations (w_i, z_i) , is assumed to satisfy the relationship

$$z_i = \beta_0 + \beta_1 w_i + e_i \quad i = 1, 2, \dots, m \quad (1)$$

Similarly, the "floating" chronology, represented by n pairs of observations (x_i, y_i) , is assumed to have the property that the pairs $(\alpha + x_i, y_i)$ satisfy the same relationship as the (w_i, z_i) for some suitable value of α . Thus (x_i, y_i) must satisfy the equation

$$y_i = \beta_0 + \beta_1 (\alpha + x_i) + e_i \quad i = 1, 2, \dots, n \quad (2)$$

In the above nomenclature, w represents the absolute tree-ring age with corresponding observed radiocarbon date z ; x is the arbitrary tree-ring age of a sample in the "floating" chronology with corresponding radiocarbon age y . The parameter α represents the position on the true timescale of the arbitrary zero of the floating chronology. Finally, e is the random fluctuation,

comprising measurement errors in the dating process and possible random fluctuations representing deviations from the underlying straight line relationship which is assumed to exist between the tree-ring dates and the radiocarbon dates.

The principal interest lies in the determination of an estimate and confidence limits for α . Thus, equation 2 is rewritten in the form

$$y_i = \gamma + \beta_1 x_i + e_i \quad i = 1, 2, \dots, n \quad (3)$$

where

$$\gamma = \beta_0 + \beta_1 \alpha$$

Using the method of least squares, estimates (b_0, c, b_1) of the parameters (β_0, γ, β_1) are obtained, and hence the estimate of α is given by

$$a_1 = \frac{c_1 - b_0}{b_1} \quad (4)$$

The essential assumption of the method is that the parameters β_0 and β_1 , representing the slope and gradient of the straight line, are the same in equations 1 and 2. Logically, it is not possible to verify this assumption with regard to β_0 , but a statistical test is used for testing whether the slope β_1 is the same for the two sets of data. The final step in the analysis calculates confidence limits for the estimate of the zero point of the floating chronology. A Fortran IV computer programme has been written for this analysis and is presented in Appendix 2. Certain of the procedures involved in the calculation, solution of the matrix equation, linear regression and matrix inversion are performed by NAGLIB subroutines, available on the NUMAC network.

Calibration of the "floating" chronologies analysed in this research, against the appropriate sections of the bristlecone pine/radiocarbon record, has been performed. Data for the master chronology were obtained by extrapolation from the original calibration curve (Suess, 1970a) and from Houtermans (1971). In each case, a 5% significance level is adopted for the comparison of gradient F-test and 95% confidence limits for the arbitrary zero point, based on the appropriate percentile of a t-distribution with the relevant degrees of freedom, are calculated. The results are presented in Table 5-3.

The results indicate that, in the case of the longer oak chronologies from Cullykhan and Stolford, the null hypothesis of a common gradient for both master and "floating" chronologies is rejected. Figs. 5-9 and 5-10 show the positions of these two floating chronologies, relative to the master bristlecone pine chronology. It is evident that the least squares estimates for the gradients of the "floating" chronologies (Table 5-1) are different from those displayed in the relevant sections of the bristlecone pine chronology and that, in both cases, agreement between the U.K. and American data is not convincing. Furthermore, reduction in the sampling frequency of the "floating" chronology, by omission of alternate analyses (Cullykhan), or by averaging adjacent analyses (Stolford), does not alter the outcome of the F-test. (For Cullykhan, reduction in the sampling frequency produces a calculated F statistic significant at the 1% level). Therefore, it is concluded that there

TABLE 5-3: STATISTICAL CALIBRATION OF FLOATING CHRONOLOGIES AGAINST
A MASTER CHRONOLOGY

Master	Floating	Estimate of zero point years B.P.	Tabulated F statistic	Calculated F statistic	95% confidence limits for zero point estimate years B.P.
Bristlecone pine	Cullykhan (oak)	2541	4.06	13.27	2458 - 2643
Bristlecone pine	Cullykhan (half frequency)	2543	4.12	6.84	2479 - 2613
Bristlecone pine	Stolford (oak)	6010	4.04	70.50	5940 - 6079
Bristlecone pine	Stolford 5 (half frequency)	6078	4.13	20.88	6001 - 6158
Bristlecone pine	Borth 4 (oak)	4300	4.14	0.06	4154 - 4409
Bristlecone pine	Borth 1 (pine)	6124	4.21	0.54	6108 - 6338
Bristlecone pine	Ynyslas (pine)	5749	4.21	0.21	5667 - 5830

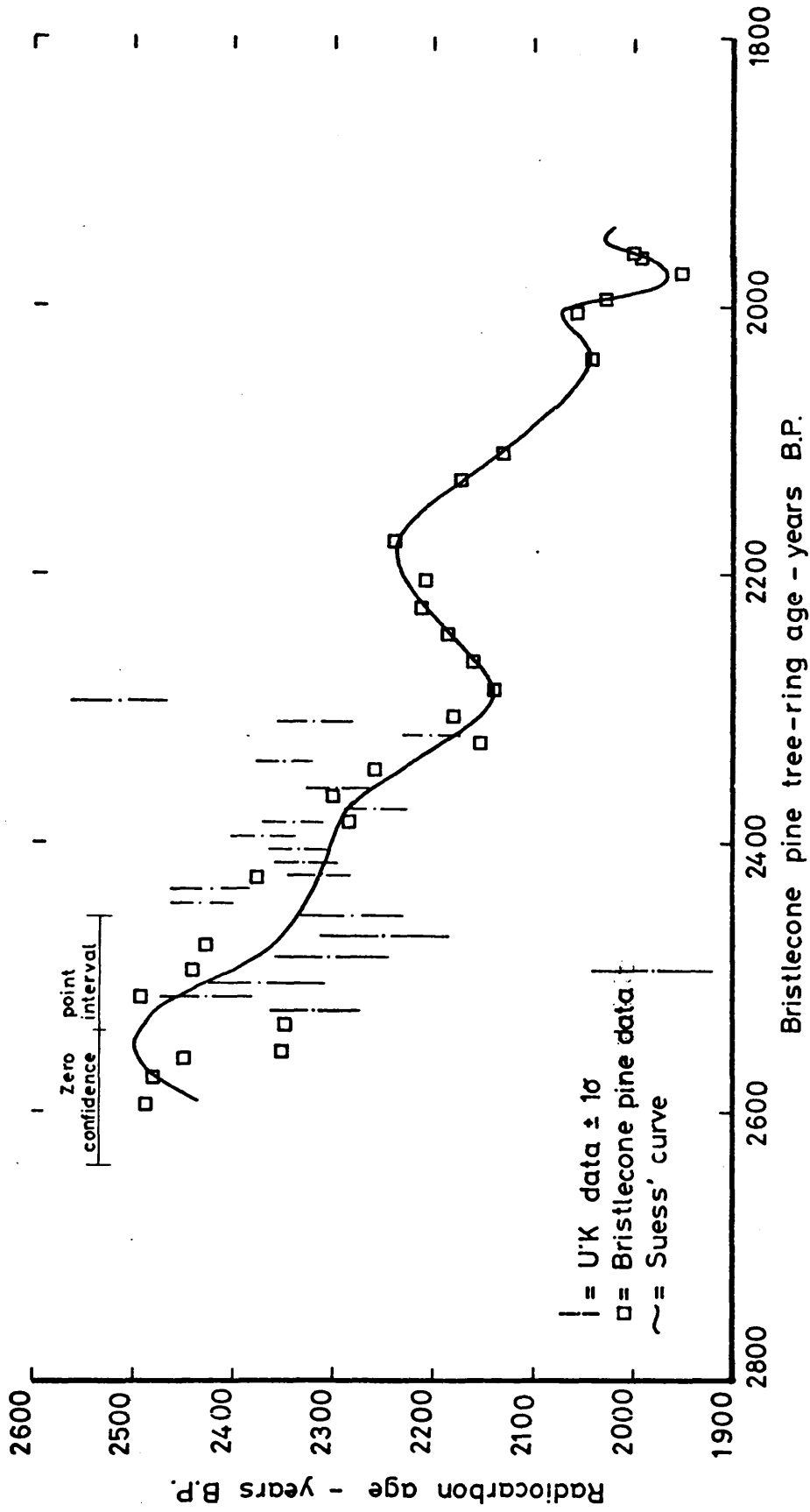


FIGURE 5-9: Statistical calibration of Cullykhan oak chronology against bristlecone pine

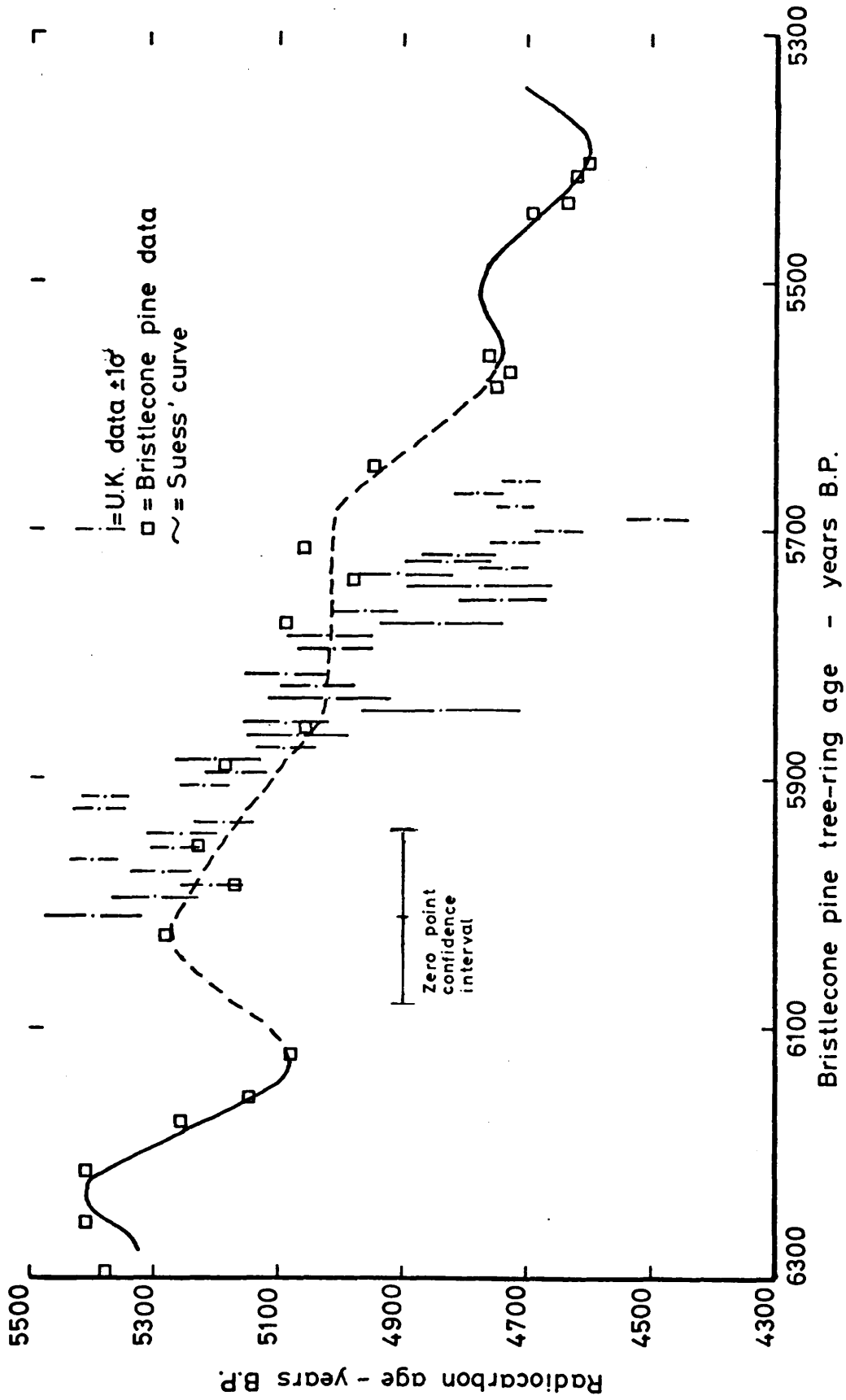


FIGURE 5-10: Statistical calibration of Stolford oak chronology against bristlecone pine

are differences between the U.K. and American data. Of course, such discrepancies, evaluated here as differing gradients, may be resolved with a higher sampling frequency in the bristlecone pine data record.

Because of the large fluctuations described for the Borth 6 oak section (Table 3-3-4), only the smoother Borth 4 has been subjected to the statistical analysis. In this case, and in the case of the two short pine sections, Borth 1 and Ynyslas 1, the null hypothesis of common gradient cannot be rejected. These comparisons are presented in Figs. 5-11 and 5-12. The 95% confidence interval for the zero point of the Borth 4 chronology extends across 255 years of the master chronology tree-ring timescale. Nevertheless, there is reasonable agreement between both chronologies and also adequate correlation against Suess' hand drawn curve. The positioning of the two pine chronologies against the master chronology in some way overcomes the difficulties arising from the dendro-chronological studies and, furthermore, allows indirect comparison of the "floating" oak and pine chronologies. Firstly, there is reasonable agreement between the "floating" and master bristlecone pine chronologies, despite the wide difference in the sampling frequencies. The analysis places the zero point of the Borth chronology 375 years older than the zero point of the Ynyslas chronology and therefore the latter will overlap with the main Stolford oak tree-ring sequence. The relative positions of these two pine and oak chronologies are shown in Fig. 5-13, indicating the excellent agreement

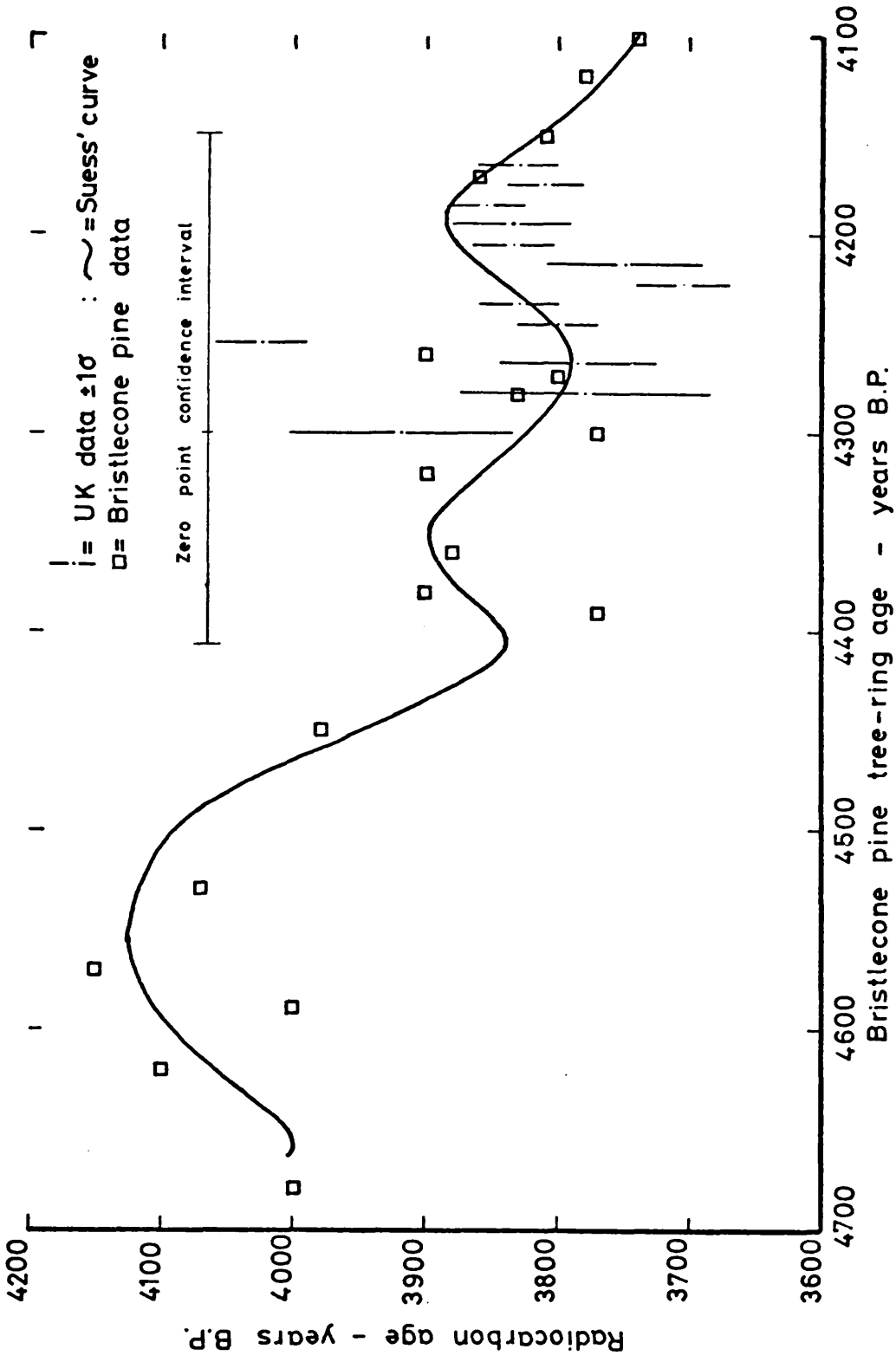


FIGURE 5 -11: Statistical calibration of Borth 4 oak chronology against bristlecone pine

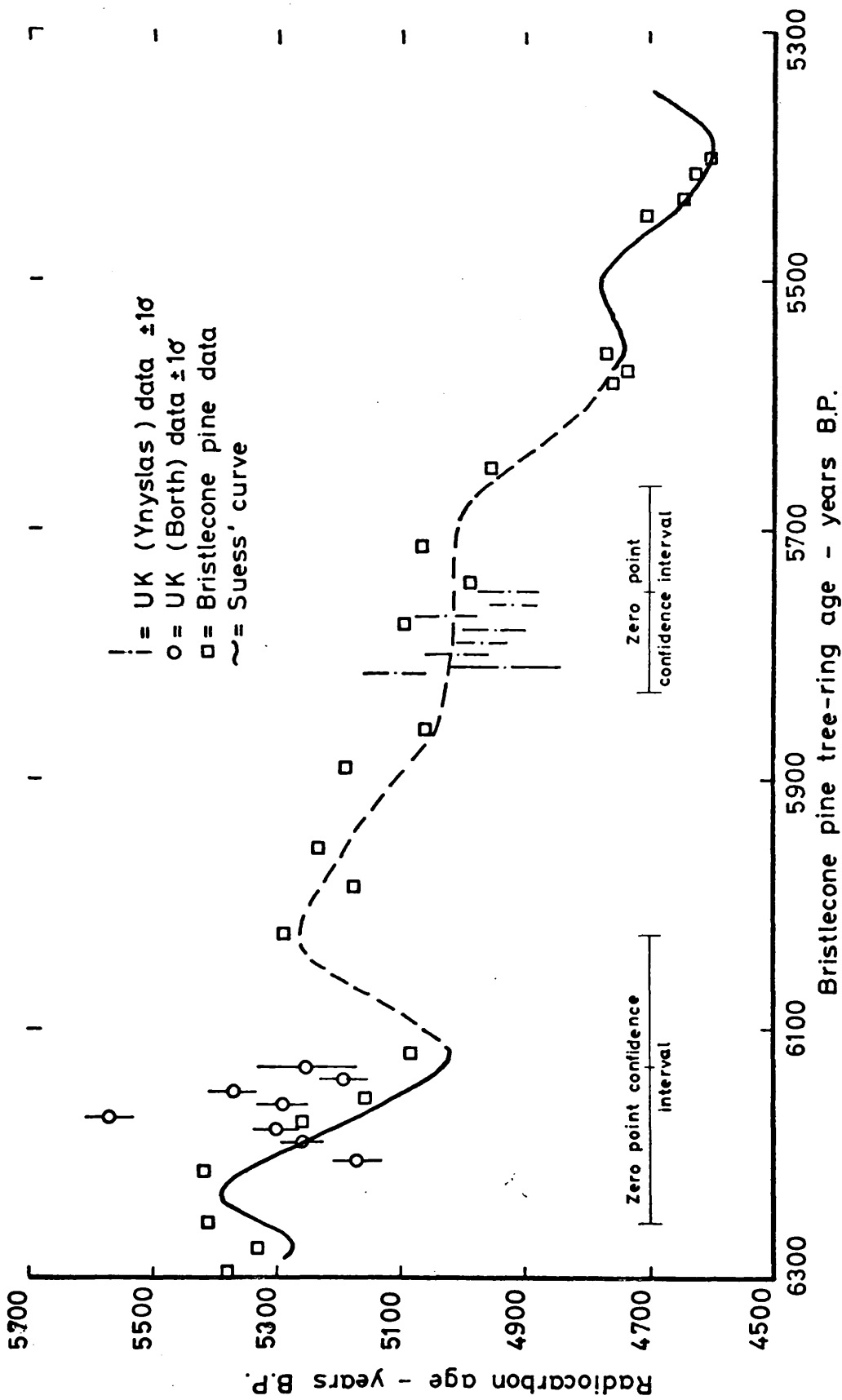


FIGURE 5-12: Statistical calibration of Borth & Ynyslas pine chronologies against bristlecone pine

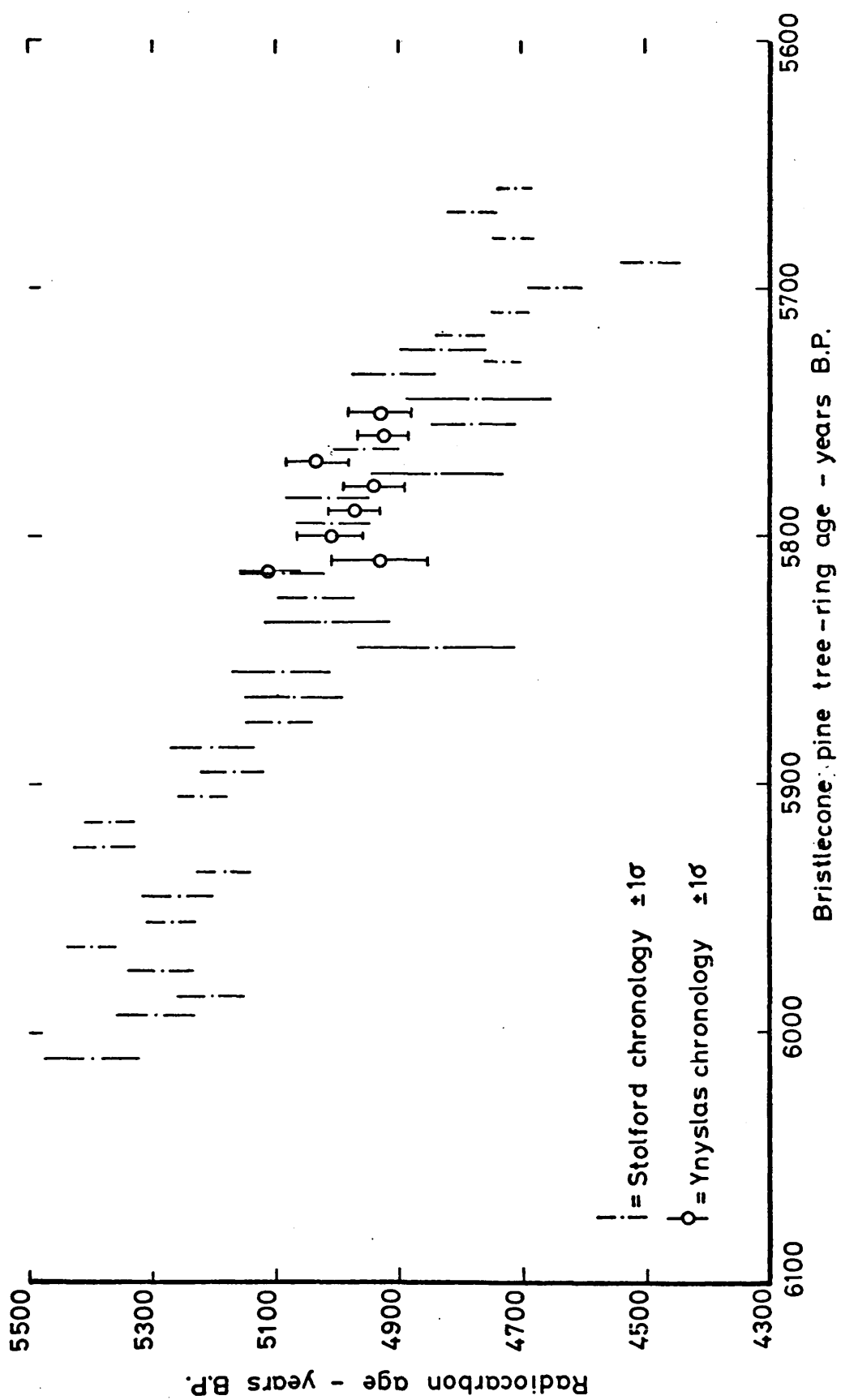


FIGURE 5-13: Statistical calibration against bristlecone pine: relative positions of Stolford (oak) & Ynyslas (pine) chronologies

between the overlapping Ynyslas and Stolford sections.

One of the main criticisms of the bristlecone pine calibration is the possibility that this wood may be atypical of normal organic matter (Aitken, 1970; Berger, 1970; Libby and Lukens, 1973; Harkness and Burleigh, 1974). These authors have suggested that the ^{14}C content of bristlecone pine may be abnormally high resulting from the extreme growth conditions of the tree. Consequently, bristlecone pine wood should yield a radiocarbon age younger than "normal" organic material of the same age. The results of the statistical comparisons of U.K. "floating" chronologies and bristlecone pine wood, however, indicate that no such difference exists.

5.4 Conclusions and implications

Although the development of an absolute dendro-chronology for the United Kingdom, based on wood from submerged forests, is at a preliminary stage, the findings of this research illustrate features which are significant to the question of the realistic accuracy of radiocarbon dates, conventional and calibrated. ^{14}C assay of tree-ring samples from "floating" chronologies have shown a considerable degree of scatter, typically a range of dates of ~ 500 years has been obtained from a 250 ring sequence. This variability has been accentuated by the high sampling frequency used in this study compared to similar projects. In view of the rigorous experimental technique employed, long count times and a high degree of long-term counter stability, the short-term fluctuations observed in the data are confidently assumed to exceed

the analytical errors, assessed by replicate analysis standardisation. Allied to the non-random nature of the ^{14}C scatter, the secular pattern of ^{14}C variations can be assumed true changes in atmospheric ^{14}C content rather than random or experimental noise.

The different time-spans analysed have indicated that certain periods of the recent past have been "stormier" than others, with respect to the magnitude and frequency of the observed fluctuations. Thus, during the first half of the second millenium B.P. (radiocarbon years), several fluctuations of the order of 2 - 3%, occurring over 40 - 50 years, have been observed, whereas, around 5,000 B.P. (radiocarbon years), much smoother changes in atmospheric radiocarbon are observed, with superimposed occasional fluctuations of 2 - 3% again over 40 - 50 years. These short-term variations are generally not apparent in bristlecone pine data, however, this may be solely because of the lower frequency of the American work. On the other hand, the perturbations may be a result of local effects connected with more rapid annual growth of the "normal" wood producing a higher sensitivity to extremely short-term atmospheric ^{14}C variations.

Statistical comparisons of the U.K. "floating" chronologies against the absolute bristlecone pine/radiocarbon calibration have not detected reported systematic differences between the latter data and "typical" organic material of the same age grown at sea-level. The intercomparisons have, however, shown that, for extended tree-ring sequences, there appear to be

differences between the record of atmospheric radiocarbon concentrations as reflected in U.K. wood, compared to that from the U.S.A. These discrepancies, both in trend and short-term variability, may be related to the disparate sampling frequencies employed in the two studies. A complete assessment of the situation will only be available when the "floating" chronologies become fixed on an absolute scale and when many more bristlecone pine/ ^{14}C analyses have been performed.

In view of the proven existence of short-term fluctuations in atmospheric ^{14}C levels, the interpretation of single conventional radiocarbon ages is necessarily constrained to a minimum uncertainty commensurate with the magnitude of these wiggles. Furthermore, continuing research leading in the long-term, to an absolute calibration scale for the U.K. will, unavoidably, involve a greater calibration error, irrespective of the ultimate form of the selected calibration function. Two types of radiocarbon/tree-ring relationship are possible. Firstly, the calibration function may accurately express the irregular variations in past ^{14}C concentrations or secondly, it may take the form of a "confidence envelope". More precise radiocarbon/tree-ring measurements will increase the resolution of these past variations and perhaps lead to a geochemical evaluation of the causal factors producing them. It is, however, not feasible to produce from more precise measurements a calibration curve involving a greatly reduced calibration error, since this uncertainty level is unrealistic compared to the precision routinely attained by most commercial laboratories.

The most recent version of the bristlecone pine calibration (Clark, 1975) gives the uncertainty on a calibrated date as ± 200 years. Although the considerations applied to the data presented here are different from Clark's statistical approach, it is concluded that this level of uncertainty is of the same order as suggested by this work.

CHAPTER 6

APPLICATIONS OF RADIOCARBON DATING TO ARCHAEOLOGY6.1 Radiocarbon dates for South Cadbury - Camelot

One of the main difficulties in applying radiocarbon dating to archaeological studies is the reconciliation of theoretical and radiometric timescales and, in general, it arises through lack of appreciation of the limitations of the ^{14}C dating technique. The correct evaluation of effectiveness of radiocarbon dating as a research tool in prehistory cannot be achieved solely by the proper manipulation of the statistical uncertainty (McKerrell, 1971), the error term usually expressed with an age determination, as this term cannot take into account all of the factors which influence the reliability of a radiocarbon age determination.

It is proposed here, through delineating these other sources of error, and noting their application to a real situation, that the inability of ^{14}C age determinations to predict accurately the timing of events in prehistory, although unsatisfactory to the archaeologist, is, however, an inevitable consequence of the constraints imposed by the radiometric dating method itself.

It is convenient to consider the measurement of age by the ^{14}C dating technique as comprising three parts, each containing sources of error which may or may not be quantifiable. These three categories are (a) the collection of samples, (b) the ^{14}C analysis and (c) the calibration of ^{14}C ages.

a) The sample error

It is most common for apparent discrepancies between radiocarbon and expected dates to be attributed to sample contamination, and in a large number of cases this may indeed be a major contributing factor. The form of the contamination determines in which sense the radiometric age is discrepant, namely contamination by modern or old carbon making the sample date respectively too recent or too old. Certainly, in the case of this chemical contamination effect, it is the duty of the dating laboratory to ensure that rigorous chemical pretreatment procedures are employed to counteract and minimise such errors. It is also, however, the responsibility of the field worker to maintain high standards on site to reduce such problems, for the rigour of the chemical pretreatment is largely determined by the physical condition of the sample, and, of course, by the quantity available for analysis. Exhaustive chemical pretreatments generally involve considerable (~50%) loss of sample material so that satisfactory dating normally requires an initial sample weight of the order of 100g, rather than a few grams of mixed sample fragments and earth which are often submitted. Of some concern also, is the possibility that, where close contact between submitter and dating laboratory does not exist, the resultant date of such an unsuitable sample may be used to support an erroneous hypothesis. Some of the blame for such an outcome should, of course, rest with the dating laboratory for uncomplainingly analysing low quality samples and then failing to clearly define the gross uncertainty associated with the ^{14}C assay. Sample

contamination error contributions cannot, in general, be quantified, yet as they apply to virtually every sample submitted and analysed, some subjective assessment of their magnitude must be undertaken.

In selecting suitable samples for radiometric dating, it is necessary to establish the relation of the sample to the archaeological context, in terms of the time elapsed between the organic death of the sample - the radiometric age - its utilisation by the culture and the time when it reached its final resting place in an archaeological deposit. This interval can originate in various ways. Firstly, the sample material may continue to grow even although the part ultimately dated is dead. An obvious example of this is tree-ring growth. Unless it is possible to identify the outermost rings of a large timber, or the bark, an error of as much as 200 years may be incurred. Thus, random wood samples or wood charcoal should be considered as yielding maximum ages for particular archaeological horizons. A similar error, although of perhaps several decades only, must apply to ^{14}C dating of collagen from adult skeleta, the organic fraction of bone being highly inert towards carbon turnover in life. Secondly, the material collected for analysis may have been dead for a significant period of time before it was utilised by man. A peculiarly relevant example of this concerns the submerged forest wood which has provided the larger number of samples for this research. At the present time, this preserved wood is being recovered by the local inhabitants for incorporation in construction work - the average age of this wood being 4,000 to 5,000 years! In the third

instance, certain materials can be re-used by man, so that structural timbers may, in fact, date a previous phase of construction. Finally, unless samples were buried during or immediately after a disaster, there is a high probability that these will have remained on the horizon surface for some years after the event and been buried with younger material.

Thus, in terms of dating a particular event, charcoal or even fossil wood, despite being excellent materials as far as reliable ^{14}C assay is concerned, can provide age data which should be treated with caution. Short-lived organic samples, on the other hand, such as twigs, grain and food remains, would appear to be more reliable indicators. There are, however, inevitable drawbacks concerning such short-lived samples. In the event of the final criterion outlined above being significant, there is a considerable risk of contamination by more recent materials becoming mixed with the original sample material. Of course, this is also likely to affect the age estimate assigned to a more recent occupation level. Furthermore, the possible occurrence of short-term fluctuations in atmospheric ^{14}C concentrations, as reported by Baxter and Walton (1971), Baxter and Farmer (1973) and Lavrukhina et al. (1973), will increase the uncertainty of radiocarbon analyses on these short life-span materials. Such variations, by as much as $\pm 1.5\%$ ($\Delta^{14}\text{C}$ units), could introduce a further ± 120 year age uncertainty, thereby precluding their use as accurate event markers.

b) The analytical error

The error quoted with a radiocarbon age determination is normally based on what is called "counting statistics", and quantifies the uncertainty of the random process under measurement, namely radioactive decay. The counting error also includes a contribution from the uncertainty arising from the stable carbon isotope enrichment measurement, $\delta^{13}\text{C}$, used in the calculation of $\Delta^{14}\text{C}$ and finally of radiocarbon age. The calculation of errors on sample, modern standard and background count rates has been outlined in the preceding chapters and will not be discussed further. Chapter 4 details an investigation into possible sources of non-counting error, such as pretreatment, isotopes fractionation in the synthesis of the counting material - in the case of GU and SRR, this is benzene - and possible geometry errors. It was concluded, from replicate analyses of homogenised and aged wood, that for this laboratory, these non-counting errors contribute only a small amount over and above the defined counting error. Nevertheless, natural radiocarbon assay remains one of the few analytical procedures which fails to quantify experimental precision based on replicate analyses of typical sample materials (not of N.B.S. oxalic acid), and, more conventionally, via a wide range of internationally accepted secondary standards. The reasons underlying this deficiency are probably related to the length of time required for each analysis and a productivity commitment in terms of producing new analytical data. It is, surely, presumptuous for ^{14}C analyses to require high levels of accuracy from sample-submitters without themselves experimentally measuring their own reproducibility.

In general, the component errors within the "counting statistics" uncertainty are closely defined. Certain radio-

carbon laboratories, however, do not perform a stable carbon isotope enrichment ($\delta^{13}\text{C}$) measurement and the ultimate radiocarbon date may therefore be calculated without consideration of carbon isotope fractionation in nature, or in the laboratory. Such total omission of this correction term may introduce an error up to ± 200 years, the magnitude being determined largely by the sample type, being largest for shells and smallest for wood. Many commercial laboratories require an extra payment for $\delta^{13}\text{C}$ assay, usually 15 - 20% of the cost of the ^{14}C analysis, and the sample submitter may consider this expense better deployed in additional radiocarbon dates. As a compromise, it is possible to use a reference table presenting average $\delta^{13}\text{C}$ values for different biospheric materials typically submitted for ^{14}C age assessment (Polach, 1969; 1975). The use of such tables is preferable to complete omission of the stable carbon isotope correction, since it will only introduce an additional ± 10 years to the counting error. These methods, however, do not take account of laboratory fractionation effects which may involve errors of greater magnitude. A further uncertainty which may, in future, require consideration is the unresolved possibility that isotopic fractionation against the heavier carbon isotopes may not be precisely proportional to the mass difference between the competing isotopes. It has been assumed that the fractionation of ^{14}C against ^{12}C is twice that for ^{13}C against ^{12}C (Craig, 1954). This empirical relationship may, however, not hold as a result of different thermodynamic and kinetic restraints on isotopic behaviour, thus introducing a further small

uncertainty to the overall analytical error.

The random errors associated with the experimental procedures involved in natural ^{14}C assay, including the "counting errors" outlined above, may be quantified by series of replicate analyses and the introduction of realistic secondary working standards. Besides these random errors, however, there are potential sources of systematic error in ^{14}C assay. Conventional radiocarbon dates are calculated using the Libby half-life of 5568 years. Despite recent, more accurate determinations of the half-life indicating a value of 5730 ± 40 years (Mann et al., 1961; Watt et al., 1961; Godwin, 1962), it has been decided by successive International conferences to continue the use of the shorter half-life, since revision of a vast number of previously reported dates would inevitably lead to considerable confusion. It is to be anticipated that eventually a ^{14}C half-life value will be precisely determined and adopted as convention. In the meantime, the uncertainty on the half-life is unknown and no consideration is given to this source of variability in calculating radiocarbon ages.

Further systematic inaccuracy results if the reference activity, against which sample activities are compared, is not representative of the sample activity during its participation in the dynamic carbon cycle. The N.B.S. Oxalic Acid standard activity is directly related to the specific activity of the "undisturbed" atmosphere. Shells, calcareous deposits and marine organisms, however, assimilate their carbon from an equilibrium system which is depleted in radiocarbon through oceanic residence, ground water retention and hard water effects. Obviously, this error

would be considerably reduced with the introduction of appropriate dating standards of the same composition and origin.

Systematic errors may also be induced in laboratories which have a significant non-counting and random contribution to experimental uncertainty. This arises since most laboratories retain and reanalyse the same N.B.S. counting gas/liquid over long time periods. If the single preparation of that reference sample introduces any error component, all subsequent sample analyses measured relative to that standard will be systematically erroneous. Interlaboratory calibration and replicate analysis of N.B.S. standard samples both serve to eliminate this effect, but it is doubtful whether radiocarbon laboratories in general pay sufficient regard to these procedures.

In conclusion then, it must be appreciated that the conventional ^{14}C data which quote only counting errors, largely because these are readily quantifiable, do, in reality, underestimate accuracy by an extent which can, in part, be readily assessed by intra-laboratory standardisation. Recently, several research laboratories have begun to quote extreme levels of accuracy (Stuiver, 1977). This, of course, is achieved given abundant experimental time and financial support, and is naturally impractical for service laboratories. Fortunately, for general archaeological dating purposes it is likely that the uncertainties associated with the samples, the distribution of natural radiocarbon in nature and the calibration of the ^{14}C timescale, are far in excess of the experimental errors.

c) The calibration error

Since the original Suess calibration curve was published in 1970, a large variety of calibration methods have been introduced (Chapter 1). There are two extreme views of the relationship between the timescales of radiocarbon and bristlecone pine. On the one hand, Suess (1970a) produced a hand-drawn curve intended to reflect the variations of natural radiocarbon during the past millenia, which consequently displayed a large number of kinks or wiggles. Clark (1975), on the other hand, has produced a calibration system without these wiggles, which were apparently not justified by the precision of the data. Between these extremes there are many different calibration functions which are derived by smoothing techniques - curve approximation and averaging for example - and which are essentially simplifications of the Suess method since the degree of smoothness has been subjectively determined. There are two unfortunate but unavoidable consequences of the geometry of these subjectively derived calibration curves. Firstly, a single radiocarbon date may correspond to more than one tree-ring age, and secondly, a calibrated radiocarbon date may appear to be more accurate than the original radiometric age. The questions which have recently been posed concerning the global applicability of the bristlecone pine chronology will further affect the uncertainty associated with calibration. Superimposed upon this possible systematic difference is a potential further uncertainty arising from local variations in atmospheric ^{14}C concentrations. The only realistic

solution to these uncertainties at present is to include a major calibration error term, say of the order of 100 - 150 years. Only Clark's calibration procedure fulfils this requirement.

Common to each error contribution discussed so far is the additional uncertainty of human error, which may arise through mistaken assignment of archaeological context, mislabelling of samples, carelessness in experimentation and faulty data handling. This source of variability is naturally unquantifiable.

The application of these considerations to an actual situation is now illustrated through the radiocarbon analyses on material from the excavations at South Cadbury - Camelot. These samples were submitted to the Glasgow and SRR radiocarbon laboratories in 1976 by Professor L. Alcock (University of Glasgow) and were intended to rationalise one of the most common problems caused by the dating method, namely the apparent non-agreement of radiocarbon data with archaeological hypothesis. It is relevant here to give an outline of the archaeological background of the samples.

During the years 1970-1973 archaeological excavations at South Cadbury had led to the formulation of hypotheses concerning the structural history of the defences. These hypotheses showed that on the site was represented a long series of both structural and ceramic phases from some kind of Ultimate Bronze Age, through various phases of Iron Age to a massacre which brought native culture to an abrupt end around the middle of the first century A.D. At this stage, however, only one radiocarbon date had been obtained (I-5971: 925 ± 90 B.C., Buckley, 1976) from a supposed Neolithic level.

In 1973, however, a series of well stratified charcoal samples was collected thus presenting an opportunity to check the hypotheses and to compile a detailed site chronology for the first millenium B.C. period. Of the twelve dates, five were related to pre-rampart deposits and were both consistent between two laboratories (I and SRR) and in agreement with dates for the same ceramic phase from other sites in southern England. The remaining 7 dates were associated with successive structural phases of the rampart, all of the analyses being performed by SRR (Table 6-1). With the exception of one date, SRR 446, these dates were all in agreement with the stratification and were separated by intervals which corresponded well with archaeological expectations. The problem, from the archaeological viewpoint, was simply that the latest of the sequence, for a remodelling of the fortifications on the eve of the Roman sack of Cadbury, was 444 ± 40 A.D. Correspondingly, at the start of the sequence, was a date of 264 ± 110 B.C. In terms of the hypotheses for the site history, these dates appeared about 400 years late (Alcock, pers. comm.).

This apparent discrepancy may originate from the archaeological hypotheses for the site being in error. It is possible that in the model for the history of the fortifications, the structures and the dates proposed for them were out of step by a whole phase. In archaeological parlance, the Early PR1A defence, Rampart A, was perhaps really Middle PR1A, and the supposed Ultimate PR1A remodelling, Rampart D2, was, in fact, Arthurian. The further

TABLE 6-1: RADIOCARBON DATES FOR SOUTH CADBURY - CAMELOT

Site feature number	Laboratory number	Conventional ^{14}C date $\pm 1\sigma$	Structural Phase	Expected date	Comments
SC/KX 022	SRR 444	A.D. 444 \pm 40	Rampart D1/D2 Cadbury 9B	pre A.D. 60	Historical date
SC/KX 029	SRR 445	272 \pm 45 B.C.	Pre-Rampart D1 Cadbury 9A	1st cent. B.C.	Residual rubbish in fill
SC/KX 031	SRR 447	A.D. 246 \pm 55	Rampart C Cadbury 8	2nd cent. B.C.	Material cannot be Romano-British
SC/KX 031	SRR 446	2072 \pm 270 B.C.	Rampart C Cadbury 8	2nd cent. B.C.	Out of sequence
SC/KX 038	SRR 449	2 \pm 60 B.C.	Rampart B Cadbury 7	5th - 4th cent. B.C.	
SC/KX 039A	SRR 450	111 \pm 50 B.C.	Rampart B1 Cadbury 7	5th - 4th cent. B.C.	
SC/KX 034	SRR 448	264 \pm 110 B.C.	Rampart A Cadbury 5/6	6th cent. B.C.	
SC/KX 016	SRR 443	870 \pm 110 B.C.	Fossil soil	<div style="border: 1px solid black; padding: 5px;"> 8th cent. B.C. or earlier back to 10th cent. B.C. or earlier </div>	Agreement between samples from different locations and different laboratories, and with expected date is food.
SC/K 618	I 5971	925 \pm 90 B.C.	pre-Rampart A with Y.B.A.		
SC/KX 906	SRR 451	955 \pm 140 B.C.	pottery		
SC/K 530	I 5973	985 \pm 90 B.C.	Cadbury 4/5		
SC/KX 016	SRR 442	1064 \pm 75 B.C.			

implication arising from this reasoning would be that the cultural material associated with each structural phase was entirely residual.

The other archaeological evidence on the site, however, ruled this explanation out. Firstly, if Rampart D is to be dated to the 5th-6th centuries A.D. on the basis of the single radiocarbon analysis, then there is a supernumerary defence work, Rampart E, to be fitted in between the 6th century and the early 11th century to which a mortared stone wall of Rampart F has been attributed. No historical context could be suggested for such a rampart. Furthermore, the character of Rampart D is exactly comparable with that of the Ultimate PRIA gateway which is situated only some 15 metres away. The final event in the history of that gateway has been securely dated to the middle decades of the first century A.D. by brooches, weapons and pottery associated with a group of mutilated human bodies. In short, to suggest that this material should date to the 5th century A.D. would be running counter to a large body of archaeological and historical evidence.

Although the best way to examine this inconsistency would clearly have involved collection and analysis of samples from the same levels, these had been subsequently back-filled. As an alternative, however, the massacre level had yielded abundant samples of carbonised grain, twigs and timbers of known archaeological context and closely inferred historical date. Ten samples were collected and submitted to this laboratory (7) and to SRR (3).

The gate structure, from which the latter materials were collected, had been destroyed by fire during the sack of Cadbury Castle. The guard chamber and passage-way of the structure had been strewn with corpses, weapons and jewellery and other metal objects (all suggestive of a battle and massacre at the gate). The floor of the guard chamber, in context, SC/K 659, was a destruction layer sealed by collapse of the rear wall of the chamber. This contained carbonised twigs and large timbers, probably from the roof of the chamber, and carbonised grain, presumably food for the garrison. This carbonised material provided six samples. Context SC/K 747, the threshold of the gate, provided one further sample of carbonised wood, presumably from the gate structure.

It was assumed at first that this situation was evidence for the sack of Cadbury by troops under the command of Vespasian during the first phase of the conquest of southern Britain: a military action comparable with that at Maiden Hill (Wheeler, 1943) and Hod Hill (Richmond, 1968) in the neighbouring county of Dorset. If that were so, then a date after A.D. 43 - say about A.D. 45 - would be indicated. But it was then realised that some of the brooches and pottery associated with the final heightening of the rampart and with destruction of the gate were of types unlikely to be current before the 40's A.D. Moreover, an actual Roman presence, perhaps in the form of a police-post, was indicated by Roman military fittings and by Samian pottery of types which might have been as late as the 70's A.D. On balance, historical considerations led to the view that the final heightening of Rampart D, the blocking of the gate and the subsequent

military action and massacre, all mark a south-western rising of Boudicca and its suppression in A.D. 61. Thus the terminus ante quem for the samples must be A.D. 61.

The results of the radiocarbon analyses performed in this laboratory, presented initially in Table 3-2-1 are reproduced in Table 6-2 along with those obtained by SRR. Three forms of calibration curve have been utilised in this study: the original Suess curve (Suess, 1970a) and the most recent calibration by Clark (1975), both based on the Libby half-life, and the MASCA calibration curve (Ralph et al., 1973), based on the 5730 year half-life. The radiocarbon-calendar age calibration results are presented as an age range based on the one sigma counting errors quoted with the ^{14}C dates. Sample SC/K 659 (iv), GU 648, was of extremely poor quality and was not suitable for dating. Nevertheless, an analysis was carried out mainly to illustrate the problems of sample variability, but the result of the assay is not considered hereafter.

It is immediately obvious from Table 6-2 that, based solely on the radiocarbon data, it would not be possible to assign a precise date to the massacre level, rather, the data indicate that the event occurred sometime during the first or second century A.D. Bearing in mind the arguments outlined above, the samples which should, in theory, give the best concordance with the date predicted by the historico-archaeological evidence are those comprising twig charcoal and carbonised grain, namely

TABLE 6-2: RADIOCARBON DATES FOR SOUTH CADBURY "MASSACRE"

Sample Code	GU/SRR code	Sample material	^{14}C date $\pm 1\sigma$		Suess	Calibrated ^{14}C dates		MASCA
			years B.P.	$t_{1/2}=5568\text{y}$		$t_{1/2}=5730\text{y}$	Clark	
SC/K 659(i)	GU 645	twig charcoal	1814 \pm 31	1868 \pm 31	AD 170 - AD 240	AD 156 - AD 242	AD (130-110) - AD 180	
SC/K 659(i)	SRR 693	twig charcoal	1845 \pm 45	1900 \pm 45	AD 90 - AD 200	AD 106 - AD 228	AD 70 - AD 160	
SC/K 659(ii)	GU 646	charcoal-large timber	1961 \pm 27	2020 \pm 27	(AD 47, AD 1, 31 BC, 84 BC) - AD 57	34 BC - AD 115	(AD 10-60 BC) - AD 60	
SC/K 659(iii)	GU 647	charcoal-large timber	1839 \pm 26	1894 \pm 26	AD 100 - AD 200	AD 126 - AD 225	AD 100 - AD 160	
SC/K 659(iv)	GU 648	charcoal	2214 \pm 43	2280 \pm 43	405 BC - (340, 275 BC)	415 BC - 203 BC	410 BC - (250-380)BC	
SC/K 659(v)	GU 649	carbonised grain	1949 \pm 26	2007 \pm 26	AD 60 - AD 70	AD 10 - AD 129	AD 20 - AD 70	
SC/K 659(v)	SRR 691	carbonised grain	1776 \pm 50	1829 \pm 50	AD 160 - AD 275	AD 187 - AD 276	AD 140 - AD (250-230)	
SC/K 659(vi)	GU 650	carbonised grain	1765 \pm 47	1818 \pm 47	AD 180 - AD 250	AD 190 - AD 274	AD 180 - AD 260	
SC/K 659(vi)	SRR 692	carbonised grain	1666 \pm 50	1829 \pm 50	AD 250 - AD (360, 410)	AD 252 - AD 396	AD (250-220) - AD 390	
SC/K 747	GU 651	charcoal	1825 \pm 48	1880 \pm 48	AD 100 - AD 230	AD 127 - AD 241	AD 90 - AD (200-180)	

SC/K 659 (i), SC/K 659 (v) and SC/K 659 (vi). In these cases sufficient material was collected to allow independent analyses by GU and SRR, and the results indicate that the agreement between laboratories is good thus reinforcing the interlaboratory calibration illustrated previously in Table 3-1-1. Yet ^{14}C measurements on these short-lived samples show a spread of almost 300 years about an arithmetic mean of 1802 years B.P. (A.D. 148), which is more recent than the predicted date. It is curious to note, though probably coincidental, that the longer-lived samples, whose apparent relationship to the archaeological context is less well defined than that of the twigs and grain, yield closer agreement with the "expected" date.

The discrepancy between the ^{14}C data and the expected date is further widened by calibration of the radiocarbon timescale, indicating that the sack of Cadbury Castle occurred in the 2nd or 3rd centuries A.D. There is, naturally, good agreement between the different calibration systems, but the disadvantages indicated previously, namely the possibility of multiple calendar ages and more accurate calibrated dates, are clearly illustrated in this series of measurements. For example, SC/K 659 (ii) has, for the lower 1σ age limit ($1961-27 = 1934$ years B.P.), four possible calendar ages using the Suess calibration and a range of ages resulting from the MASCA tables. Also, there are several instances where the calibrated ^{14}C ages appear to be more accurate than the radiometric ages. It is hardly surprising that the statistically derived curve does not exhibit this anomalous behaviour.

The generally greater discrepancy between the calibrated ^{14}C ages and the historical date may, in part, be explained by a systematic error in the application of the bristlecone pine calibration, so that calibrated dates appear more recent. Such a systematic difference would be of the same magnitude and in the same sense as previously observed apparent discrepancies between bristlecone pine and European materials (Suess and Strahm, 1970; Clark and Sowray, 1974). It is, however, more probable that, in view of the considerable variation within the data as a whole, there is a significant contribution stemming from incorporation of non-contemporaneous carbon into the sampling area, and for the short-lived samples where the scatter is more marked, a further contribution arising from short-term fluctuations in natural ^{14}C . This would imply that short-lived samples are not suited for precise dating purposes, even if sample-collection and age-calibration procedures could be accomplished without large additional uncertainties being incurred.

It has therefore been shown that, in terms of the sources of error outlined above, and through the example of the Cadbury samples, the constraints imposed upon radiocarbon age determinations precludes the use of the ^{14}C method as a precise dating tool in archaeology. In this particular case, the precise date of the massacre, derived so exactly on historico-archaeological evidence, cannot be assigned closer than sometime during the first or second (or even third) century A.D.

The sources of uncertainty which so limit the ^{14}C method, outlined previously are presented in Table 6-3. It is important that these possible sources of error are fully understood when the results of radiocarbon age-measurements are being interpreted. It is most likely that the uncertainties associated with sampling and calibration are far greater than those pertaining to the actual ^{14}C analysis. This philosophy should not, however, result in laboratories being complacent about their own reproducibility. Many of the categories comprising the total uncertainty of a radiocarbon measurement, particularly those associated with sampling and age-calibration, are unquantified. For sampling, the different types of material submitted for analysis have, as it has been shown, inherent uncertainties such as the association of sample and event, the occurrence of short-term fluctuations in ^{14}C and unavoidable (and avoidable) sample contamination, combinations of which may give rise to errors typically of the order of ± 100 years, but in some cases, of greater magnitude. With respect to radiocarbon age-calibration, since the past fluctuations in natural ^{14}C concentrations are insufficiently defined, the use of approximate calibration procedures will inevitably lead to large uncertainties, although these may not be apparent on application of a particular method. At present, Clark's curve (Clark, 1975), with its significant error terms, is most probably the best calibration procedure to adopt until understanding of past ^{14}C variations improves beyond its present rather tenuous state.

TABLE 6-3 : SOURCES OF ERROR IN RADIOCARBON ASSAY

Source of Error	Size of Error	Precaution
Samples		
(i) Human	Unquantifiable	Care in identification, interpretation and collection.
(ii) Sample type Long-lived Sample re-use Short-lived	Up to 200 years Unquantifiable + 120 years	Close definition of sample - event association
(iii) Contamination	Unquantifiable	Large, high quality samples (~100g) >1 sample to observe spread Exhaustive pretreatment
Analysis		
(i) Human	Unquantifiable	Careful analysis
(ii) Counting	Quantifiable	Minimise by large samples and long counting times. Stable isotope fractionation correction.
(iii) Experimental	Quantifiable	Replicate standardisation Interlaboratory calibration
(iv) Systematic	e.g. Shells dating 400 years old	System of "realistic" reference standards Half-life revision Reduction of replicate error
Calibration		
(i) Random	Unquantifiable	Careful selection of calibration procedure, large errors unavoidable
(ii) Systematic	Unquantifiable 50-90 years?	Require replacement tree-ring ¹⁴ C calibration for sea-level
GENERAL COMMENT:	Close contact between sample-submitter and radiocarbon analyst is essential to realistic assessment of data and can, in favourable cases, lead to some, even if subjective, estimate of total error.	

6.2 The 1976 British-Ecuadorean Expedition to the
Los Tayos Caves.

In his much publicised work "The Gold of the Gods" (1973), Erich von Däniken has described in fantastic terms, a system of caves in the tropical rain-forests of South Eastern Ecuador. The regular structure of the underground system, square cross-section passageways and large galleries were, in his opinion, not naturally formed but probably constructed thousands of years ago by extra-terrestrial beings. In his account of the caves, von Däniken describes the fantastic treasures found in the caves, stone furniture, skeletons coated in precious metal, a metal library - large numbers of metal plaques with inscriptions etched in the surface - and a pile of gold which remained in the cave. There is, however, no photographic record of any of these findings because of mysterious radiation which prevented the use of a camera. Further artifacts created, presumably, by the local tribesmen, recovered from the cave show these spacemen wearing the gadgetry of advanced telecommunications and space travel.

In 1976, a multi-discipline scientific expedition, backed by a contingent of the British Army Adventure Training Programme, set out to investigate the Los Tayos Cave system. The party of 25 scientists included not only geologists, speleologists and archaeologists, but also a number of zoologists and botanists whose aim was to make as wide a study as possible of the fauna of the underground system and also of the flora and fauna of the surrounding, unexplored, rain-forest.

The base camp for the expedition was situated at Teniente Ortiz, an Ecuadorean Army outpost close to the disputed border with Peru, on the right bank of the Santiago River, which is one of the many tributaries of the Amazon river system. Advance camp was established at the cave site, 20 miles away at the headwaters of the Coangas River and the members of the party were ferried to the camp by helicopter by river or by foot - certainly not by Toyota Jeep as reported by von Däniken.

The cave system was explored by a team from the British Cave Research Association and a survey was conducted over a length of 4,900 metres at a depth of 186 metres, which placed the Los Tayos caves as one of the largest underground systems on the South American continent. The development of the cave system is classic, the rectangular section forms are a result of cavern collapse and a massive collapse formed the huge galleries, the largest, called "Stanley Hall" after the expedition co-ordinator, having a floor dimension of 250m by 90m. The "glaze" on the walls of the cave has been produced by crystallisation of salts from water running over the surfaces, and not by the blast from electron ray guns.

There is an abundance of animal life in the caves. Many types of spiders, scorpions and other insects inhabit the floor of the cave and the roof is a roosting area for large colonies of fruit and nectar bats and Tayos, or oil birds. These nocturnal creatures leave the caves at dusk to feed on fruit, abundant in the dense forest. During the breeding season, the parent birds collect large quantities of food to satiate the young Tayos. The

fledglings convert the food into fat reserves and it is for this commodity that the local tribesmen hunt the birds, gaining access to the cave system by series of vine ladders. The oil which they collect forms the basis of local trade.

Under the roosting areas large mounds of guano and seed remains accumulate. From one of these deposits, at a depth of 2.3 metres, a sample of "soil" was collected for radiocarbon analysis, the result being given in Table 3-2-1. The slightly positive $\delta^{14}\text{C}$ value suggests that this material was deposited at the onset of the bomb effect in the late 1940's or early 1950's, indicating an accumulation rate of 1 metre per decade. There are, however, several uncertainties which may substantially affect this rate. The figure could be an underestimation due to the Suess effect, or percolating ground water giving an erroneous $\delta^{14}\text{C}$ value. Also an overestimate would be obtained if more modern carbon was introduced as a result of the hunting activities of the Indians. A more probable effect is that from time to time the roosting places for both bats and Tayos have changed and numbers of creatures at a particular roost has similarly varied so that periods of more rapid and then reduced guano accumulation would alternate.

The only material of archaeological importance was found close by the guano pile from which the ^{14}C sample was collected. The artifacts collected consisted of decorated pottery, clay statuettes and some shells. At the present time, very little archaeological work has been

performed in the rain-forests and so the estimation of the age of the finds on the expedition was based on stylistic comparison with materials excavated at coastal sites. This pottery from the main cave was assigned an archaeological age of 2,000 - 800 B.C. and samples have been submitted for thermoluminescence dating. There was no trace whatsoever of the treasures reported by von Däniken and consequently there must be considerable doubt concerning the authenticity of his work.

Two archaeological sites were excavated within the grounds of a Roman Catholic Mission one mile downstream from the base camp. The first site, on the football field, revealed almost complete earthenware vessels stacked one on top of another, reminiscent of so-called "chimney-burials" discovered on the coast. A charcoal sample yielded a date of 1012 ± 66 years B.P. (Table 3-2-1, GU 652) which is in agreement with the archaeological estimate of 500 - 1000 years B.P.

The second site, situated in a nearby banana plantation, yielded decorated pottery in an apparent chronological sequence spanning an estimated age range 1000 - 500 B.C. The ^{14}C analyses on charcoal samples collected from a stratigraphic cut are, however, in considerable disagreement with this estimate being only 150 - 250 years old (GU 653, 654). Furthermore, the sample from the lower level (GU 654, OMST 1/5) gives a younger date than the overlying charcoal. Archaeological interpretation has not yet been completed and no reason for this discrepancy has been forthcoming.

The findings of the expedition are soon to be published in a report and in a book of photographs contributed by the members of the expedition.

A P P E N D I X 1

THE BACKGROUND COUNT RATE

The background of a coincidence mode liquid scintillation spectrometer may be divided into three components:

1. Accidental coincidences between the two photomultiplier tubes,
2. coincident light pulses in the sample itself, i.e. in the part of the system common to both photomultiplier tubes
- and 3. coincidence from light pulses which originate in one photomultiplier and are seen by the other photomultiplier.

Component 1 arises mainly from thermionic emission from the photocathodes and may be reduced to well below 0.1c.p.m. by cooling the detector chamber and by using a short resolving time. Component 2, light pulses in the sample, is caused by extraneous radiation and by radioactivity in the glass of the scintillation vials, mainly ^{40}K and natural series isotopes, and may be reduced by shielding and by selection of low radioactivity materials. Little improvement is obtained beyond 10cm lead shielding or equivalent (Hartley and Church, 1974). This component can further be reduced by energy discrimination which eliminates the high energy cosmic-ray components and the γ -background. Component 3 originates from two sources, namely, light pulses associated with the operation of the photomultipliers and those caused by cosmic rays and radioactivity of the photocathode window. Some of the light from these processes will reach the other photo-

multiplier and may trigger the coincidence circuit causing a background count to register. Background arising from component 3 will be referred to as cross-talk.

Procedures for the optimisation of the liquid scintillation counting system have been described in Chapter 2 and the established background count rate for a standard 10 ml counting vial has been recorded as 7.44 ± 0.01 c.p.m. using both benzene, synthesised from marble chips and commercially produced scintillation grade benzene (Tables 2-4 and 2-5). Before discussing the contributions to this background count rate, however, it is important to establish that there is no variation in this observed count rate between different scintillation vials, as a function either of vial weight or of the amount of screening on each. Any relationship between the latter factor and the observed background count rate will, furthermore, be a function of the variability in the volumetric procedures used in preparation of vials for counting (Chapter 4).

A tray of fifty standard low potassium vials was selected and the individual vials were weighed, minus their plastic caps. These weighings are presented as a grid in Table A1-1. Fifteen vials were selected from the tray. The choice was not completely random, but aimed at covering the complete range of weights in the sample batch. Each vial was prepared to the standard size (Chapter 2) using, as background material, scintillation grade benzene. The group of samples was counted for a

TABLE A1-1: WEIGHT OF SCINTILLATION VIALS IN A 50-VIAL TRAY

	0	1	2	3	4	5	6	7	8	9
0	13.96366	14.09245	13.97195	13.73006	13.89732	14.22175	13.98906	14.07949	13.75937	13.92666
1	13.28117	13.96122	13.96378	13.78395	14.00642	13.78618	13.65225	13.78121	14.13763	13.79109
2	13.77182	13.80572	13.72280	13.90535	13.73850	13.79532	13.83974	13.94643	13.72720	13.96420
3	13.65289	13.86451	13.74400	13.74587	13.69770	13.79527	13.97515	13.90575	13.63133	13.94532
4	13.95452	13.88322	13.85838	13.79266	13.87195	13.94755	13.81982	13.80052	13.82872	14.18204

Mean value = 13.85782 ± 0.14812

total of 4,600 minutes per vial. The results are presented in Table A1-2, the sample code being the row-column number of the vial in the tray grid. Figure A1-1 shows the variation of background count rate versus weight of vial. There is no significant correlation between these two variables. (The average background count rate, 7.19 c.p.m., is lower than the value used in the calculation of radiocarbon data, that is 7.44 c.p.m. Shortly after this experiment was conducted, the counting conditions altered as a result of malfunction and subsequent repair of the sample of elevator. It is assumed that this alteration would not affect the results of the experiment under the reset conditions). Furthermore, the small variations, ± 1 mm, in the "clear height", that part of the vial not masked off, are seen not to affect the background count rate significantly (Fig. A1-2).

The contributions to the background count rate arising from the three components outlined previously can be assessed by varying the presentation of the sample vial in the counting chamber. Firstly, however, the contribution arising from accidental coincidences can be calculated without any counting using the following empirical relationship. If the thermal noise rates for two photomultiplier tubes a and b are N_a and N_b counts per minute respectively and the coincidence resolving time for the system is τ seconds, then the rate of accidental coincidence, A, is given by

$$A = \frac{2 \cdot N_a \cdot N_b \cdot \tau}{60} \text{ c.p.m.}$$

TABLE A1-2 : BACKGROUND COUNT RATE FOR SELECTED VIALS

Vial number row-column	Weight of vial g	Clear height mm	Count rate $\pm 1\sigma$ c.p.m.
0-1	14.09245	20.70	7.15 \pm 0.04
0-5	14.22175	21.10	7.17 \pm 0.04
0-7	14.07949	20.95	7.16 \pm 0.04
1-0	13.28117	21.45	7.16 \pm 0.04
1-4	14.00642	20.35	7.12 \pm 0.04
1-6	13.65225	20.70	7.21 \pm 0.04
1-8	14.13763	21.55	7.19 \pm 0.04
2-5	13.79532	21.75	7.07 \pm 0.04
2-6	13.83974	21.15	7.20 \pm 0.04
3-0	13.65289	20.55	7.23 \pm 0.04
3-1	13.86451	21.00	7.14 \pm 0.04
3-4	13.69770	20.35	7.22 \pm 0.04
3-8	13.63133	20.85	7.34 \pm 0.04
4-2	13.85838	21.65	7.18 \pm 0.04
4-9	14.18204	21.30	7.27 \pm 0.04

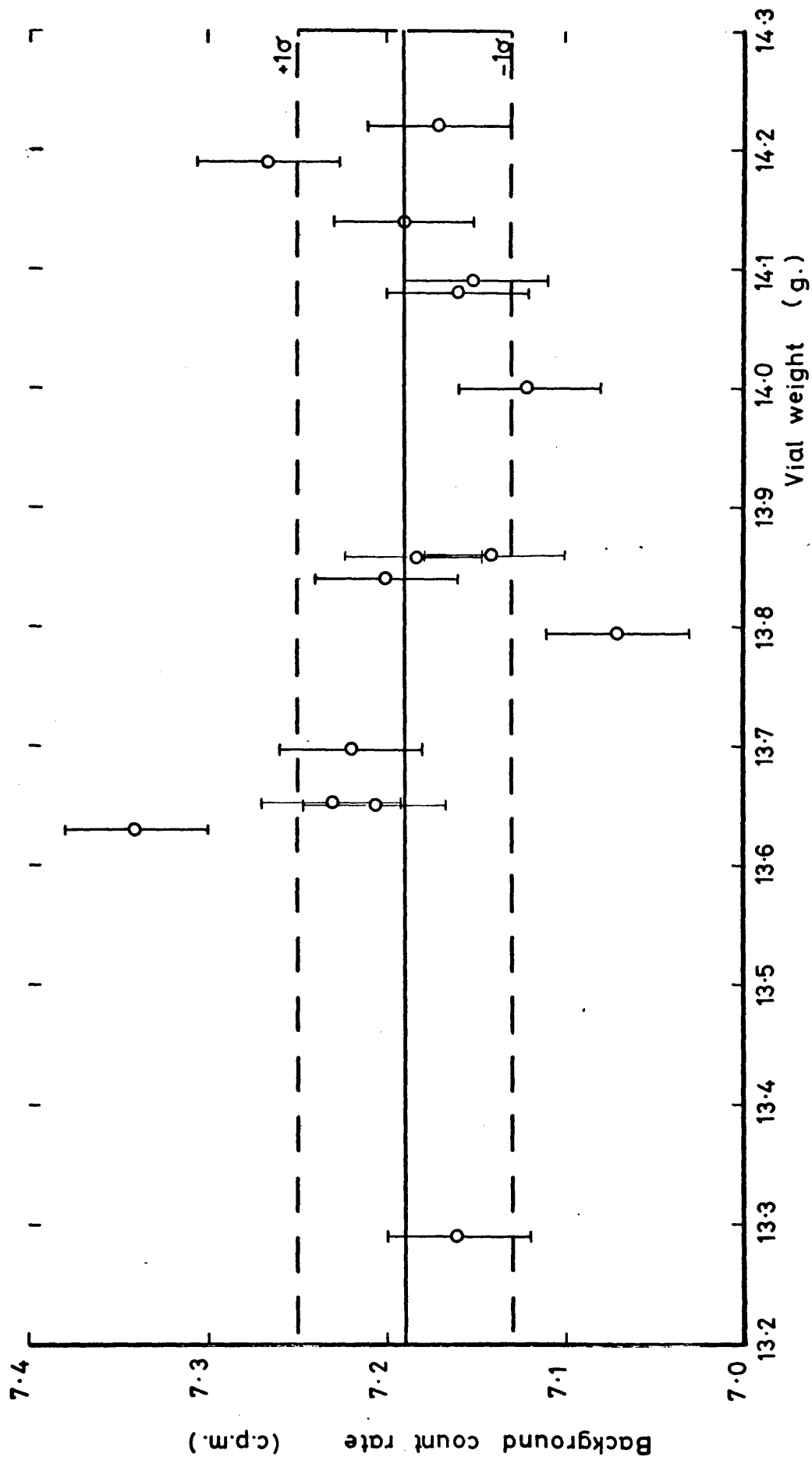


FIGURE A1-1: Background count rate (10ml. geometry) versus scintillation vial weight

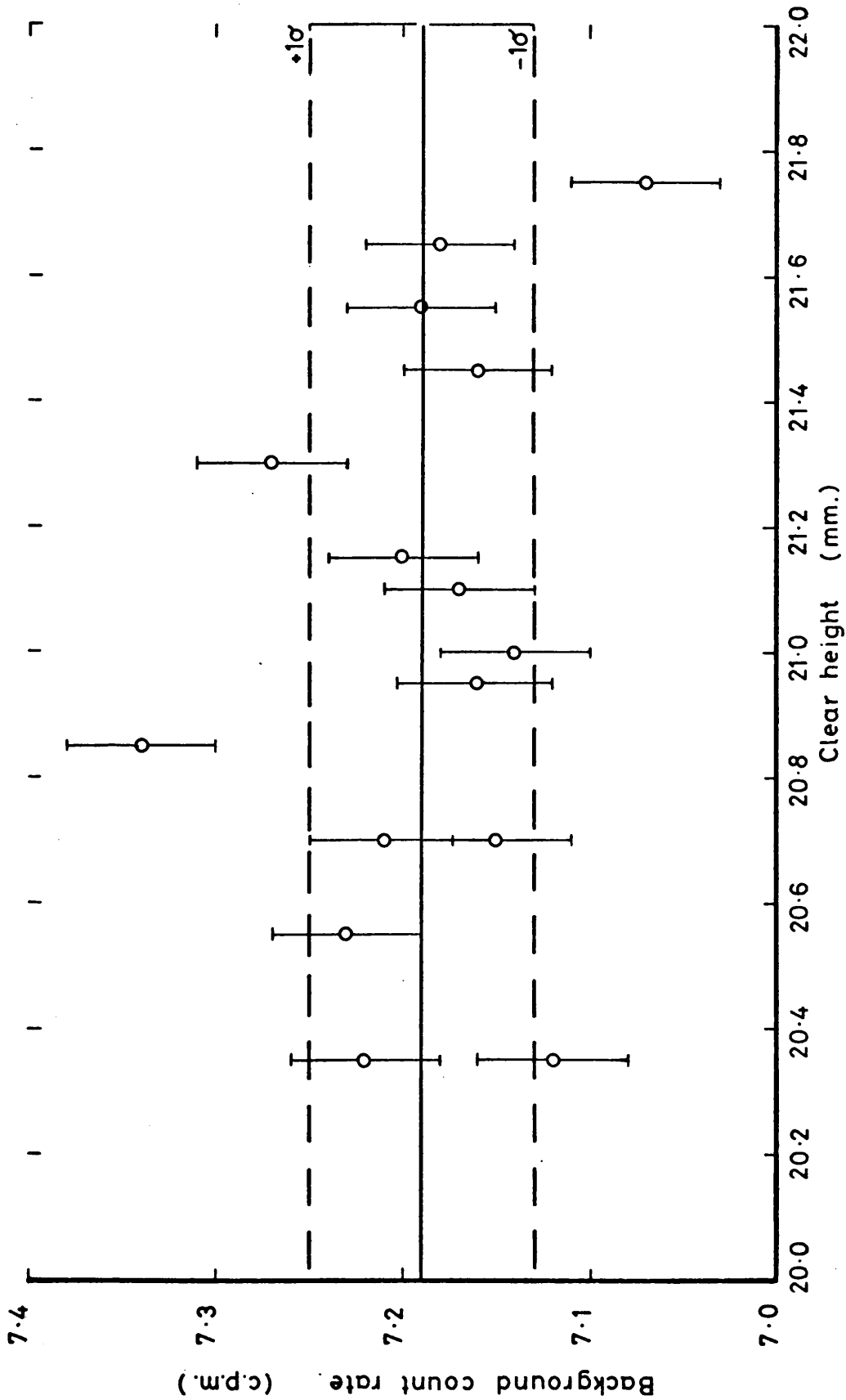


FIGURE A1-2: Background count rate (10ml. geometry) versus clear height

N_a and N_b vary with temperature and at the operating temperature of 0°C the thermal noise rate is estimated to be $1 \times 10^4 - 2 \times 10^4$ c.p.m. Thus, with $\tau = 20$ nanoseconds, the accidental coincidence rate has a value of $0.07 - 0.27$ c.p.m. The discriminator settings adopted will result in rejection of most of the accidental pulses since these occur at the lower energy end of the pulse height spectrum and hence it is estimated that this source of background will contribute <0.1 c.p.m. ($\sim 1\%$) to the total observed count rate for a 10 ml standard vial.

The different modes of presentation of the sample vial in the optical chamber and the count rates obtained are presented in Table A1-3. From these data it is possible to derive qualitatively the contribution to the background count rate from each of the previously outlined sources. The first component, arising from thermionic coincidences in the photomultiplier tubes, has already been estimated at <0.1 c.p.m. Cases 1 and 2 provide information on the cross-talk. Thus, with the empty chamber the total cross-talk rate is $1.3 - 2.4$ c.p.m. Placing a totally masked vial in the optical chamber reduces the cross-talk such that the photons which are detected are those which have "leaked" around the outside of the vial, amounting to $0.6 - 0.7$ c.p.m. Natural radioactivity in the glass of the vial, ^{40}K and natural series isotopes, will contribute to the background count rate in two ways. Firstly, radiation associated with decay of radionuclides may give rise to Cerenkov radiation. Cerenkov radiation is produced when a charged particle passes through a transparent medium

TABLE A1-3 : BACKGROUND COUNT RATE OBSERVED
UNDER DIFFERENT COUNTING CONDITIONS

Counting conditions	Observed count rate $\pm 1\sigma$ c.p.m.
Empty chamber	2.38 \pm 0.04
Chamber plus completely masked glass vial	0.64 \pm 0.02
Chamber plus partially masked glass vial (10ml size)	3.43 \pm 0.04
Chamber plus unmasked glass vial	5.95 \pm 0.05
Chamber plus standard 10ml vial containing 10ml scintillation cocktail	7.44 \pm 0.01
Chamber plus unmasked vial containing 10ml scintillation cocktail	9.31 \pm 0.07

(the Cerenkov generator) at a relative phase velocity greater than the speed of light in the same medium. From Case 3 it can be seen that this source of light photons contributes as much as 3.5 - 3.6 c.p.m. when the cross-talk and noise rates are subtracted. Reduction in these background components is achieved by masking the part of the scintillation vial above the level of the standard counting volume. It is reasonable to assume that this will result in an equal reduction, of approximately half, in cross-talk and Cerenkov radiation. Therefore, for the standard 10 ml counting vial, the contributions from these sources are approximately 0.8 - 0.9 c.p.m. and 1.7 - 1.8 c.p.m. respectively.

The addition of scintillant to the 10 ml geometry vial produces an increase of 4 counts in the observed background count rate. This rise is accounted for by production of photons arising from a further contribution of Cerenkov radiation in the scintillation solvent derived from decay events in the glass of the vial, and the interaction of ambient radiation and cosmic rays with the scintillator system. The contribution to the background resulting from interaction of cosmic rays with the scintillator is not likely to be substantial, since the effective cross-sectional area of the detection system, $\sim 10\text{cm}^2$, is very small. The omnidirectional cosmic-ray flux at sea-level has been estimated as $1.2 \text{ ray min}^{-1} \text{ cm}^{-2}$ (Blatz, 1959). Shielding of the detection chamber and energy discrimination, however, will result in a probable cosmic-ray component of $< 0.5 \text{ c.p.m.}$ An independent estimate of the ^{40}K content of a scintillation vial has been made via γ -spectrometry, using a Ge(Li) detector.

These measurements indicate that the maximum γ -activity arising from ^{40}K is 2 d.p.m. per vial, so the maximum total β activity will be ~ 16 d.p.m. per vial. (McKinley, pers. comm.). It is, however, unlikely that the detection efficiency will be greater than 15 - 20% as a result of geometry restrictions and energy discrimination. Thus, a maximum total contribution to the background of 2.5 - 3 c.p.m. may be expected to arise from ^{40}K in the glass of the scintillation vial. Thus, probably 1 - 1.5 c.p.m. of the increase in count rate observed upon the introduction of scintillant will be due to ^{40}K -derived radiation in the vial material. Ambient radiation from the surrounding materials will be considered as producing the remaining contribution of $\sim 2 - 2.5$ c.p.m.

It is interesting to note that, for unmasked vials, the increase in background count rate produced by introduction of the scintillation cocktail is less by 0.6 c.p.m. than in the case of the partially masked vials. This discrepancy may be accounted for through increased light loss by scattering.

Table A1-4 summarises these contributions to the observed background count rate. Clearly one of the major components is radioactivity, principally ^{40}K , in the glass of scintillation vials, in this case accounting for almost half of the observed rate. The utilisation of vials, constructed from different synthetic materials and also from quartz has been reviewed by Painter (1974). Plastic vials have, in general, been rejected for ^{14}C dating because of contamination of sample with inactive carbon, quenching through dissolution of the plastic, diffusion of

TABLE A1-4 : BACKGROUND COMPONENTS FOR A STANDARD
10ML GEOMETRY VIAL

Sources of background	Estimated contribution to total background
Cosmic Radiation	6%
Photomultiplier tube thermal noise	1%
Cross-talk	
(i) incident on vial	10 - 15%
(ii) leakage around vial	8 - 10%
Radioactivity, ^{40}K and natural series isotopes, in glass of vial	30 - 40%
Ambient radiation	25 - 35%

atmospheric components containing radioactivity through the container walls, ineffective sealing and a tendency of plastics to become distorted and brittle when cooled. Teflon vials, however, appear to have advantages over the customary low potassium glass vials although these are not yet commercially available. Calf (1977) has shown that it is possible, using thick walled teflon vials, to achieve a much enhanced figure of merit for ^{14}C through both a reduction in background and an increase in ^{14}C detection efficiency. These experiments were conducted using virtually identical conditions to those in this research. The observed background count rate of 3.00 c.p.m. for a teflon vial achieved by elimination of a ^{40}K contribution and reduction in cross-talk, therefore represents a considerable improvement over values obtained using standard glass vials. Careful design and construction of vials made from this material should overcome many of the problems encountered previously and it is anticipated that the advantages displayed by teflon will lead to their adoption by many radiocarbon laboratories once they are commercially available.

A P P E N D I X 2

COMPUTER PROGRAMMES

A Fortran IV computer programme has been written for calculation of ^{14}C data. From the input data, total number of counts in the three counting channels, total count time, weight of sample benzene and $\delta^{13}\text{C}$, the programme will calculate the quench corrected sample count rate and then $\delta^{14}\text{C}$, $\Delta^{14}\text{C}$ and conventional radiocarbon age with the respective one sigma counting errors. The printed output also contains the radiocarbon age calculated with the 5730 year half-life.

The programme is as follows:

FORTRAN IV G LEVEL 21 MAIN DATE = 77188 15/37/44

C ---THIS PROGRAMME WILL CALCULATE SMALL DELTA, CAPITAL DELTA
 C AND THE CORRESPONDING ONE SIGMA COUNTING ERRORS, ACCORDING TO THE
 C FORMULAE OF BROECKER AND OLSON, 1961, AND CALLOW ET AL., 1965.
 C THE CORRESPONDING RADIOCARBON AGES ARE THEN CALCULATED.
 C THE INPUT DATA IS AS FOLLOWS:

C CARD 1: TITLE OF SAMPLE IN 20A4 FORMAT
 C CARD 2: TOTAL NO OF COUNTS ACCUMULATED IN THE THREE
 C COUNTER CHANNELS IN 3F10.0 FORMAT
 C CARD 3: THE COUNTING TIME IN F10.0 FORMAT
 C CARD 4: THE WEIGHT OF BENZENE PRODUCED IN F10.0 FORMAT
 C CARD 5: DELTA C-13 +/- ONE SIGMA IN 2F10.0 FORMAT
 C BEFORE THE C-14/C12 RATIO IS COMPUTED THE COUNT RATES ARE
 C NORMALISED TO COMPENSATE FOR QUENCH EFFECTS

C DIMENSION TITLE(20)

C NIX=0

C ---READING INPUT DATA

C READ(5,10) NUMRUN
 C NIX=NIX+1
 C IF (NIX.GT.NUMRUN)GO TO 9999
 C WRITE(6,500)
 C READ(5,20) (TITLE(I),I=1,20)
 C WRITE(6,20) (TITLE(I),I=1,20)
 C WRITE(6,25)
 C READ(5,30) GROSS1,GROSS2,GROSS3
 C READ(5,40) TIME
 C READ(5,50) WSB
 C READ(5,60) DC13,SDC13

C ---INPUT FORMAT STATEMENTS

C

```

10 FORMAT(13)
20 FORMAT(20A4)
25 FORMAT(1H,120('**'))
30 FORMAT(3F10.0)
40 FORMAT(F10.0)
50 FORMAT(F10.0)
60 FORMAT(2F10.0)
500 FORMAT(1H1,'NEW PASS'////)

```

C
C
C

---CALCULATE COUNT RATES AND ERRORS

```

RATE1=GROSS1/TIME
RATE2=GROSS2/TIME
RATE3=GROSS3/TIME
ERATE1=(SQRT(GROSS1))/TIME
ERATE2=(SQRT(GROSS2))/TIME
ERATE3=(SQRT(GROSS3))/TIME

```

C
C
C

---CONSTANTS FOR PROGRAMME

```

BR1=3.63
EBR1=0.01
BR2=3.93
EBR2=0.01
BR3=7.44
EBR3=0.01
RMOD=63.40
EMODR=0.05
TMB=7.0
TLAPS=26.0
DF=TMB/WSB
VBR3=EBR3*EBR3
VDC13=SDC13*SDC13

```

C
C
C

---BACKGROUND SUBTRACTION

```

SRATE1=RATE1-BR1
SRATE2=RATE2-BR2
SRATE3=RATE3-BR3
ESR1=(SQRT((ERATE1*ERATE1)+(EBR1*EBR1)))
ESR2=(SQRT((ERATE2*ERATE2)+(EBR2*EBR2)))
ESR3=(SQRT((ERATE3*ERATE3)+(EBR3*EBR3)))

```


---STANDARD AGE CALCULATION

```

19 D14=(((DF*SAMR)/(0.95*EMOD))-1)*1000)
VD14=(((1000*DE)/(0.95*EMOD))*2)*(VSAMR+(((SAMR/RMOD)**2*(EMODR*
1EMODR))+(((SAMR-RMOD)**2)*VBR3)))
ED14=SQRT(VD14)
BD14=D14-(2*DC13+50)*(1+D14/1000)
IF (DC13 LT -25.0) GO TO 29
VBD14=(((1+(2*DC13+50)/1000)**2*VD14)+(4*(((1+D14)/1000)*((1+D14
1)/1000)*VDC13))
EBD14=SQRT(VBD14)
AGE1=8033*ALOG(1/(1+(0.001*(BD14+EBD14))))
CAGE2=8033*ALOG(1/(1+(0.001*BD14)))
AGE3=8033*ALOG(1/(1+(0.001*(BD14-EBD14))))
ERROR1=CAGE2-AGE1
ERROR2=AGE3-CAGE2
CAGE=CAGE2-TLAPS
DATE=CAGE-1950
DAGE=CAGE*1.03
GO TO 1000

29 VBD14=(((1+(2*DC13+50)/1000)**2*VD14)+(4*(((1+D14)/1000)*((1+D14
1)/1000)*VDC13))
EBD14=SQRT(VBD14)
AGE1=8033*ALOG(1/(1+(0.001*(BD14+EBD14))))
CAGE2=8033*ALOG(1/(1+(0.001*BD14)))
AGE3=8033*ALOG(1/(1+(0.001*(BD14-EBD14))))
ERROR1=CAGE2-AGE1
ERROR2=AGE3-CAGE2
CAGE=CAGE2-TLAPS
DATE=CAGE-1950
DAGE=CAGE*1.03

```

---OUTPUT STATEMENTS

```

1000 WRITE(6,90)
WRITE(6,91)
WRITE(6,100) TIME
WRITE(6,110) RATE1,ERATE1
WRITE(6,120) RATE2,ERATE2
WRITE(6,130) RATE3,ERATE3

```

```

WRITE(6,140) BR1,EBR1
WRITE(6,150) BR2,EBR2
WRITE(6,160) BR3,EBR3
WRITE(6,170) RMOD,EMODR
WRITE(6,180) WSB,DF
WRITE(6,190) DC13,SDC13
WRITE(6,200)
WRITE(6,210)
WRITE(6,220)
WRITE(6,230) RATIO,EFF
WRITE(6,240) SAMR,ESAMR
WRITE(6,250)
WRITE(6,260)
WRITE(6,270)
WRITE(6,280) D14,ED14,BD14,EBD14
IF (CAGE.LT.1950) GO TO 109
WRITE(6,290) CAGE,ERROR2,DATE
WRITE(6,300) DAGE,ERROR2
WRITE(6,310)
WRITE(6,320)
GO TO 7777
109 ADDATE=DATE*(-1.0)
WRITE(6,330) CAGE,ERROR2,ADDATE
WRITE(6,340) DAGE,ERROR2
WRITE(6,350)
WRITE(6,360)

C
C
C
---OUTPUT FORMAT STATEMENTS
90 FORMAT(///1H,'INPUT DATA')
91 FORMAT(1H,15('*'))
100 FORMAT(///,'COUNTING TIME FOR SAMPLE = ',F10.2,' MINUTES')
110 FORMAT(///,'CHANNEL 1 RATE +/- 1-SIGMA ---',F7.2,' +/- ',F5.3,
1' CPN ')
120 FORMAT(///,'CHANNEL 2 RATE +/- 1-SIGMA ---',F7.2,' +/- ',F5.3,
1' CPN ')
130 FORMAT(///,'CHANNEL 3 RATE +/- 1-SIGMA ---',F7.2,' +/- ',F5.3,
1' CPN ')

```

```

140 FORMAT(//, '
13, ' CPM')
BACKGROUND RATE FOR CHANNEL 1 = ', F5.3, ' +/- ', F5.
150 FORMAT(//, '
13, ' CPM')
BACKGROUND RATE FOR CHANNEL 2 = ', F5.3, ' +/- ', F5.
160 FORMAT(//, '
13, ' CPM')
BACKGROUND RATE FOR CHANNEL 3 = ', F5.3, ' +/- ', F5.
170 FORMAT(//, '
1- ', F5.3, ' CPM ')
ACTIVITY OF NBS OXALIC ACID STANDARD = ', F7.3, ' +/-
180 FORMAT(//, '
1 ' DILUTION FACTOR = ', F8.5)
WEIGHT OF BENZENE SYNTHESISED = ', F8.5, ' GRAMS'//,
190 FORMAT(//, '
200 FORMAT(1H, 120(' * '))
DELTA C-13 = ', F8.2, ' +/- ', F5.2, ' (ONE SIGMA)')
210 FORMAT(////, '
1 ' )
NORMALISATION OF COUNT RATE BY QUENCH CORRECTION
220 FORMAT(1H, 56(' - '))
230 FORMAT(////, '
13//, '
240 FORMAT(//////, '
1/- ', F5.3, ' CPM')
CORRESPONDING EFFICIENCY = ', F8.3, '%')
250 FORMAT(1H, 120(' * '))
260 FORMAT(////, '
270 FORMAT(1H, 29(' - '))
DELTA VALUES AND AGES')
280 FORMAT(//, '
1TA = ', F8.2, ' +/- ', F6.2)
SMALL DELTA = ', F8.2, ' +/- ', F6.2, 10X, 'CAPITAL DEL
290 FORMAT(//, '
10.2, ' +/- ', F6.2, ' C-14 YRS BP (' , F7.2, ' BC)')
RADIOCARBON AGE, LIBBY HALF LIFE, (5568YRS) IS ', F1
300 FORMAT(//, '
1 +/- ', F6.2, ' C-14 YRS BP')
RADIOCARBON AGE, 5730 YEAR HALF LIFE IS ', F10.2, '
310 FORMAT(//////, '
1NTING ERRORS ONLY')
N.B. ERRORS QUOTED ON RADIOCARBON DATES ARE COU
320 FORMAT(1H, 120(' * '))
330 FORMAT(//, '
10.2, ' +/- ', F6.2, ' C-14 YRS BP (A.D. ', F7.2, ' )')
RADIOCARBON AGE, LIBBY HALF LIFE, (5568YRS) IS ', F1

```

```

340 FORMAT(//, ' RADIOCARBON AGE, 5730 YEAR HALF LIFE IS ', F10.2, '
1 +/- ', F6.2, ' C-14 YRS BP')
350 FORMAT(////, ' N.B. ERRORS QUOTED ON RADIOCARBON DATES ARE COU
NTING ERRORS ONLY')
360 FORMAT(1H, 120('**'))
GO TO 7777
9999 STOP
END

```

EXAMPLE OF OUTPUT

YNYSLAS 1/3 RINGS 11-20

INPUT DATA

```

COUNTING TIME FOR SAMPLE = 2300.00 MINUTES
CHANNEL 1 RATE +/- 1-SIGMA --- 11.13 +/- 0.070 CPM
CHANNEL 2 RATE +/- 1-SIGMA --- 12.43 +/- 0.074 CPM
CHANNEL 3 RATE +/- 1-SIGMA --- 23.41 +/- 0.101 CPM
BACKGROUND RATE FOR CHANNEL 1 = 3.630 +/- 0.010 CPM
BACKGROUND RATE FOR CHANNEL 2 = 3.930 +/- 0.010 CPM
BACKGROUND RATE FOR CHANNEL 3 = 7.440 +/- 0.010 CPM
ACTIVITY OF NBS OXALIC ACID STANDARD = 63.400 +/- 0.050 CPM
WEIGHT OF BENZENE SYNTHESISED = 3.48603 GRAMS
DILUTION FACTOR = 2.00801
DELTA C-13 = -23.90 +/- 0.05 (ONE SIGMA)

```

NORMALISATION OF COUNT RATE BY QUENCH CORRECTION

RATIO OF CHANNEL 1 RATE TO CHANNEL 2 RATE = 0.882

CORRESPONDING EFFICIENCY = 99.443%

QUENCH CORRECTED COUNT RATE. (CH3) = 16.062 +/- 0.101 CPM

DELTA VALUES AND AGES

SMALL DELTA = -464.52 +/- 3.42 CAPITAL DELTA = -465.70 +/- 3.43

RADIOCARBON AGE, LIBBY HALF LIFE, (5568YRS) IS 5009.05 +/- 51.67 C-14 YRS BP (3059.05 BC)

RADIOCARBON AGE, 5730 YEAR HALF LIFE IS 5159.32 +/- 51.67 C-14 YRS BP

N.B. ERRORS QUOTED ON RADIOCARBON DATES ARE COUNTING ERRORS ONLY

The second computer programme performs the analysis outlined by Clark and Renfrew (1972), for calibration of "floating" tree-ring chronologies using radiocarbon dates. Several of the operations in the programme, linear regression, solution of linear equations and matrix inversion, are performed using NAGLIB subroutines available on the NUMAC system.

FORTRAN IV G LEVEL 21 MAIN DATE = 77229 13/32/26

FLOATING CHRONOLOGY CALIBRATION PROGRAMME

IMPLICIT REAL*8 (A-H,O-Z)

DIMENSION W(200), Z(200), X(200), Y(200), A(3,3), B(3,1),
1C(3,1), WKSP(100), TITLE(20), RESULT(20), AINV(3,3),
2 AMAT(3,3), AINT(50)

READ IN MASTER AND FLOATING DATA

READ(5,5) (TITLE(I), I=1,20)
READ(5,10) M
READ(5,20) (W(I), Z(I), I=1,M)
READ(5,30) N
READ(5,40) (X(J), Y(J), J=1,N)

INPUT FORMAT STATEMENTS

5 FORMAT(20A4)
10 FORMAT(I2)
20 FORMAT(2F10.0)
30 FORMAT(I2)
40 FORMAT(2F10.0)

ZERO ALL SUMMATION TERMS

SW=0.0
SZ=0.0
SW2=0.0
SZ2=0.0
SX=0.0
SY=0.0
SX2=0.0
SY2=0.0
SWZ=0.0
SXY=0.0

CALCULATION OF MATRIX ELEMENTS

C
C
C

```

DO 50 I=1,M
WI=W(I)
ZI=Z(I)
SW=SW+WI
SZ=SZ+ZI
SW2=SW2+WI*WI
SZ2=SZ2+ZI*ZI
SWZ=S1/2+WI*ZI

```

50

CONTINUE

```

DO 60 J=1,N
XJ=X(J)
YJ=Y(J)
SX=SX+XJ
XY=XY+YJ
SX2=SX2+XJ*XJ
SY2=SY2+YJ*YJ
SXY=SXY+XJ*YJ

```

60

CONTINUE

```

SSQ=SX2+SW2
SCP=SXY+SWZ
AM=FLOAT(M)
AN=FLOAT(N)

```

C
C
C

SET UP LEFT HAND SIDE MATRIX

```

A(1,1)=AM
A(1,2)=0.0
A(1,3)=SW
A(2,1)=0.0
A(2,2)=AN
A(2,3)=SX
A(3,1)=SW
A(3,2)=SX
A(3,3)=SSQ
DO 61 I=1,3
DO 62 J=1,3
AMAT(I,J)=A(I,J)

```



```

C      IFAIL=0
C      CALL G02CAF (M,W,Z,RESULTM,IFAIL)
C
C      REGRESSION ON FLOATING CHRONOLOGY - HARD FAILURE OPTION
C
C      IFAIL=0
C      CALL G02CAF (N,X,Y,RESULTF,IFAIL)
C
C      CONSTRUCT ANALYSIS OF VARIANCE TABLE
C
C      COMBINED REGRESSION - CR - TOTAL COMBINED S.S. - COMB. S.S. ABOUT
C      REGRESSION
C
C      NN=M+N
C      AVEZY=(SZ+SY)/MN
C      TCSSM=0.0
C      SSACRM=0.0
C      DO 70 I=1,M
C      ZI=Z(I)
C      WI=W(I)
C      TCSSM=TCSSM+((ZI-AVEZY)**2)
C      SSACRM=SSACRM+((ZI-BO-(B1*WI))**2)
C      CONTINUE
C      TCSSF=0.0
C      SSACRF=0.0
C      DO 80 J=1,N
C      XJ=X(J)
C      YJ=Y(J)
C      TCSSF=TCSSF+((YJ-AVEZY)**2)
C      SSACRF=SSACRF+((YJ-BO-(B1*(XJ+A1)))**2)
C      CONTINUE
C      TCSS=TCSSM+TCSSF
C      TSSWG=RESULTM(19)+RESULTF(19)
C      SSACR=SSACRM+SSACRF
C      CREG=TSSWG-SSACR
C      CREGDF=1.0

```

70

80

C POOLED RESIDUAL - FROM INDIVIDUAL REGRESSION

C PRES=RESULM(16)+RESULTF(16)

C PRESDF=MN-4

C DIFFERENCE BETWEEN REGRESSIONS

C DREG=SSACR-PRES

C DREGDF=1.0

C TOTAL SUM OF SQUARES - WITHIN GROUPS

C TSS=CREG+DREG+PRES

C TDF=NN-2

C MEAN SQUARE TOTALS

C DREGMS=DREG/DREGDF

C PRESMS=PRES/PRESDF

C F-STATISTIC

C F=DREGMS/PRESMS

C COMPARE CALCULATED F-STATISTIC WITH TABULATED VALUE

C CALCULATION OF CONFIDENCE LIMITS FOR ZERO POINT

C CALCULATE S2 = ESTIMATE OF VARIANCE OF RANDOM ERRORS

C S2=(PRES+DREG)/(PRESDF+1)

C

C INVERSION OF MATRIX AMAT - NAGLIB F01AAF - HARD FAILURE OPTION
 C
 C

IFAIL=0
 CALL F01AAF (AMAT,3,3,AINV,3,AINT,IFAIL)

C CHECK MATRIX INVERSION
 C

C ELEMENTS OF THE INVERTED MATRIX ARE USED TO CONSTRUCT THE QUADRATIC
 C EQUATIONS DEFINING THE CONFIDENCE LIMITS, THE 'T-VALUE' FOR A P%
 C CONFIDENCE LIMIT IS NOW READ IN
 C

READ(5,2000) T
 2000 FORMAT(F5.2)

C FOR ALGEBRAIC SOLUTIONS OF QUADRATIC LET CA, CB, CC BE THE
 C COEFFICIENTS OF THE QUADRATIC
 C

T2=T*T
 T2S2=T2*S2
 C1B0=C1-B0
 B1SQ=B1*B1
 C1BOSQ=C1B0*C1B0
 C01=AINV(3,3)
 C02=(AINV(1,3)-AINV(2,3))*2
 C03=(AINV(1,1)+AINV(2,2))-2*AINV(1,2)
 CA=B1SQ-(T2S2*C01)
 CB=(-2*B1*C1B0)-(T2S2*C02)
 CC=C1BOSQ-(T2S2*C03)
 CALL ROOTS (CA,CB,CC,ALPHA1,ALPHA2)

C PRINT RESULTS
 C
 C

```

WRITE(6,500)
WRITE(6,510)
WRITE(6,515)
WRITE(6,516)
WRITE(6,520)
WRITE(6,521)
WRITE(6,522)
WRITE(6,523)
WRITE(6,540)
WRITE(6,541)
WRITE(6,542)
WRITE(6,550)
WRITE(6,560)
WRITE(6,570)
WRITE(6,580)
WRITE(6,590)
WRITE(6,600)
WRITE(6,610)
WRITE(6,620)
WRITE(6,630)
WRITE(6,640)
WRITE(6,650)
WRITE(6,660)
WRITE(6,670)
WRITE(6,680)
WRITE(6,690)
WRITE(6,700)
WRITE(6,710)
WRITE(6,720)
WRITE(6,730)
WRITE(6,740)
WRITE(6,750)
WRITE(6,760)

(TITLE(I), I=1, 20)

(W(I), Z(I), I=1, M)

(X(J), Y(J), J=1, N)

M, N, SW, SW2, SZ, SZ2, SX, SX2, SY, SY2, SWZ, SXY, SSQ, SCP
BO, B1, C1
A1

CREGDF, CREG
DREGDF, DREG, DREGMS, F
PRESDF, PRES, PRESMS

TDF, TSS

((AINV(I, J), J=1, 3), I=1, 3)

T, S2

CA, CB, CC
ALPHA1, ALPHA2

```

OUTPUT FORMAT STATEMENTS

```

500 FORMAT(20A4)
510 FORMAT(1H,8X,60(' - '))
515 FORMAT(////, ' INPUT DATA--')
516 FORMAT(1H,13(' - '))
520 FORMAT(//,13X, ' MASTER CHRONOLOGY')
521 FORMAT(1H,11X,19(' - '))
522 FORMAT(//,3X,E15.8,5X,E15.8)
523 FORMAT(//,110(' * '))
540 FORMAT(//,9X, ' FLOATING CHRONOLOGY')
541 FORMAT(1H,7X,21(' - '))
542 FORMAT(//,3X,E15.8,5X,E15.8)
550 FORMAT(1H,3(110(' * ')),/)
560 FORMAT(//, ' LEAST SQUARES TOTALS'//
1 ' NO. OF POINTS IN MASTER CHRONOLOGY =',14/
2 ' NO. OF POINTS IN FLOATING CHRONOLOGY =',14/
3 ' SUM W =',E17.9,5X, 'SUM W2 =',E17.9/ ' SUM Z =',E17.9,5X, ' SUM Z2
4 =',E17.9/ ' SUM X =',E17.9,5X, ' SUM X2 =',E17.9/ ' SUM Y =',E17.9,5X
5 ' SUM Y2 =',E17.9/ ' SUM WZ =',E17.9,5X, 'SUM XY =',E17.9/ ' SUM SSQ
6 (SW2+SX2) =',E17.9/ ' SUM SCP (SWZ+XZY) =',E17.9)
570 FORMAT(////, ' LEAST SQUARES ESTIMATES'////, ' B0 =',E17.9,5X, ' B1 =
1 ',E17.9,5X, ' C1 =',E17.9)
580 FORMAT(//, ' LEAST SQUARES ESTIMATE OF FLOATING CHRONOLOGY-ZERO POI
1NT ON MASTER CHRONOLOGY =',E17.9)
590 FORMAT(1H,3(110(' * ')),/)
600 FORMAT(1H, ' ANALYSIS OF VARIANCE TABLE (E. J. WILLIAMS REGRE
1SSION ANALYSIS, 1959)')
610 FORMAT(1H,65(' - '))
620 FORMAT(//,10X, ' SOURCE OF VARIATION',5X, ' D.O.F.',10X, ' S.S.',10
1X, ' M.S.',10X, ' F')
630 FORMAT(1H,120(' - '))
640 FORMAT(//, ' COMBINED REGRESSION',13X,F5.1,10X,F10.1//)
650 FORMAT(//, ' DIFFERENCE BETWEEN REGRESSIONS',2X,F5.1,10X,F10.1,6
1X,F10.1,5X,F6.2//)
660 FORMAT(//, ' POOLED RESIDUAL',17X,F5.1,10X,F10.1,6X,F10.1//)

```

C
C
C

```

670 FORMAT(1H,120(' - '))
680 FORMAT(//,1 TOTAL (WITHIN GROUPS)',12X,F5.1,10X,F10.1//)
690 FORMAT(1H,2(120(' - '),//))
700 FORMAT(//,1 INVERTED MATRIX - AINV'//)
710 FORMAT(//,3(D15.8,1X))
720 FORMAT(1H,120(' - '))
730 FORMAT(//,1 T-VALUE (M+N-3 D.F.) FOR 95% CONFIDENCE INTERVAL
1=F5.2//,1 ESTIMATED VARIANCE =',F8.2)
740 FORMAT(//,1 COEFFICIENTS OF QUADRATIC EQUATION --')
750 FORMAT(//,1 CA =',D15.8//,1 CB =',D15.8//,1 CC =',D15
18//)
760 FORMAT(//,1 95% CONFIDENCE LIMITS FOR FLOATING CHRONOLOGY ZERO
1 POINT ARE',F8.2,' AND',F8.2)
STOP
END

```

```

SUBROUTINE ROOTS (CA,CB,CC,ALPHA1,ALPHA2)
B24AC=CB*CB-4.0*CA*CC
B24AC=SQRT(B24AC)
ALPHA1=(-CB+B24AC)/(2.0*CA)
ALPHA2=(-CB-B24AC)/(2.0*CA)
RETURN
END

```

EXAMPLE OF OUTPUT

INPUT DATA

MASTER CHRONOLOGY

0.54050000D 04	0.46010000D 04
0.54150000D 04	0.46180000D 04
0.54350000D 04	0.46350000D 04
0.54450000D 04	0.46950000D 04
0.55600000D 04	0.47620000D 04
0.55750000D 04	0.47320000D 04

0.55850000D 04	0.47520000D 04
0.56500000D 04	0.49490000D 04
0.57150000D 04	0.50630000D 04
0.57400000D 04	0.49810000D 04
0.57720000D 04	0.50920000D 04
0.58600000D 04	0.50630000D 04
0.58880000D 04	0.51860000D 04
0.59550000D 04	0.52290000D 04
0.59850000D 04	0.51720000D 04
0.60270000D 04	0.52860000D 04
0.61200000D 04	0.50830000D 04
0.61550000D 04	0.51520000D 04
0.61750000D 04	0.52540000D 04
0.62550000D 04	0.54030000D 04
0.62750000D 04	0.53340000D 04
0.62950000D 04	0.53810000D 04
0.62150000D 04	0.54100000D 04

FLOATING CHRONOLOGY

0.0	0.49300000D 04
0.10000000D 02	0.49240000D 04
0.20000000D 02	0.50350000D 04
0.30000000D 02	0.49460000D 04
0.40000000D 02	0.49740000D 04
0.50000000D 02	0.50090000D 04
0.60000000D 02	0.49350000D 04
0.65000000D 02	0.51060000D 04

LEAST SQUARES TOTALS

NO. OF POINTS IN MASTER CHRONOLOGY = 23

NO. OF POINTS IN FLOATING CHRONOLOGY = 8

SUM W = 0.134502000D 06 SUM W2 = 0.788595332D 09
 SUM Z = 0.115833000D 06 SUM Z2 = 0.584950863D 09
 SUM X = 0.275000000D 03 SUM X2 = 0.133250000D 05
 SUM Y = 0.398590000D 05 SUM Y2 = 0.198621035D 09
 SUM WZ = 0.679088089D 09 SUM XY = 0.137572000D 07
 SUM SSQ (SW2+SX2) = 0.788608657D 09
 SUM SCP (SWZ+SXY) = 0.680463809D 09

LEAST SQUARES ESTIMATES

B0 = 0.135266684D 03 B1 = 0.838068328D 00 C1 = 0.495356640D 04

LEAST SQUARES ESTIMATE OF FLOATING CHRONOLOGY-ZERO POINT ON MASTER CHRONOLOGY = 0.574929222D 04

ANALYSIS OF VARIANCE TABLE

E. J. WILLIAMS, REGRESSION ANALYSIS, 1959.

SOURCE OF VARIATION	D.O.F.	S.S.	M.S.	F
COMBINED REGRESSION	1.0	1435061.5		
DIFFERENCE BETWEEN REGRESSIONS	1.0	1395.1	1395.1	0.21
POOLED RESIDUAL	27.0	182787.1	6769.9	
TOTAL (WITHIN GROUPS)	29.0	1619243.8		

INVERTED MATRIX = AINV

0.16780961D 02 0.98385692D-01 -0.28621292D-02
0.98385692D-01 0.12557833D 00 -0.16824069D-04
0.28621292D-02 -0.16824069D-04 0.48942746D-06

T-VALUE (M+N-3 D.F.) FOR 95% CONFIDENCE INTERVAL = 2.02

ESTIMATED VARIANCE = 6577.94

COEFFICIENTS OF QUADRATIC EQUATION ---

CA = 0.68922199D 00

CB = 0.79233893D 04

CC = 0.22767512D 08

95% CONFIDENCE LIMITS FOR FLOATING CHRONOLOGY ZERO POINT ARE 5829.52 AND 5666.61

R E F E R E N C E S

- Aitken, M.J., 1970, Physics applied to Archaeology, I, Dating, Reports on Progress in Physics, 33, 941-1000.
- Alcock, L., personal communication.
- Alexeev, V.A., Lavrukhina, A.K. and Milnikova, Z.K., 1975, Variations of radiocarbon content in annual rings of the sequoia (1890-1916), Geokhimiya, 5, 667-675.
- Anderson, E.C., Libby, W.F., Weinhouse, S., Reid, A.F., Kirschenbaum, A.D. and Grosse, A.V., 1947, Natural radiocarbon from cosmic radiation, Phys. Rev., 72, 931-936.
- Anderson, E.C. and Libby, W.F., 1951, World-wide distribution of natural radiocarbon, Phys. Rev., 81, 64-69.
- Anscombe, F.J., 1960, Rejection of outliers, Technometrics, 2, 123-147.
- Arnold, J.R., 1954, Scintillation counting of natural radiocarbon: I. The counting method, Science, 119, 155-157.
- Arrol, W.J. and Glascock, R., 1947, Conversion of carbon dioxide to acetylene on a microscale, Nature (London), 159, 810.
- Ashby, V.J. and Catron, H.C., 1959, Tables of nuclear reaction Q values, Lawrence Radiation Lab. (Livermore, Calif.) Rept. UCRL-5419.

- Audric, B.N. and Long, J.V.P., 1954, Use of dissolved acetylene in liquid scintillation counters for the measurement of carbon-14 of low specific activity, Nature (London), 173, 992-993.
- Baillie, M.G.L., personal communication.
- Barensden, G.W., 1957, Radiocarbon dating with liquid CO₂ as diluent in a scintillation solution, Rev. Sci. Instrum., 28, 430-432.
- Barker, H., 1953, Radiocarbon dating: Large-scale preparation of acetylene from organic material, Nature (London), 172, 631-632.
- Barker, H. and Mackey, J., 1959, British Museum Natural Radiocarbon Measurements I, Am. J. Sci. Radiocarbon Suppl., 1, 81-86.
- Barker, H. and Mackey, J., 1961, British Museum Natural Radiocarbon Measurements III, Radiocarbon, 3, 39-45.
- Barker, H., Burleigh, R. and Meeks, N., 1971, British Museum Natural Radiocarbon Measurements VII, Radiocarbon, 13, 157-188.
- Baxter, M.S., 1969, Recent fluctuations of atmospheric carbon-14 concentrations, Ph.D. Thesis, University of Glasgow.
- Baxter, M.S. and Walton, A., 1970, A theoretical approach to the Suess effect, Proc. R. Soc. London, Ser. A, 318, 213-230.

- Baxter, M.S. and Walton, A., 1971, Fluctuations of atmospheric carbon-14 concentrations during the past century, Proc. R. Soc. London, Ser. A, 321, 105-127.
- Baxter, M.S. and Farmer, J.G., 1973, Radiocarbon: Short-term variations, Earth Planet. Sci. Lett., 20, 295-299.
- Berger, R., 1970, Tree-ring calibration of radiocarbon dates, Philos. Trans. R. Soc. London, Ser. A, 269, 23-36.
- Bien, G. and Suess, H.E., 1967, Transfer and exchange of ^{14}C between the atmosphere and the surface water of the Pacific Ocean, Proceedings of a conference on Radioactive Dating and Methods of Low-level Counting, Monaco, 57-68: I.A.E.A., Vienna.
- Bischof, W. and Bolin, B., 1966, Space and time variations of the CO_2 content of the troposphere and the lower stratosphere, Tellus, 18, 155-159.
- Blatz, H., ed., 1959, "Radiation Hygiene Handbook", McGraw Hill, New York.
- Bolin, B. and Keeling, C.D., 1963, Large scale atmospheric mixing as deduced from the seasonal and meridional variations of CO_2 , J. Geophys. Res., 68, 3899-3920.
- Bolin, B. and Bischof, W., 1970, Variations of the carbon dioxide content of the atmosphere of the northern hemisphere, Tellus, 22, 431-442.
- Broecker, W.S. and Olson, E.A., 1959, Lamont Radiocarbon Measurements VIII, Am. J. Sci. Radiocarbon Suppl., 1, 111-132.

- Broecker, W.S. and Walton, A., 1959, Radiocarbon from nuclear tests I, *Science*, 130, 309-314.
- Broecker, W.S. and Olson, E.A., 1960, Radiocarbon from nuclear tests II, *Science*, 132, 712-721.
- Broecker, W.S. and Olson, E.A., 1961, Lamont Radiocarbon Measurements VIII, *Radiocarbon*, 3, 176-204.
- Bucha, V., 1970, Influence of the Earth's magnetic field on radiocarbon dating, in "Radiocarbon Variations and Absolute Chronology", Proc. Twelfth Nobel Symp., Uppsala, 1969, Olsson, I.U., ed., 501-511: John Wiley, New York.
- Buckley, J.D., Trautman, M.A. and Willis, E.H., 1968, Isotopes' Radiocarbon Measurements VI, *Radiocarbon*, 10, 246-294.
- Buckley, J.D., 1976, Isotopes' Radiocarbon Measurements XI, *Radiocarbon*, 18, 172-189
- Burleigh, R. and Hewson, A., 1976, Evidence for short-term ^{14}C variations about 4,000 yrs. b.p., *Nature* (London), 262, 128-130.
- Calf, G.E., 1977, The counting of carbon-14 using thick walled vials, *Int. J. Appl. Radiat. Isot.*, 28, 735-737.
- Callendar, G.S., 1958, On the amount of carbon dioxide in the atmosphere, *Tellus*, 10, 243-248.
- Callow, W.J., Baker, M.J. and Hassal, G.I., 1965, National Physical Laboratory Radiocarbon Measurements III, Proc. Sixth Int. Conf. of Radiocarbon and Tritium Dating, Pullman, Washington, 393-395.

- Callow, W.J. and Hassal, G.I., 1968, National Physical Laboratory Radiocarbon Measurements V, Radiocarbon, 10, 115-118.
- Clark, R.M. and Renfrew, C., 1972, A statistical approach for the calibration of floating tree-ring chronologies, Archaeometry, 15, 255-266.
- Clark, R.M. and Renfrew, C., 1973, The tree-ring calibration of radiocarbon and the chronology of ancient Egypt, Nature (London), 243, 266-270.
- Clark, R.M. and Renfrew, C., 1974, Problems of the radiocarbon calendar and its calibration, Archaeometry, 16, 5-18.
- Clark, R.M. and Sowray, A., 1974, Further statistical methods for the calibration of floating tree-ring chronologies, Archaeometry, 15, 255-266.
- Clark, R.M., 1975, A calibration curve for radiocarbon dating, Antiquity, 49, 251-266.
- Craig, H., 1953, The geochemistry of the stable carbon isotopes, Geochim. Cosmochim. Acta., 3, 53-92.
- Craig, H., 1954, Carbon 13 in plants and the relationships between carbon 13 and carbon 14 in nature, J. Geol., 62, 115-149.
- Craig, H., 1957, The natural distribution of radiocarbon and the exchange time of carbon dioxide between atmosphere and sea, Tellus, 10, 243-248.

- Craig, H., 1961, Mass spectrometer analyses of radiocarbon dating standards, *Radiocarbon*, 3, 1-3.
- Damon, P.E., 1968, Radiocarbon and climate, *Meteorol. Monogr.*, 8, 151-154.
- Damon, P.E., 1970, Climatic versus magnetic perturbations of the atmospheric C14 reservoir, in "Radiocarbon Variations and Absolute Chronology", Proc. Twelfth Nobel Symp. Uppsala, 1969, Olsson, I.U., ed., 571-593: John Wiley, New York.
- Damon, P.E., Long, A. and Grey, D.C., 1970, Arizona radiocarbon dates for dendrochronologically dated samples, in "Radiocarbon Variations and Absolute Chronology", Proc. Twelfth Nobel Symp., Uppsala, 1969, Olsson, I.U., ed., 615-618: John Wiley, New York.
- Damon, P.E., Long, A. and Wallick, E.I., 1972, Dendrochronology calibration of the carbon-14 timescale, Proc. Eighth Int. Radiocarbon Dating Conf., Lower Hutt, New Zealand, A28-A43.
- Damon, P.E., Long, A. and Wallick, E.I., 1973, On the magnitude of the 11-year radiocarbon cycle, *Earth Planet Sci. Lett.*, 20, 300-306.
- von Daniken, E., 1972, "The Gold of the Gods", Corgi Books; Transworld Publishers Ltd., London .
- Drndarski, N., personal communication.
- Drndarski, N., 1977, Studies in radiocarbon geochemistry, Ph.D. Thesis, University of Glasgow.

- Eddy, J.A., 1976, The Maunder Minimum, *Science*, 192, 1189-1202.
- Edwards, I.E.S., 1970, Absolute dating from Egyptian records and comparison with carbon-14 dating, *Philos. Trans. R. Soc. London, Ser. A.*, 269, 11-18.
- Elsasser, W., Ney, E.P. and Winckler, J.R., 1956, Cosmic ray intensity and geomagnetism, *Nature (London)*, 178, 1226-1227.
- Emiliani, C., 1955, Pleistocene temperatures, *J. Geol.*, 63, 538-578.
- Fairbridge, R.W., 1961, Eustatic changes in sea level, in "Physics and Chemistry of the Earth", 4, 99-185.
- Fairhall, A.W., Schell, W.R. and Takashima, Y., 1961, Apparatus for methane synthesis for radiocarbon dating, *Rev. Sci. Instrum.*, 32, 323-325.
- Fairhall, A.W. and Young, J.A., 1970, in "Radionuclides in the Environment", Gould R.F., ed., Am. Chem. Soc., Washington.
- Ferguson, C.W., Huber, B. and Suess, H.E., 1966, Determination of the age of Swiss Lake Dwellings as an example of dendrochronologically-calibrated radiocarbon dating, *Z. Naturforschg.*, 21a, 1173-1177.
- Ferguson, C.W., 1968, Bristlecone pine: science and esthetics, *Science*, 159, 839-846.

- Ferguson, C.W., 1969, A 7104-year annual-tree ring chronology for bristlecone pine, Pinus aristata from the White Mountains, California, *Tree-Ring Bulletin*, 29, 3-29.
- Ferguson, C.W., 1970, Dendrochronology of bristlecone pine, Pinus aristata, Establishment of a 7484 year chronology in the White Mountains of eastern-central California, U.S.A., in "Radiocarbon Variations and Absolute Chronology", Proc. Twelfth Nobel Symp., Uppsala, 1969, Olsson, I.U., ed., 237-259: John Wiley, New York.
- Ferguson, C.W., 1972, Dendrochronology of bristlecone pine prior to 4000 B.C., Proc. Eighth Int. Radiocarbon Dating Conf., Lower Hutt, New Zealand, A1-A10.
- Fergusson, G.J., 1958, Reduction of atmospheric radio-carbon concentration by fossil fuel carbon dioxide and the mean life of carbon dioxide in the atmosphere, Proc. R. Soc. London, Ser. A, 243, 561-574.
- Forbush, S.E., 1954, World wide cosmic-ray variations, 1937-1952, *J. Geophys. Res.*, 59, 525-542.
- Fromm, E., 1970, An estimation of errors in the Swedish varve chronology, in "Radiocarbon Variations and Absolute Chronology", Proc. Twelfth Nobel Symp., Uppsala, 1969, Olsson, I.U., ed., 163-172: John Wiley, New York.
- De Geer, G., 1940, *Geochronologica Suecia Principales*, Kungl. Svenska, Vetensk. Akad. Handlingar, Ser. A., 18, 367 pp.

Godwin, H. and Willis, E.H., 1959, Cambridge University
Natural Radiocarbon Measurements I, Am. J. Sci.
Radiocarbon Suppl., 1, 63-75.

Godwin, H. and Willis, E.H., 1961, Cambridge University
Natural Radiocarbon Measurements III, Radiocarbon, 3,
60-76.

Godwin, H., 1962, Half-life of radiocarbon, Nature (London),
195, 984.

Godwin, H. and Willis, E.H., 1962, Cambridge University
Natural Radiocarbon Measurements V, Radiocarbon, 4,
57-70.

Godwin, H., Willis, E.H. and Switsur, V.R., 1965, Cambridge
University Natural Radiocarbon Measurements VII,
Radiocarbon, 7, 205-211.

Greig, J.C., 1970, Excavations at Castle Point, Troup,
Banffshire, Aberdeen University Reviews, 274-283.

Greig, J.C., 1971, Excavations at Cullykhan, Castle Point,
Troup, Banffshire, Scottish Archaeological Forum, 3,
15-21.

Grey, D.C., 1969, Geophysical mechanisms for ^{14}C variations,
J. Geophys. Res., 74, 6333-6340.

Grootes, P.M., 1977, Thermal diffusion isotopic enrichment
and radiocarbon dating beyond 50,000 years B.P.,
Ph.D. Thesis, University of Groningen.

Harkness, D.D., personal communication.

Harkness, D.D., 1970, Artificial carbon-14, a tracer for carbon in the atmosphere and biosphere, Ph.D. Thesis, University of Glasgow.

Harkness, D.D. and Wilson, H.W., 1972, Some applications in radiocarbon measurement at the Scottish Research Reactor Centre, Proc. Eighth Int. Radiocarbon Dating Conf., Lower Hutt, New Zealand, B101-B108.

Harkness, D.D. and Burleigh, R., 1974, Possible carbon-14 enrichment in high altitude wood, *Archaeometry*, 16, 121-127.

Hartley, P.E. and Church, V.E., 1974, A low background liquid scintillation counter for ¹⁴C, in "Liquid Scintillation Counting - Recent Developments", Proc. Int. Symp. on Liquid Scintillation Counting, Sydney, 1973, Stanley, P.E. and Scoggins, B.A., eds., 67-76: Academic Press Inc., New York .

Houtermans, J.C., 1966, On the quantitative relationships between geophysical parameters and the natural ¹⁴C inventory, *Z. Phys.*, 193, 1-12.

Houtermans, J.C., Suess, H.E. and Munk, W.H., 1967, The effect of industrial fuel combustion on the carbon-14 level of atmospheric CO₂, Proceedings of a conference on Radioactive Dating and Methods of Low-level Counting, Monaco, 57-68: I.A.E.A., Vienna.

Houtermans, J.C., 1971, Geophysical interpretations of bristlecone pine radiocarbon measurements using a method of Fourier analysis of unequally spaced data, Ph.D. Thesis, University of Bern.

- Houtermans, J.C., Suess, H.E. and Oeschger, H., 1973, Reservoir models and production rate variations of natural radiocarbon, *J. Geophys. Res.*, 78, 1897-1908.
- Jansen, H.S., 1970, Secular variations of radiocarbon in New Zealand and Australian trees, in "Radiocarbon Variations and Absolute Chronology", Proc. Twelfth Symp. Uppsala, 1969, Olsson, I.U., ed., 261-274: John Wiley, New York .
- Jelgersma, S., 1966, Sea-level changes during the last 10,000 years, *R. Met. Soc. Proceedings of a Symposium on World climate from 8,000 to 0 B.C.*, 54-71.
- Karlen, I., Olsson, I.U., Kallberg, P. and Kilicci, S., 1964, Absolute determination of the activity of two ^{14}C dating standards, *Archiv. Geofysik*, 4, 465-471.
- Kidson, C. and Heyworth, A., 1973, The Flandrian sea-level rise in the Bristol Channel, *Proc. Ussher Soc.*, 2, 565-584.
- Kigoshi, K. and Hasegawa, H., 1966, Secular variation of atmospheric radiocarbon concentration and its dependence on geomagnetism, *J. Geophys. Res.*, 71, 1065-1071.
- Kocharov, G.E. Dergachev, V.A. and Sanadze, A.A., 1974, On the secular cycle of radiocarbon content variations in the atmosphere, *Maler. Mezhdunar Semin. "Uskor Chastils Yad. Reakts. Kosmose"*, 6th 163-168 (Russian) (See also 1976, *Chem. Abs.*, 84, 138707b).

- Lal, D. and Rama, J., 1966, Characteristics of global tropospheric mixing based on man-made ^{14}C , ^3H and ^{90}Sr . *J. Geophys. Res.*, 71, 2865-2874.
- Lal, D. and Venkatavaradan, V.S., 1970, Analysis of the causes of $\text{C}14$ variations in the atmosphere, in "Radiocarbon Variations and Absolute Chronology", Proc. Twelfth Nobel Symp., Uppsala, 1969, Olsson, I.U., ed., 549-569: John Wiley, New York .
- Lavrukhina, A.K., Alexeev, V.A., Galimov, E.M. and Sulerzhitsky, L.D., 1973, Radiocarbon in the rings of sequoia, *Doklady Akad. Nauk. S.S.S.R.*, 210, 941-943.
- Léger, C. and Pichat, L., 1957, Use of paraldehyde to incorporate large quantities of labelled carbon in a liquid scintillator, *Compt. Rend.*, 224, 190-192.
- Lerman, J.C., Mook, W.G. and Vogel, J.C., 1970, $\text{C}14$ in tree rings from different localities, in "Radiocarbon Variations and Absolute Chronology", Proc. Twelfth Nobel Symp., Uppsala, 1969, Olsson, I.U., ed., 275-302: John Wiley, New York .
- Libby, L.M. and Lukens, H.R., 1973, Production of radiocarbon in tree rings by lightning bolts, *J. Geophys. Res.*, 78, 5902-5903.
- Libby, W.F., 1955, Radiocarbon Dating, 2nd ed., University of Chicago Press, Chicago.
- Lingenfelter, R.E., 1963, Production of $\text{C}14$ by cosmic ray neutrons, *Rev. Geophys.*, 1, 35-53.

- Lingenfelter, R.E. and Ramaty, R., 1970, Astrophysical and geophysical variations in C14 production, in "Radiocarbon Variations and Absolute Chronology", Proc. Twelfth Nobel Symp., Uppsala, 1969, Olsson, I.U., ed., 513-537: John Wiley, New York .
- Machta, L., 1959, in "Fallout from nuclear weapons tests, summary-analysis", Hearings of Joint Comm. Atom. Energy, Congress of the U.S.A., 3, 2191.
- McKerrell, H., 1971, Some aspects of the accuracy of carbon 14 dating, Scottish Archaeological Forum, 3, 73-84.
- McKinley, I.G., personal communication.
- Mann, W.B., Marlow, W.F. and Hughes, E.E., 1961, The half-life of carbon-14, Int. J. Appl. Radiat. Isot., 11, 57-67.
- Michael, H.N. and Ralph, E.K., 1972; Discussion of radiocarbon dates obtained from precisely dated sequoia and bristlecone pine samples, Proc. Eighth Int. Radiocarbon Dating Conf., Lower Hutt, New Zealand, A11-A27.
- Mörner, N.A., 1969, Eustatic and climatic changes during the last 15,000 years, Geol. Mijnbouw, 48, 389-399.
- Münnich, K.O. and Roether, W., 1967, Transfer of bomb ^{14}C and tritium from the atmosphere to the ocean. Internal mixing of the ocean on the basis of tritium and ^{14}C profiles, in Proceedings of a conference on Radioactive Dating and Methods of Low-level Counting, Monaco, 93-104: I.A.E.A., Vienna.

- Noakes, J.E., Isbell, A.F., Stipp, J.J. and Hood, D.W., 1962, Benzene synthesis by low temperature catalysis for radiocarbon dating, *Geochim. Cosmochim. Acta.*, 27, 797-808.
- Noakes, J.E., Kim, S.M. and Stipp, J.J., 1965, Chemical and counting advances in liquid scintillation age dating, *Proc. Sixth Int. Conf. of Radiocarbon and Tritium Dating*, Pullman, Washington, 68-92.
- Nydal, R., 1963, Increase in radiocarbon from the most recent series of thermonuclear tests, *Nature (London)*, 200, 212-214.
- Nydal, R., 1968, Further investigation on the transfer of radiocarbon in nature, *J. Geophys. Res.*, 73, 3617-3635.
- Nydal, R. and Lösveth, K., 1970, Prospective decrease in atmospheric radiocarbon, *J. Geophys. Res.*, 75, 2271-2278.
- Oeschger, H., Houtermans, J.C., Loosli, H. and Wahlen, N., 1970, The constancy of cosmic radiation from isotopic studies in meteorites and on the Earth, in "Radiocarbon Variations and Absolute Chronology", *Proc. Twelfth Nobel Symp.*, Uppsala, 1969, Olsson, I.U., ed., 471-498:
John Wiley, New York .
- Oeschger, H., Siegenthaler, U., Schotterer, U. and Gugelmann, A., 1975, A box diffusion model to study the carbon dioxide exchange in nature, *Tellus*, 27, 168-192.
- Otlet, R.L. and Slade, B.S., 1974, Harwell Radiocarbon Measurements I, *Radiocarbon*, 16, 178-191.

- Painter, K., 1974, Choice of counting vial for liquid scintillation counting: A review, in "Liquid Scintillation Counting - Recent Developments", Proc. Int. Symp. on Liquid Scintillation Counting, Sydney, 1973, Stanley, P.E. and Scoggins, B.A., eds., 431-451: Academic Press Inc., New York.
- Pietig, F. and Scharpeenseel, H.W., 1966, Age determination with the liquid scintillation spectrometer; a new catalyst for the synthesis of benzene, *Atompraxis*, 12, 95-97 (German).
- Polach, H.A., 1969, Optimisation of liquid scintillation radiocarbon age determinations and reporting of ages, *At. Energy Aust.*, 12, 21-28.
- Polach, H.A., 1975; Radiocarbon as a research tool in archaeology, hopes and limitations, Proc. Symp. Scientific Methods of Research in the Studies of Ancient Chinese Bronzes and Southeast Asian Metal and other Archaeological Artifacts, Melbourne, 255-298.
- Pringle, R.W., Turchinitz, W. and Funt, B.L., 1955, Liquid scintillation techniques for radiocarbon dating, *Rev. Sci. Instrum.*, 26, 859-865.
- Pringle, R.W., Turchinitz, W., Funt, B.L. and Danyluk, S.S., 1957, Radiocarbon age estimates obtained by an improved liquid scintillation technique, *Science*, 125, 69-70.
- Rafter, T.A. and Fergusson, G.J., 1958, Atom bomb effect - recent increase in the carbon-14 content of the atmosphere, biosphere and surface water of the oceans, *N.Z. J. Sci. Technol.*, 38, 871-883.

- Ralph, E.K., 1959, University of Pennsylvania Radiocarbon Dates III, *Am. J. Sci., Radiocarbon Suppl.*, 1, 45-58.
- Ralph, E.K. and Michael, H.N., 1970, Masca radiocarbon dates for sequoia and bristlecone pine samples in "Radiocarbon Variations and Absolute Chronology", *Proc. Twelfth Nobel Symp. Uppsala, 1969*, Olsson, I.U. ed., 619-624: John Wiley, New York.
- Ralph, E.K., Michael, H.N. and Han, M.C., 1973, Radiocarbon dates and reality, *MASCA Newsletter*, 9, 1-20.
- Reiter, R., 1973, Increased influx of stratospheric air into the lower troposphere after solar H α and X ray flares, *J. Geophys. Res.*, 78, 6167-6172.
- Revelle, R. and Suess, H.E., 1957, Carbon dioxide exchange between atmosphere and ocean and the question of an increase in atmospheric CO₂ in the past decades, *Tellus*, 9, 18-27.
- Richmond, I., 1968, "Hod Hill, Vol. II, excavations carried out between 1951 and 1958", Trustees of the British Museum London.
- Schaeffer, O.A., 1963, Information that isotopic measurements provide about space and the cosmos, *J. Chim. Phys.*, 60, 332-338.
- Schell, W.R., Fairhall, A.W. and Harp, G.D., 1965, Measurements of carbon-14 in known age samples and their geophysical implications, *Proc. Sixth Int. Conf., Radiocarbon and Tritium Dating*, Pullman, Washington, 397-414.

- Schove, D.J., 1955, The sunspot cycle 649 B.C. to A.D. 2000, *J. Geophys. Res.*, 60, 127-145.
- Shepard, F.P., 1963, Thirty-five thousand years of sea-level, in "Essays in Marine Geology", Univ. S. Calif. Press, Los Angeles.
- Simpson, J.A., 1963, The primary cosmic-ray spectrum and the transition region between interplanetary and interstellar space, *Proc. Int. Conf. Cosmic rays, Jaipur*, 2, 155-159.
- Smith, A.G., Baillie, M.G.L., Hillam, J., Pilcher, J.R. and Pearson, G.W., 1972, Dendrochronological work in progress in Belfast; the prospect for an Irish Post-Glacial tree-ring sequence, *Proc. Eighth Int. Radiocarbon Dating Conf., Lower Hutt, New Zealand*, A92-A96.
- Smith, A.G., Pearson, G.W. and Pilcher, J.R., 1974, Belfast Radiocarbon Dates VII, *Radiocarbon*, 16, 269-276.
- Starik, I.E., Arslanov, K.A. and Zharkov, A.P., 1961, Scintillation technique for counting natural radiocarbon and its use for the determination of absolute age, *Radiokhimiya*, 2, 67-68.
- Stenhouse, M.J., personal communication.
- Stuiver, M., 1961, Variations in radiocarbon concentration and sunspot activity, *J. Geophys. Res.*, 66, 273-276.
- Stuiver, M. and Suess, H.E., 1966, On the relationship between radiocarbon dates and true sample ages, *Radiocarbon*, 8, 534-540.

Stuiver, M., 1969, Yale Natural Radiocarbon Measurements IX, Radiocarbon, 545-658.

Stuiver, M., 1970, Long term ^{14}C variations, in "Radiocarbon Variations and Absolute Chronology", Proc. Twelfth Nobel Symp., Uppsala, 1969, Olsson, I.U., ed., 197-213: John Wiley, New York.

Stuiver, M., 1977, ^{14}C dating to 60,000 years B.P. with proportional counters, Proc. Ninth Int. Radiocarbon Dating Conf., Los Angeles-San Diego, in press.

Stuiver, M., personal communication.

Suess, H.E., 1954, Natural radiocarbon measurements by acetylene counting, Science, 120, 5-7.

Suess, H.E., 1955, Radiocarbon concentration in modern wood, Science, 122, 415-417.

Suess, H.E., 1965, Secular variations of the cosmic-ray-produced carbon-14 in the atmosphere and their interpretations, J. Geophys. Res., 70, 5937-5952.

Suess, H.E., 1968, Climatic changes, solar activity and the cosmic ray production rate of natural radiocarbon, Meteorol. Monogr., 8, 146-150.

Suess, H.E., 1970a, Bristlecone pine calibration of the radiocarbon time-scale 5200 B.C. to the present, in "Radiocarbon Variations and Absolute Chronology", Proc. Twelfth Nobel Symp. Uppsala, 1969, Olsson, I.U., ed., 303-312: John Wiley, New York.

- Suess, H.E., 1970b, Three causes of the secular ^{14}C fluctuations, their amplitudes and time constants, in "Radiocarbon Variations and Absolute Chronology", Proc. Twelfth Nobel Symp., Uppsala, 1969, Olsson, I.U., ed., 595-606: John Wiley, New York.
- Suess, H.E. and Strahm, C., 1970, The Neolithic of Auvernier, Switzerland, *Antiquity*, 46, 91-99.
- Switsur, V.R., 1973, The radiocarbon calendar recalibrated, *Antiquity*, 47, 131-137.
- Tamers, M.A., 1960, Carbon-14 dating with the liquid scintillation counter: Total synthesis of the benzene solvent, *Science*, 132, 668-669.
- Tamers, M.A., Stipp, J.J. and Collier, J., 1961, High sensitivity detection of naturally occurring radiocarbon - I. Chemistry of the counting sample, *Geochim. Cosmochim. Acta.*, 24, 266-276.
- Tamers, M.A., 1965, Routine carbon-14 dating using liquid scintillation techniques, Proc. Sixth Int. Conf. Radiocarbon and Tritium Dating, Pullman, Washington, 53-67.
- Tamers, M.A. and Pearson, F.J. Jnr., 1965, Isotope effect in benzene synthesis for radiocarbon dating, *Nature (London)*, 205, 1205-1207.
- Tamers, M.A., 1975, Chemical yield optimisation of the benzene synthesis for radiocarbon dating, *Int. J. Appl. Radiat. Isot.*, 26, 676-682.
- Tauber, H., 1967, Copenhagen Radiocarbon Measurements VIII, Geographic variations in atmospheric ^{14}C activity, *Radiocarbon*, 9, 246-256.

- Tauber, H., 1970, The Scandinavian varve chronology and C-14 dating, in "Radiocarbon Variations and Absolute Chronology", Proc. Twelfth Nobel Symp., Uppsala, 1969, Olsson, I.U., ed., 173-196: John Wiley, New York.
- de Vries, H., 1958, Variation in concentration of radiocarbon with time and location on earth, Proc. K. Ned. Akad. Wet., B61, 94-102.
- Wada, M. and Yamaguchi, A., 1962, Relation between ^{14}C production rate and geomagnetism, Uchusenkenkyn, 8, 168-170 (Japanese).
- Walton, A., Ergin, M. and Harkness, D.D., 1970, Carbon-14 concentrations in the atmosphere and carbon dioxide exchange rates, J. Geophys. Res., 75, 3089-3098.
- Watkins, T., ed., 1975, "Radiocarbon: Calibration and Prehistory", Edinburgh University Press, Edinburgh.
- Watt, D.E., Ramsden, D. and Wilson, H.W., 1961, The half-life of carbon-14, Int. J. Appl. Radiat. Isot., 11, 68-74.
- Welin, E., Engstrand, L. and Vaczy, S., 1972, Institute of Geological Sciences Radiocarbon Dates II, Radiocarbon, 14, 140-144.
- Welin, E., Engstrand, L. and Vaczy, S., 1972, Institute of Geological Sciences Radiocarbon Dates III, Radiocarbon, 14, 331-335.
- Wendland, W.M. and Donley, D.L., 1971, Radiocarbon-calendar age relationship, Earth Planet, Sci. Lett., 11, 135-139.

- Wenner, C.-G., 1968, Comparison of varve chronology, pollen analysis and radiocarbon dating, Stockholm Contributions in Geology, 18, 75-79.
- Wheeler, R.E.M., 1943, Maiden Castle, Dorset, Reports of the Research Committee of the Society of Antiquaries of London, No XII.
- Williams, E.J., 1959, "Regression Analysis", John Wiley, New York.
- Williams, E.T., 1977, Brooklyn College Radiocarbon Dates I, Radiocarbon, 19, 1-11.
- Willis, E. II, Tauber, M. and Münnich, K.O., 1960, Variations in the atmospheric radiocarbon concentration over the past 1300 years, Am. J. Sci. Radiocarbon Suppl., 2, 1-14.
- Young, J.A. and Fairhall, A.W., 1968, Radiocarbon from nuclear weapons tests, J. Geophys. Res., 73, 1185-1200.